



**TECHNISCHE UNIVERSITÄT
KAISERSLAUTERN**

Investigating the mechanism of cellular toxicity during aberrant branched-chain amino acid metabolism

Dem Fachbereich Biologie
der Technischen Universität Kaiserslautern
zur Erlangung des akademischen Grades
„Doktor der Naturwissenschaften“ (Dr. rer. nat.)
genehmigte Dissertation,

vorgelegt von

M.Sc. Gurleen Kaur Khandpur

Datum der wissenschaftlichen Aussprache:

03, September 2021

Prüfungskommission

1. Gutachter: Prof. Dr. Bruce Morgan
 2. Gutachter: Prof. Dr. Zuzana Storchová
- Vorsitzender: Prof. Dr. Johannes M. Herrmann

Kaiserslautern, 2021
D386

To my Family and my Friends....

Table of Contents

LIST OF FIGURES	6
LIST OF TABLES	9
ABSTRACT	10
ZUSAMMENFASSUNG	11
1 INTRODUCTION	12
1.1 Yeast: an eukaryotic model organism	12
1.2 Amino acids-elixir of life	13
1.2.1 What is an amino acid?.....	13
1.2.2 Classification of amino acids.....	15
1.3 Amino acid sensing in yeast.....	17
1.3.1 SPS signalling	17
1.3.2 Role of Gcn4 mediated GAAC control.....	19
1.4 Amino acid permeases/transporters.....	22
1.4.1 Regulation of AAT	22
1.4.2 Role of Gap1 in amino acids starved condition.....	23
1.5 Cross talk between TOR signalling and amino acids.....	24
1.5.1 TOR activation in <i>S. cerevisiae</i>	24
1.5.2 TOR signalling under the light of amino acids.....	26
1.6 Aminoacidopathies.....	27
1.6.1 Organic acidurias.....	28
1.6.2 Urea cycle related disorders	28
1.6.3 BCaa related pathologies.....	28
1.7 Branched-chain amino acids.....	31
1.7.1 BCaa synthesis in a yeast cell	32
1.7.2 BCaa and Diabetes	33
1.8 Effect of auxotrophies in yeast research.....	34
1.9 Aim of the study	36
2 MATERIALS AND METHODS	37
2.1 Molecular and Cell Biology Methods	37
2.1.1 Plasmid DNA isolation from <i>E.Coli</i>	37
2.1.2 Yeast media and growth	37
2.1.3 Yeast transformation.....	39
2.1.4 Drop dilution assay	40

2.1.5 Growth curve assay	40
2.1.6 Halo assay	40
2.1.7 Polymerase chain reaction (PCR)	41
2.2 Biochemistry Methods.....	46
2.2.1 Whole-cell Glutathione (GSH/GSSG) analysis	46
2.2.2 Quantification of Amino acids (intracellular amino acids or ¹³ C enrichment studies):	47
2.2.3 RNA Sequencing	47
2.2.4 Annexin-V staining and Microscopy	48
2.2.5 Quantification of cellular metabolites.....	49
2.2.6 Translational studies.....	50
3 RESULTS	51
3.1 Growth of <i>Saccharomyces cerevisiae</i> in the presence of increased amino acid content in the growth medium.....	51
3.1.1 The foundation stone observation	51
3.1.2 The growth of auxotrophic yeast strains is severely impacted in response to an increase in amino acid content in the solid agar and liquid growth medium	52
3.1.3 Restoring only the leucine auxotrophy in BY4742 rescues the impaired growth phenotype.....	55
3.1.4 Increasing leucine in proportion to the increase of amino acid content in the growth medium also rescues the impaired growth phenotype	56
3.1.5 Deletion or overexpression of amino acid permeases does not affect the amino acid dependent observed growth phenotype	58
3.1.6 The main bad guys: Ehrlich amino acids are inducing the impaired growth phenotype.....	59
3.1.7 Deep insights about intracellular amino acids levels of BY4742 strain	64
3.1.7a Imported versus <i>de novo</i> synthesized amino acids.....	65
3.1.7b Total intracellular arginine levels are increased as an effect of 2 X AAM.....	67
3.2 Activation of branched-chain amino acid biosynthetic pathway correlates positively with the amino acid dependent growth phenotype of the yeast cell	69
3.2.1 Role of valine and isoleucine on the growth of cell	71
3.2.2 Deleting either <i>ILV2</i> or <i>ILV3</i> rescues the growth phenotype.....	72
3.2.3 BCaa pathway NON-ACTIVATION supports the growth of BY4742 on 2 X AAM condition	78
3.2.4 Sit4 and Gcn4 act upstream to the activation of the BCaa pathway	79
3.3 Effect of AAM on the transcriptional and translational level	81
3.3.1 BCaa genes are upregulated on 2 X AAM.....	81
3.3.2 Increased amino acid content affects the cell division.....	83
3.3.2a Increased amino acid content induces apoptosis in a fraction of the yeast population.....	84
3.3.2b Increased amino acid content decreases the global translation levels.....	87
3.4 Increased amino acid content induces redox phenotype	88
3.4.1 Restoring the leucine auxotrophy in BY4742 also rescues the redox phenotype.....	90
3.4.2 Removing isoleucine and valine from the medium partially rescue the redox phenotype....	93
3.4.3 Deleting <i>ILV3</i> rescues the redox phenotype	94
3.5 The potential intermediate behind the growth phenotype	98
3.5.1 <i>ILV3</i> is potentially the switching point for observed growth phenotype	98
3.5.2 Quantification of intracellular KIV/ α -IPM levels	103

4 DISCUSSION	107
4.1 The case of leucine limitation	107
4.2 The potential role of leucine underlying the observed phenotype	108
4.3 The plausible contribution of the Gap1 permease towards the observed growth phenotype	109
4.4 pH-dependent activation of PKA pathway and TORC1 mediated signalling	110
4.5 The role of branched-chain aminotransferases	112
4.6 The role of α -keto acids.....	114
4.7 The interplay between amino acid homeostasis, mitochondrial function and the cell growth.....	115
CONCLUSION.....	118
SUPPLEMENTARY FIGURES	120
REFERENCES	122
LIST OF ABBREVIATIONS	139
CURRICULUM VITAE	141
ACKNOWLEDGEMENTS.....	143
DECLARATION	145

LIST OF FIGURES

Figure 1: The structural representation of twenty proteogenic and two special case amino acids.	14
Figure 2: Schematic representation of the catabolism pattern of ketogenic and glucogenic amino acids in humans.	16
Figure 3: A schematic representation of the degradation pattern of Ehrlich amino acids inside the <i>S. cerevisiae</i>	17
Figure 4: A schematic representation of SPS signalling in <i>S. cerevisiae</i>	18
Figure 5: Mechanism of Gcn4 translation in response to amino acids.	21
Figure 6: Mechanism of TORC1 signalling in response to preferred nitrogen sources.	25
Figure 7: Branched-chain amino acids' catabolism pathway in humans.	29
Figure 8: Overview of human branched-chain amino acids' catabolism.	30
Figure 9: Schematic diagram showing the branched-chain amino acid biosynthetic pathway in <i>S. cerevisiae</i>	33
Figure 10: Increased amino acid content (AAM) in the medium severely impacts the growth of BY4742 yeast strain as shown by Drop dilution assay.	51
Figure 11: Auxotrophic wild-type yeast strains were sensitive to increase amino acid content, unlike prototrophic wild-type strains in the presence of a fermentable carbon source.	53
Figure 12: Increased amino acid content (AAM) in the medium severely impacts the growth of BY4742 yeast strain as shown by Drop Dilution assay (A) and Growth Curve assay (B) in fermentable carbon substrate.	54
Figure 13: Restoring the auxotrophic markers in BY4742 affects the amino acid dependent growth phenotype.	55
Figure 14: Increase in extracellular leucine amounts relative to increase in AAM, also rescues the growth phenotype.	57
Figure 15: Deletion and overexpression of genes encoding the amino acid permeases Agp1, Gap1 or Bap2 have no striking effect on the observed growth phenotype.	58
Figure 16: Removing Ehrlich amino acids individually from the amino acid mix affects cell growth.	60
Figure 17: Increasing the amino acids of AAM individually to three times affects cell growth.	61

Figure 18: Increasing concentration of Ehrlich amino acids in dropout amino acid mix to three times affects cell growth.	62
Figure 19: The concentration of Ehrlich amino acids is critical for the growth of the cell.	64
Figure 20: Relative fraction of proteinogenic amino acids synthesized de novo versus imported fraction from the medium when cells were fed with ¹³ C glucose for BY4742 and wt+ <i>LEU2</i> on 1 X AAM and 2 X AAM.	66
Figure 21: Total free intracellular amino acid levels in BY4742 and BY4742+ <i>LEU2</i> on 1 X AAM and 2 X AAM.	68
Figure 22: Schematic diagram showing the branched-Chain amino acid biosynthetic pathway in <i>Saccharomyces cerevisiae</i>	69
Figure 23: The growth phenotype is lost when cells are forced to respire.	70
Figure 24: Removing isoleucine and valine from the medium rescues the growth phenotype.	71
Figure 25: Deleting <i>ILV2</i> or <i>ILV3</i> rescues the growth of cells in conditions with increased amino acid content.	73
Figure 26: <i>ILV3</i> as a potential switch point for the growth phenotype.	74
Figure 27: Relative fraction of proteinogenic amino acids synthesized de novo versus imported fraction from the medium when cells were fed with ¹³ C glucose for BY4742 and $\Delta ilv3$ deletion strain on 1 X AAM and 2 X AAM.	76
Figure 28: Total free intracellular amino acid levels in BY4742 and $\Delta ilv3$ on 1 X AAM and 2 X AAM.	78
Figure 29: Deleting <i>GCN4</i> also rescues the growth phenotype.	79
Figure 30: Sit4 and Gcn4 act upstream to possibly activate of the BCaa pathway ...	80
Figure 31: The PCA analysis and heat map representing BY4742 and $\Delta ilv3$ transcriptional changes on 1 X AAM vs 2 X AAM growth condition.	82
Figure 32: The GO plot summarizing the GO enrichment of the transcriptional changes in BY4742 on 1 X AAM versus 2 X AAM growth condition.	82
Figure 33: The expression levels for the BCaa pathway genes in BY4742 and $\Delta ilv3$ in 1 X AAM and 2 X AAM growth conditions.	83
Figure 34: Increase in the amino acid content in growth medium results in apoptosis of BY4742.	85
Figure 35: Increase in the amino acid content in growth medium results in G1 cell cycle arrest of BY4742.	86

Figure 36: Increase in the amino acid content in growth medium results in decreased global protein translation in BY4742.	88
Figure 37: Restoring the available Leucine biosynthetic pathway rescues cells from the oxidative stress-induced due to 2 X AAM growth condition.	89
Figure 38: Increased amino acid content (2 X AAM) in the medium leads to a redox phenotype.....	90
Figure 39: DTT supplementation could not rescue the growth phenotype.....	91
Figure 40: Establishment of functional leucine biosynthetic pathway or extra Leucine supplementation in the medium rescued the redox phenotype.....	92
Figure 41: Removing isoleucine and valine from the medium partially rescued the redox phenotype.....	93
Figure 42: Deleting <i>ILV3</i> rescued the redox phenotype.....	95
Figure 43: Deleting <i>GCN4</i> rescues the redox phenotype.	96
Figure 44: Overexpressing <i>BAT1</i> does not rescue the redox phenotype.....	97
Figure 45: Schematic diagram showing the possible routes and proteins involved where keto-isovalerate (KIV) can be metabolized downstream.	98
Figure 46: Deleting or overexpressing <i>LEU4</i> and <i>LEU9</i> has no rescue effect on the growth of cells in conditions with increased amino acid content in the medium.....	99
Figure 47: Overexpressing <i>BAT1</i> rescues the growth of cells in conditions with increased amino acid content in the medium.....	100
Figure 48: Elm1, Aim45, and Cir2 have no role in plausible signalling mediated via KIV or its downstream intermediates to the growth of the cell in conditions with increased amino acid content.	102
Figure 49: Schematic diagram highlighting the biochemical reactions around the <i>Ilv3</i> catalyzed step.....	103
Figure 50: The total cellular metabolites levels.....	104
Figure 51: The total cellular alpha-ketoglutarate levels.....	106
Figure 52: No significant change in the cytosolic pH in BY4742 (wt) and $\Delta ilv3$ due to increased amino acid content in the growth medium.	111
Figure 53: PKA signalling components have no plausible contribution towards the impaired growth phenotype of BY4742 in growth conditions with increased amino acid content.....	112
Figure 54: The levels of some metabolites are altered in <i>taz1</i> Δ cells and restored upon overexpression of <i>BAT1</i>	113

Figure 55: Schematic representation summarising the plausible mechanism contributing to the slow growth phenotype of leucine auxotroph BY4742 on 2 X AAM growth condition.117

Figure 56: Schematic representation summarizing the observations of the current study.....119

Figure 57: Deleting *ILV2* or *ILV3*, and not *LEU4 LEU9*, rescues the growth of cells in conditions with increased amino acid content.....121

LIST OF TABLES

Table 1: Amino acid transporters and transported substrates. 22

Table 2: Composition of the dropout mix. 38

Table 3: Recipe of Hartwell Complete media..... 38

Table 4: Plasmids transformed in BY4742 and mutant strains during this study. 39

Table 5: Program used in the thermocycler to amplify DNA in PCR..... 41

Table 6: The primers used during the study. 42

Table 7: The yeast strains used during the study. 45

Table 8: Recipe for the liquid medium composition used during the study. 52

Table 9: The concentration of the individual Ehrlich amino acid (M, I, V, F, Y) present in HC medium supplemented with either normal [1 X AAM] and triple amount [3 X AAM] of amino acid dropout mix or in the new medium. 63

ABSTRACT

Amino acids, apart from being building blocks of proteins, serve various cellular and metabolic functions^{1,2}. Changes in amino acid handling have been observed in a wide range of human pathologies, including diabetes and various metabolic disorders (aminoacidopathies)³⁻⁵. *Saccharomyces cerevisiae* is used as a model to investigate how increase in amino acid content (in the form of amino acid dropout mix: AAM) in growth medium influences cell growth. Intriguingly, it was observed that increasing the concentration of AAM in the media (double or triple times; 2 X AAM and 3 X AAM respectively), severely affects the growth of auxotrophic but not of prototrophic yeast strains in presence of glucose as carbon substrate. Increased concentration of Ehrlich amino acids, which are degraded to fusel acidic/alcoholic compounds, induced the observed slow growth phenotype of BY4742. These phenotypes can be rescued by either re-establishing the functional leucine biosynthetic pathway in BY4742 (leucine auxotroph) or increasing leucine in proportion to the increased AAM. Interestingly, the amino acid dependent growth phenotypes are absent when cells grow in media containing non-fermentable carbon sources. Furthermore, the deletion of *ILV2* or *ILV3* (genes encoding enzymes involved in the leucine biosynthetic pathway) also rescues the growth phenotype of BY4742 on 2 X AAM and 3 X AAM growth media. It was found that *Ilv3* is the potential switching point and links cellular growth to redox homeostasis. The possibility of leucine limitation *per se* or transport competition between different Ehrlich amino acids and leucine, as a cause for the observed phenotypes, is ruled out. Upregulation of the branched-chain amino acid pathway inhibits cell growth of BY4742 on 2 X AAM. Although we could not detect KIV, the α -keto acid intermediate formed by the *Ilv3*. It is proposed that KIV itself (or its unknown downstream product) leads to the onset of the observed phenotypes. Different studies suggest that oxidative stress (due to accumulation of branched-chain amino acids (BCaa) and their α -keto acids) contributes to the neurological damage of MSUD patients⁶⁻⁹. It was also observed that the trigger of the BCaa bio-synthesis pathway on 2 X AAM growth conditions also contributes to the significant oxidative stress in the cell. In conclusion, we propose that yeast can be used as a suitable model system to study how accumulation of BCaa and their α -keto acids are lead to oxidative stress that is potentially toxic to cells. Further, this knowledge and the underlying molecular mechanisms will enhance our understanding of MSUD in humans.

ZUSAMMENFASSUNG

Aminosäuren sind nicht nur Bausteine von Proteinen, sondern dienen auch verschiedenen zellulären und metabolischen Funktionen^{1,2}. Veränderungen im Umgang mit Aminosäuren wurden bei einer Vielzahl von menschlichen Pathologien beobachtet, darunter Diabetes und verschiedene Stoffwechselstörungen (Aminosäureopathien)³⁻⁵. *Saccharomyces cerevisiae* wird als Modell verwendet, um zu untersuchen, wie eine Erhöhung des Aminosäuregehalts (in Form von Aminosäure-Dropout-Mix: AAM) im Wachstumsmedium das Zellwachstum beeinflusst. Interessanterweise wurde beobachtet, dass eine Erhöhung der Konzentration von AAM im Medium (das Doppelte oder Dreifache; 2 X AAM bzw. 3 X AAM) das Wachstum von auxotrophen, aber nicht von prototrophen Hefestämmen in Gegenwart von Glukose als Kohlenstoffsubstrat stark beeinflusst. Erhöhte Konzentration von Ehrlich-Aminosäuren, die zu fuselsauren/alkoholischen Verbindungen abgebaut werden, induzierten den beobachteten langsamen Wachstumsphänotyp von BY4742. Dieser Phänotyp kann entweder durch die Wiederherstellung des funktionalen Leucin-Biosynthesewegs in BY4742 (Leucin-Auxotrophie) oder durch die Erhöhung von Leucin im Verhältnis zur erhöhten AAM gerettet werden. Interessanterweise sind die aminosäureabhängigen Wachstumsphänotypen nicht vorhanden, wenn die Zellen in Medien wachsen, die nicht fermentierbare Kohlenstoffquellen enthalten. Darüber hinaus rettet die Deletion von *ILV2* oder *ILV3* (Gene, die für Enzyme kodieren, die am Leucin-Biosyntheseweg beteiligt sind) auch den Wachstumsphänotyp von BY4742 auf 2 X AAM und 3 X AAM Wachstumsmedien. Es wurde festgestellt, dass *Ilv3* der potentielle Schaltpunkt ist und das zelluläre Wachstum mit der Redox-Homöostase verbindet. Die Möglichkeit einer Leucin-Limitierung per se oder einer Transportkonkurrenz zwischen verschiedenen Ehrlich-Aminosäuren und Leucin, als Ursache für die beobachteten Phänotypen, wird ausgeschlossen. Die Hochregulierung des verzweigtkettigen Aminosäurewegs hemmt das Zellwachstum von BY4742 auf 2 X AAM. Obwohl wir KIV, das α -Ketosäure-Zwischenprodukt, das von der *Ilv3* gebildet wird, nicht nachweisen konnten. Es wird vorgeschlagen, dass KIV selbst (oder sein unbekanntes Downstream-Produkt) zum Auftreten der beobachteten Phänotypen führt. Verschiedene Studien legen nahe, dass oxidativer Stress (aufgrund der Akkumulation von verzweigtkettigen Aminosäuren (BCaa) und deren α -Ketosäuren) zu den neurologischen Schäden von MSUD-Patienten beiträgt⁶⁻⁹. Es wurde auch beobachtet, dass die Auslösung des BCaa-Biosyntheseweges unter 2 X AAM-Wachstumsbedingungen ebenfalls zu dem signifikanten oxidativen Stress in der Zelle beiträgt. Zusammenfassend schlagen wir vor, dass Hefe als geeignetes Modellsystem verwendet werden kann, um zu untersuchen, wie die Akkumulation von BCaa und deren α -Ketosäuren zu oxidativem Stress führt, der potenziell toxisch für Zellen ist. Außerdem werden dieses Wissen und die zugrunde liegenden molekularen Mechanismen unser Verständnis von MSUD beim Menschen verbessern.

1 INTRODUCTION

1.1 Yeast: an eukaryotic model organism

Yeast is a unicellular eukaryotic organism classified as a member of the Kingdom Fungi¹⁰. They are known for use in bread making, wine production and as a core aspect in breweries since ancient times¹¹. The earliest anecdotes of yeast being used for beer making by human civilization dates to 6000 BCE in Sumaria, present-day Iran¹². The term yeast is often mistaken for *Saccharomyces cerevisiae*. Instead, based on their cell physiology, colony, and ascospore features, yeasts are classified into two separate phyla: Ascomycota and Basidiomycota. *Saccharomyces cerevisiae*, which is also known as budding yeast, belongs to the phylum Ascomycota under the order Saccharomycetales¹³. It is found diversely in nature, for example, on plant leaves or fruits or in the soil. Yeasts usually divide by asexual (*S. cerevisiae*: budding-asymmetric division; *S. pombe*: fission-direct division) or sexual reproduction. However, under nutrient depletion conditions, diploid yeasts can also undergo sporulation, forming haploid spores, which mate and form the diploid cell once normal growth conditions are restored¹⁴. They are also known to be found in the intestines of warm-blooded animals and also on their skin surfaces. *Candida albicans*, present in human gut flora, can become an opportunistic pathogen and pose a serious threat to immunocompromised patients in some circumstances¹⁵.

In 1857, Louis Pasteur discovered that yeast can convert glucose into ethanol during the fermentation process, and later, this phenomenon was famously called as respiration without air¹⁶. In the late 19 century, Eduard Buchner isolated a collection of enzymes "Zymases", catalyzing the entire fermentation process as cell-free extracts from grounded yeast cells. He was awarded the Nobel prize in 1907 for his discovery¹⁷. Earlier experiments performed by Øjvind Winge at the Carlsberg Laboratory in Denmark established that budding yeasts are heterothallic organisms. They require two haploid yeast cells to form one diploid yeast cell.

Moreover, it is also common for budding yeasts to alternate between the two forms. Winge et al. also established that the different yeast strains could be effectively crossed over for having desirable brewing traits in the end. For all his pioneering work and contribution in yeast research, Winge is popularly known as the Father of Yeast Genetics¹⁸. Since it is easy to grow yeast in liquid cultures overnight (doubling time of 90 min) with easy accessibility to select for desirable traits, it made yeasts a very popular and cost-effective entity for use in the biology research field from the mid to late 20 century till now. Many outstanding research works were carried out using yeast as the model organism which includes the discovery of cell cycle-related genes by Leland Hatwell¹⁹ and Paul Nurse²⁰. The protein vesicular trafficking studies and discovery of related SEC genes made by Randy Schekman²¹ were also done using *S. cerevisiae*. Further, the discovery of autophagy, and the associated genes involved in the process, was made in *S. cerevisiae* by Yoshinori Ohsumi^{22,23}. Scientific literature is full of many more ground-breaking discoveries that employed classical yeast genetics²⁴.

There have also been significant advancements in molecular mechanistic understanding of different human diseases by several labs across the world using budding yeast as model organism²⁵. The most important contributions include works from Jared Rutter's lab for studying the role of the *SDH5* gene (human homologue *PGL2*), which is mutated in the inherited paraganglioma cancer type and is responsible for modifying different respiratory proteins²⁶. Another example is included from work done in Susan Lindquist's lab, where they studied the role of protein aggregates in neurodegenerative diseases and their implications using the budding yeast²⁷. Many of such examples are illustrated in the literature, exemplifying the use of classical yeast genetics to address several biological questions. It is also believed in the scientific community that budding yeast can also be used as a surrogate model platform to study human diseases²⁵.

From the early days of research using *S. cerevisiae*, the reference strain S288c and its derivatives have been used in different labs across the world, where S288c was obtained by crossing different parental strains. The ability to be stable in the haploid state made it popular to work with budding yeasts in different research platforms across the world^{16,28-30}. Subsequently, it was the S288c strain of *S. cerevisiae* that became the first eukaryotic organism to have its entire genome sequenced in 1996³¹. Later various libraries were also developed with a collection of the strains that were deleted³² for single non-essential genes or had single encoded protein either overexpressed³³ or tagged with a reporter gene³⁴. Such libraries led to many publications and enhanced our understanding of different aspects of biological research.

1.2 Amino acids-elixir of life

Proteins account for 50% of the dry cellular weight and play many essential roles and diverse functions in the cell³⁵. They are made of one or more long polypeptide chains of twenty amino acids connected by a special covalent peptide linkage. The unique sequence of amino acids, encoded and inherited in the form of DNA, further defines specific structure and function of a protein¹. In addition to their role as monomeric building blocks of proteins, few amino acids (or modified forms) also function as neurotransmitters, nitrogen donors for purine and pyrimidine synthesis. They serve as precursors for synthesis of many important molecules².

1.2.1 What is an amino acid?

An amino acid is a simple organic molecule consisting of an alpha asymmetric carbon atom (chiral) linked to a basic amino group (NH_2), carboxyl group (COOH), the hydrogen atom and a particular side chain denoted by 'R'. This R group is unique and imparts different properties to every amino acid. Glycine amino acid is an exception with symmetric carbon atom (non-chiral) since it has an 'H' atom as the R group. There are twenty proteogenic amino acids that are present in proteins in all organisms¹. However, two amino acids- pyrrolysine and selenocysteine occur in proteins in exceptional cases. Selenocysteine is a cysteine analogue and is present in the active site of many enzymes like glutathione peroxidases, thioredoxins reductases etc., in some lineages and pyrrolysine is found only in a few methanogenic archaea and

bacteria^{36,37}. Figure 1 illustrates the structures of twenty proteogenic amino acids, selenocysteine and pyrrolysine, along with their alphabetical letter representations.

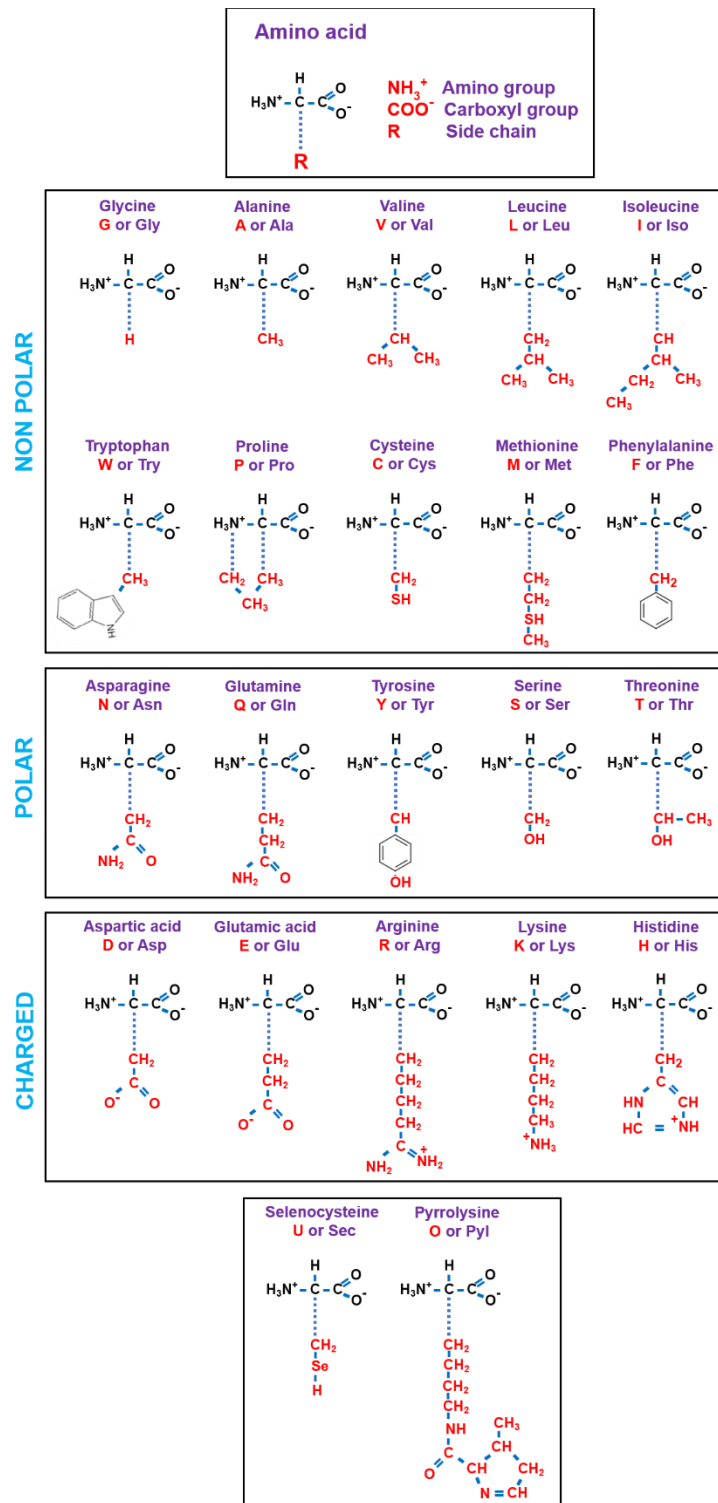


Figure 1: The structural representation of twenty proteogenic and two special case amino acids. An amino acid consists of an asymmetric carbon atom linked to the amino group, carboxyl group, the hydrogen atom, and a side residue group denoted by R. The R group imparts different properties to an amino acid. Thus, amino acids are broadly classified as non-polar, polar, and charged (negatively or positively charged) amino acids.

1.2.2 Classification of amino acids

Polar vs non-polar amino acids

Based on the properties of the side 'R' side group, they are classified as hydrophilic polar and hydrophobic non-polar amino acids (fig: 1). Polar hydrophilic amino acids include either uncharged (threonine, serine, cysteine, tyrosine, glutamine, and asparagine) or charged amino acids (positively charged: lysine, histidine, and arginine; negatively charged: glutamic acid and aspartic acid). Non-polar hydrophobic amino acids can be aromatic (tryptophan and phenylalanine) or aliphatic (valine, leucine, isoleucine, glycine, alanine, proline, and methionine) in nature². Leucine, valine, and isoleucine are also referred to as branched-chain amino acids since they have branched aliphatic side chains.

Essential vs non-essential amino acids

Unlike bacteria, yeast and plants, humans cannot synthesize some of the 20 amino acids such as leucine, isoleucine, valine, threonine, methionine, tryptophan, phenylalanine, and lysine. Hence, they are termed essential amino acids for human growth and must be supplied in the diet³⁸⁻⁴¹. However, certain amino acids are also classified as semi-essential or conditionally essential, especially for children since they are not synthesized in enough quantities at the appropriate growth phase, thus must be supplied through diet⁴⁰. These amino acids are arginine, histidine, cysteine, glycine, tyrosine, glutamine, and proline.

Proteogenic vs non-proteogenic amino acids

Next to the proteogenic amino acids, several non-proteogenic amino acids are found in nature. As the name suggests, non-proteogenic amino acids are not part of proteins. Instead, they serve several other vital functions in the cell: as ornithine and citrulline are key intermediates in the urea cycle. γ -Aminobutyric acid (GABA)-derived from glutamic acid, melatonin and serotonin derived from tryptophan etc., acts as a neurotransmitter. Further, β -alanine: is found to be a crucial precursor during Vit B₅ synthesis. These amino acids are also referred to as non-standard amino acids. A few proteogenic amino acids are not produced directly. However, they are post-translationally modified like 4-hydroxyproline, hydroxylysine (by hydroxylation of proline and lysine, respectively) and γ -carboxy glutamic acid (carboxylation of glutamic acid). These modifications are generally essential for the function and structure of respective proteins containing them.

Ketogenic vs glucogenic amino acids

Based on the catabolism pattern in humans, amino acids are also classified as ketogenic, glucogenic or mixed types⁴². The cell recycles the carbon skeleton of an amino acid after removing the amino group to form intermediates which can be fuelled further to either Krebs's cycle or can be used to form glucose via gluconeogenesis. The degradation products of ketogenic amino acids: lysine and leucine form acetyl CoA and aceto-acetyl CoA, which are funnelled to form ketone bodies and fatty acids but cannot be made into glucose. On the other hand, degradation of glucogenic amino acids to pyruvate or Krebs's cycle intermediates such as α -ketoglutarate, oxaloacetate, succinyl-CoA, or fumarate are used to form phosphoenolpyruvate (PEP) or glucose.

Lysine and leucine are the only two ketogenic amino acids, along with phenylalanine, tyrosine, isoleucine, tryptophan, and threonine belonging to the mixed type, and the remaining thirteen amino acids are glucogenic. Following figure 2 summarizes the fate of carbon atoms when a deaminated amino acid is degraded inside the cell.

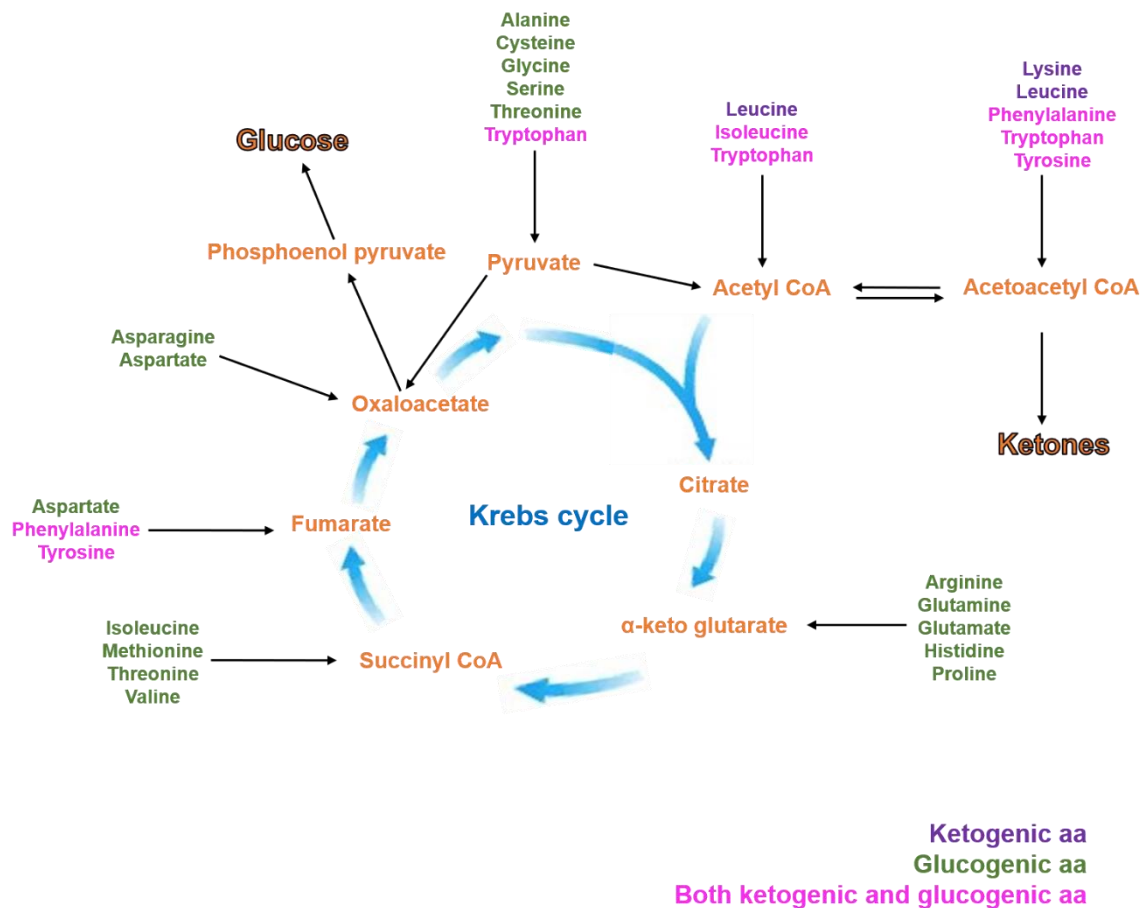


Figure 2: Schematic representation of the catabolism pattern of ketogenic and glucogenic amino acids in humans. Ketogenic, glucogenic and both ketogenic and glucogenic amino acids are represented by purple, green and pink colours, respectively. (Adapted and modified from Biochemistry 5th edition. 2002¹).

Ehrlich vs non-ehrich amino acids

In yeasts, degradation of amino acids such as leucine, valine, isoleucine, tyrosine, tryptophan, phenylalanine, and methionine lead to the formation of iso-amyl alcohols or acids, which are also known as Fusel acids or Fusel alcohols. This pathway was discovered by the scientist Felix Ehrlich, and hence they are also referred to as Ehrlich amino acids⁴³. These fusel compounds are known to add valuable flavour and aroma to yeast fermented foods and beverages. Thus, making this Ehrlich pathway of high industrial relevance and research interest in the scientific community. In general, an Ehrlich amino acid is transaminated (reversible reaction step) to an alpha-keto acid along with the concomitant conversion of 2-oxoglutarate to glutamate.

Further, the alpha-keto acid is decarboxylated to its respective fusel aldehyde. Afterwards, depending upon whether the fusel aldehyde is either oxidized or reduced, fusel acids or fusel alcohols are produced, respectively, which are known to impart quality and flavours to the yeast fermented products⁴³. The following figure 3 represents the detailed Ehrlich amino acid degradation pathway in *S. cerevisiae*.

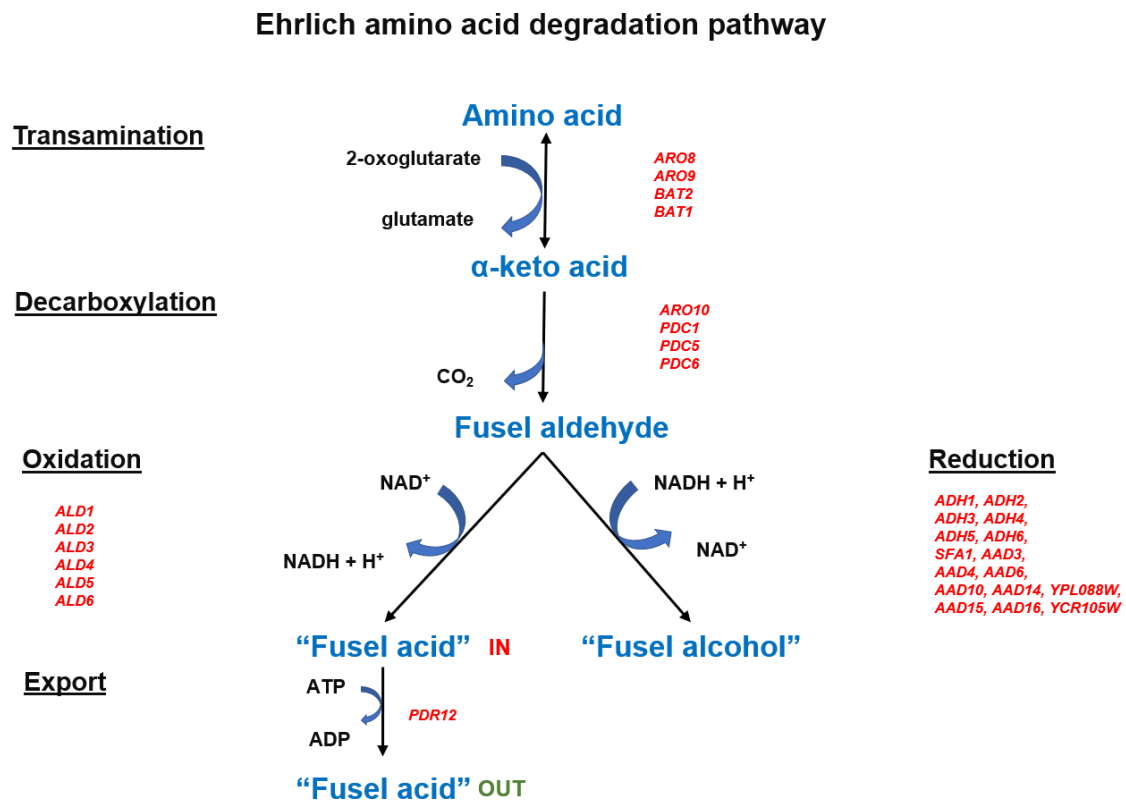


Figure 3: A schematic representation of the degradation pattern of Ehrlich amino acids inside the *S. cerevisiae*. The different genes, whose proteins products catalyze similar steps for different Ehrlich amino acids, are represented in the red colour (Adapted and modified from Hazelwood et al., 2008⁴³).

1.3 Amino acid sensing in yeast

1.3.1 SPS signalling

S. cerevisiae has a special pathway, known as the SPS pathway^{44,45}, to sense extracellular amino acids, which in turn further induces transcription of various amino acid permeases and genes related to amino acid metabolism. SPS stands for Ssy1-Ptr3-Ssy5, where Ssy1 is an extracellular amino acid receptor⁴⁶, Ssy5 is a chymotrypsin-like endoprotease. Ptr3 is a phosphoprotein that acts as an adaptor for Ssy1 and Ssy5 is a chymotrypsin-like endoprotease⁴⁷. When extracellular amino acids bind to Ssy1, it leads to conformational change and hyper-phosphorylation of Ptr3. Ultimately this activates the proteolytic activity of Ssy5, masking its active C-terminal catalytic domain from the N-terminal pro-domain⁴⁸. The Hyper-phosphorylation state

of Ptr3 is further positively regulated by two casein kinases Yck1, 2 and negatively regulated by SCF^{Grr1} E3 ubiquitin ligase and PP2A phosphatase^{49–51}. Stp1 and Stp2 are the two transcription factors responsible for inducing transcription of amino acid permeases genes, which are transcribed as inactive precursors^{49,52,53}. Due to the presence of cytoplasmic retention signals, Stp1,2 are sequestered in the cytoplasm and cannot enter the nucleus until they are processed. Even if a small part of inactive Stp1 and Stp2 reaches the nucleus, Asi1-3 proteins (present in the nucleus) bind to it and prevent its downstream action^{54,55}. The presence of extracellular amino acids activates proteolytic activity of Ssy5, which cleaves retention signals of Stp1 and Stp2⁴⁷. The small length Stp1 and Stp2 enter the nucleus, bind to the promoters, and induce expression of their target genes. Thus, Stp1-2 are key players in mediating the signal from extracellular amino acids to downstream, leading to expression of amino acid permeases on the plasma membrane, which in turn aids in importing these amino acids⁴⁸. The following figure 4 describes SPS mediated signalling in brief. It has also been shown that rapamycin-induced Stp1 degradation from the nucleus is mediated in Sit4 dependent manner⁵⁶. Thus, establishing that the SPS sensing system is linked to TOR signalling.

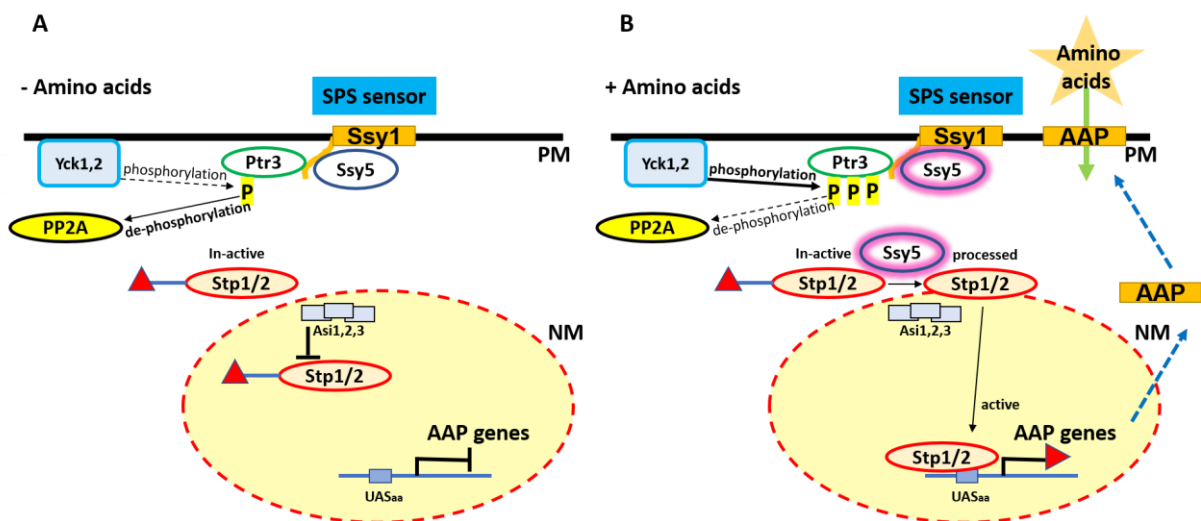


Figure 4: A schematic representation of SPS signalling in *S. cerevisiae*. SPS stands for Ssy1-Ptr3-Ssy5, where Ssy1 is the plasma membrane amino acid sensor, Ptr3 is a phosphoprotein, and Ssy5 is an endoprotease. Further, the activity of Ssy5 is enhanced due to hyperphosphorylation of Ptr3. P indicated by yellow highlighted colour represents the phosphorylation. The two casein kinases Yck1-2 and PP2A phosphatases are known to phosphorylate or dephosphorylate the Ptr3 respectively. **A:** In the absence of amino acids, Ptr3 is partially phosphorylated, and Ssy5 is inactive and cannot cleave the latent Stp1 and Stp2. Even if the full-length in-active Stp1 and Stp2 can escape to the nucleus, Whi1-3 proteins bind and inhibit its action. **B:** Binding of amino acids on Ssy1 leads to conformational changes and activation of Ssy5 protease, which cleaves and processes the in-active latent Stp1 and Stp2 to an active form, which enters the nucleus and binds to promoter regions of its target genes like AAP genes. Thus, inducing the expression of AAP on the plasma membrane and enhancing the import of amino acids. NM: nuclear membrane; PM: plasma membrane.

1.3.2 Role of Gcn4 mediated GAAC control

General Amino Acid Control (GAAC) is one of the classical examples of how a cell responds to different environmental stresses, for example, amino acid limitation by activation of Gcn2-Gcn4 mediated pathway⁵⁷⁻⁵⁹. Independent of which amino acid is limiting, induction of GAAC pathway leads to expression of several amino acid biosynthetic genes⁶⁰. In brief, GAAC functions in three steps: first, activation of Gcn2 kinase by uncharged tRNAs; second induction and stable expression of Gcn4 mRNA; and last, Gcn4 induced gene expression of several downstream targets, mainly amino acid biosynthetic genes⁶¹.

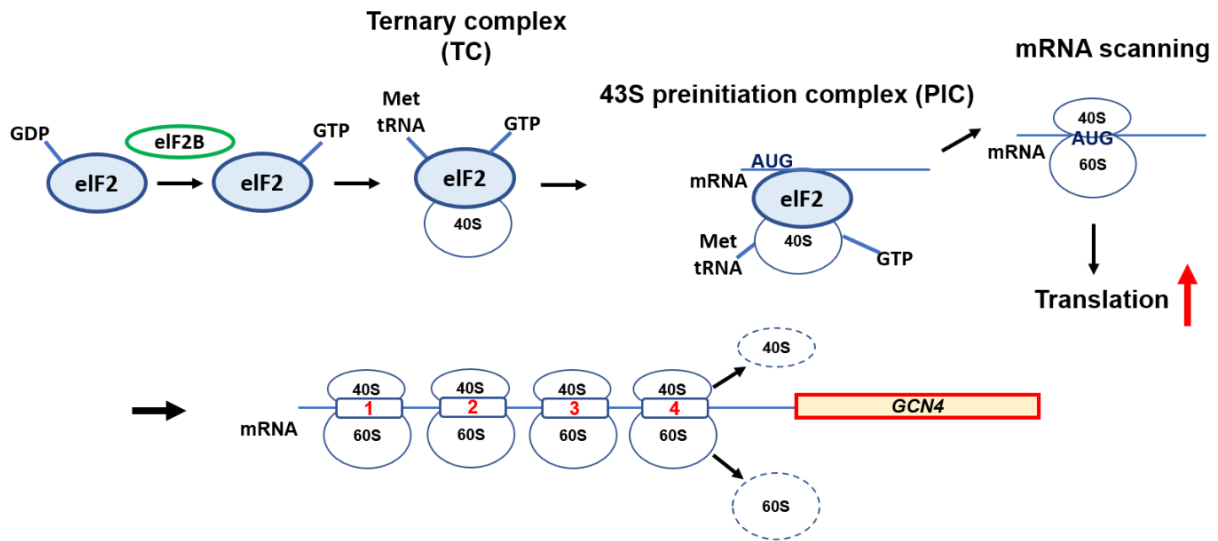
Gcn4 (General control non-depressible 4), a highly conserved protein belonging to the leucine zipper family of proteins, is a master transcription regulator of amino acid biosynthetic genes in *S. cerevisiae*⁶². Unlike its mammalian analogue Atf4⁶³, induction of Gcn4 in environmental stress and amino acids starved conditions decreases global protein synthesis capacity⁶⁴ and increases the lifespan of a yeast cell⁶⁵. However, the mechanism is still unclear as to how Gcn4 mediated signalling contributes to cell's longevity via diminished protein synthesis⁶⁴, depletion of 60S ribosomal subunits⁶⁶ and activating various amino acids biosynthesis pathway⁶⁰. In amino acid starved conditions, induction of amino acid biosynthetic genes depends on transcriptional regulator Gcn4, which operates via binding at upstream activating sequence elements located in promoter regions of its target genes⁶⁷.

Translational control of *GCN4* mRNA abundance is well characterized. In normal growth conditions, eIF2B stimulates and activates eIF2 (GTP bound, active) through its GEF activity⁶⁸. Further, eIF2B (GTP bound) associates with charged methionyl initiator tRNA and forms a tertiary complex (TC). This TC associates with the 40S small ribosomal subunit and other eIFs, which together are also known as 43S preinitiation complex (PIC)^{68,69}. The PIC further scans mRNA and recruits the larger 60S ribosomal subunit when it encounters the AUG start codon and thus leads to initiation of translation⁶⁹. *GCN4* mRNA is preceded by four upstream open reading frames (uORFs) located at its 5' UTR region, which prevents its translation by blocking the arrival of ribosomal machinery at *GCN4* mRNA and thus limiting Gcn4 abundance. Upon nutrient depletion (glucose or purines) or stress conditions such as amino acid starvation. Gcn2 kinase gets dephosphorylated and activated due to increased uncharged tRNA^{70,71} or TOR inactivation⁷². Active Gcn2 subsequently phosphorylates and inactivates its only substrate- alpha subunit of elongation factor 2 (eIF2 α), which binds more tightly to eIF2B upon phosphorylation and is sequestered mainly in GDP bound inactive state. This leads to a massive drop in TC formation, thereby inhibiting the global protein synthesis and reducing the consumption of amino acids⁶⁰. Lack of availability of TC further favours scanning of *GCN4* ORF over the uORFs region. Gcn4 subsequently enters the nucleus, binds at UAS elements of its target genes and thus enhances their transcription⁴⁸. Abundance of *GCN4* mRNA in the cell is tightly controlled by both translational control mechanisms, proteasomal degradation mediated by phosphorylation and ubiquitylation. Rawal et al. showed that two cyclin-dependent kinases: Srb10/Cdk8 and Pho85, are known to phosphorylate the activation domain of Gcn4, ultimately targeting it for proteasomal degradation in non-starving growth conditions. Srb10 or Cdk8 is known to remove the inactive Gcn4 species which

are enriched for SUMOylation in the promoter regions. Pho85 is responsible for clearing the highly active unsumoylated along with the defective Gcn4 species⁷³.

Gcn4 expression in response to amino acid starved conditions induces transcription of 539 genes, which are known to perform varied functions such as nitrogen utilization, gene expression and downstream signalling and out of which only 57 genes belong to amino acid biosynthetic pathways^{60,74,75}. Gcn4 induction is also reported to occur even under depletion of single amino acid⁷⁴. This is a good example of crosstalk among different pathways in response to stress conditions. Expression of Gcn4, in response to stress conditions, is known to exert its transcriptional role via five different levels^{60,62}. First, induction of biosynthetic pathways of 19 amino acids, with cysteine as an exception, where formation of intermediates from serine and homocysteine synthesis contributes to cysteine synthesis. Second, it activates the transcription of different genes involved in synthesizing vitamins, amino acid permeases, mitochondrial carrier proteins, peroxisomal proteins, and purines that indirectly contribute to amino acid biosynthesis. Third, it represses translation of certain transcriptional factors and ribosomal proteins, leading to reduced global protein synthesis, supporting the growth of cells in amino acid starved conditions. Fourth, it induces the expression of certain genes that are fundamental for the processes of autophagy and glycogen accumulation. Last, Gcn4 mediated transcription further enhances stress responses operating at different levels in the cell.

A Presence of amino acids or non-starved conditions



B Absence of amino acids or starved conditions

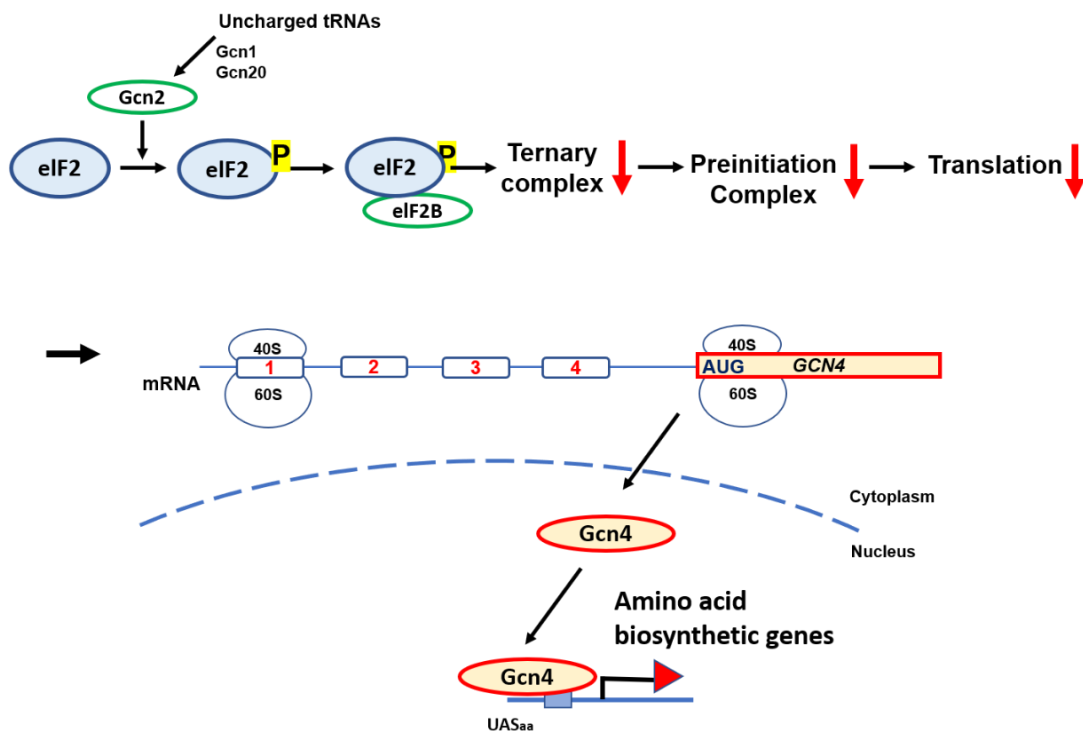


Figure 5: Mechanism of Gcn4 translation in response to amino acids. Gcn4 mRNA is preceded by four uORFs in the 5' UTR region, which prevents the arrival of ribosomal machinery on Gcn4 mRNA. Thus, controlling the translation rate and abundance of Gcn4 in the cell. **A:** In the presence of amino acids or non-starved conditions equivalent to normal growth conditions, eIF2B stimulates the eukaryotic translation initiation factor eIF2 with its GEF activity, which forms a ternary complex (TC) in association with Met-tRNA. TC gets associated with the 40S and 60S ribosomal units, forming a functional ribosome, and starts scanning the mRNA. Since the four uORFs halt and controls the translation rates, the abundance of Gcn4 is very limited. **B:** In the absence of amino acids or starved conditions, the presence of

uncharged tRNA's increases, which further stimulates Gcn2 kinase, which phosphorylates eIF2 such that it gets bounded to eIF2B very tightly. This eIF2-GDP-eIF2B complex leads to a rapid decrease in TC levels and global protein synthesis in the cell. When the TC levels are dropped, the ribosomes can reach now the Gcn4 mRNA and translate it efficiently to protein. The newly synthesized Gcn4 transcription factor further binds to promoter regions and stimulates the expression of amino acids biosynthetic genes.

1.4 Amino acid permeases/transporters

S. cerevisiae is known to express 24 amino acid permeases or transporters (AAP or AAT respectively), which are specialized to import either some or several amino acids at different rates⁷⁶. AAT contains twelve transmembrane domains and cytoplasmic oriented N and C terminal^{77,78}. Based on their regulation and expression conditions, AAP in yeast is broadly divided into two subfamilies⁷⁹. One that are expressed constitutively at the plasma membrane, and the other that is known to be expressed highly under nitrogen starved conditions. The former category includes Aat1, Aat2, Agp1, Bap2 etc. The latter category of AAPs includes Gap1, Put4, that scavenge extracellular amino acids more efficiently and support the growth of the cell⁸⁰. Thus, under nutrient-depleted or nitrogen starved conditions, Gap1 and Put4 are targeted to the plasma membrane to actively uptake amino acids. Likewise, when nutrients are replenished, these amino acid transporters are ubiquitinated and targeted for vacuolar degradation⁸¹.

Table 1: Amino acid transporters and transported substrates. The values mentioned in the brackets indicate the respective Michaelis constants (K_m) of the individual amino acids. The table is directly adapted from Ruiz et al. 2020⁸².

Transporters	Transported substrates
Agp1	His, Asp, Glu, Ser, Thr, Asn (0.29 mM), Gln (0.79 mM), Cys, Gly, Pro, Ala, Val, Ile (0.6 mM), Leu (0.16 mM), Met, Phe (0.6 mM), Tyr, Trp
Bap2	Cys, Ala, Val, Ile, Leu (37 μ M), Met, Phe, Tyr, Trp
Can1	His, Arg (10–20 μ M), Lys (150–250 μ M), Orn
Dip5	Glu (48 μ M), Asp (56 μ M), Ser, Asn, Gln, Gly, Ala
Gnp1	Ser, Thr, Asn, Gln (0.59 mM), Cys, Pro, Leu, Met
Lyp1	Lys (10–25 μ M), Met
Put4	Gly, Pro, Ala
Tat2	Gly, Ala, Phe, Tyr, Trp, Cys

1.4.1 Regulation of AAT

The amino acid permeases or transporters are subjected to a tight regulation at the gene transcription level or during intracellular trafficking and transport to the plasma membrane and lastly by its intrinsic activity⁴⁸. The expression of these AATs is highly dependent on extracellular amino acids (quality of nitrogen source) and is mediated by

SPS signalling. In the absence of nitrogen sources, transcription of AAT genes is activated⁴⁸. The transporters are co-translationally transported to the endoplasmic reticulum first, where they are further processed and modified. Further, these AATs are targeted to the plasma membrane via Golgi apparatus⁷⁷. Once normal growth conditions (good nitrogen source) are restored and the PM localized AATs are not required anymore, AATs are internalized by the arrestin-like adaptor proteins Bul1 and Bul2^{83,84}. These internalized transporters are ubiquitylated by HECT family ubiquitin ligase- Rsp5 and are ultimately targeted for vacuolar degradation via multivesicular body pathway⁸⁵⁻⁸⁷. Moreover, the Golgi-located newly synthesized transporters are ubiquitylated, translocated and degraded in the vacuole⁴⁸.

There are several studies that describe regulation of different permeases in presence of different substrates. Regulation of Gap1 permease is one of the best-studied examples and is explained briefly in the following section.

1.4.2 Role of Gap1 in amino acids starved condition

Gap1 permease belongs to the high-affinity broad permeases that can transport most of the amino acids⁸⁸. Gap1 permease is also known as a transceptor, meaning while transporting amino acids across the PM, it also senses and detects the abundance of amino acids that can further regulate its expression and activity^{89,90}. Gap1 is also studied for its function to mediate the signals downstream to the PKA pathway⁹¹ and elucidate the mechanism of how membrane transporters are trafficked and regulated at different levels in response to various stimuli in a yeast cell⁸³. Under amino acids starved conditions or non-preferred nitrogen sources, its expression is positively or negatively regulated by Gln3p, Gat1p and Ure2p transcription factors, respectively⁴⁸. In the presence of poor nitrogen sources such as urea and proline, Gap1 is not ubiquitylated and is sorted to the plasma membrane with high activity. Since Arrestin-like adaptor proteins, Bul1 and Bul2 (that mediate the ubiquitylation and targeting of Gap1 for vacuolar degradation) are phosphorylated and inactivated by Npr1 kinase, they further get associated to 14-3-3 proteins in the phosphorylated stage⁸³.

Conversely, in the presence of amino acids or preferred nitrogen source growth conditions (such as ammonium), the active Tor1 kinase phosphorylates and inactivates Npr1 kinase, leading to dephosphorylation and concomitant activation of Bul1 and Bul2 proteins^{92,93}. The dephosphorylated Bul1 proteins get disassociated from 14-3-3 proteins and ubiquitinate the Gap1 permease (at Lys9 and Lys16 residue) in Rsp5 dependent manner⁹⁴. Further, this polyubiquitylated Gap1 is endocytosed and targeted to the vacuole for degradation. However, when TORC1 activity is inhibited due to certain stress factors or presence of rapamycin, the arrestin proteins Aly1 and Aly2, together with Bul1 and Bul2, ubiquitylate and further downregulate the Gap1^{83,95}. These Bul1 and Bul2 arrestin proteins might still be in phosphorylated and bound to 14-3-3 and might target the ubiquitinated Gap1 via C-terminal for vacuolar degradation, indicating that they undergo different mechanisms to assist the Rsp5 mediated ubiquitinylation of Gap1 when TORC1 is active or in-active in response to different stimulus. Therefore, mutations in genes that help the ubiquitination of Gap1 leads to stable sorting of Gap1 on the plasma membrane. Further, it was shown that

ubiquitylation-mediated endocytosis of permeases like Gap1 and Can1 happen due to the signalling mediated by their transport-associated proteins instead of the pre-assumed idea of intracellular accumulation of their respective transport substrates (amino acids)^{83,94}.

1.5 Cross talk between TOR signalling and amino acids

1.5.1 TOR activation in *S. cerevisiae*

First discovered in budding yeast *S. cerevisiae*, the target of rapamycin (TOR), a serine-threonine kinase, is the master regulator of eukaryotic cell growth. It quickly responds to nutrients, promotes anabolic activities (protein, lipid, and nucleotide synthesis), and inhibits catabolic activities (autophagy), leading to an increase in the cell size. Its mammalian counterpart, the mechanistic target of rapamycin (mTOR), also contributes to cellular and organismal growth. The de-regulation of this pathway is known to cause various human pathologies, including cancer, diabetes, and obesity. Therefore, (m)TOR pathway has been of active interest for researchers over the decades^{96,97}.

S. cerevisiae, unlike all other eukaryotes, consists of two TOR kinases: Tor1 and Tor2, which are 67 % identical to each other and 37% to mTOR in terms of sequence similarity⁹⁸. TOR pathway comprises of two structurally and functionally distinct multi-protein complexes: TORC1 and TORC2, where TORC1 is rapamycin-sensitive and comprises either Tor1 or Tor2 kinase, Kog1, Lst8 and Tco89 subunits. TORC2 is rapamycin-insensitive and comprises Tor2 kinase, Avo1-3, Bit61 and Lst8 subunits⁴⁸. Upon inactivation of TORC1, cellular activities such as protein synthesis, ribosomes biogenesis, transcription, cell cycle, autophagy, and nutrient uptake are highly affected^{96,99}. Cellular activities such as lipid synthesis, endocytosis, actin cytoskeleton organization and cell viability are impacted upon TORC2 inactivation. Unlike in mammals, TORC1 in yeast is already tethered to the vacuolar membrane with the help of Ego1-3, which is known as EGO tertiary complex (EGOC)¹⁰⁰. Its activity is mediated by Gtr1 and Gtr2, which are the Ras family GTPases. In nutrient-rich conditions, such as in the presence of preferable nitrogen sources-glutamine and glutamate or other amino acids (especially leucine or arginine), GTP-bound Gtr1 heterodimerizes with GDP-bound Gtr2 and stimulates TORC1^{101,102}. Active TORC1 further exerts its downstream signalling by phosphorylating and activating Sch9 and Tap42 kinases^{96,103}. Once activated, Sch9 kinase promotes ribosome biogenesis and translation initiation, and Tap42 inhibits protein phosphatases, namely Sit4, PP2A, respectively. Secondly, this also reinforces hyperphosphorylation of Ure2 protein and subsequently sequestering of Gln3 and Gat1 in the cytoplasm and causing repression of NCR (nitrogen catabolite repression) and stress-responsive genes¹⁰⁴. Thirdly, TORC1 dependent phosphorylation of Mks1 bounded to Bmh1 prevents nuclear localization of transcription factors Rtg1 and Rtg3 and thus inhibiting retrograde RTG signalling pathway and synthesis of glutamate and glutamine by TCA cycle¹⁰⁵. Fourthly, phosphorylation and inactivation of Npr1 via TORC1 activity lead to Bul1-

mediated endocytosis of Gap1 and stabilization of specific amino acid permeases like Tat2 on the plasma membrane⁸³.

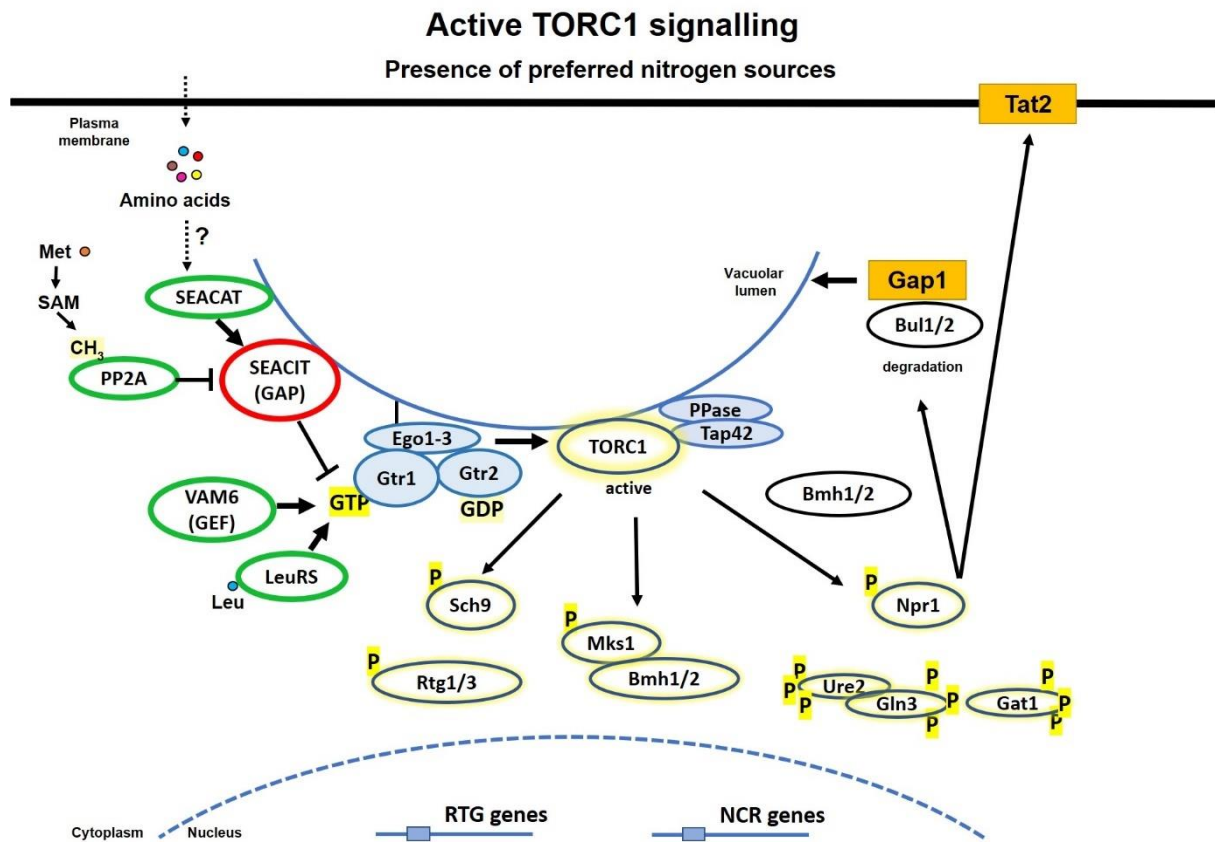


Figure 6: Mechanism of TORC1 signalling in response to preferred nitrogen sources. The presence of preferred nitrogen sources in the medium like glutamate or glutamine, leads to transcriptional repression of genes responsible for the metabolism of less preferred nitrogen sources, commonly known as nitrogen catabolite repression (NCR), by hyperphosphorylation and retention of transcriptional factors like Ure2, Gln3, and Gat1 in the cytoplasm. Also, the presence of glutamine or amino acids stimulates the vacuolar membrane-associated EGO complex, which consists of regulator proteins Ego1,3 and Ras GTPases: GTP bound Gtr1, and GDP bound Gtr2. The guanine nucleotide exchange factors (GEF's): Vam6 and Leu tRNA synthetase (LeuRS), stimulates the activity of Gtr1 by the GTP loading of Gtr1 is also negatively affected by the GAP activity of SEACIT complex, further activity of SEACIT is impacted by SEACAT and type 2 phosphatases. The stimulated EGO complex gets associated with and activates the vacuolar membrane located TORC1 complex. The active Tor1 kinase further phosphorylates its downstream targets like Sch9 kinase, Mks1, Rtg1-3, Npr1, and Tap42, where the latter inactivates several downstream phosphatases. Thus, transcriptional factors like Ure2, Gln3 and Gat1 can no longer be dephosphorylated and sequestered in the cytoplasm, along with Rtg1-3, in the hyperphosphorylated state. Phosphorylation of Npr1 also inactivates it and leads to increased expression of Tat2 permease on the plasma membrane and mediates vacuolar targeting and subsequent degradation of general amino acid permease Gap1. Conversely, in the presence of the non-preferred nitrogen sources, SEACIT complex stimulates the GDP loading of Gtr1 and thus inactivates the EGOs and subsequently cannot activate the TORC1, which leads to cytoplasmic release and activation of Tap42-phosphatase protein complex. The active phosphatases dephosphorylate the cytoplasmic Mks1, Ure2, Gln3, and Gat1 proteins. The former and the latter two lead to nuclear localisation Rtg1-3 and Gln3

and Gat1, respectively, and subsequent activation and expression of genes related to RTG and NCR signalling. RTG signalling promotes the synthesis of glutamate and glutamine via the TCA cycle, and NCR signalling promotes the synthesis of genes involved in the metabolism of non-preferred nitrogen sources. Also, the phosphatases de-phosphorylates and activate Npr1, where it phosphorylates the Bul1/2 proteins which get associated with Bmh1/2 proteins, leading to stable expression of Gap1 permease on the plasma membrane. The components which affect positively or negatively the activity of TORC1 are represented by green and red colour, respectively. The transcriptional factors whose activity gets affected by active TORC1 are represented by yellow colour. (Adapted and modified from Conrad et al. ⁴⁸).

1.5.2 TOR signalling under the light of amino acids

Several studies report different ways through which the activity of the EGO complex is affected in the presence of amino acids (mainly by leucine and arginine in mammals and leucine and glutamine in yeasts). As a key to TORC1 activation, the amino acids are known to bind and affect the guanine nucleotide-binding state of RagA-RagB/Gtr1⁴⁸.

In yeast, leucine seems to affect the TORC1 activity strongly, firstly by positively affecting the activity of Vam6 or Vps39, which is known to be the guanine nucleotide exchange factor of Gtr1¹⁰⁰. Secondly, the non-essential amino acid editing domain of the Cdc60: the leucyl-tRNA synthetase (LeuRS), is also reported to bind and interact with the yeast Gtr1 in leucine dependent manner¹⁰⁶, thus making this interaction necessary for TORC1 activation in response to leucine availability¹⁰⁶. Thirdly, it has been reported that amino acid limitation induces the transient interaction of Iml1, which is a component of SEACIT (SEAC subcomplex inhibiting TORC1 signalling) complex along with the protein subunits Npr2 and Npr3, and Gtr1 at the vacuolar membrane. This interaction activates the GAP activity of Iml1 towards GTP bound Gtr1, thus inactivating the TORC1 activity^{107,108}. This GAP activity of the SEACIT complex (or the GATOR1 complex in mammals) acting towards the GTP bound Gtr1 (or RagA/RagB in mammals), is conserved from yeast to humans¹⁰⁹. Furthermore, the Seh1-associated complex (SEAC) complex, which is also known as SEAC activating the TORC1 signalling (SEACAT), influences the activity of SEACIT complex by inhibiting it and hence positively regulates the TOR signalling^{107,108}. In mammals, leucine binds to its cytoplasmic sensor, Sestrin2, leading to its disassociation from GATOR2, thus causing the free GATOR2 to interact and inhibit GATOR1. Thus, leading to translocation of mTORC1 to lysosomes and its subsequent activation. However, the budding yeast lacks orthologues of Sestrin proteins¹¹⁰. Additionally, Whi2 has been shown to interact with plasma membrane phosphatases Psr1-2 and inhibit the TORC1 mediated signalling in the presence of low amino acid conditions (mainly leucine)¹¹¹. Although, the mechanism remains elusive.

Glutamine is known to be the preferred nitrogen substrate for the growth of the cell. It is converted to glutamate and α -ketoglutarate via the action of glutaminase (GLS) and glutamate dehydrogenase (GDH), respectively, where GDH requires leucine as a cofactor. In mammals, α -ketoglutarate further activates RagA/B via the action of prolyl hydroxylase (PHD). Though PHDs are known to be conserved from mammals to yeast, there is no evidence available in the literature so far depicting whether yeast PHDs are

also capable of activating Gtr1¹¹⁰. However, how the presence of glutamine activates the mTORC1 in a Rag/Gtr1 independent manner, remains elusive.

The lysosomal transmembrane protein-SLC38A9 has been characterized and proposed as the arginine transporter in lysosomes that affects mTORC1 activity in an arginine-dependent fashion^{112,113}. However, there is no evidence for the most closely related yeast homologues of SLC38A9 so far- the amino acid vacuolar transporters, Avt1-7, whether they also regulate TORC1 activity or not^{110,114}. Additionally, there are studies reporting the presence of cytoplasmic arginine sensors in mammals: the CASTOR1 and CASTOR2 proteins that bind to arginine similar to leucine binding to Sestrin2. Arginine binds to homo-dimers of CASTOR1 or heterodimer of CASTOR1 and CASTOR2 and disrupts its disassociation with GATOR2¹¹⁰. This leads to translocation and activation of mTORC1, similarly to the Sestrin2 mechanism.

Sutter and his colleagues showed that methionine is also known to activate the Gtr1 in S-adenosylmethionine (SAM) dependent manner, which is a methyl donor. Synthesis of SAM inhibits autophagy and leads to methylation and subsequent activation of the type 2A protein phosphatase PP2A via the action of the methyltransferase Ppm1p. The activated methylated PP2A dephosphorylates and inactivates the Npr2 kinase, which is a component of SEACIT complex, and thus eventually activates the TORC1 signalling¹¹⁵.

1.6 Aminoacidopathies

Aminoacidopathy, also known as inborn error of amino acid metabolism, is a term used to collectively refer to the various inherited disorders or syndromes caused by impaired enzymatic activity associated with amino acid metabolism or transport within the cell. This, results in either accumulation of amino acid(s) or its by-product that further affects several downstream signalling pathways and organ functions¹¹⁶. Nowadays, 1 out of 1000 people is reported to suffer from amino acid-related disorders. They are sub-grouped as organic acidurias, urea cycle related disorders and aminoacidopathies, where the latter comprises all the remaining amino acid-related disorders³. The most common aminoacidopathies include phenylketonuria, maple syrup urine disease (MSUD), homocystinuria, argininosuccinic aciduria, and tyrosinemia type 1. Depending on the age upon onset of the disease or the degree of the defect in related enzymatic function, the resulting clinical symptoms vary from individual to individual. People affected by such disorders are usually treated with special diets either restricted to natural protein content or combined with an exclusive protein diet that excludes the amino acid that has detrimental effects. Also, diet supplementing the essential amino acids due to loss of enzymatic activity, is one treatment prescribed frequently^{117,118}. Since these disorders can also commence from the neonatal stage, screening of such conditions at neonatal stage and in newborn babies (4-7 days old) is widely adopted worldwide. For detailed understanding of clinical symptoms, outcomes, and current therapeutic approaches for these aminoacidopathies, one can refer to the article "Disorders of branched-chain amino acid metabolism" by Manoli et al.¹¹⁹.

1.6.1 Organic acidurias

Individuals suffering from organic acidurias tend to accumulate carboxylic acids (mono, di or tri) in their blood (or excreted with abnormal levels in urine) along with corresponding metabolites such as coenzyme A, carnitine with or without glycine esters that are also proven to be toxic when they exceed a particular threshold limit¹²⁰. Most studied organic acid metabolic disorders include propionic acidemia, methylmalonic acidemia (methylmalonyl-CoA mutase deficiency), isovaleric acidemia, beta-ketothiolase deficiency, 3-methylcrotonyl-CoA carboxylase deficiency, 3-hydroxy-3-methylglutaric aciduria, holocarboxylase synthase deficiency, and glutaric acidemia type 1.

1.6.2 Urea cycle related disorders

Individual affected by Urea cycle disorders generally can be deficient (or have mutations) in any of the enzymes related to the urea cycle. Here, nitrogen is not able to convert into urea, leading to the accumulation of ammonia, beyond a permissive level causing to brain damage, coma or in extreme cases death. The disorders are also named according to the deficient enzymes of the urea cycle, such as ornithine transcarbamylase (OTC), argininosuccinic acid synthetase or citrullinemia, arginase, argininosuccinase acid lyase or argininosuccinic aciduria, carbamoyl phosphate synthetase, and N-acetylglutamate synthetase. OTC is a sex chromosome-linked disorder and the treatment strategy focuses on reducing the exposure of highly toxic ammonia in the brain¹²¹.

1.6.3 BCaa related pathologies

Overview of the biochemical pathway for BCaa's catabolism is represented in figure 7. The subsequent aminoacidopathies resulting from loss of the particular enzymatic function from the BCaa's catabolism pathway include: maple syrup urine disease, isovaleric acidemia, 3-methylcrotonyl-CoA carboxylase deficiency, 3-hydroxyisobutyric aciduria, methylmalonic semialdehyde dehydrogenase deficiency, propionic acidemia, methylmalonic acidemia, 3-methylglutaconic aciduria, 3-hydroxy-3-methylglutaryl-CoA lyase deficiency, 2-methyl-3-hydroxyisobutyric aciduria, isobutyryl-CoA dehydrogenase deficiency, and 3-hydroxyisobutyryl-CoA deacylase deficiency¹²².

Out of all described BCaa aminoacidopathies, MSUD is the only disorder that can be easily diagnosed (using plasma of the affected individuals) since it is caused due to loss (or reduced) of branched-chain alpha-keto-dehydrogenase (BCKDH) activity, leading to detectable accumulation of BCaa (primary leucine) and their respective keto acids¹²³.

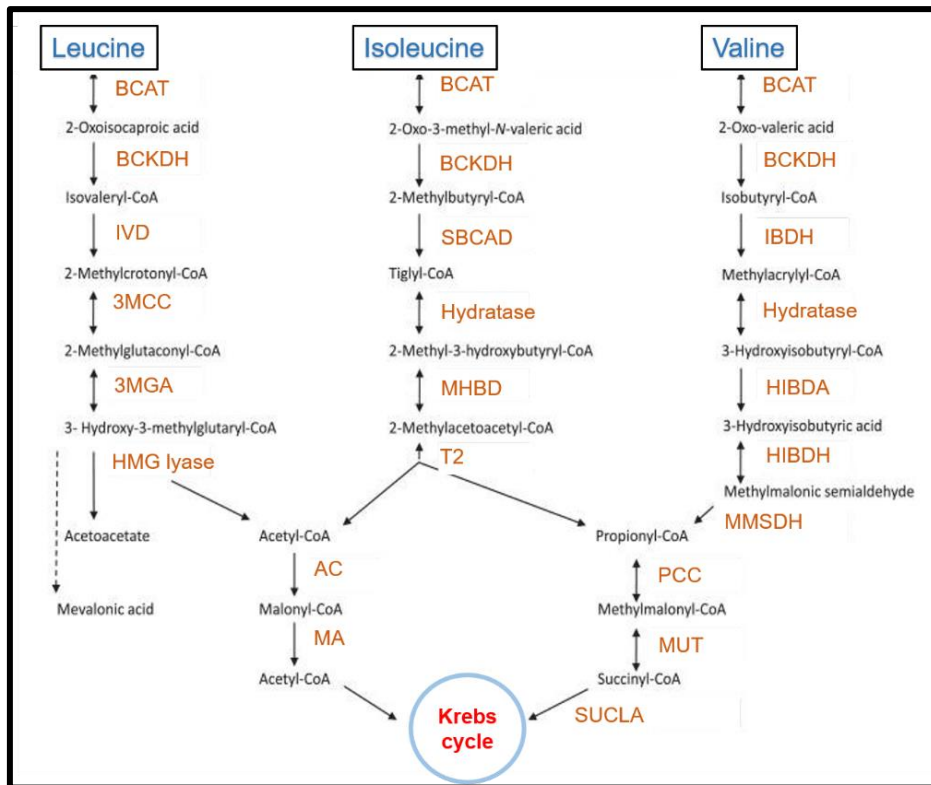


Figure 7: Branched-chain amino acids' catabolism pathway in humans. Enzymes (represented in maroon colour) catalyzing the production of different intermediates are: BCAT: branched-chain amino acid aminotransferase; BCKDH: branched-chain alpha-keto-dehydrogenase; IVD.: isovaleryl dehydrogenase; 3MCC: 3-methylcrotonyl-CoA carboxylase; 3MGA: 3-methylglutaconic-CoA hydratase; HMG lyase: 3-hydroxy-3-methyl glutaryl-CoA lyase; SBCAD: methylbutyryl CoA dehydrogenase; MHBD: 2-methyl-3-hydroxyisobutyric acid dehydrogenase; T2 or BKT: mitochondrial acetoacetyl-CoA thiolase; IBDH: isobutyryl-CoA dehydrogenase; HIBDA: 3-hydroxyisobutyryl-CoA deacylase (hydrolase); HIBDH: 3-hydroxyisobutyrate dehydrogenase; MMSHD: methylmalonic semialdehyde; PCC: propionyl-CoA carboxylase; MUT: methylmalonyl-CoA mutase; SUCLA: succinyl-CoA ligase. This figure is adapted from Manoli et al. 2016¹¹⁹.

Maple Syrup Urine Disease

MSUD is a rare autosomal recessive metabolic disorder¹¹⁹. As the name suggests, urine in the affected infants (with chronic infection) has a peculiar sweet maple syrup odour¹²³. It is reported to affect nearly 1:185,000 infants worldwide¹²⁴ and 1:200,000 infants in the United States. Whereas its occurrence rate is relatively higher in Mennonite populations, with a frequency of 1:350 live births; in the Ashkenazi Jewish population, it is estimated to be 1:26,000¹²⁵, and in the Galician population of Spain with a frequency of 1:52,500 births¹²⁶. This clinical condition arises due to missing activity (or incomplete) of branched chain alpha-keto dehydrogenase (BCKDH) enzyme complex, which catalyzes the second step in the BCaa catabolism pathway. This, leads to accumulation of leucine, isoleucine, valine and their respective alpha-keto acids in the blood of affected infants¹²⁷.

In the mitochondria of skeletal muscle cells, kidney, liver, and brain tissues, the BCaa leucine, isoleucine and valine are reversibly converted to KIC, KMV and KIV respectively, by aminotransferases (BCAT), with the formation of glutamate from alpha keto-glutarate (fig: 8). Further, these alpha-keto acids are catalyzed by branched-chain alpha-keto dehydrogenase enzyme complex (BCKDH) to isovaleryl, or isobutyryl Co-A, which are degraded to acetyl Co-A and intermediates, and fed to Kreb's cycle¹²⁸. The BCKDH is located in the inner mitochondrial membrane along with pyruvate dehydrogenase and alpha-keto dehydrogenase in a super complex. It consists of E1: alpha-keto dehydrogenase (α and β), E2: dihydrolipoyl transacylase, and E3: dihydrolipoamide dehydrogenase subunits^{119,123}. Its activity is further reported to be tightly regulated by BCKDH phosphatase and kinase. E1 decarboxylates alpha-keto acids in the presence of thiamine pyrophosphate, E2 catalyzes the transfer of acyl group from E1 to CoA and E3 re-oxidizes and regenerates the lipoic acid residue of E2, using FAD as a cofactor. E1 α , E1 β and E2 enzymes are encoded by BCKDHA, BCKDHB and DBT genes, respectively.

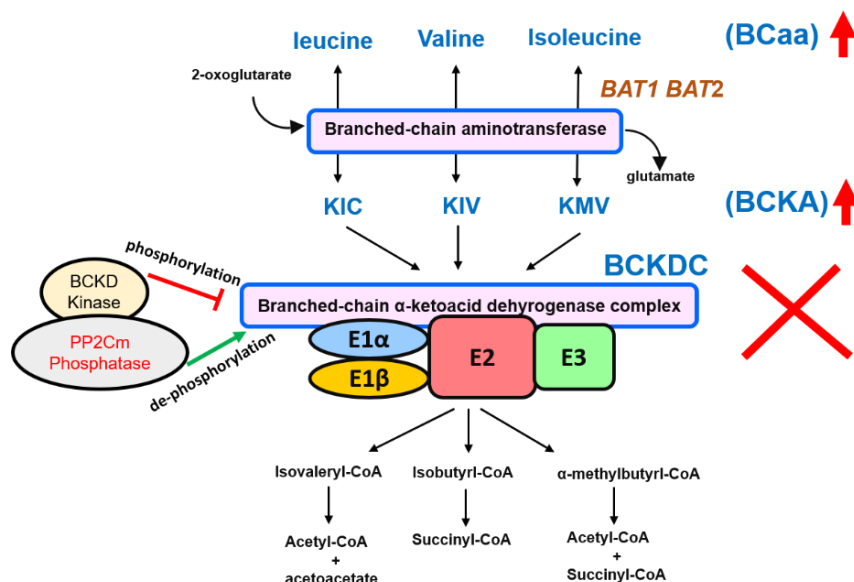


Figure 8: Overview of human branched-chain amino acids' catabolism. Deficiency in the activity of BCKDH leads to accumulation of BCaa, i.e., leucine, valine, and isoleucine, and their α -keto acids KIC, KIV and KMV, respectively. The activity of BCKDHC is further known to be regulated negatively and positively by phosphorylation and de-phosphorylation mediated by BCKD kinase and PP2Cm phosphatase, respectively. BCAT: branched-chain amino acid aminotransferase; BCKDHC: branched-chain alpha-keto-dehydrogenase complex. This figure was modified from Blackburn et al., 2017¹²⁸.

MSUD is classified as the classic, intermediate, intermittent, thiamine responsive and E3 deficient depending upon the residual activity of BCKDH. In the classical (severe) form of MSUD, with less than 2% of residual activity of BCKDH, the BCaa and their α -keto acids levels are reported to increase abnormally in the blood of asymptomatic infants immediately after a few hours of their birth. If not treated immediately, the early

symptoms begin with irritability, anorexia, lethargy, encephalopathy, and apnea to critical cerebral edema, coma, and central respiratory failure. The onset of remaining MSUD types: intermediate, intermittent and the thiamine responsive types is reported to be variable with 3 to 30%, 5 to 20%, and 2 to 40% of residual activity BCKDH, respectively¹²³.

The treatment options include first-aid like approaches to reduce or eliminate the branched-chain amino acids from the diet. Techniques such as peritoneal dialysis, exchange transfusions, and haemodialysis are possible but not recommended for infants. Positive results reported for MSUD management after administering balanced solutions (with minus BCaa formulations, electrolytes, and calories) intravenously or using very slow nasogastric drips to patients¹²⁷.

Patients suffering from MSUD have profound brain damage, but the underlying mechanism remains elusive¹²⁹. Several studies have been done on larvae of zebrafish and mice models to understand the neurological consequence of the disease. These studies report the presence of oxidative stress, brain energy deprivation, reduced antioxidants defences, decreased levels of glutamate, possibly contributing to aberrant CNS function^{6,130,131}. Also, high levels of lipid peroxidation and protein oxidation have been detected in the plasma of MSUD patients^{132,133}. In a study with C6 glioma cells, chemical induction of MSUD phenotype using 5 mM of BCaa(s) induced actin cytoskeleton re-organization causing reduction in GSH levels and increased NO production⁹. These findings increased our understanding of the underlying neurological impact in MSUD patients.

1.7 Branched-chain amino acids

Leucine, valine, and isoleucine are also called branched-chain amino acids (BCaa) since they have branched side chain (R group). Only archaeobacteria, eubacteria, fungi and plants can synthesize BCaa needed for growth^{134–138}. hence, they are also classified as essential amino acids for human beings and must be supplied in the diet^{40,41}. Since mammals cannot synthesize BCaa, the BCaa pathway genes serve as an attractive solution and are studied extensively as potential targets for drug development against fungal pathogens¹³⁹. During evolution, functions of the enzymes catalyzing different steps remained largely the same. However, localization, organization, compartmentalization, and regulation of the enzymes varied from organism to organism. For example, the BCaa pathway genes are organized in the form of operons in *E. coli*; in spinach, these genes are located in chloroplasts¹³⁷, whereas in yeast and other fungi¹⁴⁰, these genes are located on different chromosomes in the nucleus.

BCaa accounts for 14% of the total amino acids content in the skeletal muscles. When genes involved in the catabolism of BCaa are disrupted, it leads to various diseases in humans¹¹⁹, which were briefly described in the above section. Thus, the study of BCaa metabolism holds high importance in the scientific community.

1.7.1 BCaa synthesis in a yeast cell

The BCaa share the first few steps of their bio-synthesis pathway in the yeast cell, mainly the *Ilv2*, *Ilv5* and *Ilv3* catalyzed steps^{140,141}. Valine and isoleucine are synthesized in the mitochondria from two molecules of pyruvate and ketobutyrate, respectively¹⁴². The intermediates KIV or KMV can also be transported outside the mitochondria and transaminated to valine and isoleucine by *Bat2*¹⁴³. Inside the mitochondria, KIV is converted to α -IPM by the action of α -isopropyl malate synthase, encoded by *Leu4* and *Leu9*, and is further transported to the cytoplasm to convert into leucine¹⁴⁴. Also, KIV present in the cytoplasm can be converted to α -IPM by the short form of *Leu4p*, eventually forming leucine. In the absence of leucine in the medium, *Leu3* acts as a transcriptional activator of the BCaa synthesis pathway¹⁴⁵. In physiological or leucine replete conditions, the activation domain of *Leu3* is masked due to its intramolecular interactions and is present in the inactive state in the nucleus¹⁴⁶. The binding of α -IPM to *Leu3* leads to unmasking of its activation domain^{147,148}. This α -IPM-*leu3* complex further acts as a positive regulator for the expression of target genes: BCaa pathway genes (*ILV2*, *ILV5*, *LEU4*, *LEU1* and *LEU2*), ultimately leading to the synthesis of BCaa¹⁴⁹. The detailed synthesis mechanism of the BCaa in *S. cerevisiae* is depicted in figure 9.

The *LEU4* and *LEU9*, encoding the α -isopropyl malate synthase I and II, share 83% sequence similarity, where the former is known to account for 80% of the total α -isopropyl malate synthase activity in the wild-type yeast cell¹⁵⁰. Since *LEU4* mRNA contains two starting AUG codons, it is known to be translated in two versions, long and short (*l* and *s*), where *l* contains N-terminal mitochondrial targeting sequence (MTS) and thus is localized in the mitochondria and the *s* form devoid of the MTS is localized in the cytoplasm^{151,152}.

It is quite interesting to note that primarily leucine synthesis is compartmentalized in a yeast cell¹⁴⁴. There are many explanations available in the scientific literature regarding the compartmentalization of leucine biosynthesis in a yeast cell. Firstly, the first intermediates of leucine biosynthesis, KIV and acetyl-CoA, are primarily formed (and probably accumulated) in the mitochondria¹⁴², making it evident for α -IPM synthase I and II to be present in the mitochondria as well. Secondly, the presence of two isoforms of α -IPM synthase (*l* and *s*) is equally intriguing. It is speculated that under conditions like glucose repression, anaerobic growth conditions, where the yeast cells have few and poorly developed mitochondria¹⁵³, *Leu4l*, and *Leu9* might not be stable. The presence of *Leu4s* in the cytoplasm can easily overtake and suffice the α -IPM synthase activity and the cellular needs of leucine synthesis since other leucine biosynthetic enzymes are also located in the cytoplasm¹⁴⁴.

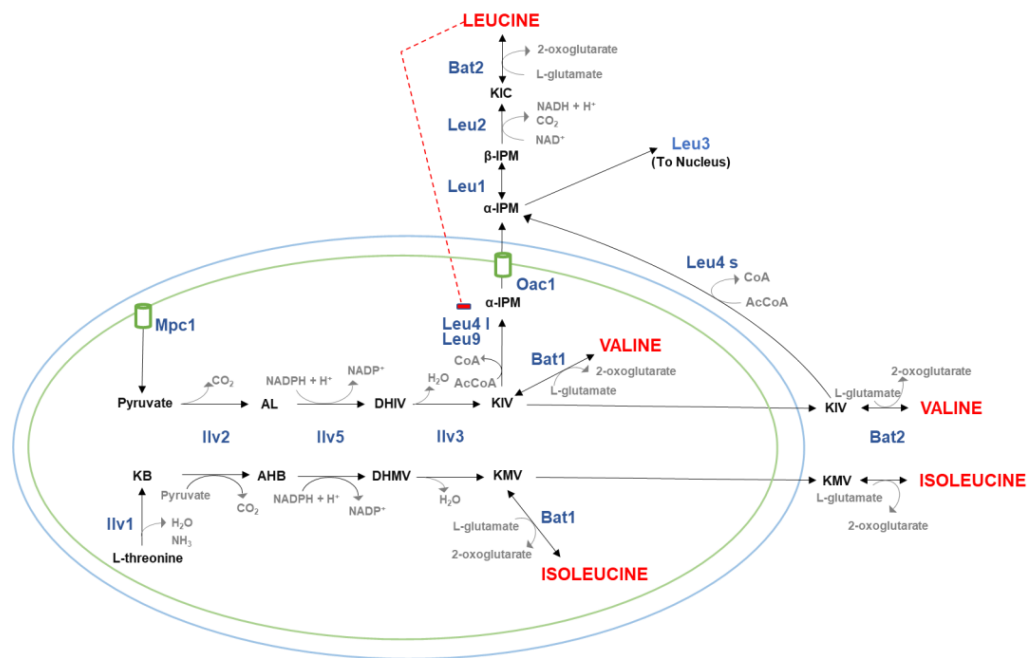


Figure 9: Schematic diagram showing the branched-chain amino acid biosynthetic pathway in *S. cerevisiae*. Leucine and valine are synthesized from pyruvate, and isoleucine is synthesized from ketobutyrate, derived from threonine. The intermediates KIV or KMV can be transported out of mitochondria and converted to valine and isoleucine, respectively. KIV can also be converted to α -IPM in the mitochondria, which is further converted to leucine in the cytoplasm. The blue coloured labelled are the enzymes that catalyze the different steps during the synthesis of the BCaa. The double arrow depicts that the respective enzymes Bat1 and Bat2 can catalyze the reaction in both directions. The enzymes and the intermediates involved and formed respectively, in the BCaa pathway are as follows: Ilv1: threonine deaminase, Ilv2: acetohydroxy acid synthase-catalytic subunit, Ilv5: acetohydroxy acid reductoisomerase, Ilv3: dihydroxy acid dehydratase, Bat1 and Bat2: mitochondrial and cytosolic branched-chain amino acid aminotransferases, Leu4 and Leu9: α -isopropyl malate synthase I and II respectively where I and s represent the long and the short form of Leu4, Leu1: α -isopropyl malate isomerase, Leu2: β -isopropyl malate dehydrogenase, AL: acetylacetyl-CoA, DHIV: α,β -dihydroxyisobutyrate, KB: α -ketobutyrate, AHB: α -aceto α -hydroxybutyrate, DHMV: α,β -dihydroxy β -methyl valerate, KIV: α -keto-isovalerate, KMV: α -keto β -methyl valerate, α -IPM: α -isopropyl malate, β -IPM: β -isopropyl malate and KIC: α -keto-isocaproate. Mpc1 and Oac1: mitochondrial pyruvate carrier and oxaloacetate carrier1 are the membrane transporters for pyruvate and α -IPM, respectively.

1.7.2 BCaa and Diabetes

The elevated blood plasma levels of BCaa and phenylalanine and tyrosine, aromatic amino acids, are predicted to be the early-biomarkers for type-2 diabetes (T2D) with more pronounced correlation found in men compared to women^{4,5,154}. The exact mechanism remains elusive but is investigated to be partly mediated via insulin resistance with ramifications such as hyperglycemia, oxidative stress and dyslipidaemia^{155–157}. Interestingly, a plant-based diet has shown tremendous results in decreasing the blood plasma levels of the BCaa compared to the animal protein-based diet in humans^{158–160}. Furthermore, intake of a low protein (LP) diet not only reduces the plasma BCaa levels but also promotes metabolic health and extends lifespan in mice when supplemented from an early development stage^{161–163}. Western diet, which

is rich in sugars, calories and saturated fats, is investigated to be linked with high rates of obesity and Type- 2 Diabetes (T2D). It is also shown that reducing the dietary levels of either total proteins (all amino acids) or specifically BCaa, can reverse the pathological conditions of the diet-induced obese mice by transiently inducing the expression of FGF21 (Fibroblast growth factor 21) and increasing the energy expenditure. This study strongly elicited that it was possible to circumvent the complications associated with metabolic diseases such as T2D by reducing the intake of the BCaa while maintaining adequate nutrition (without calorie restriction) in the diet¹⁶⁴. In conclusion, all these data indicate relevance of BCaa in sustaining metabolic health of an individual.

So far, many of the studies have investigated the physiological impact of the three BCaa. However, there is recent evidence emerging which states that the three BCaa might have different effects on the metabolic health of an individual. A recent study found that restricting the dietary valine and isoleucine content, but not leucine, is sufficient and necessary to recapitulate the beneficial effect of the LP-based diet to a diet-induced obesity mice model, where the latter has a more pronounced effect. They also found that increased content of isoleucine in the diet promotes increased body-mass index in humans, whereas restricting isoleucine in the diet promotes FGF21 expression, browning of the white adipose tissues and the energy expenditure¹⁶⁵.

1.8 Effect of auxotrophies in yeast research

There are several examples in the literature that talk about correlation between the growth phenotypes and the choice of auxotrophic marker used to delete the yeast gene. Meaning that the resulting phenotypes are mediated not due to abolishment of gene function *per se* but rather is dependent on the background of the antibiotic cassette or auxotrophic marker gene used to delete the gene¹⁶⁶. In the latter case, the secondary effects are usually caused by limitation of the auxotrophically required nutrients in the growth medium. For example, cells deleted for *ATH1*, the vacuolar acid trehalase, exhibited increased growth rate and biomass yields, which were not due to deletion of *ATH1* but rather due to introduction of *URA3* for generating the *ATH1* deletion strain¹⁶⁷. Further, in cells deleted for *PDA1*, the E1 α subunit of pyruvate dehydrogenase complex (PDH), along with the abolishment of PDH activity, the deletion strain had an increased rate of petite colonies (ρ^0) and experienced a slow growth rate which was rescued by increased leucine supplementation in the growth medium¹⁶⁸. When grown in the presence of 80 mg/mL of leucine concentration in the medium, leucine limited or auxotroph cells grew not only slower (arrested at late G1 cell cycle stage) but also exhibited altered cell and vacuolar morphology¹⁶⁹. It was also shown that the expression of *SPT15-300* dominant mutant allele in BY4741, the leucine auxotrophic yeast strain, enhanced its growth on the defined medium with low leucine levels and improved its ethanol tolerance compared to the wild type with *SPT15*. It was found to be associated with enhanced leucine uptake and or its utilisation^{170,171}. It was observed that the growth defect of *ero1-1 leu2* strain could be rescued by supplementing increased leucine concentration (180 mg/mL) in the synthetic growth medium or by transforming the strain with wild type *LEU2*¹⁷². Restoring the missing *LEU2* in strain background *leu2 Δ ura3 Δ his3 Δ* or *leu2 Δ ura3 Δ met15 Δ* , but not in strain background of *leu2 Δ ura3 Δ his3 Δ met15 Δ* ,

resulted in a positive effect on the growth rate of the auxotrophic strains¹⁷³. All these studies suggest that auxotrophic markers, especially leucine auxotrophy, have a profound impact on the growth of yeast cells in undefined medium conditions. Extreme precautions should be employed while designing/choosing growth medium to avoid the growth artefacts. The background differences due to auxotrophic markers have a profound impact on the gene expression and metabolism, where the genetic background affected 83% of the coding genome. They still retained a strong metabolic signature even though the normal growth rate is restored by enough supplementation of auxotrophically required nutrients¹⁷⁴. Rather prototrophic yeast strains should be employed instead of auxotrophic yeast strains to eliminate the biases in the metabolic and physiological studies until the auxotrophy is the subject of study^{173,175}.

Proteins account for 40% of the total dry cellular weight in a yeast cell, wherein leucine accounts for 10% of the total protein biomass¹⁷⁵. It is shown experimentally that at least a minimum concentration of 240 mg/mL leucine in the growth medium is required to support the growth (with maximum cell density) of *S. cerevisiae* leucine auxotrophs¹⁷⁶. Later Dijken et al. proposed to use nearly 25% extra amounts of experimentally derived concentrations of auxotrophically required nutrients to grow auxotrophic yeast cells in the synthetic growth medium. For example, 400 mg/mL of leucine must be supplemented in the growth medium for cultivating leucine auxotrophs to rule out the leucine limitation case and avoid non-specific results¹⁷⁷.

Effects of leucine auxotrophy have also been extensively studied. It is known that auxotrophic yeast strains grew slowly on synthetic complete (SC) medium (supplemented with 76 mg/L of all 20 amino acids) in comparison to YPD medium. Further, this growth phenotype could be rescued upon overexpression of *LEU2*, *BAP2* or *TAT1* genes in auxotrophic yeast cell¹⁷⁸. It was shown that defective leucine transport was the underlying cause for slow growth of auxotrophic strains, which could be overcome by either re-establishing functional leucine biosynthetic pathway or enhancing the leucine transport across the plasma membrane¹⁷⁸. Further, Gomes et al. showed that starvation of essential amino acids (the auxotrophy complementing amino acids) leads to the production of oxidative stress in *S. cerevisiae*, premature ageing phenotypes, shorter life span, and G2/M cell cycle arrest of cells with appearance of sub population with G0-G1 phase. The results indicated that cells experienced cell death possibly due to starvation of essential amino acids, especially leucine, which was successfully rescued by five times supplementation of the essential amino acids in the growth medium¹⁷⁹.

It is quite well established that different auxotrophies, particularly leucine auxotrophy, has a strong impact on the transcription and metabolism of the auxotrophs¹⁷⁴. In the current study, similar findings are observed where growth of BY4742 *S. cerevisiae* strain was severely impacted upon increase in the amino acid content in the growth medium. Further, this growth phenotype is rescued by either re-establishing the functional leucine biosynthetic pathway in BY4742 (leucine auxotroph) or increasing leucine in proportion to the increased amino acid content in the growth medium. Though, the initial findings spoke for the leucine limitation case underlying this observation. This assumption was also ruled out after studying the intracellular amino acids levels. Therefore, I decided to investigate the mechanistic underpinnings of this slow growth phenotype in detail as a part of my doctoral study.

1.9 Aim of the study

We observed that the growth of the lab wild type *S. cerevisiae* strain- BY4742 (MAT α his3 Δ 1 leu2 Δ 0 lys2 Δ 0 ura3 Δ 0) was impacted in response to increase in the total amino acid concentration in the growth medium. This fascinating observation intrigued me to study the molecular mechanistic basis underlying the slow growth phenotype as part of my doctoral study in more detail. The following objectives are addressed during this study.

- a) To investigate whether the observed amino acid dependent growth phenotype is common to all budding yeast strains.
- b) To investigate whether the auxotrophic background of the yeast strain is relevant for this growth phenotype.
- c) To address the plausible role of leucine limitation as the underlying cause of the observed phenotype by studying the role of specific AATs and interrogating the intracellular amino acids pool.
- d) Specifically, which amino acid(s) from amino acid dropout mix contribute to slow growth of BY4742 in the presence of increased amino acid in the growth medium.
- e) To study activation of the BCaa pathway under growth conditions with increased amino acid content in the media and look for its upstream partners.
- f) To study the effect of increased amino acid content in the growth conditions on transcriptional and translational level, cell division and possibly at the oxidative stress handling capacity of the cell.
- g) To investigate the potential causative key intermediate leading to onset of these phenotypes.

2 MATERIALS AND METHODS

2.1 Molecular and Cell Biology Methods

2.1.1 Plasmid DNA isolation from *E.Coli*

MH1 strain of *E. coli* was cultivated in liquid LB medium (Sigma Aldrich) or on LB agar plates (or plus 100 µg/ml ampicillin). Plasmids that were used in the study were transformed into *E. coli* using the standard bacterial transformation protocol. A single colony from transformation plates was inoculated in LB (supplemented with 100 µg/ml ampicillin) medium and incubated overnight at 37°C, 230 rpm. The next day, cells from 3 mL of culture were harvested and processed with NucleoSpin Plasmid-Kit (Macherey-Nagel) kit using the instructions as described by the manufacturer. The concentration and purity of isolated plasmid DNA were further checked using the Nanodrop.

2.1.2 Yeast media and growth

During this study yeast cells were cultured either in complex, rich YP(D) medium or synthetic, defined Hartwell Complete (HC) medium (or selective medium) depending upon experimental requirements. The detailed recipes of the medium (or plates) are as follows:

YP media: The respective amount of 1% (w/v) Yeast extract, 2% (w/v) Peptone was weighed, dissolved in water (pH adjusted to 5.5 using HCl), and was autoclaved. 2% (w/v) sugar (D: Dextrose, G and E: glycerol and ethanol, Gal: Galactose: usually made as 40% (w/v) stock solutions) was added as a carbon source in the autoclaved media. For having YP-plates, 2% (w/v) of agar was added to the YP media before autoclaving, and afterwards, the mix was poured in petri plates under sterile conditions. For antibiotics YPD plates: 100 µg/mL cloNAT, 150 µg/mL G418, or 200 µg/mL Hygromycin as final concentration were supplemented in the YPD media before pouring plates.

Hartwell Complete (HC) media: This media was initially used in Lee Hartwell's lab and later used by various yeast biology labs worldwide. It comprises sugar as a carbon source, Yeast nitrogen base as the nitrogen source, amino acid dropout mix. Nucleotides (Uracil and Adenine) and few amino acids (Lysine, Leucine, Tryptophan, and Histidine) are added from the top, which could be subsequently dropped out from the medium for plasmid selection. Amino acid dropout mix consists of 10 amino acids (listed in the table below) is referred to as amino acid mix (AAM) in this study.

Table 2: Composition of the dropout mix. Amino acids were weighed, added to 1 litre of sterile water, heated up to 70°C, and then filter sterilized.

10 x Dropout mix (AAM)	10 x (g/L)
L-Methionine	0.2
L-Tyrosine	0.6
L-Isoleucine	0.8
L-Phenylalanine	0.5
L-Glutamic acid	1.0
L-Threonine	2.0
L-Aspartic acid	1.0
L-Valine	1.5
L-Serine	4.0
L-Arginine	0.2

Yeast nitrogen base (YNB): 67 g of YNB mix was weighed, as stated by the supplier for making 10X stock.

Glucose solution: 40% (w/v)

Uracil solution: 1 g/L

Adenine solution: 1 g/L

Lysine solution: 10 g/L

Tryptophan solution: 10 g/L

Leucine solution: 20 g/L

Histidine solution: 10 g/L

All above components were weighed accordingly and were added to 1 litre of distilled water separately, sterile filtered and stored at RT.

Table 3: Recipe of Hartwell Complete media.

Hartwell Complete Media (1 L)	mL
10 x Dropout mix (AAM)	100
10 x YNB	100
40% Glucose	50
Uracil	35
Adenine	20
L-Lysine	12
L-Tryptophan	8
L-Leucine	4
L-Histidine	2
Sterilized H ₂ O	669

For having HC-plates (or selection), 2% (w/v) of agar was added to the water and autoclaved separately. Afterwards, all the above sterile-filtered components were added, and the mix was stirred and poured into Petri plates under sterile conditions. Depending on the selection marker, amino acids were left out accordingly to have HC (selective medium) plates for plasmid selection.

Yeast strains were freshly streaked from glycerol stocks after three weeks on YPD agar plates. Cells were inoculated from plates either into YPD or HC (or minus amino acid for selection) media and cultivated at 30°C, 140 rpm. All the plates were incubated at 30°C.

2.1.3 Yeast transformation

In order to transform the yeast cells with the required plasmid, the standard lithium-acetate based transformation protocol was followed, which is described below¹⁸⁰. Cells (800 µL) from an overnight yeast culture were harvested by centrifugation (3000 rpm, 1560 x g, 3 min at RT) and were subsequently washed with 1 mL of miliQ H₂O. The pellet was redissolved in 100 µL of one-step buffer (0.2 M lithium acetate, 40% PEG 3350 (50% w/v), 100 mM DTT). Then, 5 µL of 10 mg/mL single-stranded salmon sperm DNA (already heat-denatured at 96°C for 10 min and cooled on ice) and 1 µL of ~500 ng/µL plasmid DNA were added to the mix. The transformation mix was vortexed briefly and was incubated at 42°C for 30 min. Further, cells were harvested (3000 rpm, 1560 x g, 3 min at RT) and resuspended in 150 µL of miliQ H₂O and plated on appropriate selective medium plates. The plates were incubated at 30°C for 2-3 days.

Table 4: Plasmids transformed in BY4742 and mutant strains during this study.

S. No.	Plasmid	Auxotrophic markers	Source
1.	p415 TEF empty	<i>LEU2</i>	Dominik et al. ¹⁸¹ ; ATCC 87366
2.	p416 TEF empty	<i>URA3</i>	Dominik et al. ¹⁸¹ ; ATCC 87368
3.	pHLUK	<i>HIS3, LEU2, URA3, LYS2</i>	Muelleder et al. ¹⁸² ; (Addgene # 64181)
4.	pHUK	<i>HIS3, URA3, LYS2</i>	Muelleder et al. ¹⁸² ; (Addgene # 64183)
5.	pHluorin	<i>HIS3</i>	Miesenboeck et al. ¹⁸³ ; Maresová et al. ¹⁸⁴

For homologous recombination and for integrating the DNA cassette at the desired location, cells (~2-3 mL) from exponential phase yeast culture were harvested, washed, and resuspended in 200 µL of One-step buffer. 10 µL of ss-DNA and 10 µL of PCR amplified cassette (instead of plasmid DNA) were used following the same procedure described in the above paragraph. Next, the appropriate volume of transformed mix or cells were plated as 90% and 10% on YPD agar plates containing the suitable antibiotics for selection.

2.1.4 Drop dilution assay

Yeast cells were cultured in HC complete medium (or selective medium for transformed cells) with a normal amount of amino acid dropout, i.e., 1 X AAM, overnight at 30°C, 140 rpm and diluted 1:10 in fresh medium next morning and further incubated for 3-4 hours till the cells reach the logarithmic growth phase. Further, 2 O.D.₆₀₀ units of cells were harvested, washed, and resuspended in 1 mL of ddH₂O. Cells were five-fold serially diluted and spotted in the form of drops of 5 µL on agar plates which were incubated for 42 hours at 30°C. The first drop in every row corresponded to the number of cells from the culture with 2 O.D.₆₀₀ units, and the following drops were derived from its fivefold serial dilutions. All experiments were performed at least three times (or unless mentioned) using independent cultures made on separate days.

2.1.5 Growth curve assay

Unlike drop dilution assay, growth curve assay is a quantitative assay that can also be used to determine the doubling rate of yeast cells under different conditions. For this assay: yeast cells were cultured overnight at 30°C, 140 rpm in the liquid medium (Hartwell Complete or selective medium) with the usual amount of amino acid dropout, i.e., 1 X AAM. 1 O.D.₆₀₀ units of cells were harvested, washed, and resuspended in 1 mL of ddH₂O. Further, 90 µL of fresh HC medium and 10 µL of above cell suspension were added in 96 well plates (with round bottom) to reach the starting O.D.₆₀₀ 0.1. The plate was sealed using an easy breath membrane and placed in ELx808™ Absorbance Microplate Reader (BioTek®, BMG Labtech). The absorbance (OD₆₀₀) of the cells was measured after every 10 min intervals at 30°C for 72 hours, with continuous shaking conditions. The data was exported and plotted using MS excel. All experiments were performed at least three times using independent cultures made on separate days. The graphs represent the average of three independent repeats, where error bars represent the standard deviation.

2.1.6 Halo assay

Halo assay is used to study the effect of different chemicals on the growth of yeast cells. In the current study, I performed a Halo assay to study the impact of the exogenous addition of H₂O₂ on the growth of yeast cells under different growth conditions. The radius of the Halo formed elucidates the sensitivity or resistance of the strain in response to the addition of the chemical on the filter disc (9mm, Carl Roth, Germany) in the centre of the plate. The different yeast strains were cultured overnight in HC (or selective medium to maintain the plasmid selection), diluted the next day, and grown to log phase, cells were harvested and washed. Subsequently, 100 µL of cell suspension containing 0.001 O.D.₆₀₀ units of cells were spread uniformly using the sterile glass beads on plates containing either normal [1 X AAM] or double [2 X AAM] amount of amino acid dropout mix, supplemented with 2% glucose as carbon substrate. 10 µL of 6 M H₂O₂ was added to the filter disc kept in the middle of the plate. The plates were scanned following incubation at 30°C for two days.

2.1.7 Polymerase chain reaction (PCR)

PCR thermocycler was used to amplify the DNA fragments, which was further used as a template for homologous recombination or to confirm the site-specific integration of the DNA cassettes.

Standard PCR using S1 and S2/S4 primers

This PCR was used to amplify NatNT2 or KanMX4 or hphNT2 cassette using either S1 and S2 primers (resulting in gene deletion) or S1 and S4 primers (resulting in N terminal tagging or promoter exchange). S1, S2 and S4 primers were synthesized as described by Janke et al.¹⁸⁵. For one reaction of PCR (50 μ L): 10 μ L of 5 X buffer, 1.25 μ L of each 1:10 diluted primers (100 μ M), 1.25 μ L of dNTPs (10 mM), 1-1.5 μ L of pDNA (~100 ng), 0.45 μ L of Phusion polymerase, MiliQ H₂O up to 50 μ L were taken. For amplifying the NatNT2 cassette, GC rich buffer was used, and for KanMX4 and hphNT2 cassette, the HF buffer was used. Gene-specific PAGE purified primers used are enlisted in the table. The standard PCR program mentioned in the table followed was used. Further, PCR amplified products were analyzed using an agarose gel electrophoresis run.

Confirmation PCR

This PCR was used to confirm the integration of the above-integrated cassettes at the specific gene locus either using gene-specific confirmation primers (forward and reverse) or one of the gene-specific primers (forward or reverse) along with the integrated cassette confirmation primer (reverse or forward). The primers are enlisted in the table. The standard PCR program mentioned in the table followed was used with 30 X cycles and 5 mins final elongation time. For one reaction of PCR (25 μ L): 5 μ L of 5 X buffer, 0.75 μ L of each 1:10 diluted primers (100 μ M), 0.75 μ L of dNTPs (10 mM), 1-1.5 μ L of DNA (~100-200 ng), 0.25 μ L of Phusion polymerase, MiliQ H₂O up to 25 μ L were taken. DNA from each colony was obtained by simply heating a tip full of cells dissolved in 30 μ L volume of 0.2% SDS in an Eppendorf tube for 10 mins at 96°C and centrifugation >10,000 X g for 1 min. Further, PCR amplified products were analyzed using an agarose gel electrophoresis run.

Table 5: Program used in the thermocycler to amplify DNA in PCR.

Temperature	Time	Cycle Number	Reaction
96°C	1 min		Initial denaturation of DNA
96°C	30 s	35 X	DNA denaturation
55-60°C	1 min		Primer annealing
72°C	1min/kb		Elongation
72°C	10 min		Final elongation
4°C	∞		Cooling

The following table enlists the Primers, which were synthesized as described by Janke et al.¹⁸⁵ and were used to generate the mutant yeast strains used in this study (enlisted in the table) by replacing the functional ORF with the desired antibiotic gene cassette by Homologous recombination.

Table 6: The primers used during the study. All the primers were ordered from Sigma Aldrich. S1/2/4 primers had oligonucleotides sequences upstream or downstream of specific genes followed by standard S1, S2, or S4 sequences as described by Janke et al.¹⁸⁵. The oligonucleotides sequences "CC_FP or CC_RP" primers corresponded to sequences 100-200 base pair upstream or downstream regions of the respective genes.

NO.	Name	Sequence 5' --> 3'	Comment
P1	natNT2_CC_FP	GCGCTCTACATGAGCATGCC	Confirmation of Nat-Cassette insertion
P2	natNT2_CC_RP	CATCCAGTGCCTCGATG	Confirmation of Nat-Cassette insertion
P3	KanMX4_CC_FP	TGATTTTGATGACGAGCGTAAT	Confirmation of KanMx4 Confirmation
P4	KanMX4_CC_RP	CTGCAGCGAGGAGCCGTAAT	Confirmation of KanMx4 Confirmation
P5	hphNT1_CC_FP	GGAAGGAGTTAGACAACCTG	Confirmation of hphNTI-cassette insertion
P6	hphNT1_CC_RP	GATAAACATAACGATCTTTGTAG	Confirmation of hphNTI-cassette insertion
P7	ILV5-S1	AACCTATTCCTAGGAGTTATATTTTTTACCCTACCAGCA ATATAAGTAAAAAATAAACATGCGTACGCTGCAGGTC GAC	Deletion of <i>ILV5</i>
P8	ILV5-S2	TGATGTTGCAAAAATTCGAAGAGAAAAAGTTCCAGCA CTTGATATTATTTCTCTTTAATCGATGAATTCGAGCTC G	Deletion of <i>ILV5</i>
P9	ILV5_CC_FP	GGCTTTTACACCCAGTATTTCCCTTT	Confirmation of <i>ILV5</i> deletion
P10	ILV5_CC_RP	CAGAAAAACAGGGCTTCTAGTGAC	Confirmation of <i>ILV5</i> deletion
P11	ILV2-S1	CCCTTTGAGCTAAGAGGAGATAAATACAACAGAATCAA TTTTCAAATG CGTACGCTGCAGGTCGAC	Deletion of <i>ILV2</i>
P12	ILV2-S2	GTCTGCATTTTTACTGAAAATGCTTTTGAATAAATGTT TTTGAATTCA ATCGATGAATTCGAGCTCG	Deletion of <i>ILV2</i>
P13	CC_ILV2_FP	CCCTAATTAATAATTCAGATCTACGTCACACCG	Confirmation of <i>ILV2</i> deletion
P14	CC_ILV2_RP	CGAGTTAAAACACACCATTTGAATACATATGCTACG	Confirmation of <i>ILV2</i> deletion
P15	ILV3-S1	GCGCCTGTAATCTTTAGTAACGGATTCTTGTATTTTTTTG TAAACAGCCAAGAAAAAGTAGAGATGCGTACGCTGC AGGTCGAC	Deletion (or promoter exchange) of <i>ILV3</i>
P16	ILV3-S2	GCGAACAAAAAAGATGATGGAAAAGGAGAATCTCTAT ATATATATTCATCGATTGGGGCCTATAATGCATCAATCG ATGAATTCGAGCTCG	Deletion of <i>ILV3</i>
P17	ILV3-S4	TAGAGAATTGTCTAGATGTAGCAACTTTCGTTAACAAGC CCATCGATGAATTCTCTGTCG	Promoter exchange of <i>ILV3</i>
P18	ILV3_CC_FP	CTTGTATCCATTCCGTCCTCGTGAACCC	Confirmation of <i>ILV3</i> deletion
P19	ILV3_CC_RP	GGCTTTAGTGGCAGCAAAGCAGAGTTAATTTTCGTAG	Confirmation of <i>ILV3</i> deletion
P20	LEU4-S1	GGATTCTCACACTAGAAGTTTACTGTAGACTTTTTCTT ACAAAAAGACAAGGAACAATCATGCGTACGCTGCAGG TCGAC	Deletion (or promoter exchange) of <i>LEU4</i>
P21	LEU4-S2	GGAAGTAAATAAATAAGTATAGAAATAAATAGAAGCG AATAAGTCTGAAATACAGAAAAGTTCTTAATCGATGA ATTCGAGCTCG	Deletion of <i>LEU4</i>
P22	LEU4-S4	AGGCCGATGCTCAGCAAGAGCAATAATACTCTCTTTA ACCATCGATGAATTCTCTGTCG	Promoter exchange of <i>LEU4</i>
P23	LEU4_CC_FP	GGTTCGATGTTTTCTCCTCTGGGTCAGCC	Confirmation of <i>LEU4</i> deletion
P24	LEU4_CC_RP	CGGGTCACCCACACGTAATTTGGTTCAAG	Confirmation of <i>LEU4</i> deletion
P25	LEU9-S1	CGGCTTATAAGGGTCTTCTCCTTAGGATAATACTATCGG CACATTATCATTTAGCCGCTAGCCATGCGTACGCTGCA GGTCGAC	Deletion (or promoter exchange) of <i>LEU9</i>
P26	LEU9-S2	GCCATTTATAAATAAATAACATATATATAACATGAG TAATCATAAGCTACTCCTTTCTATTAATCGATGAATTCGA GCTCG	Deletion of <i>LEU9</i>
P27	LEU9-S4	TACTAGCATGCTCAGCTAGCGCTATGAACGAATGTTTTA CCATCGATGAATTCTCTGTCG	Promoter exchange of <i>LEU9</i>

P28	LEU9_CC_FP	GAATGACTCATATTTTTCCATCTCTTTCCGGCCTTGCC	Confirmation of <i>LEU9</i> deletion
P29	LEU9_CC_RP	GGTGGGTGGGCTGGGTAATGTTTCACG	Confirmation of <i>LEU9</i> deletion
P30	LEU1-S1	GCAGTCAACAAATATAAGAATATTGAAATTGACAGTT TTTGTGCTATCGATTTTTATTATTGCTGTTTTAAATCA TGCGTACGCTGCAGGTCGAC	Deletion of <i>LEU1</i>
P31	LEU1-S2	GGTGTGCTTGTGCTGAGACACATGTTATTGACGCCAG GTTTGGACGTTGTTTTTCACTGTCTAATCGATGAATTCG AGCTCG	Deletion of <i>LEU1</i>
P32	LEU1_CC_FP	GGCTTCATGAGTCGGCTCAATAGTAGTTG	Confirmation of <i>LEU1</i> deletion
P33	LEU1_CC_RP	GAGGGATAATGTTGCATTTAAAGTACATGTTCC	Confirmation of <i>LEU1</i> deletion
P34	BAT1-S1	CGTTAGAATAAATCACCTATAAACGCAAAATCAGCTA GAACCTTAGCATACTAAAACATGCGTACGCTGCAGGTC GAC	Deletion (or promoter exchange) of <i>BAT1</i>
P35	BAT1-S2	CCTCTGAGAGGAATTCTGTTTTTTTTTTGGGGGGGG AGGGGATGTTTACCTTCATTATCATTAAATCGATGAATTC GAGCTCG	Deletion of <i>BAT1</i>
P36	BAT1-S4	TGATGGAGAATTTCCCAACTTCAAGGAATGTCTCTGCA ACATCGATGAATTCCTGTGCG	Promoter exchange of <i>BAT1</i>
P37	BAT1_CC_FP	GGCCCATCCGATCCATATTGCCTTCTATGACTC	Confirmation of <i>BAT1</i> deletion
P38	BAT1_CC_RP	GGTCAACAATTTCAAAAAGCGTAAGAAGCCGC	Confirmation of <i>BAT1</i> deletion
P39	BAT2-S1	GACTAACTACTAAAATTTAGAAATTTAAGGGAAAGCA TCTCCACGAGTTTTAAGAACGATATGCGTACGCTGCAG GTCGAC	Deletion (or promoter exchange) of <i>BAT2</i>
P40	BAT2-S2	CGCTCTAGTTTTATTCTTTTTAACTTTAATTACTTTACGT AGCAATAGCGATACTTCAATCGATGAATTCGAGCTCG	Deletion of <i>BAT2</i>
P41	BAT2-S4	TAGTTATCTTAACTTTGGAGGCGTCTAGGGGTGCCAAG GTCATCGATGAATTCCTGTGCG	Promoter exchange of <i>BAT2</i>
P42	BAT2_CC_FP	GATCCGACTCTTTTTCTTTTTGGTGTGCTTCTCTATGTC CG	Confirmation of <i>BAT2</i> deletion
P43	BAT2_CC_RP	GCTTCTAAGGTATGTATGGGCCCTTTTCTATCCGCGC	Confirmation of <i>BAT2</i> deletion
P44	GCN4-S1	CTAAAGTTTTGTTTACCAATTTGTCTGCTCAAGAAAATA AATTAATAACAATAAAATGCGTACGCTGCAGGTCGAC	Deletion (or promoter exchange) of <i>GCN4</i>
P45	GCN4-S2	CGTTATACACGAGAATGAAATAAAAATATAAAATAAA AGGTAAATGAAATCAATCGATGAATTCGAGCTCG	Deletion of <i>GCN4</i>
P46	GCN4-S4	CCATTGGATTTAAAGCAAATAAACTTGGCTGATATTCGG ACATCGATGAATTCCTGTGCG	Promoter exchange of <i>GCN4</i>
P47	GCN4_CC_FP	GTTACCAATTGCTATCATGTACCCGTAGAA	Confirmation of <i>GCN4</i> deletion
P48	GCN4_CC_RP	CCTAACCAGTAAATACCAGAACATACGCGCAG	Confirmation of <i>GCN4</i> deletion
P49	ECM1-S1	AGCTTGCCATAAAATAGGGAAATTTTACTCACAATAT GCGTACGCTGCAGGTCGAC	Deletion (or promoter exchange) of <i>ECM31</i>
P50	ECM1-S2	GTTTTTCCCTATGCAATGATTTTTATCTATATTTTTAA TCGATGAATTCGAGCTCG	Deletion of <i>ECM31</i>
P51	ECM31-S4	ATCGCTTAGAGGAGGTGCATAATTGTCTTTTATTATAT TCATCGATGAATTCCTGTGCG	Promoter exchange of <i>ECM31</i>
P52	ECM1_CC_FP	CTCTTACAGTTGCTCGATGG	Confirmation of <i>ECM31</i> deletion
P53	ECM1_CC_RP	ATACAATTCGGGTTCTACC	Confirmation of <i>ECM31</i> deletion
P54	CIR2-S1	TAAGCTAGACAGGAAAATCCACTCTGGGAAAGGGAAA ATGCGTACGCTGCAGGTCGAC	Deletion (or promoter exchange) of <i>CIR2</i>
P55	CIR2-S2	ATGAATAAAATAATTAATAAATAATGAATCCTGTGATT AATCGATGAATTCGAGCTCG	Deletion of <i>CIR2</i>
P56	CIR2-S4	TTCGGATCCCTCTAATTAAGTTCTCGTTAGTGAACCTAA TCATCGATGAATTCCTGTGCG	Promoter exchange of <i>CIR2</i>
P57	CIR2_CC_FP	CTAAACCGTTAGAGGTGGAC	Confirmation of <i>CIR2</i> deletion
P58	CIR2_CC_RP	AATATGCCGTACAACTTGC	Confirmation of gene deletion of <i>CIR2</i>
P59	AIM45-S1	CTACCATTAACGGTAAAGCAGCTAATTGTTAATTTCTAT GCGTACGCTGCAGGTCGAC	Deletion (or promoter exchange) of <i>AIM45</i>

P60	AIM45-S2	GCGAAGAGATGAATATATTTAGAAAGTTAAGAATTTATT TAATCGATGAATTCGAGCTCG	Deletion of <i>AIM45</i>
P61	AIM45-S4	CCTTGCTAGCTCTAGGCAAGACAGCAGCCAATGATTTA AACATCGATGAATTCCTGTCTCG	Promoter exchange of <i>AIM45</i>
P62	AIM45_CC_FP	ATGCTTTACATGGATTGAGC	Confirmation of gene deletion of <i>AIM45</i>
P63	AIM45_CC_RP	TGTATTATTGGTGCATCCTG	Confirmation of gene deletion of <i>AIM45</i>
P64	LEU2-S1	ACTAAAGGGAATGGTCAGATCATCAGGCCAACGGCAA ATGCGTACGCTGCAGGTCGAC	Deletion of <i>LEU2</i>
P65	LEU2-S2	AACATTTTGATGGACAATGAATTTCTCTAATTTTAACTCA ATCGATGAATTCGAGCTCG	Deletion of <i>LEU2</i>
P66	LEU2_CC_FP	CACCTGCCAGTAAGTGATTG	Confirmation of <i>LEU2</i> deletion
P67	LEU2_CC_RP	TGATCGAGAACATATTGAAGG	Confirmation of <i>LEU2</i> deletion
P68	ILV1-S1	GCCACATTTAAACTAAGTCAATTACACAAAGTTAGTGAT GCGTACGCTGCAGGTCGAC	Deletion of <i>ILV1</i>
P69	ILV1-S2	AAGTTGTTGCGTAAATTTATAAGTAAATTGTCGGTTTT AATCGATGAATTCGAGCTCG	Deletion of <i>ILV1</i>
P70	ILV1_CC_FP	CCTTTTCCTGACTACCAAGAC	Confirmation of <i>ILV1</i> deletion
P71	ILV1_CC_RP	ACATGGCTATGTGGAAGAAG	Confirmation of <i>ILV1</i> deletion
P72	ELM1-S1	TTTGAACGCCAGGTTAACAATAATTACTTAGCATGAAAT GCGTACGCTGCAGGTCGAC	Deletion (or promoter exchange) of <i>ELM1</i>
P73	ELM1-S2	CTAACCAATCCGACAGATATCATCCTGTAGTTTCATCT AATCGATGAATTCGAGCTCG	Deletion of <i>ELM1</i>
P74	ELM1-S4	CCCATTCCGGAATTAATGTCGGTATAAGCTGTCGAGGT GACATCGATGAATTCCTGTCTCG	Promoter exchange of <i>ELM1</i>
P75	ELM1_CC_FP	TCGAGGAACCTACTTGATCC	Confirmation of <i>ELM1</i> deletion
P76	ELM1_CC_RP	CAATTTACTTCCGCGATTTTC	Confirmation of <i>ELM1</i> deletion
P77	IML1-S1	GAAATAACTCAGCACTGACAAGGGACACTTTTTAAGGA TGCGTACGCTGCAGGTCGAC	Deletion (or promoter exchange) of <i>IML1</i>
P78	IML1-S2	TACTTTGTGAAGAACTCATCCATGTCATGGGGCTACTC AATCGATGAATTCGAGCTCG	Deletion of <i>IML1</i>
P79	IML1-S4	AAGAAATTGGTCTTTGTTTCTCCCATGCAATTTAGCGA ACATCGATGAATTCCTGTCTCG	Promoter exchange of <i>IML1</i>
P80	IML1_CC_FP	TGGGGAAGGGTACTAGATTC	Confirmation of <i>IML1</i> deletion
P81	IML1_CC_RP	CCATTGGAATCTGTCAAGTC	Confirmation of <i>IML1</i> deletion
P82	SIT4-S1	AAGCTCAAAAACATCCATAATAAAAGGAACAATAACAA TGCGTACGCTGCAGGTCGAC	Deletion (or promoter exchange) of <i>SIT4</i>
P83	SIT4-S2	TTTTTATTCGTCGAGTTAGGGAGGGCATGCCGTCGTGTT AATCGATGAATTCGAGCTCG	Deletion of <i>SIT4</i>
P84	SIT4-S4	TCTTTATTGTTTCAAGCCATTCGTCGGGGCCTCTAGATA CCATCGATGAATTCCTGTCTCG	Promoter exchange) of <i>SIT4</i>
P85	SIT4_CC_FP	CTTTCTGCGGGTAATAAGTC	Confirmation of <i>SIT4</i> deletion
P86	SIT4_CC_RP	CTCCCGAGTGTTGATTAAG	Confirmation of <i>SIT4</i> deletion
P87	LEU3-S1	CAACCTGCCTCAAGTAAAAATCGCTTCGTAACATTAATA CAAATCTTTTTGCAATTATGCGTACGCTGCAGGTCGAC	Deletion (or promoter exchange) of <i>LEU3</i>
P88	LEU3-S2	CATTACATAACATTTTTTCGAGGGTAAGTAAACATTACG CAAAAAAGAAAAGGACTTTAATCGATGAATTCGAGCT CG	Deletion of <i>LEU3</i>
P89	LEU3-S4	TTCACTATGGCTCATTTCACTTCCGGACTGTGAAGTCGC CACAAAATCTGATCTTCTCT'CATCGATGAATTCCTGT CG	Promoter exchange of <i>LEU3</i>
P90	LEU3_CC_FP	GACTCGCTGCGTAAAACCTCTCTTC	Confirmation of <i>LEU3</i> deletion
P91	LEU3_CC_RP	GTGAGCGCTTACGAATCTTCGC	Confirmation of <i>LEU3</i> deletion

Table 7: The yeast strains used during the study. The wild-type strains of *S. cerevisiae* used were obtained from the resource of the Biochemistry Department, University of Saarland. The mutant strains were obtained by homologous recombination in BY4742 background during this study.

Prototrophic strains	
CEN.PK113-1A	
CEN.PK113-7D	
SGA query	MAT α his3 Δ 0 leu2 Δ lys2+/lys2+ met15 Δ ura3 Δ can1::STE2pr-spHis5 lyp1::STE3pr-LEU2
D273-10 b	
Auxotrophic strains	Genotype
BY4742	MAT α his3 Δ 1 leu2 Δ 0 lys2 Δ 0 ura3 Δ 0
YPH499	MAT α ura3-52 lys2-801_amber ade2-101_ochre trp1- Δ 63 his3- Δ 200 leu2- Δ 1
W303	MAT α /MAT α {leu2-3,112 trp1-1 can1-100 ura3-1 ade2-1 his3-11,15} [phi+]
The following mutant strains were made by homologous recombination in BY4742 (MAT α his3 Δ 1 leu2 Δ 0 lys2 Δ 0 ura3 Δ 0) background	
Mutants	Genotype
Δ ilv1	ILV1::HphNTI
Δ ilv2	ILV2::natNT2
Δ ilv5	ILV5::natNT2
Δ ilv3	ILV3::natNT2
Δ leu4 Δ leu9	LEU4::KanMX4 LEU9::HphNTI
Δ leu1	LEU1::HphNTI
Δ leu3	LEU3::natNT2
Δ bat1	BAT1::HphNTI
Δ bat2	BAT2::kanMX4
Δ ecm31	ECM31::natNT2
Δ aim45	AIM45::natNT2
Δ cir2	CIR2::natNT2
Δ elm1	ELM1:: natNT2
Δ gcn4	GCN4::natNT2
Δ sit4	SIT4::natNT2
Δ iml1	IML1:: KanMX4
Δ agp1	AGP1::natNT2
Δ gap1	GAP1::natNT2
Δ bap2	BAP2::natNT2
ILV3 OE	KanMX4-pTEF ILV3
LEU4 OE	KanMX4-pTEF LEU4
LEU9 OE	KanMX4-pTEF LEU9
BAT1 OE	natNT2-pTEF BAT1
BAT2 OE	KanMX4-pTEF BAT2
ECM31 OE	natNT2-pTEF ECM31
AIM45 OE	KanMX4-pTEF AIM45
CIR2 OE	KanMX4-pTEF CIR2

<i>ELM1</i> OE	KanMX4-pTEF <i>ELM1</i>
<i>LEU3</i> OE	natNT2-pTEF <i>LEU3</i>
<i>GCN4</i> OE	KanMX4-pTEF <i>GCN4</i>
<i>SIT4</i> OE	KanMX4-pTEF <i>SIT4</i>
<i>IML1</i> OE	KanMX4-pTEF <i>IML1</i>
<i>AGP1</i> OE	KanMX4-pTEF <i>AGP1</i>
<i>GAP1</i> OE	KanMX4-pTEF <i>GAP1</i>
<i>BAP2</i> OE	natNT2-pTEF <i>BAP2</i>

2.2 Biochemistry Methods

2.2.1 Whole-cell Glutathione (GSH/GSSG) analysis

This assay was developed by Biswas et al.¹⁸⁶ and modified by Morgan et al.¹⁸⁷ to determine whole-cell GSSG/GSH levels in yeast. Total glutathione (GSX) and oxidized glutathione (GSSG) levels were measured using a simple DTNB (5,5'-dithio-bis(2-nitrobenzoic acid or Ellman's reagent) recycling assay. This assay works on the principle that two molecules of GSH react with DNTB, forming free TNB chromophore (which absorbs at 412 nm) and TNB-GS molecule recycled back to GSH and TNB via the action of Glutathione Reductase (GR) in the presence of NADPH. The rate of formation of yellow-coloured TNB in the reaction (linear range for change in the absorbance nm min^{-1} is convenient to calculate) is linearly proportional to the concentration of GSH present in the sample.

The detailed method is summarized as follows. Yeast strains (or transformed) were inoculated (using a preculture) and cultured overnight in liquid medium (Hartwell Complete or selective medium) with normal and double amount of amino acid dropout, i.e., 1 X AAM or 2 X AAM, at 30°C, 140 rpm overnight until cells reached the late exponential growth phase (O.D.₆₀₀ in the range of 3-3.5). The next day, 50 O.D.₆₀₀ units of cells were harvested, washed, resuspended in SSA-HCl buffer (1.3% w/v sulfosalicylic acid, 8mM HCl), and cells were opened using 0.5 mm beads and mechanical shearing. The lysate collected after cell debris removal via centrifugation (3000 rpm, 1560 x g, 1 min at RT) was further incubated for 15 min on ice (for precipitating proteins) and centrifuged (>16,000 x g, 15 min at 4°C) to obtain a clear cell lysate (it was carefully harvested from middle of the organic phase to another fresh Eppendorf tube). For measuring GSSG in the samples, 100 μl of this cell lysate and the known GSSG standards (also made in SSA-HCl buffer) were further incubated with 2 μl of Vinyl pyridine and 40 μl 1 M MES/TRIS buffer (pH 7.0) for 60 mins with intermittent vortexing to slowly alkylate the reduced glutathione (GSH) such that only the GSSG present in the sample could be analyzed. Meanwhile, for determining the total whole-cell glutathione concentration (GSX) in the sample, the above lysate was diluted 1:100 in KPE buffer (100 mM K_2HPO_4 , 5 mM EDTA, pH 7.5 set by the addition of 100 mM KH_2PO_4) and was further used.

20 μl volume of samples (GSH or GSSG fraction) and respective known GSH or GSSG standard were incubated with 120 μl DNTB and NADPH mix in 96 well plates. The reaction started with the addition of glutathione reductase, and the rate of yellow-coloured TNB reaction by-product was recorded. The whole-cell concentrations of

GSX/GSSG in unknown samples were calculated using the regression curve generated from the known GSH and GSSG standards. The amounts of GSH were further calculated by subtracting double GSSG values from GSX values since GR also reduces GSSG to 2 molecules of GSH.

2.2.2 Quantification of Amino acids (intracellular amino acids or ¹³C enrichment studies):

The different yeast strains (or transformed) were inoculated (using a preculture) and cultured in liquid medium (Hartwell Complete) with normal and double amount of amino acid dropout, i.e., 1 X AAM or 2 X AAM, at 30°C, 140 rpm overnight and were processed next day (O.D.₆₀₀ at the time of harvest was in the range of 3-3.5) as described below. Also, only in the case of ¹³C labelled enrichment amino acids analysis, yeast cells were fed with 2% (w/v) of ¹³C labelled glucose (Cambridge Isotope Laboratories, Tewksbury, MA, USA) while inoculating for the main culture.

For quantification of either intracellular amino acids (iAA) or ¹³C labelled enrichment amino acids studies, the fast filtration sampling method was adapted for sample harvesting. 4 mL (for iAA) or 12 mL (¹³C enrichment analysis) of cell suspension was very quickly pipetted from flasks to another flask equipped with filter paper (25 mm cellulose nitrate, 0.2 µm pore size, Sartorius, Göttingen, Germany) and vacuum pump. The filter membrane was also quickly washed with MiliQ water, harvested, and incubated with 2 mL of MiliQ water (supplemented with 220.63 µM of alpha Aminobutyric acid as an internal standard for quantification of iAA studies only, as described by Bolten et al.¹⁸⁸ at 100 °C for 15 min for extraction of cellular metabolites. The whole sampling time for each sample from harvesting till boiling took less than a minute. Subsequently, the cellular lysate was cooled on ice for 10 min, collected in 2 mL Eppendorf tubes, and centrifuged at high speed 16,000 X g for 5 min at 4 °C. The clear lysate was carefully transferred to another fresh tube. For each test condition, at least three independent samples were harvested and measured. These samples were further processed by Dr Michael Kohlstedt (Wittman group, University of Saarland) using the following protocol, as part of the collaboration work.

In the case of determination of intracellular amino acids, 500 µL of harvested lysate was directly used for injection (during injection itself, the samples were mixed with reagents and derivatized in an automated way) and quantified using HPLC as described by Wittmann et al.¹⁸⁹. For ¹³C labelled enrichment amino acids analysis, the cell lysates were dried under Nitrogen stream, pre-derivatized, and quantified using GC-MS. The co-relation factor $CDW = 0.50 \text{ O.D.}_{600} \times g \text{ L}^{-1}$) as described for *S. cerevisiae* was used for normalizing and represent the data in µmol/CDW units¹⁹⁰.

2.2.3 RNA Sequencing

The RNA samples were prepared from the BY4742 and *ILV3* mutant strain grown on 1 X AAM and 2 X AAM growth conditions using the procedure described below. Subsequent sample processing, RNA sequencing and subsequent data analysis was performed by Dr Kathrin Kattler (Walter's group, University of Saarland) as a part of collaboration work. The following protocol followed and provided by Dr Kathrin is quoted exactly for this thesis work and the manuscript.

RNA isolation

The different yeast strains were cultured overnight, in the medium with normal and double amount of amino acid dropout, i.e., 1 X AAM or 2 X AAM and harvested in the late exponential phase the next day. 2 O.D.₆₀₀ units of cells were harvested, washed, and snap-frozen at -80°C. Further, the cell pellet was dissolved in 1 mL of TRI Reagent (Zymo Research), homogenized using FastPrep homogenizer (3 cycles of 20 s, speed 8.0 m/s) and centrifuged (highest speed, 5 min, 2°C) to obtain clear lysate. The clear lysate was added to the spin column provided in the kit. Further, the protocol, as instructed by the supplier (Zymo Research), was followed to isolate RNA from the above isolated cell lysate. The concentration of isolated RNA samples was checked using Nano-drop and was quickly frozen to -80°C.

mRNA-seq library preparation and Next Generation Sequencing (NGS)

cDNA synthesis was carried out based on a SMARTseq2-like protocol¹⁹¹ modified for bulk RNA sequencing. Briefly, at least 100 ng total RNA was used for reverse transcription with 6 cycles of cDNA pre-amplification. Libraries were prepared using the Nextera DNA Library Prep Kit (Illumina) with 7 cycles of enrichment PCR followed by 0.9 X Ampure XP Beads (Beckman Coulter) purification. Normalized libraries were sequenced on a HiSeq2500 (Illumina) using TruSeq SBS Kit v3 – HS Chemistry in single read runs with read lengths of 94 bp.

NGS data processing

Reads were trimmed using Trim galore! (v0.4.2) to remove 3' ends with base quality (http://www.bioinformatics.babraham.ac.uk/projects/trim_galore/) below 20 and adaptor sequences. Reads were aligned to *Saccharomyces cerevisiae* S288C genome assembly R64 using STAR¹⁹² with per sample 2-pass mapping strategy. PCR duplicates were detected using MarkDuplicate from Picard tools (version 1.115; <http://broadinstitute.github.io/picard/>). Gene-wise read counts for RNA-seq data were estimated using RSEM¹⁹³.

RNA-seq data analysis

Expression values were normalized as log CPM + 1 (counts per million). Genes with average log CPM < 0.5 were excluded. The 1000 most variable genes were used for Principal Component Analysis (PCA). EdgeR¹⁹⁴ was used for the calculation of scaling factors and robust estimation of dispersion in order to detect differentially expressed genes with significance thresholds of maximal FDR adjusted p-value of 0.01 and minimal absolute logFC of 1. Gene ontology overrepresentation analysis was done using DAVID¹⁹⁵ with at least 3 genes per GO term and p < 0.05.

2.2.4 Annexin-V staining and Microscopy

I prepared the microscopic slides (as described in the following paragraph) in the laboratory of Storchová group, TU-Kaiserslautern. These slides were further processed for imaging and data analysis by Dr Galal Metwally as a part of the collaboration work.

The different yeast strains were cultured overnight in the liquid medium (Hartwell Complete) with regular and double amounts of amino acid dropout, i.e., 1 X AAM or 2

X AAM. The next day, 1 O.D.₆₀₀ units of cells were harvested (700 X g, 3 min) in the late exponential phase, washed using sorbitol buffer (1.2 M sorbitol, 0.5 mM MgCl₂, 35 mM potassium phosphate, pH 6.8). Further, the pellet was dissolved in 400 µl of Tris/DTT Buffer (100 mM Tris/Cl, pH 9.4, 10 mM DTT) and incubated at 30°C for 15 min (with mild shaking conditions). Afterwards, the cell suspension was centrifuged (700 X g, 3 min), the resultant pellet was rewashed and resuspended in sorbitol buffer containing Zymolase (3 mg/gm wet weight of pellet) and incubated for 30-40 mins at 30°C (with mild shaking conditions). The incubated mix was centrifuged (100 X g, 1-2 min), the resultant protoplast pellet was carefully washed with and resuspended in 30 µL volume of binding sorbitol buffer (0.6 M sorbitol, 10 mM Hepes/NaOH, pH 7.4, 140 mM NaCl, 2.5 mM CaCl₂). Further, 50 µl volume of the pre-diluted Annexin-V and Propidium Iodide (PI) stain (Annexin-V-FLUOS staining kit, Sigma Aldrich) was added to the protoplast suspension. Meanwhile, incubation of this suspension mix in the dark for 20 mins, the wells of the microscopic slides were coated using 1:1 poly-lysine solution (50 mg/ml stock solution) for 20 mins and subsequent PBS (1 X) wash. Afterwards the incubation step, the stained cells were washed with PBS (1 X) (100 X g, 1-2 min) and were further incubated with 50 µl of DAPI (1 µg/ml) staining solution for 10 mins in the dark. Afterwards, the stained cell suspension was washed and added to the poly-lysine coated slides. Following incubation for 15-20 minutes in the dark, the wells were very carefully washed with PBS (1 X) and were sealed using coverslips. Further, these slides were imaged using a Zeiss inverted microscope (AxioObserver Z1) equipped with a CSU-X1 spinning disk confocal head (Yokogawa). Either 40X air or 60X oil objective lens was used to acquire images using the CoolSnap HQ camera (Roper Scientific), which were further processed for quantification using the Slidebook software, version 6.0.6 (Intelligent Imaging Innovations). For each test condition, at least three independent biological replicates were processed and subsequently imaged.

2.2.5 Quantification of cellular metabolites

For measuring KIV, α-IPM, Valine, and α-KG in the yeast, the cold quenching sampling method was employed¹⁹⁶. The yeast strains were inoculated (using a preculture) and cultured in the liquid medium (Hartwell Complete) with normal and double amounts of amino acid dropout, i.e., 1 X AAM or 2 X AAM, at 30°C, 140 rpm overnight. 7-12 mL (O.D.₆₀₀ of at the time of harvest was around ~ 3) of culture was quickly pipetted in the pre-cooled falcon tubes containing quenching buffer (95% Acetonitrile, 25 mM formic acid, pre-cooled at -20 °C) in the ratio of ~1:4. The appropriate amount of internal standard (keto caproic acid) was added to the above mix immediately. The mix was incubated on ice for 15 min, vortexed thoroughly in between, and was clarified of cell debris (15,000 x g, 4 °C, 5 min). The supernatant was harvested, and the pellet fraction was further washed with supercooled deionized water, and the supernatant was harvested again. Afterwards, the two supernatant fractions were combined, frozen at -80 °C. These samples were further processed by Dr Michael Kohlstedt (Wittman group, University of Saarland) using the following protocol, as part of the collaboration work. The frozen lysates were lyophilized, re-dissolved in 200 µL volume of resuspension buffer (100 µL MeOX + 100 µL MSTFA, 4 °C), and filtered before injecting to GC-MS. Quantification of the analyzed metabolites (KIV, Valine, α-KG, and IPM) was done using the standard curves generated from known concentration of these purified compounds (bought from Sigma Aldrich), which were also treated and injected to GC-MS like other samples. Since, the whole-cell broth (with no separation

of biomass and supernatant fraction) was harvested during the extraction process. Thus, the concentration of the cellular metabolites is representative of the intracellular plus extracellular fraction of metabolite.

2.2.6 Translational studies

The following experiments with puromycin incorporation, budding index, and FACS were performed by Dr Galal Metwally (Storchová group, TU-Kaiserslautern) as a part of the collaboration work. The protocol followed by Dr Galal is described below in brief.

Puromycin incorporation

The different yeast strains were cultured overnight, in liquid medium (Hartwell Complete) with the average and double amount of amino acid dropout, i.e., 1 X AAM or 2 X AAM, diluted in the morning. While growing in the exponential phase, cultures were treated with puromycin (final con. 10 μ M) for 15 min (30 min, 140 rpm). Further, cells equivalent to 5 O.D.₆₀₀ were harvested (3000 rpm, 3 min), washed twice, and cell lysates were prepared for western blot.

Flow cytometry analysis of DNA content (FACS)

The different yeast strains were cultured overnight (30 min, 140 rpm) in liquid medium (Hartwell Complete) with normal and double amount of amino acid dropout, i.e., 1 X AAM or 2 X AAM, diluted in the morning, and were grown to mid-exponential growth phase for 3-4 hours. Further, cells equivalent to 1 O.D.₆₀₀ were harvested (6000 rpm, 1 min), resuspended in 1 mL of 70% (v/v) ethanol overnight. The next day, cells were harvested, washed, and resuspended in 250 μ L FxCycle™ PI/RNase staining solution (Life Technologies, #F10797). The cell suspension was incubated in the dark for 30 min at RT and then subsequently stored for 72 hours at 4°C. After 3 days, samples were sonicated for 20 secs at 30 % amplitude and run on an Attune™ Flow Cytometer. The FlowJo™ software, version 10, was used to analyze the data. A histogram of cell count against PI intensity was plotted, and samples were gated for single cells. The percentage of cells with 1C DNA and 2C DNA content, where C represents the copy number of DNA, were determined using the area under the histogram where for 1N: 0 – 2.7 x 10⁵ PI intensity and 2N: 2.7 x 10⁵ – 4.5 to 7 x 10⁵ PI intensity, values of area under the histogram were used, respectively.

Budding index determination

The different yeast strains were cultured overnight (30 min, 140 rpm) in liquid medium (Hartwell Complete) with normal and double amount of amino acid dropout, i.e., 1 X AAM or 2 X AAM, diluted in the morning, and were grown to mid-exponential growth phase for 3-4 hours. Further, cells equivalent of 1 O.D.₆₀₀ were harvested (3000 rpm, 3 min), resuspended in 1 mL of 70% (v/v) ethanol for 30 min, washed two times with PBS (1 X). These samples were used to count budded and non-budded cells in several random fields using a Zeiss inverted microscope (AxioObserver Z1) equipped with a CSU-X1 spinning disk confocal head (Yokogawa). Further, the 40X air or 60X oil objective lens was used to acquire images using the CoolSnap HQ camera (Roper Scientific), which were further processed for computing the budding index using the Slidebook software, version 6.0.6 (Intelligent Imaging Innovations).

3 RESULTS

3.1 Growth of *Saccharomyces cerevisiae* in the presence of increased amino acid content in the growth medium

3.1.1 The foundation stone observation

A former student helper made this serendipitous observation where she saw the unexpectedly slow growth of *S. cerevisiae* BY4742 wild type strain using the drop dilution assay. It was later figured out that it resulted from an experimental mistake where instead of the usual amount of amino acid dropout mix, accidentally, the double amount of dropout mix was used to make the solid agar medium plates. This exciting observation raised many questions, such as why the yeast cell grows slow in response to the extra amino acid content in the growth medium? And what is the molecular basis of this phenotype? When I further increased the amounts of amino acid dropout mix by three times in the medium (fig: 10), it further impaired the growth of the cell. This observation intrigued my interest and motivated me to study and explore the mechanisms and underpinnings behind this observation as a part of my doctoral study. The straightforward question "**Why is this so?**" for the slower growth of the BY4742 strain under condition with increased amino acid content in the medium became the foundation stone of my doctoral study.

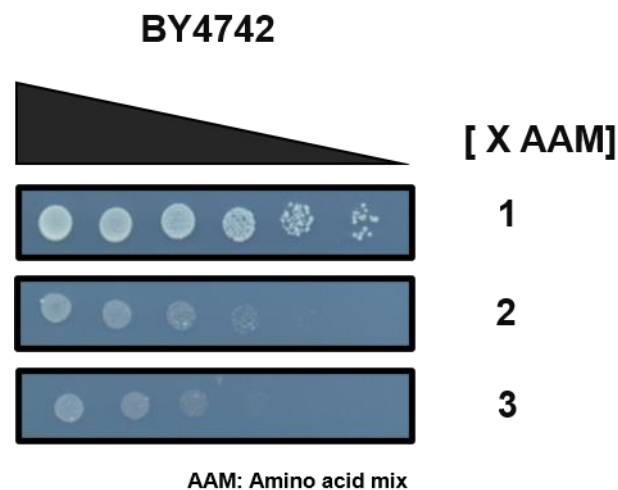


Figure 10: Increased amino acid content (AAM) in the medium severely impacts the growth of BY4742 yeast strain as shown by Drop dilution assay. BY4742 strain was cultured overnight in HC medium, diluted next day and grown to log phase, cells were harvested and washed, fivefold serially diluted and spotted on plates containing normal [1 X AAM], double [2 X AAM] or triple [3 X AAM] amount of amino acid dropout mix, containing 2% glucose as carbon substrate. The plates were scanned following incubation at 30°C for 42 hours. The top black bar corresponds to the decreasing cell density from left to right. This figure is one of the representative examples from at least three independent experiments performed on different days.

3.1.2 The growth of auxotrophic yeast strains is severely impacted in response to an increase in amino acid content in the solid agar and liquid growth medium

During this study, Hartwell Complete medium was used to grow the yeast cells. It consists of glucose as carbon substrate, yeast nitrogen base as nitrogen source and amino acid dropout mix of ten amino acids (which is represented as [AAM]). Additionally, four amino acids (histidine, leucine, lysine, and tryptophan) and nucleotides (uracil and adenine) were added separately from the amino acid dropout mix since they could be dropped out from the medium to maintain the plasmid selection.

Table 8: Recipe for the liquid medium composition used during the study. 1 X AAM represents the exact Hartwell Complete medium recipe. However, when the amount of amino acid dropout mix is increased to either two or three times in the medium from its usual normal amount, it is represented as 2 X AAM and 3 X AAM, respectively. While making the solid agar plates with 1 X AAM, 2 X AAM, or 3 X AAM medium composition, 2% (w/v) agar was added to the water and autoclaved separately. Afterwards, all the above sterile-filtered components were added, and the mix was stirred and poured into petri plates under sterile conditions.

Medium components	1 X AAM (mL)	2 X AAM (mL)	3 X AAM (mL)
10 X Dropout mix (AAM)	100	200	300
10 X YNB	100	100	100
40% Glucose	50	50	50
Uracil (1 g/L)	35	35	35
Adenine (1 g/L)	20	20	20
L-Lysine (10 g/L)	12	12	12
L-Tryptophan (10 g/L)	8	8	8
L-Leucine (20 g/L)	4	4	4
L-Histidine (10 g/L)	2	2	2
Sterilized H ₂ O	669	569	469

As the first step to gain insights into the amino acid dependent slow growth phenotype, I asked whether this phenotype is strain-specific or not? For addressing this question: The amount of amino acid dropout mix only in the Hartwell Complete medium was increased to double and triple amounts of its normal concentration (referred to as [2 X AAM] and [3 X AAM] respectively, from now onwards (refer to the table: 8)). The growth of seven different laboratory yeast strains were compared by performing a drop dilution assay on the HC agar plates. The HC plates were supplemented with either the usual amount (which is represented as [1 X AAM] from now onwards) or double ([2 X AAM]) and triple amount ([3 X AAM]) of amino acid dropout mix, respectively. The drop dilution assay is a qualitative growth assay. 2 O.D.₆₀₀ units (where 1 O.D.₆₀₀ unit is equivalent to 1 ml of culture with 1.5×10^7 cells) of cells were harvested from an exponential phase culture. The cells were washed, resuspended in 1 mL of distilled water, and serially diluted 1:5 with every fold dilution. 5 μ L of the undiluted and these five serial dilutions were spotted left to right on the HC medium agar plates. These plates were

incubated at 30°C for 42 hours and were scanned afterwards. All yeast strains were observed to grow similar to each other on 1 X AAM growth condition. Except for the YPH499, which was observed to grow slower when harvested from exponential phase culture than stationary phase culture (data not shown).

Interestingly, significant growth differences of distinct yeast strains were observed on the 2 X AAM growth condition as compared to their growth on 1 X AAM (fig: 11). The growth of three yeast strains: BY4742, YPH499, and W303, were severely impaired by the increase in amino acid concentration: while the growth of the other four yeast strains: SGA, D270-10b, CEN.PK strains were not changed. Also, further increasing the amounts of amino acid dropout mix to three times ([3 X AAM]) severely impacted the growth of BY4742, YPH499, and W303 strains whilst the growth of SGA, D270-10b, CEN.PK strains were not affected. The striking difference in the growth pattern of these different yeast strains was that BY4742, YPH499, and W303 yeast strains are auxotrophic while SGA, D270-10b, CEN.PK strains are prototrophic in nature. The auxotrophic strains have few genes missing from their amino acid or nucleotide biosynthetic pathway, which are generally used as selection markers to maintain the plasmid selection. Thus, the auxotrophic yeast strains are not able to synthesize a few of their amino acids or nucleotides, unlike the prototrophic strains, which can synthesize all their amino acids or nucleotides. As the next step, I, therefore, asked whether one or more amino acid or nucleotide auxotrophies underlie the observed growth phenotype in the presence of increased amino acid content in the medium?

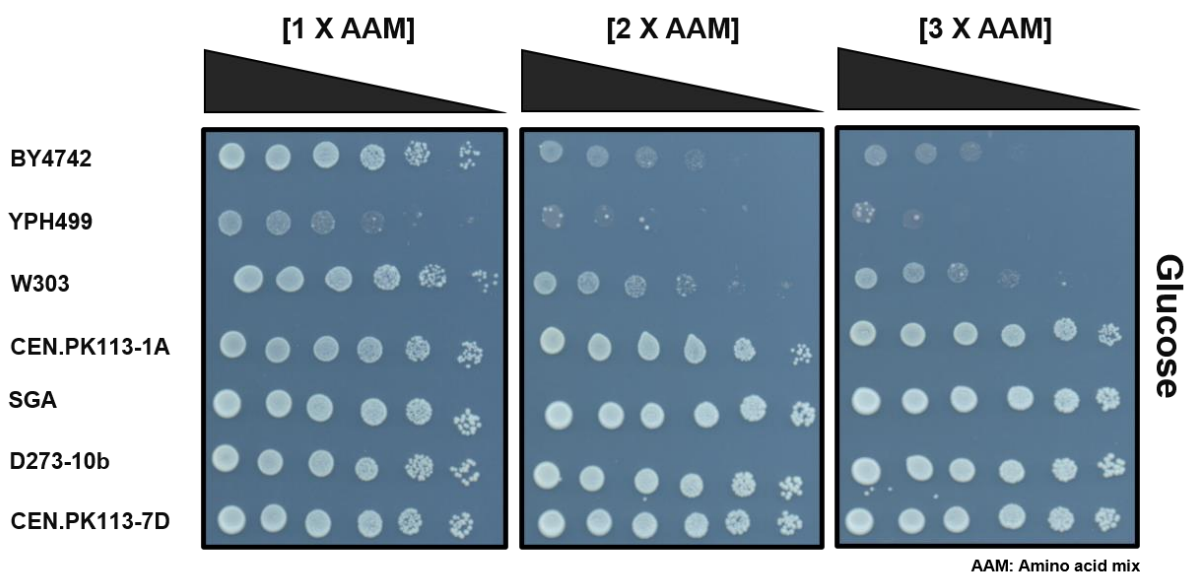


Figure 11: Auxotrophic wild-type yeast strains were sensitive to increase amino acid content, unlike prototrophic wild-type strains in the presence of a fermentable carbon source. Prototrophic yeast strains (CEN.PK 113-1A/7D, SGA, and D273-10 b) were unaffected by increased amino acid content. In contrast, the growth of auxotrophic yeast strains (BY4742, YPH499, and W303) was severely impacted in the presence of glucose as a carbon substrate. All strains were cultured overnight in HC medium, diluted the next day, and grown to log phase. Cells were harvested, washed, fivefold serially diluted, and spotted on plates containing normal [1 X AAM], double [2 X AAM] or triple [3 X AAM] amount of amino

acid dropout mix, containing 2% glucose as carbon substrate. The plates were scanned following incubation at 30°C for 42 hours. The top black bar corresponds to the decreasing cell density from left to right. This figure is one of the representative examples from at least three independent experiments performed on different days.

The next intriguing question to address was if the amino acid dependent impaired growth phenotype of auxotrophic yeast strains is limited to the solid HC agar plates or is it also present in liquid growth medium. Therefore, the auxotrophic BY4742 was also cultured in the liquid growth medium, and its growth was monitored at 30°C for nearly 72 hours using BioTek microplate reader (ELx808, BioTek instruments). It was observed that the growth of BY4742 in liquid culture medium (graph, fig: 12) was also negatively impacted, like its growth on solid HC medium agar plates in response to the increased amino acid content in the liquid medium.

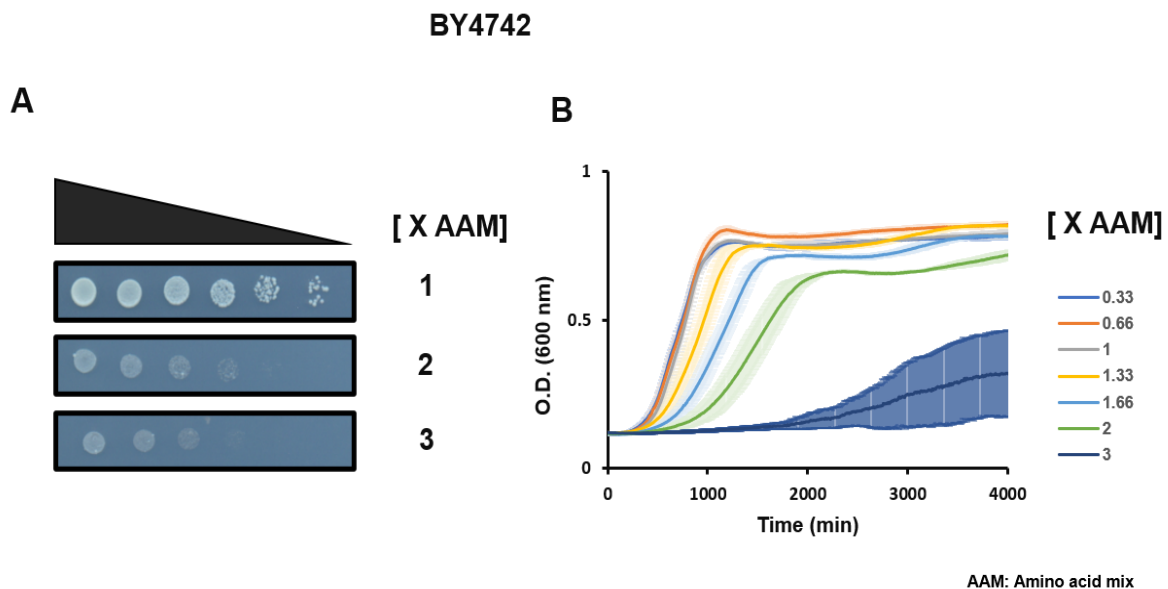
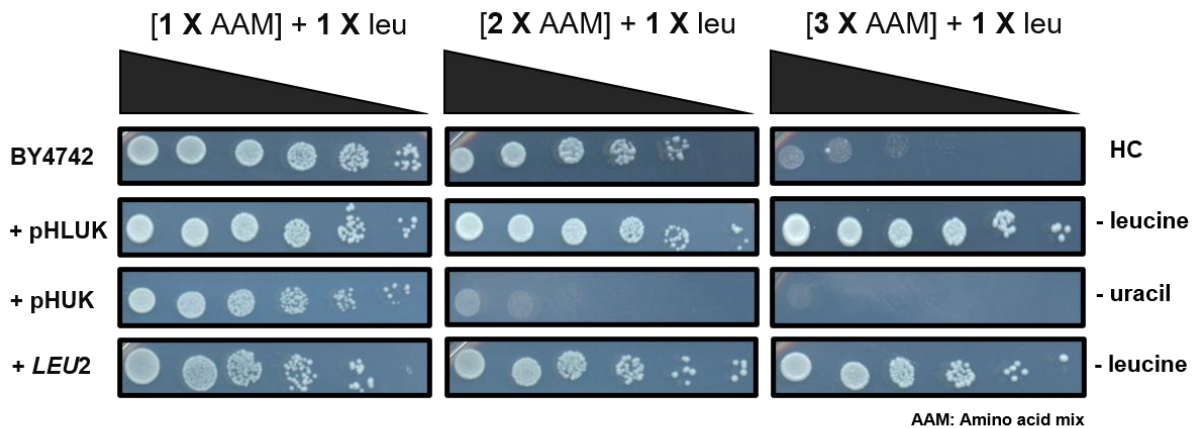


Figure 12: Increased amino acid content (AAM) in the medium severely impacts the growth of BY4742 yeast strain as shown by Drop Dilution assay (A) and Growth Curve assay (B) in fermentable carbon substrate. A: BY4742 strain was cultured overnight in HC medium, diluted the next day, and grown to log phase. Cells were harvested, washed, fivefold serially diluted, and spotted on plates containing normal [1 X AAM], double [2 X AAM], or triple [3 X AAM] amount of amino acid dropout mix, containing 2% glucose as carbon substrate. The plates were scanned following incubation at 30°C for 42 hours. The top black bar corresponds to the decreasing cell density from left to right. This figure is one of the representative examples from at least three independent experiments performed on different days. **B:** Cells from an overnight culture were inoculated in different mediums (containing different amounts of amino acid dropout mix) in a 96 well plate supplemented with 2% glucose as carbon substrate. Cell growth was continuously monitored at 30°C for 72 hours under constant shaking conditions, using BioTek microplate reader (ELx808, BioTek instruments). The graphs represent the average of three independent repeats performed on different days, where error bars represent standard deviation.

3.1.3 Restoring only the leucine auxotrophy in BY4742 rescues the impaired growth phenotype

Since the growth of prototrophic yeast strains, which can make all amino acids, was unaffected by increased amino acid content in the medium. I wondered whether restoring the missing auxotrophies in an auxotrophic yeast strain would render it insensitive to the increased amino acid content in the growth medium? If yes, which auxotrophy or auxotrophies are important for the observed slow growth phenotype?



BY4742: MAT α his3 Δ 1 leu2 Δ 0 lys2 Δ 0 ura3 Δ 0

pHLUK: plasmid encoding *HIS3 LEU2 LYS2 URA3*

pHUK: plasmid encoding *HIS3 LYS2 URA3*

Figure 13: Restoring the auxotrophic markers in BY4742 affects the amino acid dependent growth phenotype. BY4742 cells and or transformed with either pHLUK or pHUK plasmids or p415 empty vector (containing *LEU2* as selection marker) were cultured overnight in respective selective (or complete) HC medium, diluted the next day, and grown to log phase. Cells were harvested, washed, fivefold serially diluted, and spotted on plates containing normal [1 X AAM], double [2 X AAM] or triple [3 X AAM] amount of amino acid dropout mix (and without Leucine or Uracil to maintain the selection for cells transformed with plasmids), containing 2% glucose as carbon substrate. The plates were scanned following incubation at 30°C for 42 hours. The top black bar corresponds to the decreasing cell density from left to right. This figure is one of the representative examples from at least three independent experiments performed on different days.

As a first step to address this question, I transformed the BY4742 yeast strain with pHLUK plasmid¹⁶⁶, which encoded all its missing auxotrophic genes: *HIS3*, *LEU2*, *LYS2* and *URA3*. Interestingly, the pHLUK transformed BY4742 strain became resistant to the increased amino acid content in the growth medium in comparison to non-transformed BY4742 (fig: 13; row 1 and 2). This clearly shows that either one or more auxotrophic markers underlie the slow growth phenotype in response to changes in the amino acid content in the growth medium. The next question I asked was which specific auxotrophy or combination of auxotrophies was essential for this growth phenotype? It was also noticed that the three auxotrophic strains, which exhibited

amino acid dependent growth phenotype, have common auxotrophies for leucine, uracil, and histidine (fig: 11). Therefore, there are chances that any of these or all of these three in combination are leading to the growth phenotype. To gain further insights, the BY4742 was transformed with pHUK¹⁶⁶ plasmid, which replaced the auxotrophic genes *HIS3*, *LYS2*, *URA3*, but not the *LEU2*. Surprisingly, we observed that the pHUK plasmid could not rescue the growth of BY4742, unlike the pHLUK plasmid upon increased amino acid content in the medium. This result clearly pointed out that leucine auxotrophy is the reason for the observed slow growth phenotype. The pHUK transformed BY4742 strain (selected using uracil as selection marker) grew relatively slower than the non-transformed BY4742 (fig: 13; row 1 and 3) in response to the increased amino acid content in the medium. This slower growth phenotype was observed several times during this study (data not shown) when transformed yeast cells were forced to synthesize uracil and maintain the respective plasmid containing the *URA3* gene. The mechanistic basis of this phenotype is not clear at this moment and was not investigated during this study. Thus, to avoid the uracil dependent effects in the following experiments, pHUK transformed yeast cells were selected using histidine.

As a final proof of principle to confirm that leucine auxotrophy is essential for the observed growth phenotype: BY4742 was transformed with p415 TEF plasmid¹⁸¹ (which had the *LEU2* as a selection marker gene) was alone able to rescue the slow growth phenotype (fig: 13; row 4). In conclusion, the slow growth phenotype of BY4742 auxotrophic yeast strain upon supplementation of increased amino acid content in the medium is linked to leucine auxotrophy.

3.1.4 Increasing leucine in proportion to the increase of amino acid content in the growth medium also rescues the impaired growth phenotype

So far, it was established that leucine auxotrophy is the only important auxotrophy underlying the growth phenotype. The Hartwell Complete growth medium also has leucine and nucleotides (uracil and adenine) along with the other amino acids (histidine, lysine, and tryptophan), which are added separately along with the amino acid dropout mix to the medium. I further wondered how the amount of these nucleotides and amino acids in the growth medium, especially the leucine, affects the observed growth phenotype?

To address this question, the growth of the BY4742 strain was tested on HC plates supplemented with double the usual amounts of the amino acids: lysine, histidine, tryptophan, and leucine which were increased either individually or all together in combination with 2 X AAM. Interestingly, the growth of BY4742 was rescued in all situations where leucine was supplemented twice to its normal amounts (fig 14A). Remarkably, the growth phenotype of BY4742 was also rescued on [3 X AAM] when the leucine amount was increased to three times its normal amount in the HC medium (Second row, fig 14B). It was concluded from these findings that the ratio of leucine to the other amino acids present in the medium is significant for the growth of an auxotrophic yeast cell.

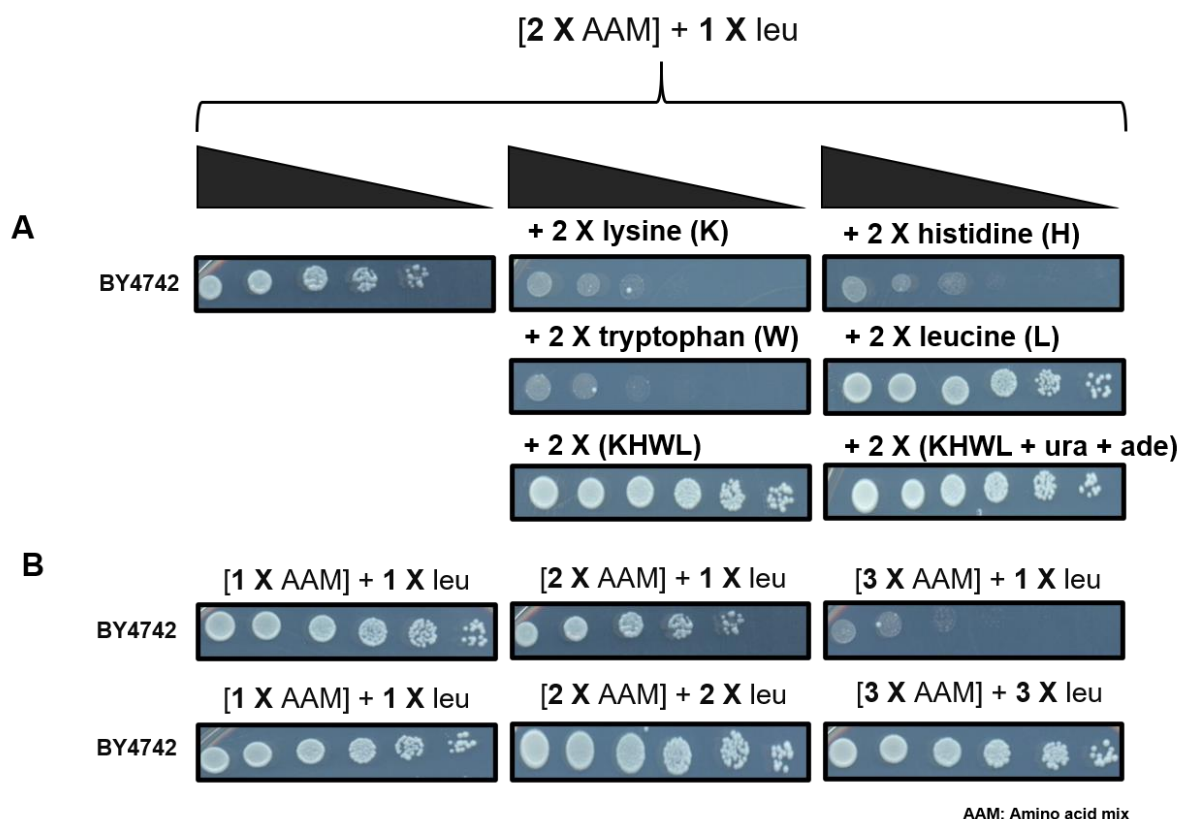


Figure 14: Increase in extracellular leucine amounts relative to increase in AAM, also rescues the growth phenotype. A: Other medium components, along with a double amount of amino acid dropout mix [2 X AAM], were increased two folds either individually or all together with uracil and adenine. **B:** In addition to the increase in amino acid dropout mix, the amount of leucine was also increased in proportion to the AAM while making the plates. In the top row, which served as a control, the amount of Leucine was kept constant. BY4742 strain was cultured overnight in HC medium, diluted the next day, and grown to log phase. Cells were harvested, washed, fivefold serially diluted, and spotted on different plates (as described above), containing 2% glucose as carbon substrate. The plates were scanned following incubation at 30°C for 42 hours. The top black bar corresponds to the decreasing cell density from left to right. This figure is one of the representative examples from two independent experiments performed on different days.

So far, it was observed that the re-establishment of the leucine biosynthetic pathway or increasing leucine in proportion to the increase in amino acid dropout mix (AAM) in the medium could rescue the observed slow growth phenotype. These results further raised the possibility that whether the observed phenotypes could be explained by the fact that cells cannot import enough leucine? Is there a leucine limitation under such growth conditions?

3.1.5 Deletion or overexpression of amino acid permeases does not affect the amino acid dependent observed growth phenotype

To gain more insights into the possibility of leucine limitation, which might explain the observed growth phenotype, genes encoding different amino acid permeases (AAPs), responsible for transporting specific or general amino acids across the plasma membrane in a yeast cell, were either deleted or overexpressed.

The high-affinity branched-chain AAP Bap2 with its paralog Bap3 is known to transport the branched-chain amino acids leucine, isoleucine and valine across the plasma membrane¹⁹⁷. It is also reported that in wild-type yeast, Bap2 also transports phenylalanine in the presence of leucine¹⁹⁸. Agp1 is a low-affinity broad-spectrum amino acid transporter whose expression is also induced by the presence of several extracellular amino acids¹⁹⁹. Both Agp1 and Gap1 play a substantial role in the transport and utilization of several amino acids, unlike the Put4 or Can1 amino acid transporters which transports selected amino acids (proline and arginine, respectively)¹⁹⁹. As mentioned before, expression of Gap1 permease is induced upon the presence of poor nitrogen source and is further tightly controlled at post-translational level^{198,200}. With these insights from literature about the expression of amino acid permeases in yeast, I chose to initially delete and overexpress the *AGP1*, *GAP1* and *BAP2* genes and study their effect on the observed growth phenotype.

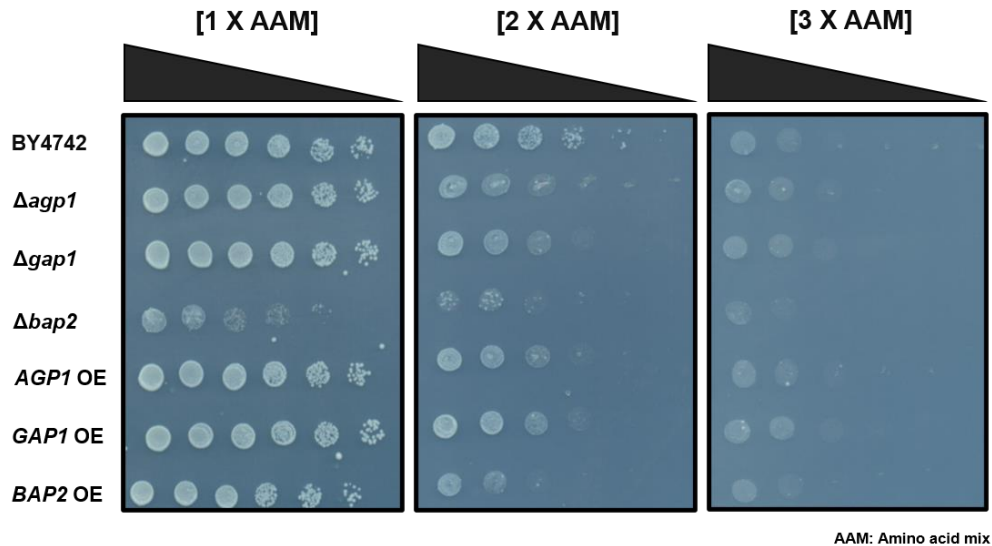


Figure 15: Deletion and overexpression of genes encoding the amino acid permeases *Agp1*, *Gap1* or *Bap2* have no striking effect on the observed growth phenotype. Strains with either deletion or over-expression of amino acid permeases genes *AGP1*, *GAP1* and *BAP2* were generated using homologous recombination. All the different yeast strains were cultured overnight in HC medium, diluted the next day, and grown to log phase. Cells were harvested, washed, fivefold serially diluted, and spotted on different plates (as described above), containing 2% glucose as carbon substrate. The plates were scanned following incubation at 30°C for 42 hours. The top black bar corresponds to the decreasing cell density from left to right. This figure is one of the representative examples from at least three independent experiments performed on different days.

As observed from figure 15, knockout and overexpression of AAP's Agp1 and Gap1 had no striking effect on the growth phenotype upon the increase in amino acid content in the growth medium. Further, both deletion and overexpression of Bap2 resulted in more slow growth of the yeast cell. It was complicated to interpret this result. It is known that the transcriptional regulation of several amino acid permeases is influenced by the presence of different nitrogen sources in the medium. Additionally, several adaptor proteins for different permeases whose expression levels and activity are further known to regulate the post-translational targeting of amino acid permeases to the plasma membrane⁴⁸. Hence, simply overexpressing an amino acid permease gene doesn't ensure overexpression of these transporters on the plasma membrane. Further, different experimental approaches are needed to confirm and validate the over expression of AAP's on the plasma membrane. It is still complicated to rule out transport competition of several amino acids like phenylalanine with leucine in the current growth conditions. Surprisingly, the deletion of Agp1 and Gap1 did not further influence the observed growth phenotype. If limited leucine import would have led to the observed growth phenotype, the deletion of genes encoding Agp1 and Gap1 would severely impact the growth phenotype upon the increase in amino acid content in the medium. However, these results nonetheless hinted that the observed growth phenotype might not be the result of the leucine limitation case *per se*.

3.1.6 The main bad guys: Ehrlich amino acids are inducing the impaired growth phenotype

So far, it was interesting to observe that how the presence of increased amino acid dropout mix affected the growth of auxotrophic yeast cells. Also, either restoration of functional leucine pathway or increasing leucine in proportion to that of the amino acid dropout mix could rescue this growth phenotype. I further wondered how the composition of the amino acid dropout mix contributed to this growth phenotype. Is the growth phenotype dependent on one or more specific amino acids, or is it simply an effect of amino acid mix in general? The amino acid dropout mix consists of ten amino acids: threonine, arginine, serine, glutamate, aspartate, methionine, isoleucine, valine, phenylalanine, and tyrosine. The growth of the BY4742 yeast strain was determined in the growth conditions where all the ten amino acids (present in the amino acid dropout mix) were either omitted individually (fig: 16) or increased to three times individually (fig: 17).

Interestingly, missing only a few amino acids (namely Ehrlich amino acids: methionine, phenylalanine, tyrosine, isoleucine, and valine) from the amino acid dropout mix contributed slightly to rescuing the growth phenotype of BY4742 (fig: 16) as compared to control (top row HC; fig: 16), where all amino acids were present. Also, omitting glutamate from the growth medium severely impacts the growth of BY4742.

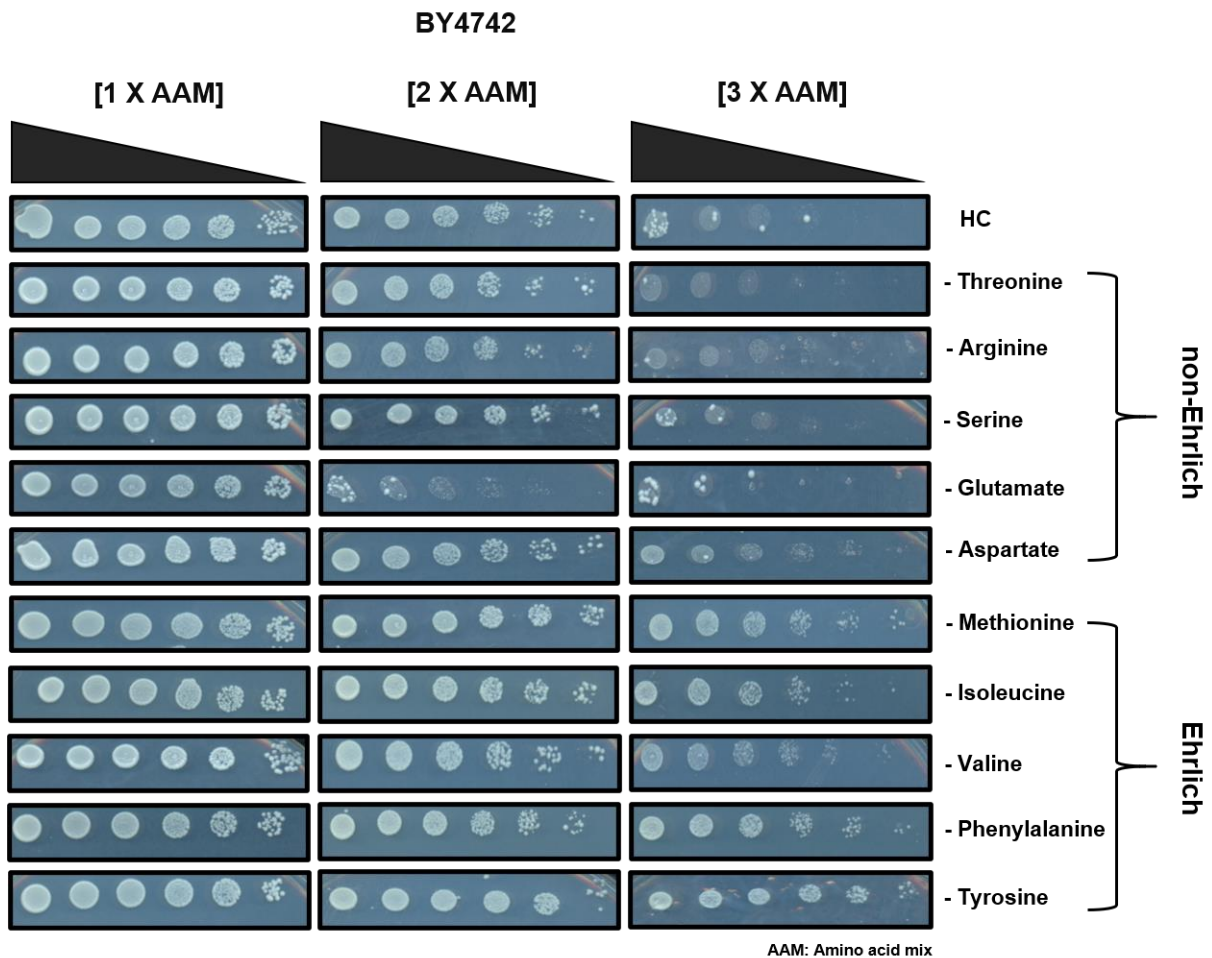


Figure 16: Removing Ehrlich amino acids individually from the amino acid mix affects cell growth. Ehrlich and non-Ehrlich amino acids were removed individually from the amino acid dropout mix, and plates were made further with these respective conditions. The top row HC, where all the ten amino acids were present in the amino acid dropout mix, served as a control. BY4742 strain was cultured overnight in HC medium, diluted the next day, and grown to log phase. Cells were harvested, washed, fivefold serially diluted, and spotted on different plates (as described above), containing 2% glucose as carbon substrate. The plates were scanned following incubation at 30°C for 42 hours. The top black bar corresponds to the decreasing cell density from left to right. This figure is one of the representative examples from at least three independent experiments performed on different days.

Likewise, increasing concentration of individual Ehrlich amino acids only in the growth medium to three times, where others were present in a standard concentration, also had a minor impact on the growth phenotype of the BY4742 yeast strain (fig: 17). These results gave a strong hint that Ehrlich amino acids could be the real causative agents inducing the observed growth phenotype on 2 X AAM and 3 X AAM growth conditions.

Amino acids like phenylalanine, methionine, tyrosine, tryptophan, and branched-chain amino acids: isoleucine, valine, and leucine are classified as Ehrlich amino acids. Ehrlich amino acids were proposed by the famous German Biochemist Felix Ehrlich since they all share a common degradation pathway in the cell²⁰¹. Inside the yeast cell, these amino acids are transaminated, decarboxylated, and further degraded to fusel acids or alcohols, which add flavour and aroma to fermented yeast products^{43,202}. This

pathway is of utmost interest and research value in the food and beverage industry. However, the Ehrlich amino acids tryptophan and leucine do not belong to the amino acid dropout mix composition but were added separately to the medium. Therefore, they were excluded from the Ehrlich amino acid description in the following text and were used in usual amounts as described for the composition 1 X AAM condition (refer to table 3), unless specified.

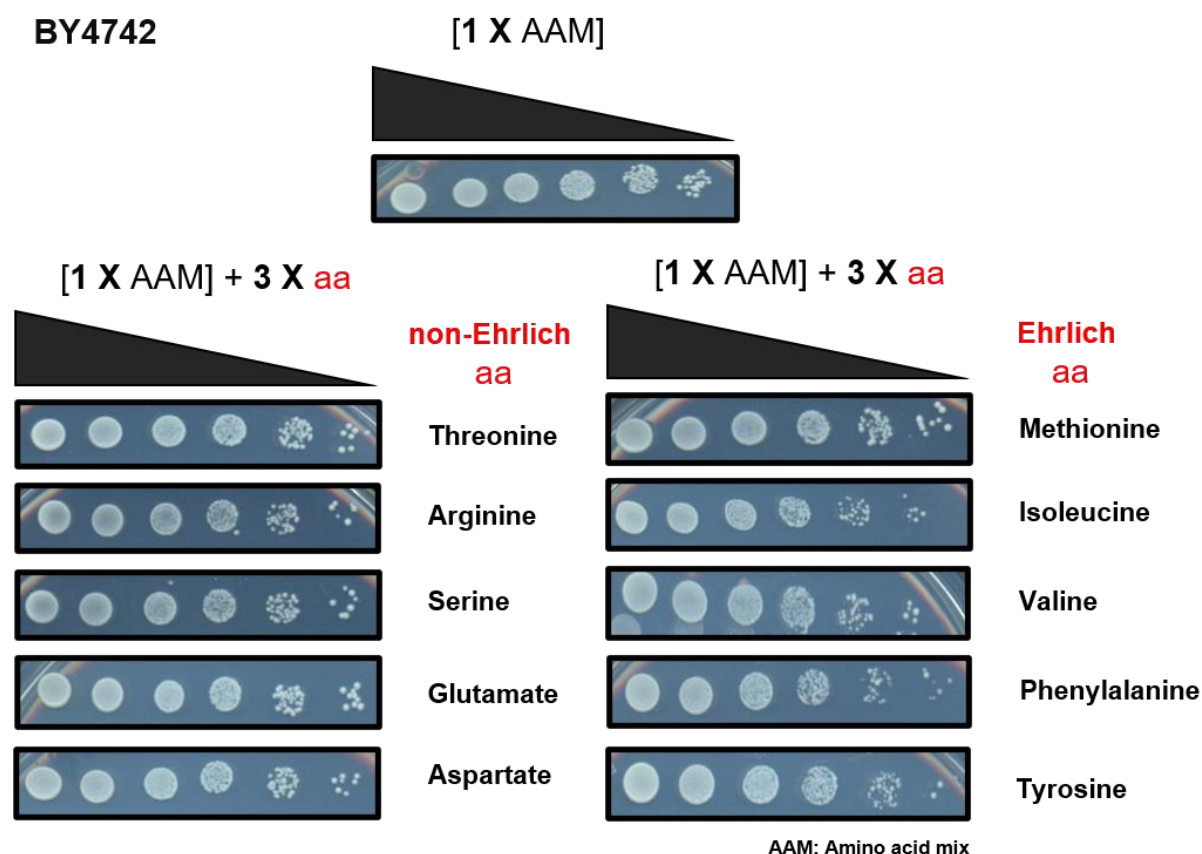


Figure 17: Increasing the amino acids of AAM individually to three times affects cell growth. Ehrlich or non-Ehrlich amino acids' concentration was increased individually to three times in the amino acid dropout mix, and plates were made further with these respective conditions. The top row 1 X AAM, where all the ten amino acids in the dropout mix were present in a standard concentration, served as a control. BY4742 strain was cultured overnight in HC medium, diluted the next day, and grown to log phase. Cells were harvested, washed, fivefold serially diluted, and spotted on different plates (as described above), containing 2% glucose as carbon substrate. The plates were scanned following incubation at 30°C for 42 hours. The top black bar corresponds to the decreasing cell density from left to right. This figure is one of the representative examples from two independent experiments performed on different days.

While investigating the effect of the composition of amino acid dropout mix on the growth of the cell, it was observed that the Ehrlich amino acids could potentially contribute to the slow growth phenotype (fig: 17; right column) of BY4742 in 2 X AAM and 3 X AAM growth conditions. To further validate this preliminary hypothesis, the effect of the composition of Ehrlich amino acids on the observed growth phenotype was studied in detail in the following section.

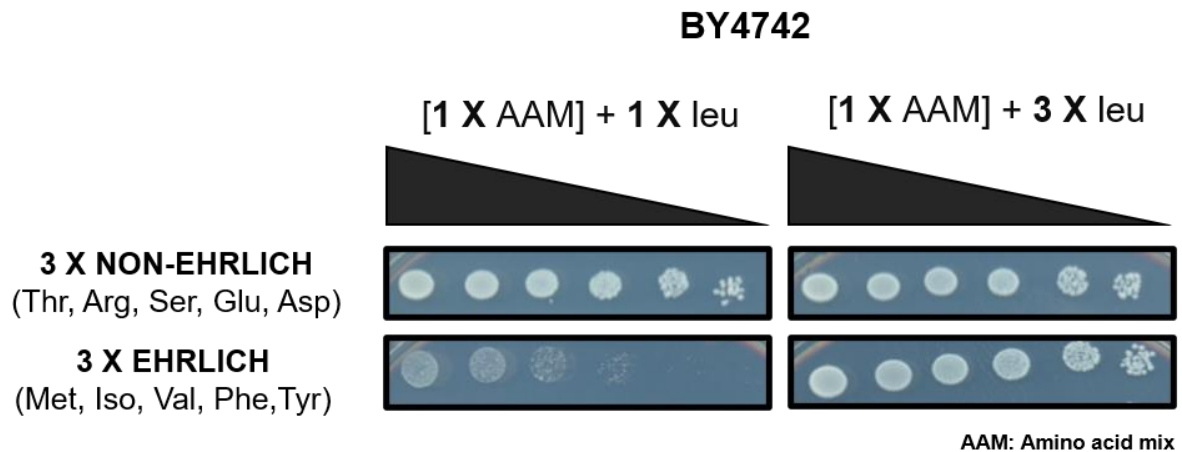


Figure 18: Increasing concentration of Ehrlich amino acids in dropout amino acid mix to three times affects cell growth. Ehrlich or non-Ehrlich amino acids' concentration was increased three times in the amino acid dropout mix, and plates were made further with these respective conditions. The second column [1 X AAM] + 3 X Leu, where leucine was added 3 times that of the usual concentration, served as a control. BY4742 strain was cultured overnight in HC medium, diluted the next day, and grown to log phase. Cells were harvested, washed, fivefold serially diluted, and spotted on different plates (as described above), containing 2% glucose as carbon substrate. The plates were scanned following incubation at 30°C for 42 hours. The top black bar corresponds to the decreasing cell density from left to right. This figure is one of the representative examples from at least three independent experiments performed on different days.

Firstly, the concentration of all Ehrlich amino acids was increased to three times while keeping the concentration of the non-Ehrlich amino acid constant as present in [1 X AAM] condition and vice versa. Interestingly, when the concentration of Ehrlich amino acids only was increased to three times in the growth medium, it resulted in a similar slow growth phenotype of BY4742. As expected, when the concentration of non-Ehrlich amino acids only was increased to three times in the growth medium, it did not affect the growth of BY4742 (fig: 18; first column, top row). As observed earlier, the increase in leucine concentration in proportion to the increase in Ehrlich amino acids in the growth medium rescued the observed growth phenotype (fig: 18; second column, bottom row) and thus served as the control.

From these findings, it was concluded that the ratio of leucine to the Ehrlich amino acids (namely methionine, isoleucine, valine, phenylalanine, and tyrosine referred to as Ehrlich amino acids in this study) was essential for the growth of the cell. Probably, any disturbance to this ratio resulted in the observed growth phenotype.

The next question to address was to figure out whether the increased concentration of which single Ehrlich amino acid or combination of which two or more Ehrlich amino acids contribute to the observed growth phenotype of BY4742? Since the concentration of these amino acids in the medium is very different (refer to table: 9, second column), it was complicated to address this question. Therefore, a new medium composition was designed which had the same components (and their concentrations)

as that of HC medium except for namely five Ehrlich amino acids (M, I, V, F, Y), whose concentration was fixed to 600 μM in the new medium (the table: 9, third column).

Table 9: The concentration of the individual Ehrlich amino acid (M, I, V, F, Y) present in HC medium supplemented with either normal [1 X AAM] and triple amount [3 X AAM] of amino acid dropout mix or in the new medium.

Ehrlich amino acids	1 X AAM Molarity (μM)	3 X AAM Molarity (μM)	New medium 1 X AAM Molarity (μM)	New medium [5 X] Molarity (μM)	New medium [10 X] Molarity (μM)
Methionine (M)	134	402	600	3000	6000
Isoleucine (I)	610	1830	600	3000	6000
Valine (V)	1280	3840	600	3000	6000
Phenylalanine (F)	303	909	600	3000	6000
Tyrosine (Y)	331	993	600	3000	6000
TOTAL MOLARITY IN MEDIUM	2658	7974	-	-	-

As expected, supplementation of standard, double, or triple amounts of Ehrlich amino acids in the new growth medium condition also severely impacted the growth of BY4742 (fig: 19A, 1 X leu). As observed earlier, the simultaneous increase in leucine concentration in proportion to the increase in Ehrlich amino acids in the new growth medium also rescued the growth phenotype (fig 19A, 2 X leu, 3 X leu) and served as the control.

Further, each of these five Ehrlich amino acids (M, I, V, F, Y) were increased individually either to five times (3000 μM , [5 X aa]) or to ten times (6000 μM , [10 X aa]) (fig: 19B). The concentration of the rest of the Ehrlich amino acids was kept constant to 600 μM , and that of non-Ehrlich amino acids was also kept the same as present originally in HC medium amino acid dropout mix [1 X AAM] (refer to the table: 2 from methods section 2.1.2). The [5 X aa] + 5 X leu condition also served as the control condition, where leucine concentration was increased to five times in proportion to the increase in individual Ehrlich amino acid in the medium. Excess of phenylalanine and tyrosine and, to a minor extend, isoleucine impacted the growth of BY4742 (fig: 19B, 1st and 2nd column). As expected, in control conditions where leucine was increased in proportion to the increase in the individual Ehrlich amino acids ([5 X aa] + 5 X leu), the BY4742 grew normally (fig: 19B, 3rd column).

Hence, it was concluded from these findings that the ratio of leucine, particularly to that of phenylalanine and tyrosine, is important for the growth of the cell.

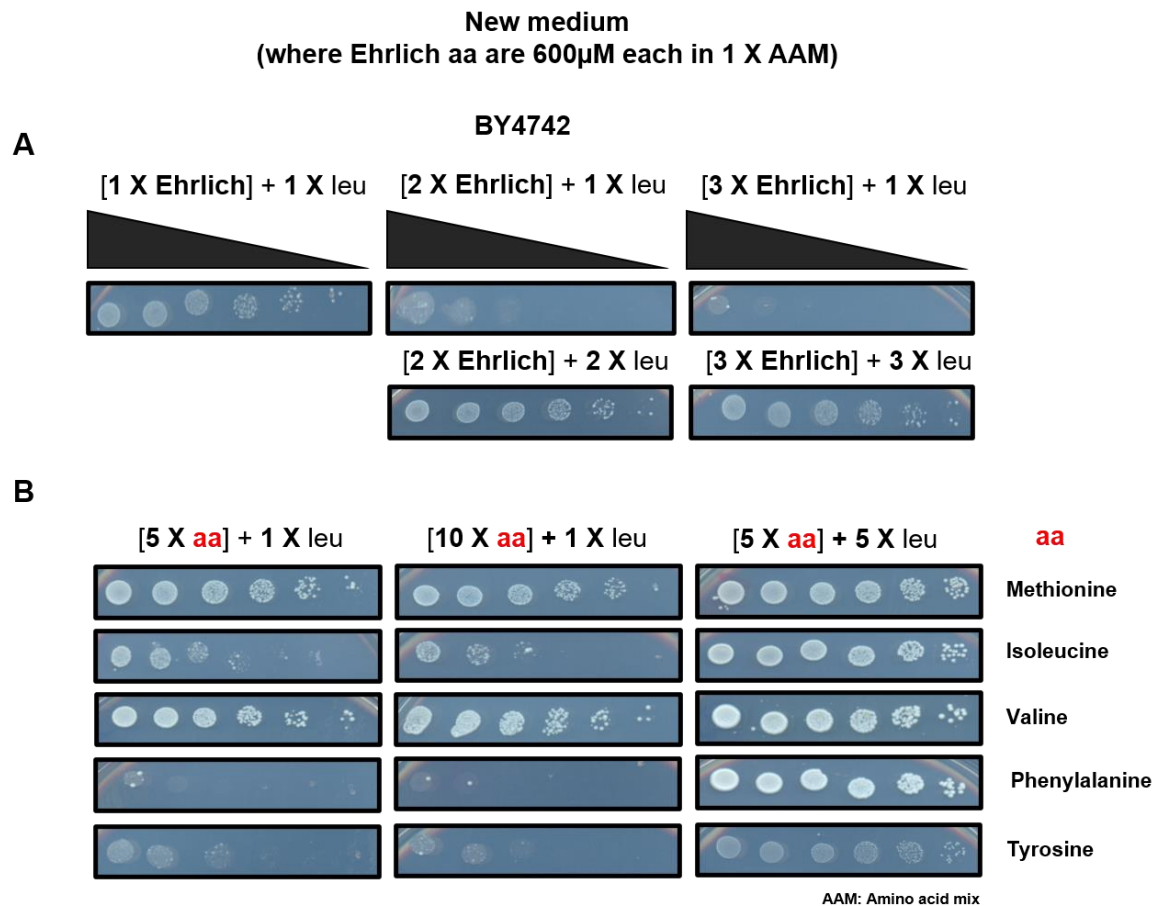


Figure 19: The concentration of Ehrlich amino acids is critical for the growth of the cell.
A: A new medium was made where the concentration of all Ehrlich amino was set to 600 μ M. Further, average, double, or triple amounts of this new dropout mix were added while making plates, where leucine concentration was kept constant. The second row, where leucine's concentration was increased proportionally along with the new dropout mix while making plates, served as a control. **B:** Further different dropout mixes were made. The concentration of all Ehrlich amino acids was set to five times (5 X corresponding to 3000 μ M) or ten times (10 X corresponding to 6000 μ M) individually. The remaining amino acids were present in their average concentration. Further, plates were made with these respective dropout mixes, where leucine concentration was kept constant. The third column served as a control where leucine concentration was increased proportionally along with a new dropout mix while making plates. BY4742 strain was cultured overnight in HC medium, diluted the next day, and grown to log phase. Cells were harvested, washed, fivefold serially diluted, and spotted on different plates (as described above), containing 2% glucose as carbon substrate. The plates were scanned following incubation at 30°C for 42 hours. The top black bar corresponds to the decreasing cell density from left to right. This figure is one of the representative examples from two independent experiments performed on different days.

3.1.7 Deep insights about intracellular amino acids levels of BY4742 strain

So far, it was observed that the increased presence of Ehrlich amino acids in the growth medium, namely phenylalanine and tyrosine, contributed to the observed growth phenotype of the BY4742. This result further leads to an intriguing question:

whether the leucine transport across the plasma membrane is hampered, possibly due to competition between leucine and the Ehrlich amino acids (mainly phenylalanine and tyrosine), which could be leading to the observed growth phenotype? It is also known that the leucine transport across the human blood-brain barrier is competitively inhibited by the transportation of the large neutral amino acids (tyrosine, phenylalanine, isoleucine, valine, histidine, methionine, glutamine, and threonine) through their common transporter, the Lat1^{119,131,203}. From our previous observations, even though we already have the hint that it is probably not the leucine limitation case from deletion of AAP's Agp1 and Gap1 (section 3.1.5: fig: 15). It was crucial to address the possibility of transport competition for leucine and other Ehrlich amino acids by investigating the amino acid levels in the current study.

To gain further insights into the relevance of leucine limitation possibility underlying the observed growth phenotype upon the increase in the amino acid content in the growth medium. The imported versus *de novo* synthesized fraction and total free intracellular amino acid levels in the cells were investigated in collaboration with the Wittman group at the Saarland University. Since BY4742 transformed with p415 empty vector (*LEU2*) did not exhibit the growth phenotype (fig: 13), it was used as a control for these studies.

3.1.7a Imported versus *de novo* synthesized amino acids

The BY4742 and BY4742+*LEU2* were grown in a medium supplemented with ¹³C labelled glucose until they reached the required cell density and then were harvested using a fast filtration procedure and processed for ¹³C enrichment analysis. Amino acids (fig: 20), which were synthesized *de novo*, incorporated labelled ¹³C (represented by blue coloured bars), and the amino acids which were imported from the medium remained unlabelled (represented by grey coloured bars). Keeping in mind that this approach was a qualitative analysis, one cannot get information about the absolute levels of amino acids that were either synthesized *de novo* or imported. Nevertheless, these results indicated that under 2 X AAM growth condition, the yeast cell synthesized more amino acids, such as alanine, glycine, valine, methionine, serine, threonine, cysteine, and tyrosine *de novo*, relative to the amounts imported from the medium as compared to the 1 X AAM condition (fig: 20). Since the BY4742 yeast strain of *S. cerevisiae* is auxotrophic for lysine, histidine, and leucine, they were imported completely from the medium.

Interestingly, BY4742 synthesized massive levels of valine, as compared to BY4742 +*LEU2*, which synthesized both valine and leucine on 2 X AAM. It was inferred that on 2 X AAM growth condition, BY4742 cells tried to make leucine, but since they missed *LEU2* and could not synthesize leucine. Therefore, they ended up synthesizing massive levels of valine instead. Whereas for BY4742+*LEU2*, which had the leucine biosynthetic pathway restored, synthesized more of leucine and relatively fewer levels of valine on 2 X AAM growth condition. In conclusion, these results firmly pointed out that the leucine and valine synthesis pathway are triggered on 2 X AAM growth condition. Nonetheless, it could still be the case of transport competition between leucine and Ehrlich amino acids, which could possibly be leading to the observed slow growth phenotype.

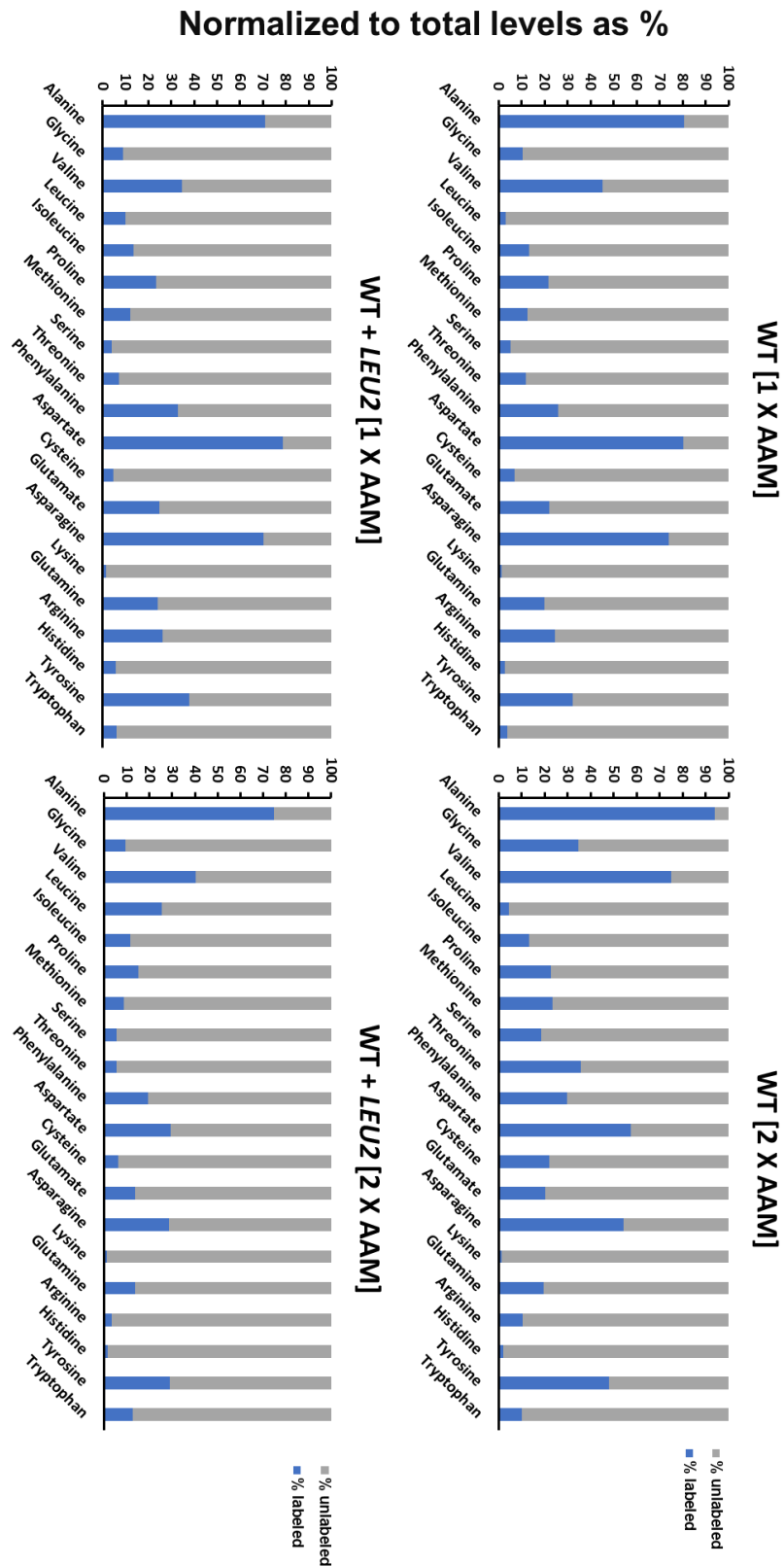


Figure 20: Relative fraction of proteinogenic amino acids synthesized de novo versus imported fraction from the medium when cells were fed with ^{13}C glucose for BY4742 and wt+LEU2 on 1 X AAM and 2 X AAM. BY4742 and BY4742 transformed with p415 empty vector (LEU2) were cultured overnight in HC medium and were inoculated in fresh HC medium the next day (with normal [1 X AAM] and double amount [2 X AAM] of amino acid dropout mix), supplemented with ^{13}C glucose and grown to late exponential phase. The following day, using

a fast filtration procedure, cells were harvested on a filter membrane, which was quickly collected in a box (with 2 mL of dH₂O) and further subjected to incubation at 100 °C for 15 min and subsequently cooled on ice for 10 min. The cell lysate was collected and cleared of cell debris by centrifugation. Further, the free amino acids present in the cellular lysate were dried under Nitrogen stream, pre-derivatized with MBDSTFA, and ¹³C enrichment was quantified using GC-MS. The graphs represent labelled and unlabelled fractions of individual amino acids, in the form of percentages normalized to total levels, generated from the average of three independent biological replicates. The unlabelled fraction of amino acid imported from the medium is represented in grey. In contrast, labelled fraction, which is *de novo* synthesized in the cell, is represented in blue. Data were corrected for naturally occurring isotopes. In this experiment, I prepared the different cell lysates, which were further processed and analyzed by Dr Michael Kohlstedt (Wittman's group, at the Saarland University) as a part of the collaboration work.

3.1.7b Total intracellular arginine levels are increased as an effect of 2 X AAM

It was not possible to quantify the absolute amounts of both *de novo* synthesized and the imported fraction of amino acids from ¹³C enrichment studies. The total free intracellular amino acid levels in the cells were investigated. The cells were grown to reach the required cell density, harvested using a fast filtration procedure and processed for intracellular amino acid analysis. Alpha-amino butyric acid was used as an internal standard during the harvesting procedure to quantify amino acid levels. Sky blue, orange, dark blue and green coloured bars in figure: 21, represented the free intracellular amino levels from BY4742 [1 X AAM], BY4742 [2 X AAM], BY4742+LEU2 [1 X AAM] and BY4742+LEU2 [2 X AAM] respectively. Interestingly, there was no change in the total intracellular amounts of leucine and valine in BY4742 and BY4742 +LEU2 on 1 X AAM vs 2 X AAM growth condition. If Ehrlich amino acids were competing with leucine during cellular import, there would have been a drop in the total intracellular levels of leucine, which was not the case. This finding completely ruled out the possibility of leucine limitation and its potential contribution towards the observed growth phenotype. Secondly, only the levels of arginine changed significantly on 2 X AAM growth condition in BY4742 cells. In combination with the relative information for imported versus the synthesized fraction of amino acids in the cells (fig: 21), it was inferred that BY4742 imported massive arginine levels on 2 X AAM growth condition. Secondly, these results also supported the idea that leucine and valine synthesis was triggered on 2 X AAM growth condition.

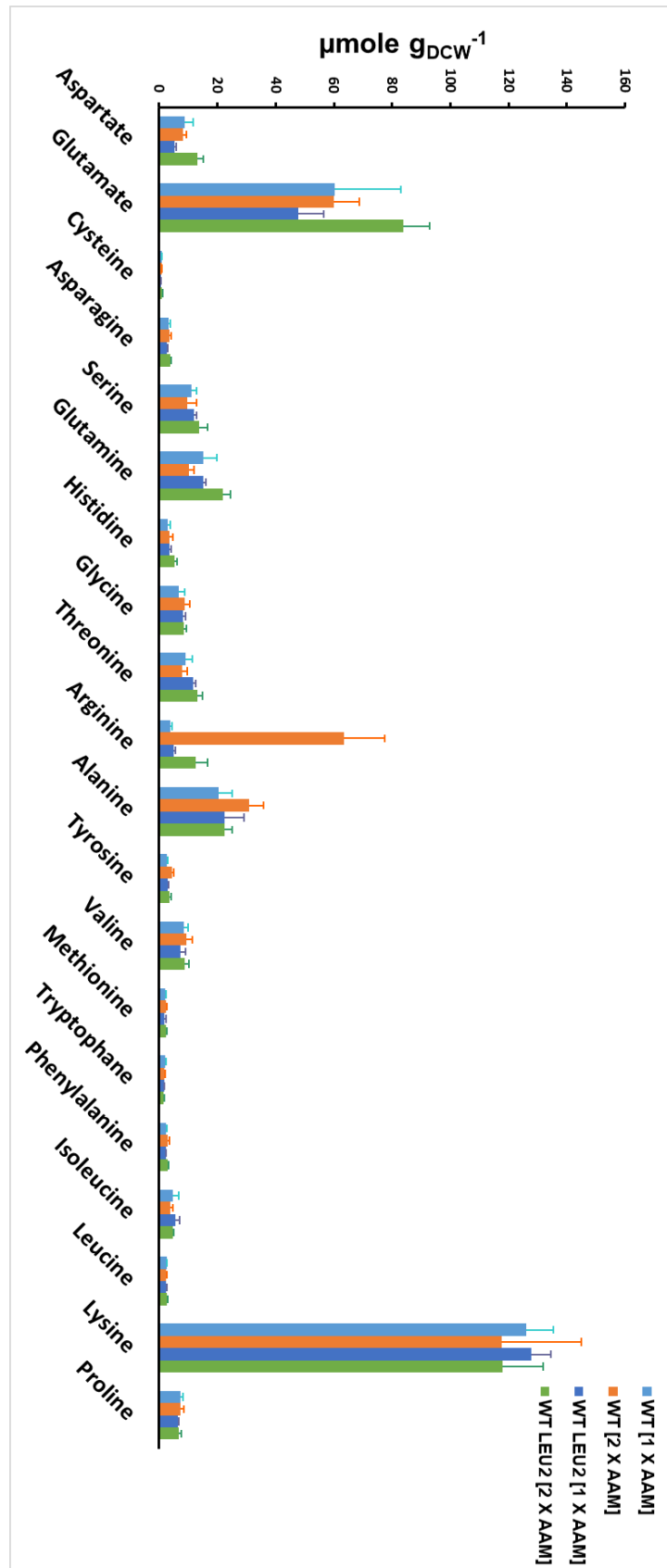


Figure 21: Total free intracellular amino acid levels in BY4742 and BY4742+LEU2 on 1 X AAM and 2 X AAM. BY4742 and BY4742 transformed with p415 empty vector (*LEU2*) were cultured overnight in HC medium and inoculated in fresh HC medium (with normal [1 X AAM] and double amount [2 X AAM] of amino acid dropout mix) the next day were and grown till late

exponential phase. The following day, using a fast filtration procedure, cells were harvested on a filter membrane, which was quickly collected in a box (with the appropriate amount of alpha-amino butyric acid, as internal standard, in 2 mL of dH₂O) and further subjected to incubation at 100 °C for 15 min, cooled on ice for 10 min. The cell lysate was collected and cleared of cell debris by centrifugation. The clear lysate was injected and simultaneously was mixed with reagents and derivatized in an automated way and quantified using HPLC. The graphs represent individual amino acid levels (µmol per cell density weight) generated from an average of three independent biological replicates. Sky blue, orange, dark blue and green coloured bars represent free intracellular amino levels from BY4742 [1 X AAM], BY4742 [2 X AAM], BY4742+LEU2 [1 X AAM] and BY4742+LEU2 [2 X AAM] respectively. In this experiment, I prepared the different cell lysates, which were further processed and analyzed by Dr Michael Kohlstedt (Wittman's group, at the Saarland University) as a part of the collaboration work.

3.2 Activation of branched-chain amino acid biosynthetic pathway correlates positively with the amino acid dependent growth phenotype of the yeast cell

Leucine, valine, and isoleucine are known as branched-chain amino acids and share partial steps of their synthesis in mitochondria and cytosol¹⁴⁰ (fig: 22). Interestingly, both leucine and valine pathways seem to be activated in the presence of [2 X AAM]. Further, the growth of different yeast strains were studied in response to the increased amino acid content in the growth medium on non-fermentable carbon sources glycerol.

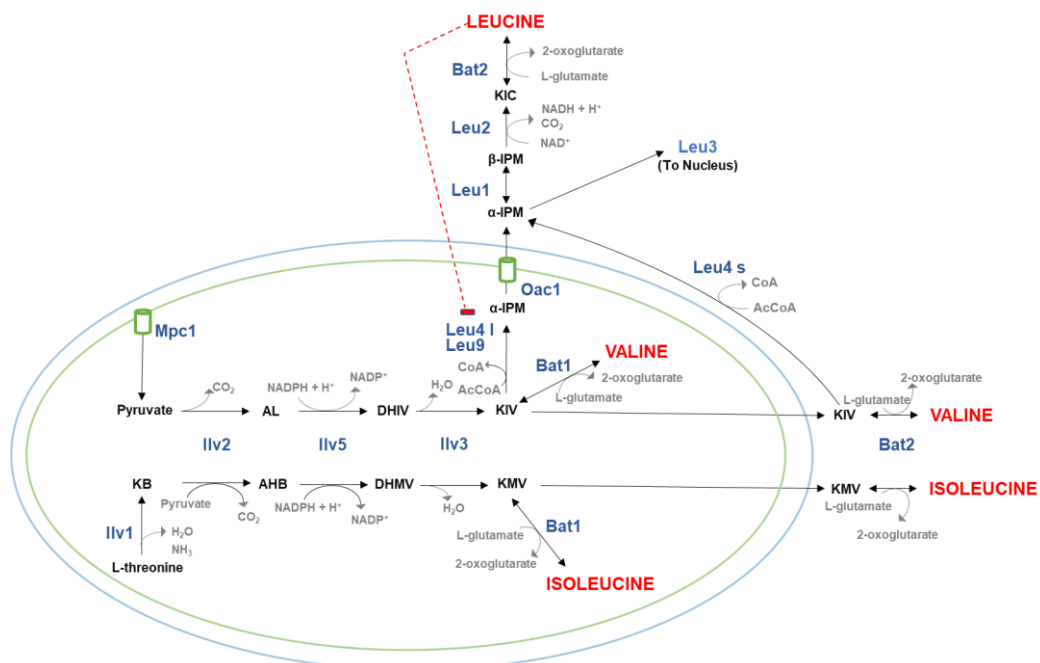


Figure 22: Schematic diagram showing the branched-Chain amino acid biosynthetic pathway in *Saccharomyces cerevisiae*. Leucine and valine are synthesized from pyruvate, and isoleucine is synthesized from ketobutyrate, derived from threonine. The intermediates KIV or KMB can be transported out of mitochondria and converted to valine and isoleucine, respectively. KIV can also be converted to α -IPM in the mitochondria, which is further converted to leucine in the cytoplasm. The blue coloured labels are the enzymes that catalyze

the different steps during the synthesis of the BCaa. The double arrow depicts that the respective enzymes Bat1 and Bat2 can catalyze the reaction in both directions. The enzymes and the intermediates involved and formed respectively, in the BCaa pathway are as follows: Ilv1: threonine deaminase, Ilv2: acetohydroxy acid synthase-catalytic subunit, Ilv5: acetohydroxy acid reductoisomerase, Ilv3: dihydroxy acid dehydratase, Bat1 and Bat2: mitochondrial and cytosolic branched-chain amino acid aminotransferases, Leu4 and Leu9: α -isopropyl malate synthase I and II respectively where I and s represent the long and the short form of Leu4, Leu1: α -isopropyl malate isomerase, Leu2: β -isopropyl malate dehydrogenase, AL: acetolactate, DHIV: α,β -dihydroxyisobutyrate, KB: α -ketobutyrate, AHB: α -aceto α -hydroxybutyrate, DHMV: α,β -dihydroxy β -methyl valerate, KIV: α -keto-isovalerate, KMV: α -keto β -methyl valerate, α -IPM: α -isopropyl malate, β -IPM: β -isopropyl malate and KIC: α -keto-isocaproate. Mpc1 and Oac1: mitochondrial pyruvate carrier and oxaloacetate carrier1 are the membrane transporters for pyruvate and α -IPM.

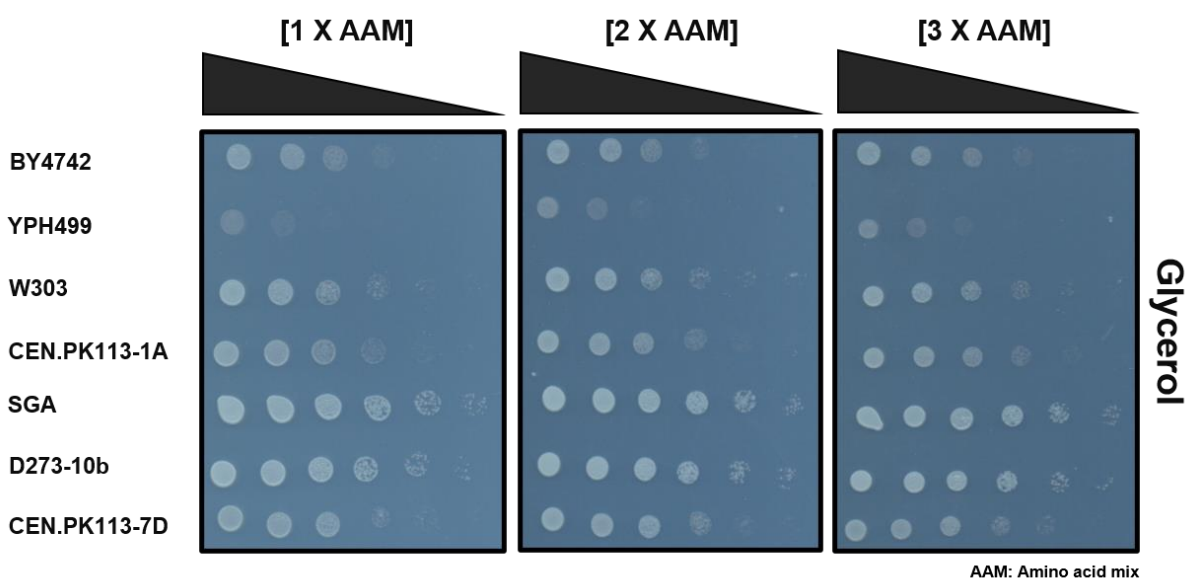


Figure 23: The growth phenotype is lost when cells are forced to respire. All strains were cultured overnight in HC medium, diluted the next day, and grown to log phase. Cells were harvested, washed, fivefold serially diluted, and spotted on plates containing normal [1 X AAM], double [2 X AAM] or triple [3 X AAM] amount of amino acid dropout mix, containing 2% glycerol as carbon substrate. The plates were scanned following incubation at 30°C for 42 hours. The top black bar corresponds to the decreasing cell density from left to right. This figure is one of the representative examples from at least three independent experiments performed on different days.

Interestingly, unlike in the presence of glucose, when cells are forced to respire using glycerol as a carbon substrate, all the auxotrophic, and prototrophic strains grew similar to each other on 2 X AAM and 3 X AAM growth condition (fig: 23). Auxotrophic yeast strains tend to lose their amino acid dependent growth phenotype while consuming the non-fermentable carbon source. As expected, all the yeast strains grew comparatively slower on glycerol than on glucose as fermentation is known to promote faster growth^{204,205}. However, why and how the amino acid dependent slow growth phenotype is lost when cells are forced to respire, unlike in the presence of glucose as the carbon substrate, cannot be explained at this moment.

3.2.1 Role of valine and isoleucine on the growth of cell

Despite the presence of increased extracellular amino acids in the growth medium, BY4742 synthesized massive levels of valine on 2 X AAM. Either restoration of functional leucine biosynthetic pathway or extra supplementation of leucine in the medium rescued the cells from the observed growth phenotype. These findings indicated that the branched-chain amino acid biosynthetic pathway must play an essential role in response to the increased amino acid content in the growth medium. Therefore, I further investigated the relevance of the BCaa pathway towards the observed growth phenotype.

The other two branched-chain amino acids- namely valine and isoleucine, are also present in the amino acid dropout mix. As a first approach, I omitted these two amino acids (in combination) from the amino acid mix and studied the effect on cell growth. Surprisingly, removing valine and isoleucine from the medium made the growth of BY4742 better on 2 X AAM and 3 X AAM (fig: 24), as compared to the control where valine and isoleucine were still available in the growth medium. These results enormously strengthen the idea that the BCaa pathway plays an important role in the growth of auxotrophic yeast cells in response to increased amino acid content in the medium.

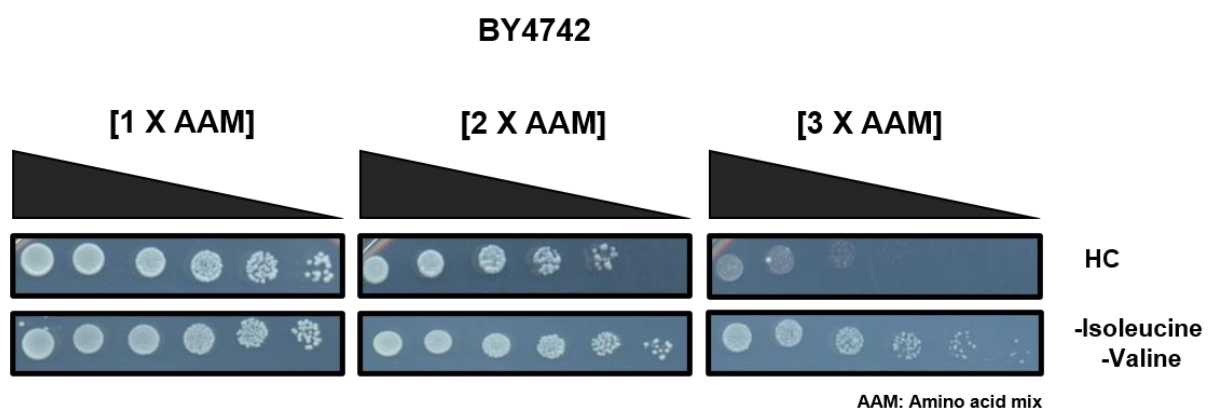


Figure 24: Removing isoleucine and valine from the medium rescues the growth phenotype. Isoleucine and valine were removed from the amino acid dropout mix, and other plates were made using the double or triple amount of this dropout mix. The top row HC, with all the ten amino acids in the amino acid dropout mix, served as a control. BY4742 strain was cultured overnight in HC medium, diluted the next day, and grown to log phase. Cells were harvested, washed, fivefold serially diluted, and spotted on different plates (as described above), containing 2% glucose as carbon substrate. The plates were scanned following incubation at 30°C for 42 hours. The top black bar corresponds to the decreasing cell density from left to right. This figure is one of the representative examples from at least three independent experiments performed on different days.

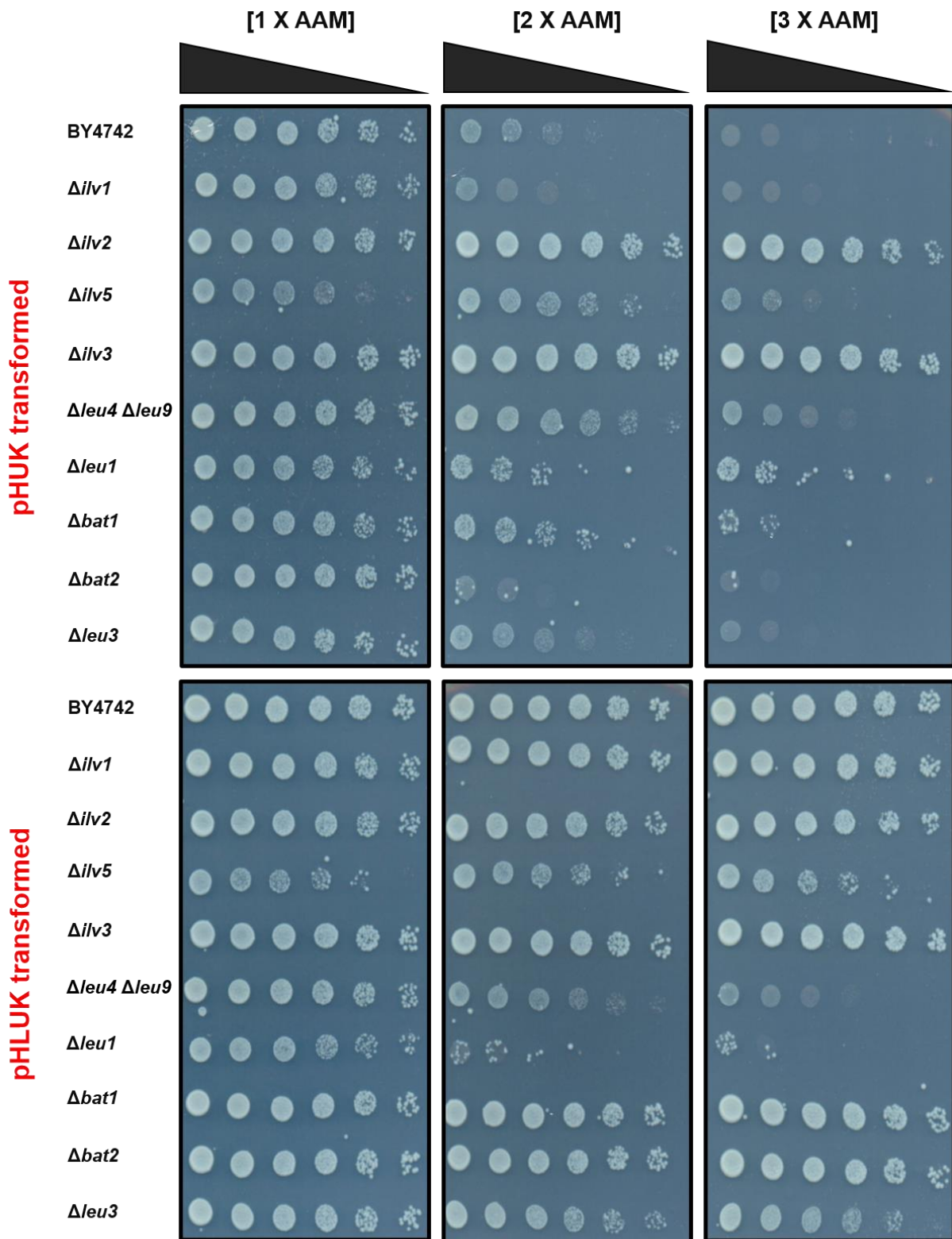
3.2.2 Deleting either *ILV2* or *ILV3* rescues the growth phenotype

The branched-chain amino acid biosynthetic pathway is conserved in yeast, plants, and bacteria^{134–138}. During evolution, humans have lost the capability to make BCaa. As they are essential amino acids, they have become indispensable in the human diet. Synthesis of isoleucine and valine occur in mitochondria or the cytoplasm¹⁴⁰. However, leucine synthesis only occurs in the cytoplasm after its key intermediate alpha-isopropyl malate (α -IPM) is transported across the mitochondrial membrane via oxaloacetate carrier 1 (Oac1) transporter²⁰⁶. The detailed steps of the BCaa synthesis pathway are summarized in figure 23.

To gain more insights into the role of the BCaa biosynthetic pathway in response to the increased extracellular amino acids, I sequentially deleted the genes encoding proteins that catalyzed the different enzymatic steps in the BCaa pathway and studied their effect on the observed growth phenotype. Thus, several mutants of the BCaa pathway were made during this study via homologous recombination.

Since these mutants were constructed in a BY4742 genetic background (which also lacks *LEU2*, whose product is known to be involved in the leucine biosynthesis pathway), it was necessary to transform all these mutants with a plasmid containing the missing *LEU2*. This control assured that the growth effect observed corresponded to a single-gene deletion and is not due to the additive effect of the *LEU2* deletion. I transformed all the BCaa mutants with pHLUK plasmid¹⁶⁶ and selected them using the histidine (*HIS3*) marker gene. Further, pHUK plasmid¹⁶⁶ transformed yeast deletion strains served as a control for the corresponding pHLUK transformed cells. As observed from figure 25, the growth of either pHUK or pHLUK transformed BCaa mutants depicted an exciting pattern. Deleting either *ILV2* or *ILV3* rescued the slow growth phenotype of BY4742 on 2 X AAM or 3 X AAM growth conditions.

Similarly, deletion of any gene downstream of *ILV3* exhibited the observed growth phenotype like BY4742 in 2 X AAM and 3 X AAM growth conditions. Interestingly, the mutant $\Delta ilv1$ also retained the slow growth phenotype like BY4742, implying that isoleucine synthesis or its intermediates have no contribution towards the observed phenotype. Deleting *ILV5* also made the cell grow better on 2 X AAM and 3 X AAM but not entirely as compared to $\Delta ilv2$ and $\Delta ilv3$ deletion cells. This is plausible as *Ilv5* performs a dual function inside the cell, i.e., alongside its role in the BCaa synthesis pathway, it is also known to bind and stabilize the mt DNA²⁰⁷. It was also observed that only the pHUK transformed double mutant $\Delta leu4 \Delta leu9$ grew better than its BY4742 counterpart, but not comparable to $\Delta ilv2$ and $\Delta ilv3$ deletions. To understand the growth of the double mutant $\Delta leu4 \Delta leu9$ more clearly, the growth of these BCaa mutants was also monitored after 24 hours. I observed that after 24 hours of growth, only the $\Delta ilv2$ and $\Delta ilv3$ strains but not the $\Delta leu4 \Delta leu9$ strain were growing faster than BY4742 (supplementary figure 57). Hence, we could conclude that deleting any gene upstream and including *ILV3* rescued the amino acid dependent growth phenotype of BY4742 on 2 X AAM and 3 X AAM. This result also strengthened our previous idea that leucine starvation is not the underlying cause for the observed growth phenotype. If a transport competition between leucine and Ehrlich amino acids in the current scenario had occurred, $\Delta ilv3$ mutant would have suffered like BY4742 upon increasing amino acid content in the growth medium, which was not the case.



BY4742: MAT α his3 Δ 1 leu2 Δ 0 lys2 Δ 0 ura3 Δ 0

pHLUK: plasmid encoding *HIS3 LEU2 LYS2 URA3*

pHUK: plasmid encoding *HIS3 LYS2 URA3*

Figure 25: Deleting *ILV2* or *ILV3* rescues the growth of cells in conditions with increased amino acid content. Several mutants of the BCaa pathway were made during this study via homologous recombination. To restore the missing *LEU2*, which also belongs to this BCaa

pathway, the BY4742 and all mutants were transformed with either pHUK or pHLUK plasmids. All the transformed strains were cultured overnight in HC (minus histidine, to maintain the plasmid selection), diluted the next day, and grown to log phase. Cells were harvested, washed, fivefold serially diluted, and spotted on plates containing normal [1 X AAM], double [2 X AAM] or triple [3 X AAM] amount of amino acid dropout mix (without histidine to maintain the selection for cells transformed with plasmids), containing 2% glucose as carbon substrate. The plates were scanned following incubation at 30°C for 42 hours. The top black bar corresponds to the decreasing cell density from left to right. This figure is one of the representative examples from at least three independent experiments performed on different days.

There seems to be a switch point around the *Ilv3* catalyzed step that could completely switch the observed growth phenotype of BY4742 on 2 X AAM and 3 X AAM growth conditions on or off. If this preliminary hypothesis holds true, the overexpression of *ILV3* must be able to exhibit the previously observed growth phenotype in contrast to the deletion of *ILV3*. Interestingly, when *Ilv3* was expressed under the control of the TEF promoter, the overexpression of *ILV3* leads to even slower growth of cells than BY4742 on 2 X AAM and 3 X AAM (fig: 26).

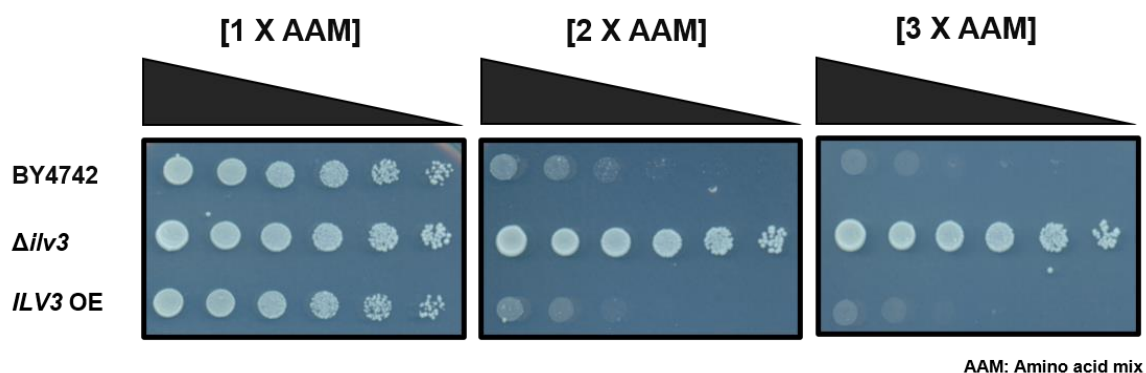


Figure 26: *ILV3* as a potential switch point for the growth phenotype. To verify the rescuing phenotype of the *ILV3* deletion, an *ILV3* overexpression strain was generated using homologous recombination. All strains were cultured overnight in HC medium, diluted the next day, and grown to log phase. Cells were harvested, washed, fivefold serially diluted, and spotted on plates containing normal [1 X AAM], double [2 X AAM] or triple [3 X AAM] amount of amino acid dropout mix, containing 2% glucose as carbon substrate. The plates were scanned following incubation at 30°C for 42 hours. The top black bar corresponds to the decreasing cell density from left to right. This figure is one of the representative examples from at least three independent experiments performed on different days.

Thus, it was concluded that the *Ilv3* catalyzed step is the potential switch point for the growth phenotype in response to the increased amino acid content in the growth medium. Therefore, in the following experiments, a $\Delta ilv3$ strain was used as a positive control, whose growth is unaffected in 2 X AAM or 3 X AAM growth condition compared to the growth of BY4742. Next, I also investigated the imported versus the *de novo* synthesized amino acids fraction and the total intracellular amino acid levels in a $\Delta ilv3$ deletion strain compared to BY4742, grown on 1 X AAM and 2 X AAM.

Normalized to total levels as %

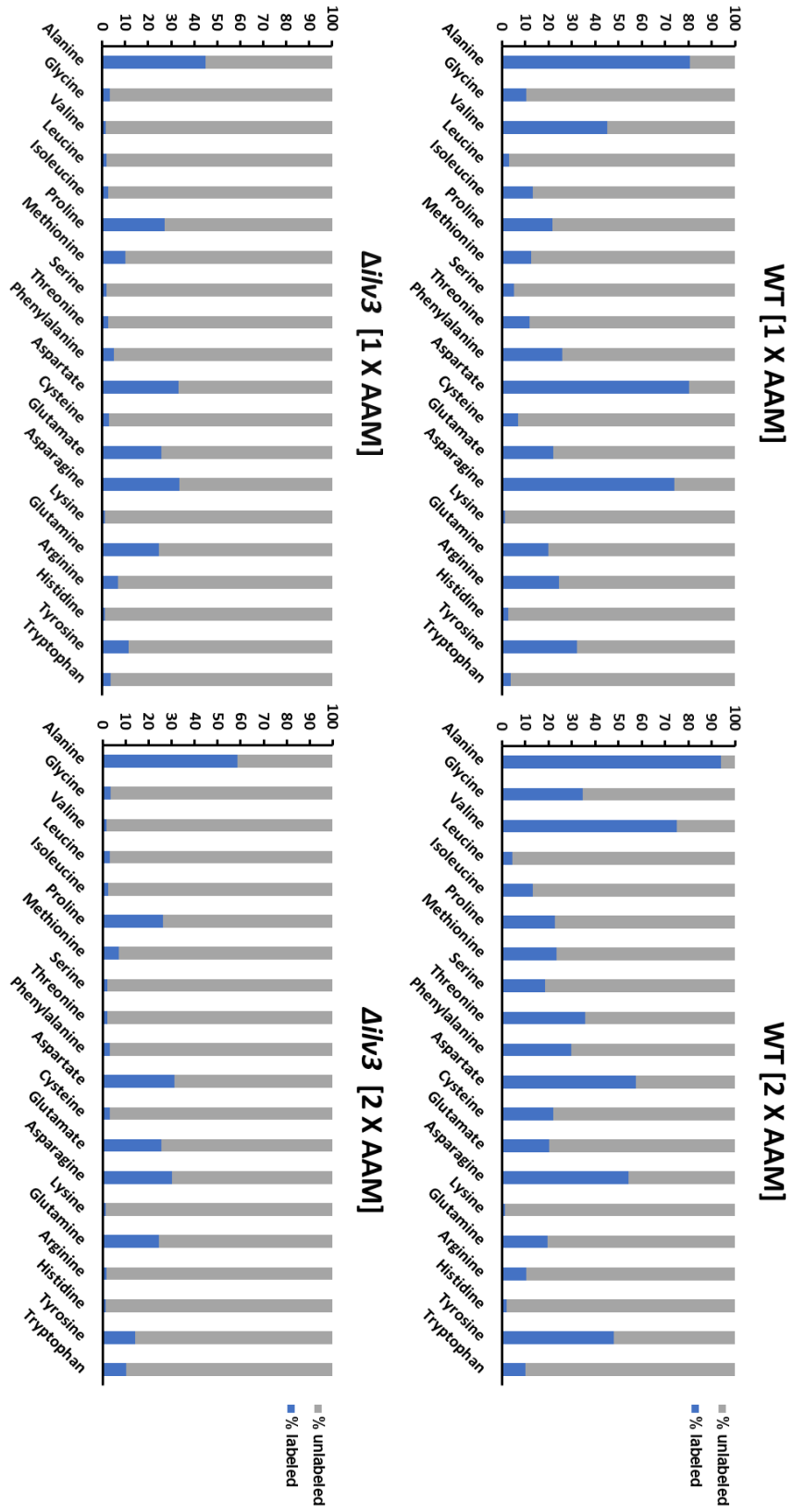


Figure 27: Relative fraction of proteinogenic amino acids synthesized *de novo* versus imported fraction from the medium when cells were fed with ^{13}C glucose for BY4742 and $\Delta ilv3$ deletion strain on 1 X AAM and 2 X AAM. BY4742 and $\Delta ilv3$ deletion strains were cultured overnight in HC medium and were inoculated in fresh HC medium the next day (with normal [1 X AAM] and double amount [2 X AAM] of amino acid dropout mix), supplemented with ^{13}C glucose and grown to late exponential phase. The following day, using a fast filtration procedure, cells were harvested on a filter membrane, which was quickly collected in a box (with 2 mL of dH_2O) and further subjected to incubation at 100 °C for 15 min and subsequently cooled on ice for 10 min. The cell lysate was collected and cleared of cell debris by centrifugation. Further, the free amino acids present in the cellular lysate were dried under Nitrogen stream, pre-derivatized with MBDSTFA, and ^{13}C enrichment was quantified using GC-MS. The graphs represent labelled and unlabelled fractions of individual amino acids, in the form of percentages normalized to total levels, generated from the average of three independent biological replicates. The unlabelled fraction of amino acid imported from the medium is represented in grey. In contrast, the labelled fraction, which is *de novo* synthesized in the cell, is represented in blue. Data were corrected for naturally occurring isotopes. In this experiment, I prepared the different cell lysates, which were further processed and analyzed by Dr Michael Kohlstedt (Wittman's group, at the Saarland University) as a part of the collaboration work.

From the first glance, unlike the BY4742, $\Delta ilv3$ imports a larger fraction of its amino acids than synthesizing them *de novo* (fig: 27) on both 1 X AAM and 2 X AAM. Interestingly, the previous observation regarding the synthesis of amino acids (like alanine, glycine, valine, methionine, serine, threonine, cysteine, and tyrosine), rather than importing from the medium, in BY4742 on 2 X AAM, as compared to 1 X AAM was not observed for $\Delta ilv3$. The co-relation of these findings to the observed growth phenotype upon increased amino acid content in the growth medium cannot be explained yet. Surprisingly, the total amino acid levels also did not change in $\Delta ilv3$ as compared to BY4742 when grown on 1 X AAM versus 2 X AAM growth condition (fig: 28) except for arginine levels as observed previously in the case of BY4742.

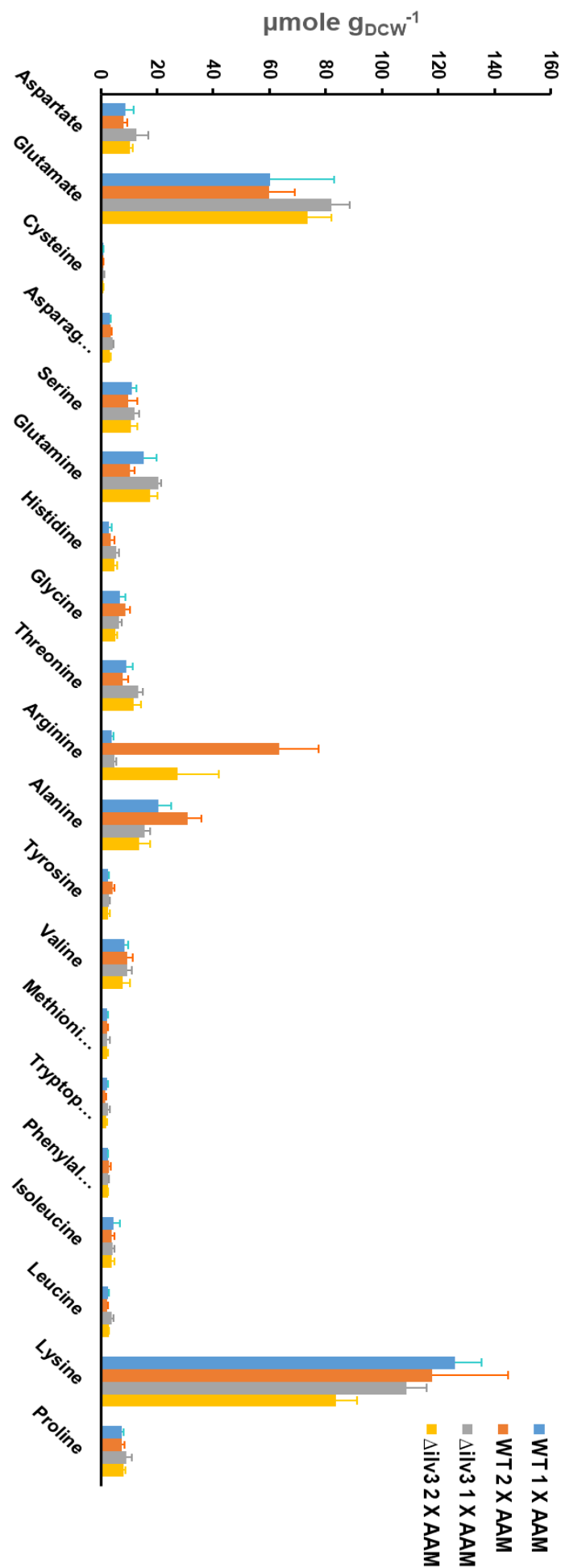


Figure 28: Total free intracellular amino acid levels in BY4742 and $\Delta ilv3$ on 1 X AAM and 2 X AAM. BY4742 and $\Delta ilv3$ deletion strain were cultured overnight in HC medium and inoculated in fresh HC medium (with normal [1 X AAM] and double amount [2 X AAM] of amino acid dropout mix) the next day were and grown till late exponential phase. The following day, using a fast filtration procedure, cells were harvested on a filter membrane, which was quickly collected in a box (with the appropriate amount of alpha-amino butyric acid, as internal standard, in 2 mL of dH₂O) and further subjected to incubation at 100 °C for 15 min, cooled on ice for 10 min. The cell lysate was collected and cleared of cell debris by centrifugation. The clear lysate was injected and simultaneously was mixed with reagents and derivatized in an automated way and quantified using HPLC. The graphs represent individual amino acid levels (μ mol per cell density weight) generated from an average of three independent biological replicates. Sky blue, orange, dark blue and green coloured bars represent free intracellular amino levels from BY4742 [1 X AAM], BY4742 [2 X AAM], BY4742+*LEU2* [1 X AAM] and BY4742+*LEU2* [2 X AAM] respectively. In this experiment, I prepared the different cell lysates, which were further processed and analyzed by Dr Michael Kohlstedt (Wittman's group, at the Saarland University) as a part of the collaboration work.

3.2.3 BCaa pathway NON-ACTIVATION supports the growth of BY4742 on 2 X AAM condition

It was interesting to see that the auxotrophic BY4742 yeast strain instead synthesized more of the amino acids itself than simply importing them from the medium on 2 X AAM growth condition. However, this was not the case for $\Delta ilv3$, which was observed to import the majority fraction of its amino acids from the growth medium. It was also observed from the ¹³C amino acid labelling studies that there is possibly no trigger for amino acid synthesis in $\Delta ilv3$, especially that of the BCaa, on 2 X AAM. This observation is plausible since the $\Delta ilv3$ deletion strain lacks the *Ilv3* enzyme, which catalyzes the third step in the BCaa synthesis pathway and thus, it cannot produce its BCaa. As the next step, to confirm the initial idea that the BCaa bio-synthesis pathway is triggered on 2 X AAM growth condition in BY4742: I intended to study the observed growth phenotype of BY4742 in a way where the BCaa pathway is not activated on 2 X AAM growth condition.

It is established that under nutrient depletion and amino acids starvation conditions, Gcn4 kinase is activated upon activation by Gcn2 kinase by uncharged tRNA's⁶⁰. Gcn4 further activates the biosynthesis of several amino acids, independent of which amino acid is depleted from the growth medium⁷⁴. Next, I intended to verify the role of Gcn4 in mediating the activation of the BCaa pathway on 2 X AAM growth condition. It was fascinating to observe that the deletion of *GCN4* renders the cell to grow better than BY4742 (fig: 29) on 2 X AAM and 3 X AAM growth conditions. This result strongly suggested that Gcn4 activity mediates the activation of the BCaa pathway on 2 X AAM condition. Its subsequent signalling is probably the cause of the observed growth phenotype of BY4742.

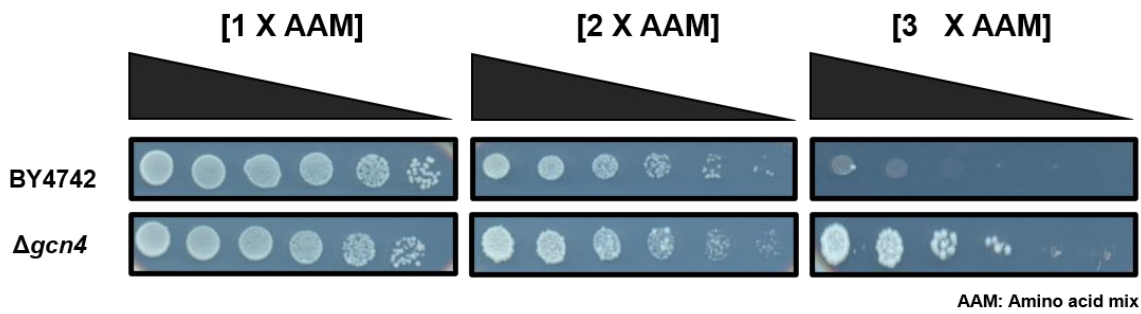


Figure 29: Deleting *GCN4* also rescues the growth phenotype. To verify the rescue of the growth phenotype from non-activation of BCaa pathway, $\Delta gcn4$ deletion strain was generated by homologous recombination. BY4742 and *GCN4* deletion strain were cultured overnight in HC medium, diluted the next day, and grown to log phase. Cells were harvested, washed, fivefold serially diluted, and spotted on plates containing normal [1 X AAM], double [2 X AAM] or triple [3 X AAM] amount of amino acid dropout mix, containing 2% glucose as carbon substrate. The plates were incubated at 30°C for 42 hours. The top black bar corresponds to the decreasing cell density from left to right. This figure is one of the representative examples from at least three independent experiments performed on different days.

3.2.4 Sit4 and Gcn4 act upstream to the activation of the BCaa pathway

Following the previous observation that Gcn4 leads to the activation of the BCaa pathway on 2 X AAM growth condition, the following questions were raised: what comes upstream for activation of Gcn4? Does the TORC1 pathway have any putative role upstream of Gcn4 in activating the BCaa pathway in BY4742 on 2 X AAM growth condition? Sit4 and Iml1 were chosen as potential candidates to address this question since Sit4 is a type 2A-related serine/threonine phosphatase known to play diverse roles in the cellular processes ranging from TOR signalling, DNA repair to actin cytoskeleton organization, G1/S phase transition during mitosis, etc^{208,209}. Iml1 acts as GTPase activating protein (GAP) for Gtr1p (EGOC subunit) and is a subunit of Seh1-associated complex or SEACIT complex along with other subunits Npr2p and Npr3p, leading to the inactivation of TORC1 signalling^{107–109}. Therefore, strains with either deletion or overexpression of *SIT4* and *IML1* were generated by homologous recombination.

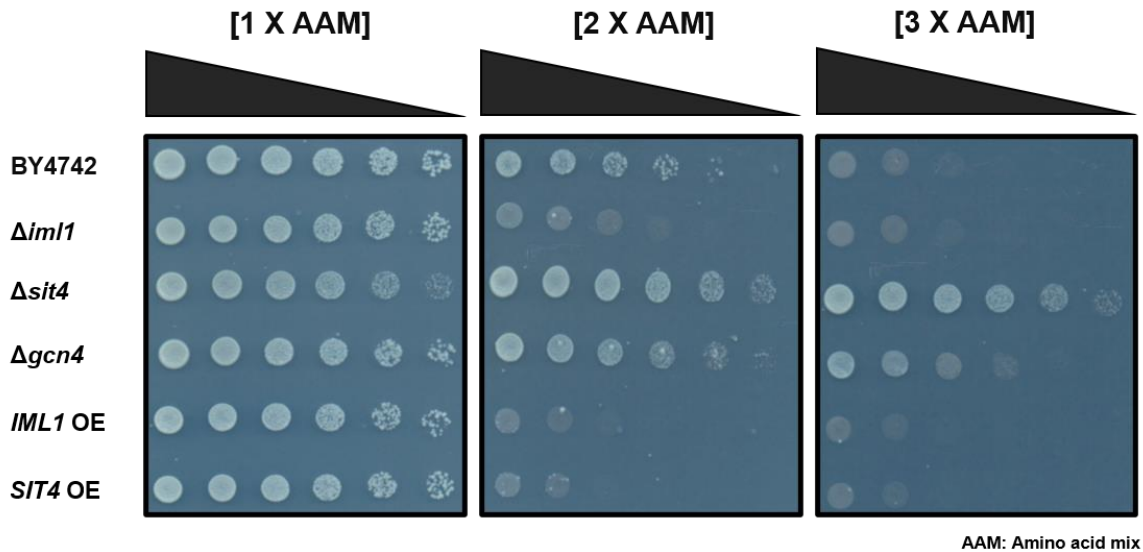


Figure 30: Sit4 and Gcn4 act upstream to possibly activate of the BCaa pathway. To verify upstream partners leading to the activation of the BCaa pathway, strains with either deletion or overexpression of *IML1* and *SIT4* were generated by homologous recombination. All strains were cultured overnight in HC medium, diluted the next day, and grown to log phase. Cells were harvested, washed, fivefold serially diluted, and spotted on plates containing normal [1 X AAM], double [2 X AAM] or triple [3 X AAM] amount of amino acid dropout mix, containing 2% glucose as carbon substrate. The plates were incubated at 30°C for 42 hours. The top black bar corresponds to the decreasing cell density from left to right. This figure is one of the representative examples from at least three independent experiments performed on different days.

As observed from the figure: 30, knockout of *SIT4* rescued, whereas its overexpression further worsened the observed growth phenotype indicating that Sit4 is potentially acting upstream of Gcn4. It is also known that the activation of Sit4 phosphatase upon TOR inactivation phosphorylates and activates the Gcn2 kinase, which further phosphorylates and inactivates elf2αB⁷². The inactive elf2αB further inhibits the global translation and thus leading to the increased transcription rates of Gcn4 and resultant Gcn4 mediated signalling⁶⁰. Also, the knockout of *IML1* could not rescue the growth phenotype in response to the increased amino acid content in the growth medium. It indicated that it was not possible to activate the TORC1 mediated signalling by diminishing the GAP activity of the SEACIT complex, which in turn could rescue the observed growth phenotype. However, the overexpression of *IML1* further worsened the growth phenotype due to higher GAP activity of SEACIT complex, probably completely diminished the TORC1 mediated signalling (if present). Though, we need more experimental evidence to establish the potential role of TORC1 inactivation on 2 X AAM growth condition. Nonetheless, these findings gave us an initial hint that the TORC1 inactivation underlies the observed growth phenotype, where possibly the active Sit4 phosphatase (activated upon inactivation of TORC1) further activates the Gcn2 kinase, leading to stable expression of Gcn4 mRNA. Further, the Gcn4 transcription factor binds to promoters of several amino acid genes leading to the synthesis of different amino acids, especially that of the BCaa.

3.3 Effect of AAM on the transcriptional and translational level

So far, we observed how the increased presence of Ehrlich amino acids in the growth medium illicit the slow growth phenotype for leucine auxotrophic yeast strain BY4742. Also, establishing the functional leucine bio-synthesis pathway or deleting any gene upstream of or *ILV3* rescued the observed growth phenotype. We also observed that activation of Sit4 phosphatase (possibly due to diminished TORC1 signalling) and resultant activation of the Gcn4 transcription factor underlies the observed growth phenotype. In summary, we learned about the factors responsible for contributing or rescuing the observed growth phenotype. However, we still lack the detailed mechanistic understanding of this growth phenotype on transcriptional and translational levels upon increased amino acid content in the growth medium. To gain more insights into the underlying mechanism, I also studied the transcriptional changes by performing RNA sequencing studies for BY4742 on 1 X AAM versus 2 X AAM growth conditions compared to $\Delta ilv3$.

3.3.1 BCaa genes are upregulated on 2 X AAM

I prepared the RNA samples from the BY4742 and $\Delta ilv3$ grown on 1 X AAM and 2 X AAM growth conditions. Further, the samples were processed, RNA sequencing and subsequent data analysis were performed in collaboration with Dr Kathrin Kattler, from the Walter group, at the Saarland University.

The PCA analysis is a commonly used method to reduce the dimensionality of the generated data. It makes it easier to detect the variability between different test conditions and biological or technical outliers. As observed from figure: 31, one could see the variance in differential expression of genes among the different biological replicates, which is frequently observed in such experimental analysis. These variances are considered while normalizing and processing the raw data. It is also good to observe that all the replicates are clustered together. The heat map shows z scores or the relative expression changes for all differentially expressed genes (DEG) in the dataset (DEG roughly ~650 genes for the current study). A correlation between different samples further clusters the DEG, and accordingly, we could see an evident separation between the different replicates and comparison groups (BY4742 and $\Delta ilv3$; 1 X AAM and 2 X AAM) during the study.

Interestingly, we observed the upregulation of the BCaa biosynthetic pathway in BY4742 when grown on 2 X AAM (fig: 32) in comparison to 1 X AAM growth condition, which was not the case for $\Delta ilv3$ (data not shown). This observation makes sense since the *ILV3* deletion lacks a dihydroxy-acid dehydratase enzyme, catalysing the BCaa intermediates DHMV or DHIV to KMV or KIV, respectively. Therefore, it cannot synthesize its BCaa and possibly could not upregulate this pathway. Further, we also observed how the expression levels of the individual BCaa genes changed for BY4742 and $\Delta ilv3$ on 1 X AAM vs 2 X AAM growth conditions (fig: 33).

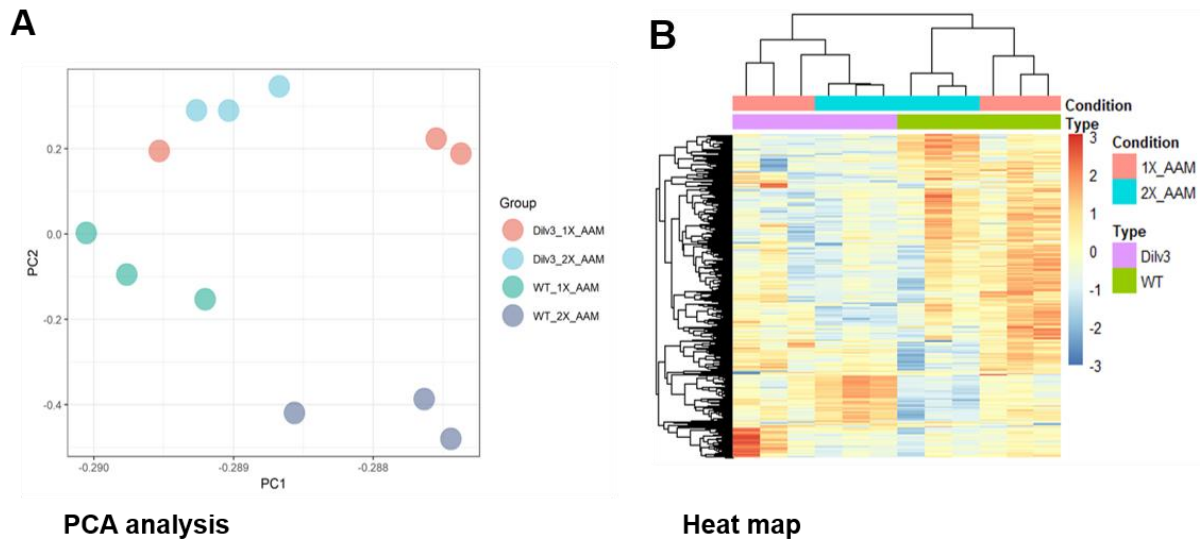


Figure 31: The PCA analysis and heat map representing BY4742 and $\Delta ilv3$ transcriptional changes on 1 X AAM vs 2 X AAM growth condition. A: The individual circles represent one biological replicate. **B:** Every column in the heat map represents a biological replicate. It shows the relative expression changes for all differentially expressed genes in the dataset. BY4742 and $\Delta ilv3$ cells grown in 1 X AAM and 2 X AAM growth conditions are represented by different colors. In this experiment, I prepared the RNA samples, which were processed for RNA sequencing. The subsequent data analysis was performed by Dr Kathrin Kattler (Walter's group, Saarland University) as a part of the collaboration work.

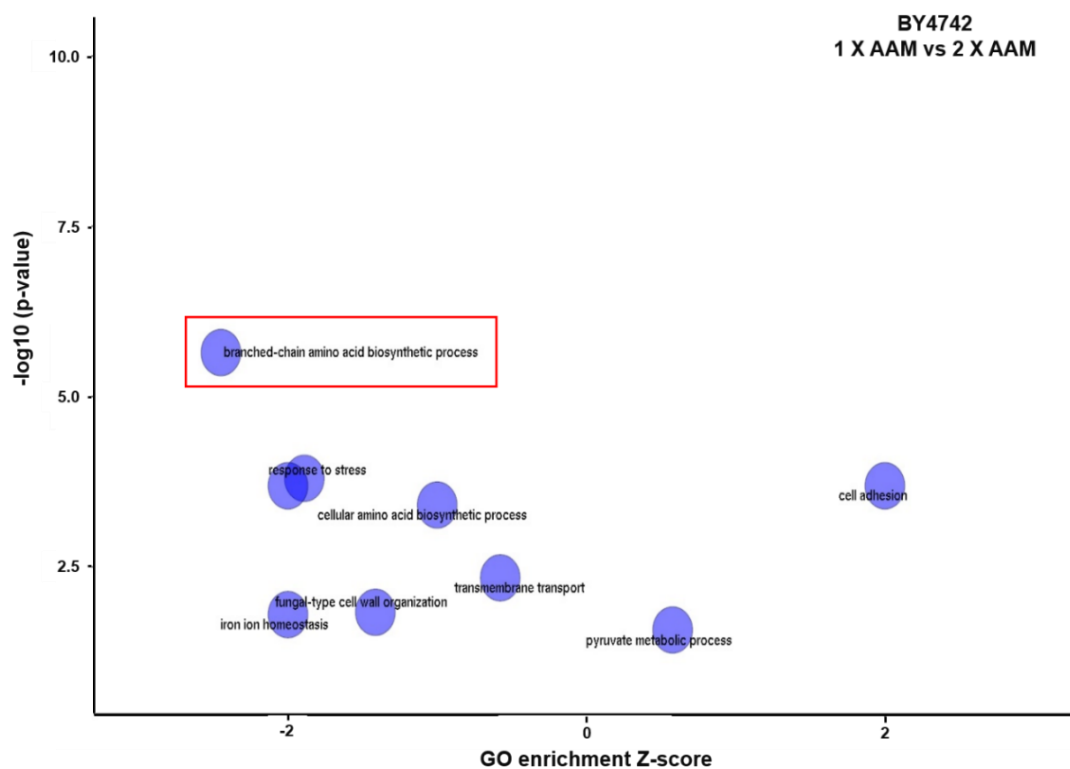


Figure 32: The GO plot summarizing the GO enrichment of the transcriptional changes in BY4742 on 1 X AAM versus 2 X AAM growth condition. The GO enrichment analysis was done on all differentially expressed genes with $|\log_{2}FC| > 1$ and $FDR < 0.01$. The y axis represents $-\log_{10} p$ -value. The x-axis represents an enrichment z-score that means a relative

enrichment of the GO enrichment term's genes. A positive Z score represents higher enrichment of GO term in the first test condition under observation and vice versa. The size of the bubble corresponds to the number of differential genes associated with the GO term.

This observation further strengthened our previous idea that BCaa biosynthetic pathway is upregulated in BY4742 on 2 X AAM, compared to the 1 X AAM growth condition. Furthermore, we did not see any striking changes at the transcription level for other related pathways (data not shown), which could have increased our understanding of the observed growth phenotype.

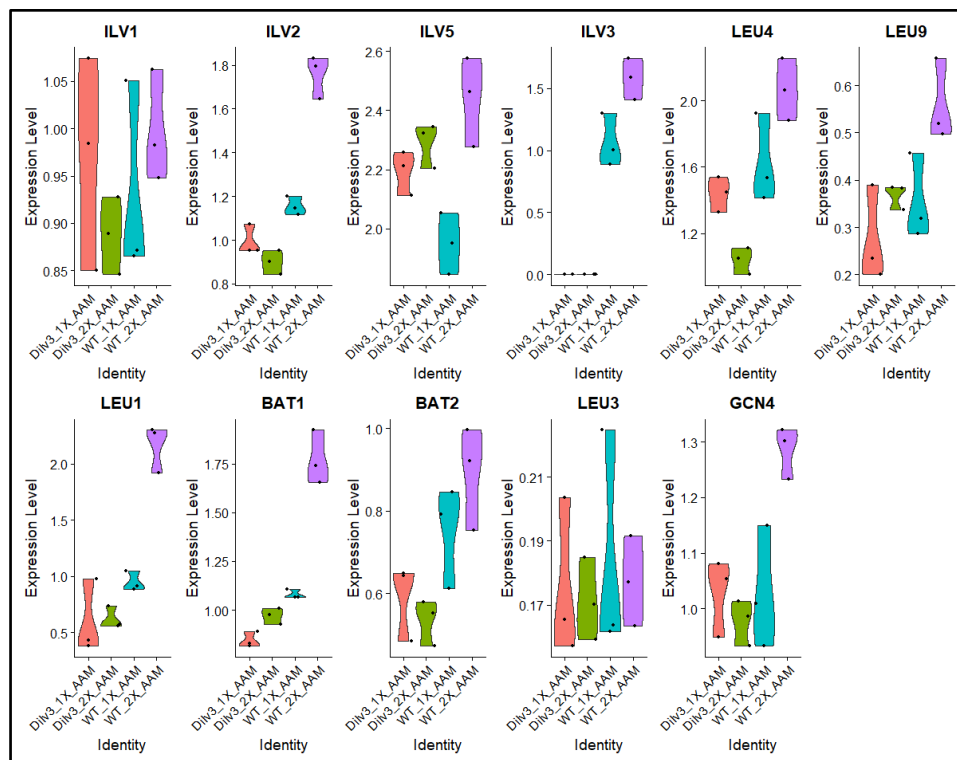


Figure 33: The expression levels for the BCaa pathway genes in BY4742 and $\Delta ilv3$ in 1 X AAM and 2 X AAM growth conditions. The genes involved in the synthesis of BCaa and *GCN4* expression levels are represented in violin plots. The expression levels of respective genes in individual biological replicates across the different samples under investigation can also be observed.

3.3.2 Increased amino acid content affects the cell division

We observed from the drop dilution and the growth curve assay (fig: 12) that BY4742 is growing slower on 2 X AAM in comparison to 1 X AAM. There is almost no or poor growth of BY4742 on 3 X AAM growth condition compared to 1 X AAM growth condition (control). This amino acid dependent slow growth (2 X AAM) and almost no growth (3 X AAM) observation of BY4742 further raised an exciting question: Are these cells viable and cell cycle arrest, or are the cells dead?

3.3.2a Increased amino acid content induces apoptosis in a fraction of the yeast population

To address how increased amino acid content in the growth medium affects the cell division cycle and results in the slow growth phenotype of BY4742: I decided to perform Annexin-V/PI staining of BY4742 when cultured in 1 X AAM and 2 X AAM liquid medium. Since we also observed that the $\Delta ilv3$ deletion was resistant to the increased amino acid content and did not exhibit the slow growth phenotype, $\Delta ilv3$ cells were used as a positive control. Annexin-V binding assay is a fast, precise, and reliable method to identify and quantify the apoptotic cells from a population via microscopic or flow cytometry analysis²¹⁰⁻²¹². The phospholipid: Phosphatidylserine (PS) residue is present usually on the inner PM leaflet but is transitioned to the upper PM leaflet in response to the early apoptotic signals. Thus, PS gets exposed to the plasma membrane and acts as an early apoptotic marker^{213,214}. Annexin-V is known to bind to the exposed PS residue on the outer plasma membrane.

Further, co-staining the cells with the propidium iodide (PI) helps to distinguish between the early apoptotic and late apoptotic stage. PI binds to the DNA only in the later apoptotic stage or necrosis. Thus, Annexin-V positive, PI negative: indicates early apoptosis stage; Annexin-V negative, PI-positive: indicates necrosis; and Annexin-V positive, PI-positive: indicates late apoptosis stage, where apoptosis gradually resulted in necrosis²¹⁵. I prepared the microscopic slides for annexin-V stained BY4742 and $\Delta ilv3$ cells grown on 1 X AAM and 2 X AAM growth conditions (using the protocol described in detail under section 2.2.4). Further, these slides were imaged, processed and subsequent data analysis was performed by Dr Galal Metwally (Storchová group, TU-Kaiserslautern) as a part of the collaboration work.

Interestingly, a significant percentage of BY4742 cells (nearly 20 %) were stained with apoptotic stain Annexin-V when grown on 2 X AAM (fig: 34) in comparison to 1 X AAM growth condition. Further, there was no significant change in the percentage of annexin-V stained $\Delta ilv3$ cells for 1 X AAM versus 2 X AAM growth condition, which served as a control. It was fascinating to observe that the increased amino acid content, mainly Ehrlich amino acids, in the growth medium resulted in apoptosis of ~20% of the cell population of BY4742. The exact mechanism by how the increased amino acid content resulted in apoptosis of leucine auxotrophic BY4742 is still elusive.

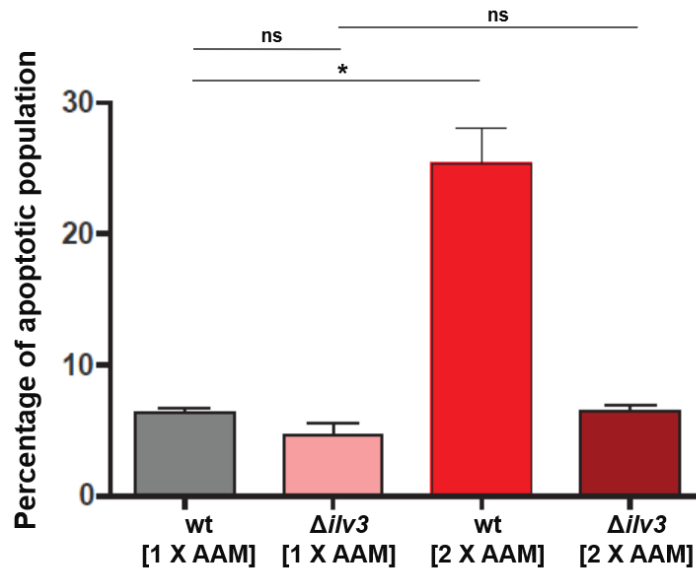


Figure 34: Increase in the amino acid content in growth medium results in apoptosis of BY4742. BY4742 and $\Delta ilv3$ deletion strains were cultured overnight in HC medium and were inoculated in fresh HC medium the next day (with either normal [1 X AAM] or double amount [2 X AAM] of amino acid dropout mix) and grown till late exponential phase. The following day, 1 O.D.₆₀₀ units of cells were harvested, washed using sorbitol buffer; the resultant pellet was dissolved in Tris/DTT Buffer and further incubated at 30°C for 15 min. Afterwards, the cell suspension was rewashed and resuspended in sorbitol buffer containing zymolase and incubated for 30-40 mins at 30°C. The resultant protoplast pellet was carefully washed with and resuspended in binding sorbitol buffer. Further, the pre-diluted Annexin-V and Propidium Iodide (PI) stain (Annexin-V-FLUOS staining kit, Sigma Aldrich) was added to the protoplast suspension and incubated in the dark for 20 mins. These stained cells were washed with PBS (1 X) and were further incubated with DAPI staining solution for 10 mins in the dark. Afterwards, the stained cell suspension was washed, added to the poly-lysine coated slides, and incubated for 15-20 min in the dark, washed with PBS, and sealed using coverslips. Further, these slides were imaged using either 40X air or 60X oil objective lens on a Zeiss inverted microscope (AxioObserver Z1), equipped with CSU-X1 spinning disk confocal head (Yokogawa) and the CoolSnap HQ camera (Roper Scientific). The Slidebook software, version 6.0.6 (Intelligent Imaging Innovations), was used to quantify and analyze the acquired images. The bar graph represents the average percentage of apoptotic cell populations derived from three independent biological replicates, where error bars represent standard deviation and 'ns', '*', '***', '****' represents <0.05, <0.005, and <0.001 p-values, respectively. In this experiment, I prepared the microscopic slides, which were imaged, processed, and analyzed by Dr Galal Metwally (Storchova group, TU-Kaiserslautern) as a part of the collaboration work.

After learning that increased amino acid content in the growth medium resulted in the apoptosis of BY4742 (by nearly 20 % of the cell population). Then what happens to the remaining cell population? To address this question, I decided to look at 2 N copy of DNA and the budding index of BY4742 and $\Delta ilv3$ when grown on 1 X AAM versus 2 X AAM growth conditions.

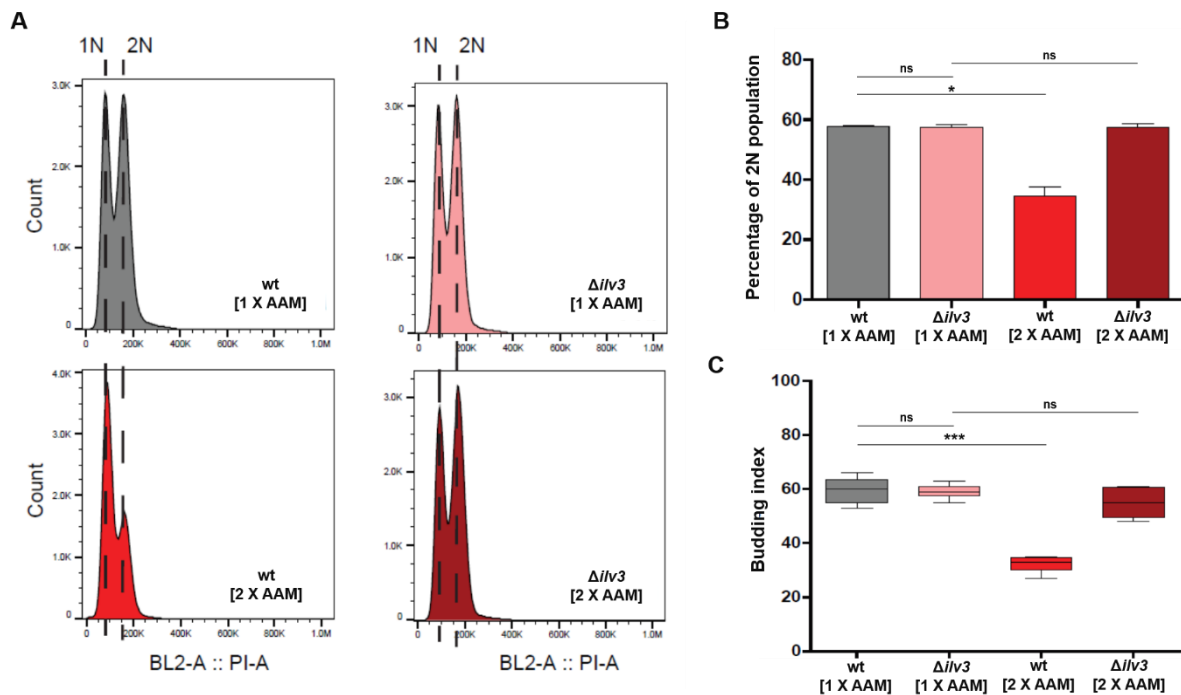


Figure 35: Increase in the amino acid content in growth medium results in G1 cell cycle arrest of BY4742. **A:** The flow cytometry histograms represent the count of cells having either 1N or 2N copy of DNA. **B:** The graph represents the average percentage of a population containing a 2N copy of DNA derived from three independent biological replicates, where error bars represent standard deviation. **C:** The box plot represents the budding index of BY4742 and $\Delta ilv3$ cells computed from three independent experiments. BY4742 and $\Delta ilv3$ were cultured overnight in HC medium and were inoculated in fresh HC medium the next day (with either normal [1 X AAM] or double amount [2 X AAM] of amino acid dropout mix) and grown till late exponential phase. The following day, 1 O.D.₆₀₀ units of cells were harvested in 2 sets (one for computing budding index, the other for PI/FACS analysis), resuspended in 1 mL of 70% (v/v) ethanol. One set of samples was processed directly to count budded and non-budded cells in several random fields using the Zeiss inverted microscope (AxioObserver Z1), which was equipped with a CSU-X1 spinning disk confocal head (Yokogawa). Further, the 40X air or 60X oil objective lens was used to acquire images using the CoolSnap HQ camera (Roper Scientific), which were further processed for computing the budding index using the Slidebook software, version 6.0.6 (Intelligent Imaging Innovations). In contrast, the other set of samples was stored overnight for the PI/FACS analysis. The next day, cells were further washed and resuspended in 250 μ L FxCycle™ PI/RNase staining solution (Life Technologies, #F10797). The cell suspension was incubated in the dark for 30 min at RT and then subsequently stored for 72 hours at 4°C. After three days, samples were sonicated for 20 secs at 30 % amplitude and run on an Attune™ Flow Cytometer. The FlowJo™ software, version 10, was used to analyze the data. A histogram of cell count against PI intensity was plotted, and samples were gated for single cells. The percentage of cells with 1C DNA and 2C DNA content, where C represents the copy number of DNA, were determined using the area under the histogram where for 1N: 0 – 2.7 $\times 10^5$ PI intensity and 2N: 2.7 $\times 10^5$ – 4.5 to 7 $\times 10^5$ PI intensity, values of area under the histogram were used, respectively. The ‘*’, ‘**’, ‘***’ represents the <0.05, <0.005, and <0.001 p-values, respectively. This experiment set was performed by Dr Galal Metwally (Storchová group, TU-Kaiserslautern) as a part of the collaboration work.

This experiment set was performed by Dr Galal Metwally (Storchová group, TU-Kaiserslautern) as a part of the collaboration work. As observed from fig: 35, BY4742 grown on 2 X AAM growth condition had significant less percentage of cells with 2N copy of DNA along with quite a significant percentage of cells with fewer buds (computed using the budding index), in comparison to the cells grown on 1 X AAM growth condition. However, for $\Delta ilv3$ cells, there was no change in the percentage of cells with 2N copy of DNA and for budding index when cells were grown in 1 X AAM versus 2 X AAM growth condition.

As a conclusion, we observed that the presence of increased amino acid content in the growth medium (2 X AAM) resulted in apoptosis for a significant percentage of BY4742 cells. Also, a significant percentage of the BY4742 cell population had fewer buds which perfectly correlated with the observation of a smaller percentage of cells with a 2N copy of DNA, indicating that cells were probably arrested at the G1 stage of cell division.

3.3.2b Increased amino acid content decreases the global translation levels

We observed that increased amino acid content in the growth medium resulted in apoptosis of BY4742 by nearly 20 %. Also, a significant percentage of cells were arrested in the G1 stage of cell division. I further decided to study the effect of increased amino acid content in the growth medium on the global protein translation rate. Puromycin is an antibiotic produced by *Streptomyces alboniger*, which acts as a translation inhibitor for prokaryotes and eukaryotes^{216–218}. Thus, puromycin uptake by the cells disrupts the peptide transfer on ribosomes, thus causing the premature termination of protein synthesis. Dr Galal Metwally (from Storchová group, TU-Kaiserslautern performed this experiment as a part of the collaboration work) studied the relative incorporation of puromycin during the exponential growth phase of BY4742 and $\Delta ilv3$ on 1 X AAM versus 2 X AAM growth condition.

As observed from fig: 36, BY4742 grown on 2 X AAM growth condition had significantly less incorporation of puromycin compared to growth of cells on 1 X AAM. However, there was no significant change in the relative rate of puromycin incorporation for $\Delta ilv3$ for 1 X AAM versus 2 X AAM growth condition. These results indicated that BY4742 cells, when grown on 2 X AAM, already had less protein synthesis and therefore incorporated a relatively less fraction of the puromycin.

Since we also observed that activation of the Gcn4 transcription is involved on 2 X AAM growth conditions (fig: 29), which is also contributing to the observed growth phenotype. Further, it is also known that induction of the Gcn4 mediated signalling inhibits the global protein translation in the cell⁶⁴. Therefore, the current observation of lower protein synthesis in BY4742 on 2 X AAM growth condition makes complete sense and is probably an effect of active Gcn4 mediated signalling in response to the increased amino acid content in the growth medium.

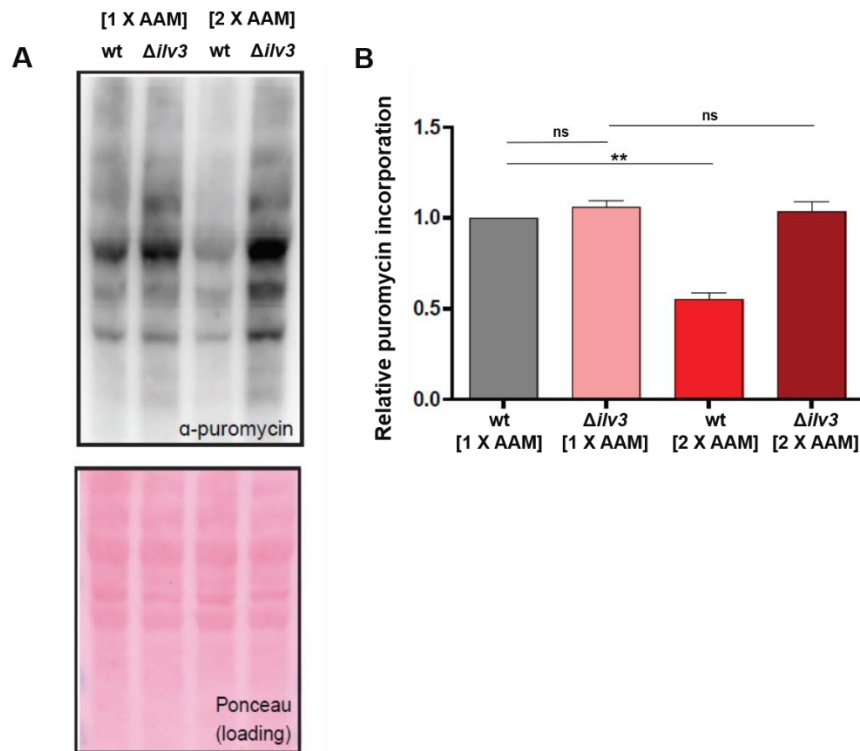


Figure 36: Increase in the amino acid content in growth medium results in decreased global protein translation in BY4742. **A:** The western blot performed using α -puromycin antibody after the addition of puromycin to the liquid culture of BY4742 and $\Delta ilv3$ and the corresponding Ponceau staining. **B:** The bar graph represents the average of the quantified data from the relative puromycin incorporation generated from three independent biological replicates, where error bars represent standard deviation. BY4742 and $\Delta ilv3$ were cultured overnight in HC medium (with either normal [1 X AAM] or double amount [2 X AAM] of amino acid dropout mix). They were diluted 1:10 in the fresh medium the following day. While growing in the exponential phase, cultures were supplemented with puromycin (final con. 10 μ M) for 15 min (30 min, 140 rpm). Further, cells equivalent to 5 O.D.₆₀₀ units were harvested, washed twice, and cell lysates were prepared for western blot. The relative levels of puromycin incorporation in wt under 1 X AAM growth condition was normalised and taken as value 1, which was used as a reference to plot other values. The ‘*’, ‘**’, ‘***’ represents the <0.05, <0.005, and <0.001 p-values, respectively. This experiment set was performed by Dr Galal Metwally (Storchová group, TU-Kaiserslautern) as a part of the collaboration work.

3.4 Increased amino acid content induces redox phenotype

One of the exciting aspects that I wanted to investigate further was to see how the cells grown on 2 X AAM responded to other stress conditions such as oxidative stress. As a first step, I performed a halo assay for BY4742 or the BY4742 transformants (transformed with either pHLUK, pHUK or p415 TEF plasmids). A halo assay is an informative assay to study the effect of different chemicals on the growth of yeast cells. The chemical is added to the centre of the filter disc, where it diffuses radially in a concentration dependent manner around the disc and could potentially affect the growth of the yeast cells. Thus, the radius of the halo-zone elucidates the sensitivity of

the strain in response to the exogenous addition of the chemical on the filter disc (which is usually kept in the centre of the plate). I looked at the effect of the addition of oxidant H_2O_2 when cells are grown on either 1 X AAM or 2 X AAM growth conditions. As observed from figure 37, it was interesting to note that cells grown on 2 X AAM growth condition, were very sensitive to H_2O_2 and had a bigger halo zone in comparison to the cells grown on 1 X AAM. It seems that cells grown on 2 X AAM growth condition were already experiencing oxidative stress and further couldn't handle the additional oxidative stress in the form of H_2O_2 . As observed earlier, the restoration of the functional leucine biosynthetic pathway helped rescue the observed growth phenotype upon increased amino acid content in the growth medium. Likewise, restoring the available leucine pathway in the leucine auxotrophic yeast strain was also able to rescue the oxidative stress, induced probably due to the increased amino acid content in the growth medium.

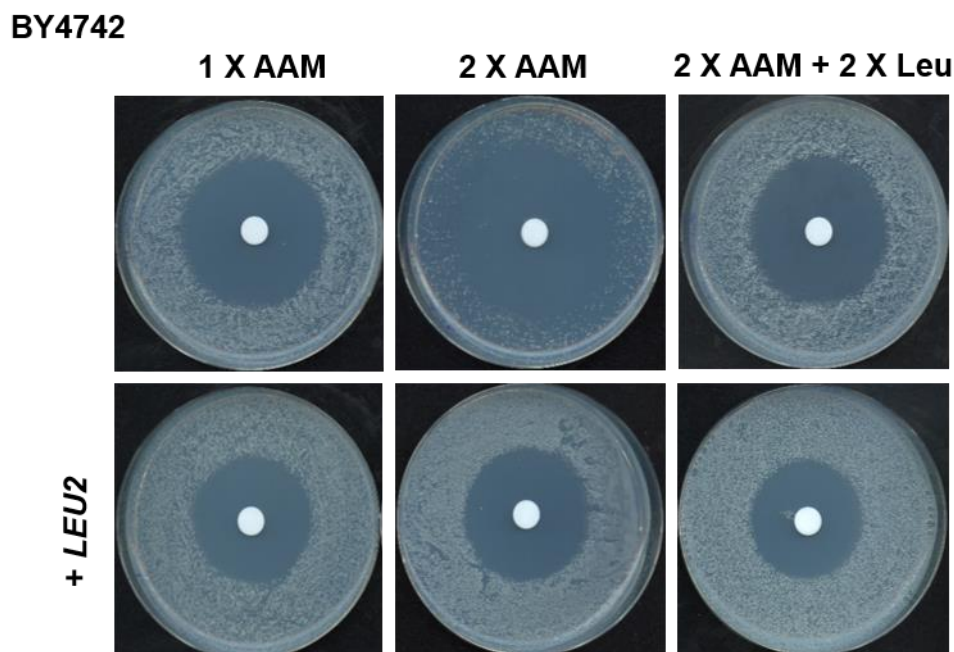


Figure 37: Restoring the available Leucine biosynthetic pathway rescues cells from the oxidative stress-induced due to 2 X AAM growth condition. All yeast strains were cultured overnight in HC (or selective medium to maintain the plasmid selection), diluted the next day, and grown to log phase, cells were harvested and washed, and subsequently, 0.001 O.D.₆₀₀ unit of cells were spread uniformly using the sterile glass beads on plates containing either normal [1 X AAM] or double [2 X AAM] amount of amino acid dropout mix, supplemented with 2% glucose as carbon substrate. 10 μ L of 6 M H_2O_2 was added to the filter disc in the middle of the plate. The plates were scanned following incubation at 30°C for two days. This figure is one of the representative examples from at least three independent experiments performed on different days.

3.4.1 Restoring the leucine auxotrophy in BY4742 also rescues the redox phenotype

It was shown with in-vitro studies using mice model for MSUD that the BCaa and their α -keto acids reduced the anti-oxidative capacity in the brain isolates and stimulated lipid peroxidation, possibly by increased production of free-radicals. Thus, strengthening the potential contribution of oxidative stress towards the neurological damage to MSUD patients⁶⁻⁹. It was also observed from the halo assay results (fig: 37) that BY4742, when grown on 2 X AAM growth condition were more sensitive towards additional oxidative stress in the form of H_2O_2 . It was quite fascinating to observe that increased amino acid content in the medium also induced oxidative stress, likewise reported for patients (and animal models) suffering from MSUD. I further decided to study this redox phenotype of the cells in detail and see how it correlates with the growth of leucine auxotrophic BY4742 yeast cells in different growth conditions.

There are several ways to determine the oxidative state of the cell by investigating and studying the dynamics of H_2O_2 or GSH levels *in-vivo* in separate cell compartments using genetically-encoded sensors roGFP2-Tsa2 Δ Cr or roGFP2-GRX1 respectively or looking at the total whole-cell levels of glutathione^{187,219}. As a first step to address this question, I chose to look at the whole-cell levels of glutathione under the different growth conditions in this study, where oxidized glutathione (GSSG) levels are an indication of oxidative stress to the cell²²⁰.

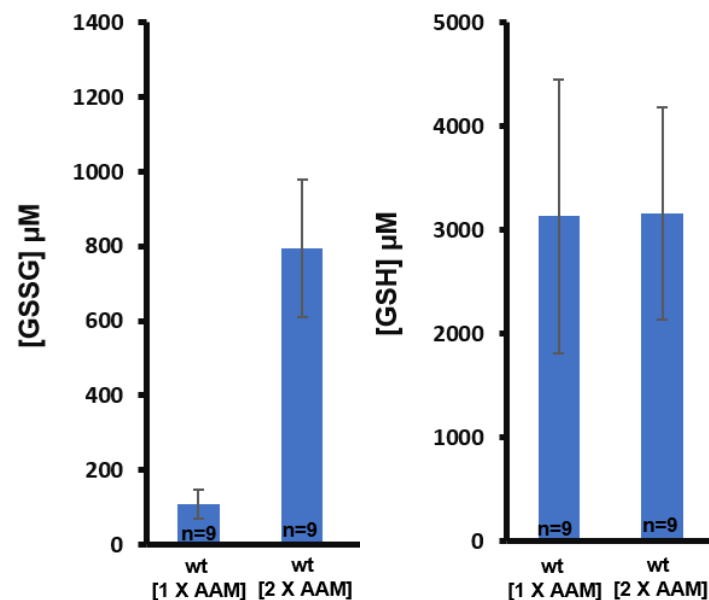


Figure 38: Increased amino acid content (2 X AAM) in the medium leads to a redox phenotype. BY4742 cells were cultured overnight in 1 X AAM and 2 X AAM liquid medium to log phase. Total glutathione (GSX) and oxidized glutathione (GSSG) levels were measured using a DTNB recycling assay. The whole-cell concentrations of the total and the oxidized glutathione were calculated using the regression curve generated from the known GSH and GSSG standards. The amounts of GSH were further calculated by subtracting double GSSG values from GSX values.

Surprisingly, there was a massive increase in GSSG levels (with no significant changes in the total GSH levels) for BY4742 when cultured in 2 X AAM liquid medium compared to 1 X AAM (fig: 38). It was intriguing to observe that increased amino acid content in the medium (2 X AAM) also had a redox phenotype effect. These observations of growth and redox phenotype further raised several questions, such as whether these phenotypes are linked to each other in such a pattern where either of them could be causing the other one? Or there could be a third unknown factor that is simultaneously leading to both growth and redox phenotypes independently of each other on 2 X AAM growth condition.

Since on 2 X AAM cells had massive GSSG levels indicating cells were experiencing oxidative stress, I decided to supplement DTT in the medium and see whether it could rescue the growth effect, which was only possible if growth phenotype was caused due to oxidative stress. The presence of 1 mM DTT in the HC agar plates couldn't rescue this growth effect. It could be very well possible that oxidative stress is not leading to growth effect or even the presence of 1 mM DTT in the agar plates (supplemented with double or triple amounts of amino acid dropout mix) was not enough to rescue this growth effect (fig: 39). The correlation between growth and redox phenotype couldn't be addressed with this experiment.

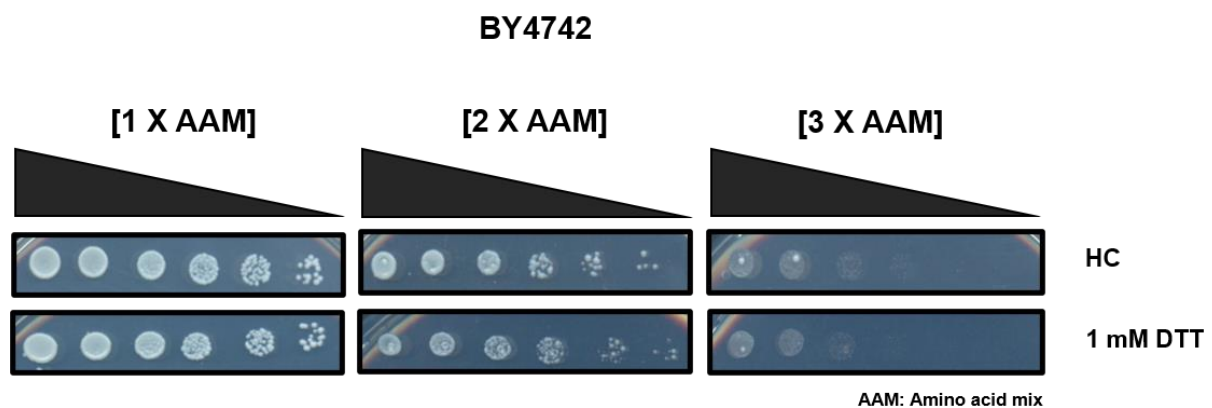


Figure 39: DTT supplementation could not rescue the growth phenotype. BY4742 was cultured in HC medium to log phase, fivefold serially diluted and spotted on plates containing normal [1 X AAM], double [2 X AAM] or triple [3 X AAM] amount of amino acid dropout mix, containing 2% glucose as carbon substrate. The plates were incubated at 30°C for 42 hours. The top black bar corresponds to the decreasing cell density from left to right. This figure is one of the representative examples from two three independent experiments performed on different days.

Likewise, for the growth phenotype, either establishing functional leucine biosynthetic pathway or increasing leucine amounts in proportion to the increased amino acid content in the growth medium rescued the cells from this redox phenotype (fig: 40). As observed previously, pHUK transformed yeast cells grew slower in the liquid medium. Interestingly, they also accumulated massive levels of GSSG as compared to the untransformed BY4742 when grown in 2 X AAM (fig: 40).

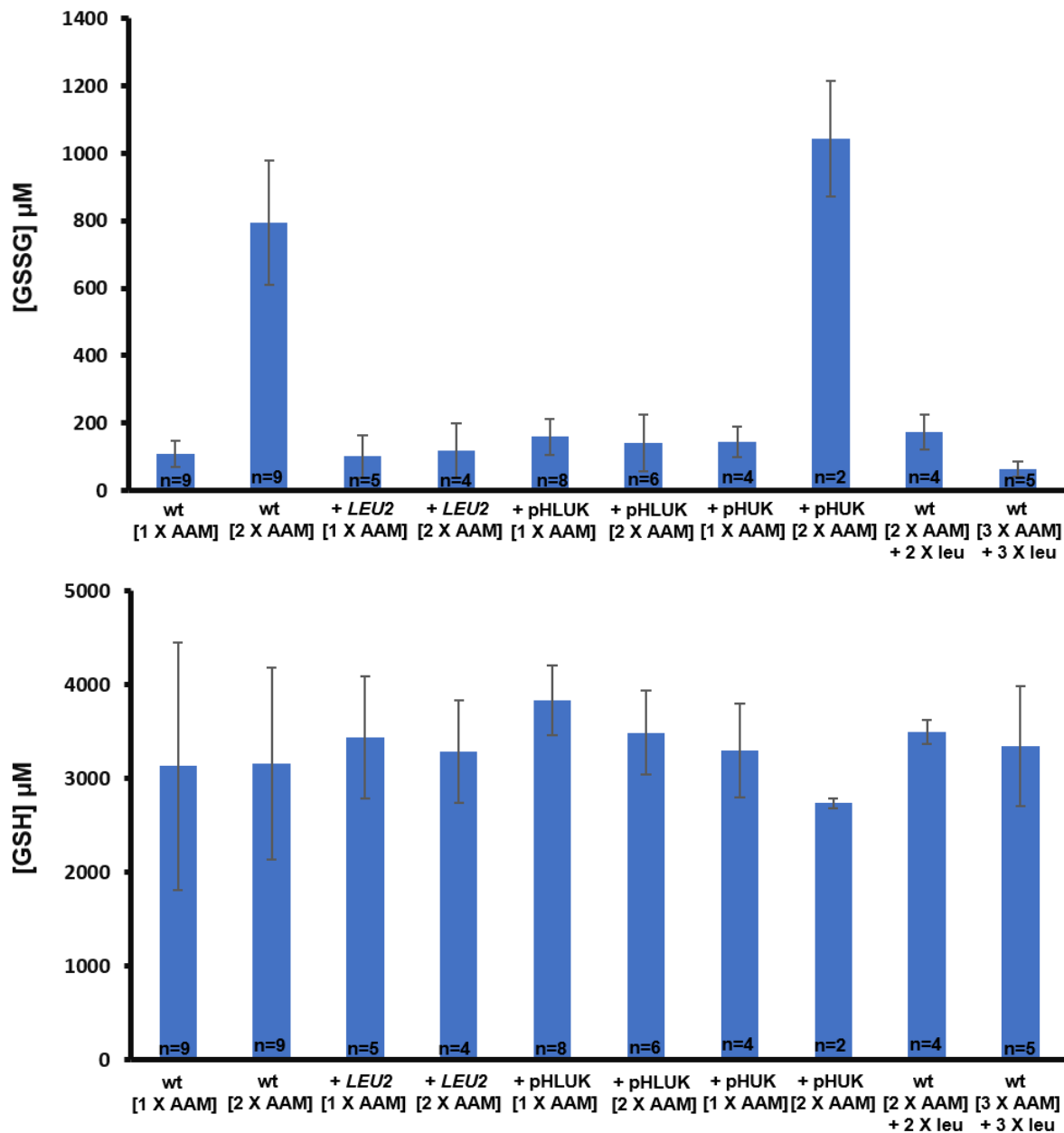


Figure 40: Establishment of functional leucine biosynthetic pathway or extra Leucine supplementation in the medium rescued the redox phenotype. BY4742 cells and or transformed with either p415 empty vector (containing *LEU2* as selection marker) or with pHLUK or pHUK plasmids were cultured overnight in 1 X AAM and 2 X AAM liquid medium (or with increased Leucine in proportion to AAM) or respective selective HC medium to log phase. Total glutathione (GSX) and oxidized glutathione (GSSG) levels were measured using a DTNB recycling assay. The whole-cell concentrations of the total and the oxidized glutathione were calculated using the regression curve generated from the known GSH and GSSG standards. The amounts of GSH were further calculated by subtracting double GSSG values from GSX values.

3.4.2 Removing isoleucine and valine from the medium partially rescue the redox phenotype

It was also observed that by removing valine and isoleucine from the medium, the amino acid dependent growth phenotype of BY4742 was rescued (fig: 24). Interestingly, the redox phenotype was partially rescued when cells were cultured in the medium with minus isoleucine and valine (fig: 41). These results further gave a hint that, like growth phenotype in the presence of increased amino content in the medium, redox phenotype might also be linked to the BCaa pathway.

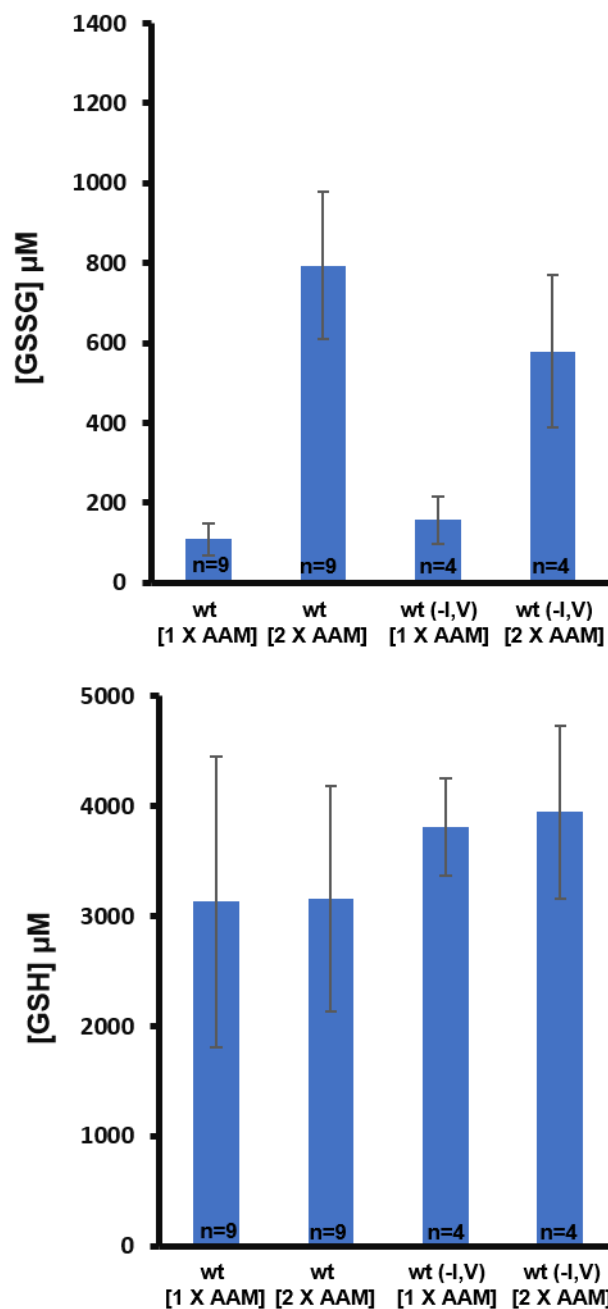


Figure 41: Removing isoleucine and valine from the medium partially rescued the redox phenotype. BY4742 cells were cultured overnight in 1 X AAM and 2 X AAM liquid medium and in -I, V (minus isoleucine and valine) medium to log phase. Total glutathione (GSX) and

oxidized glutathione (GSSG) levels were measured using a DTNB recycling assay. The whole-cell concentrations of the total and the oxidized glutathione were calculated using the regression curve generated from the known GSH and GSSG standards. The amounts of GSH were further calculated by subtracting double GSSG values from GSX values.

3.4.3 Deleting *ILV3* rescues the redox phenotype

With our previous observation that the growth phenotype is related to the BCaa biosynthetic pathway, the next step to address was to check whether the redox phenotype is also related to the BCaa biosynthetic pathway or not? As the next step, the whole-cell GSX and GSSG levels were determined in BCaa pathway mutants grown on 1 X AAM and 2 X AAM growth conditions. Interestingly, like for growth phenotype, a similar pattern was observed in the whole-cell GSSG levels of BCaa mutants. Compared to BY4742, deletion of *ILV2* and *ILV3* decreases the GSSG levels (fig: 42) significantly on 2 X AAM, where deletion of the latter had a profound effect on GSSG levels. As mentioned before, *Ilv5* has dual roles in mitochondria, and its deletion leads to the other secondary products, thus possibly elevating the GSSG levels in general. There was no significant change in the total glutathione levels of these BCaa mutants when grown on 1 X AAM versus 2 X AAM growth conditions. Therefore, it was inferred that deleting *ILV2* or *ILV3* rescued the redox phenotype. Deleting the genes downstream to *ILV3* in the BCaa pathway exhibited the same redox phenotype as BY4742 on 2 X AAM growth condition. In conclusion, like for the observed growth phenotype, the *Ilv3* catalyzed step acted as a switching point for the redox phenotype upon increasing the amino acid content in the growth medium.

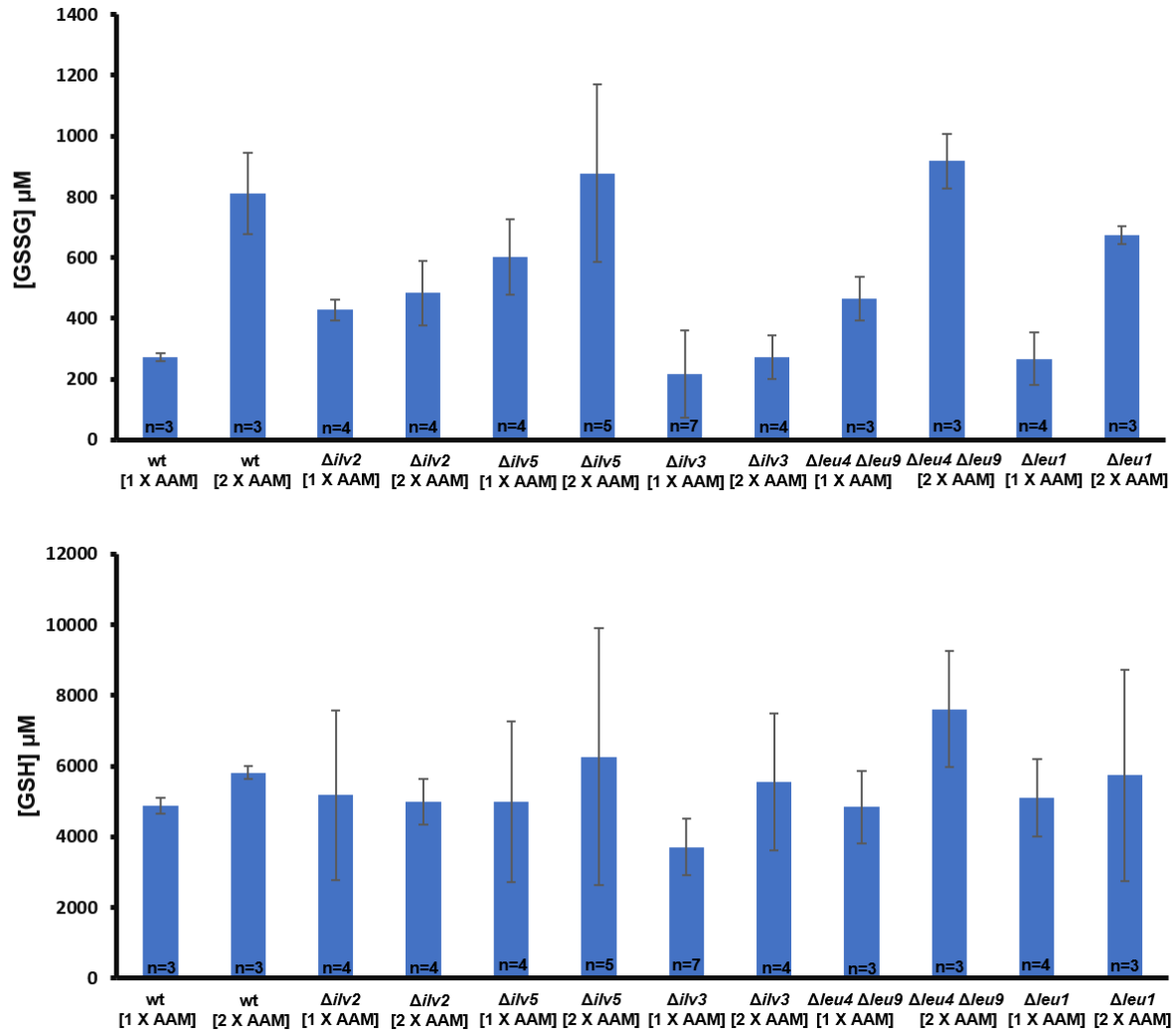


Figure 42: Deleting *ILV3* rescued the redox phenotype. BY4742 and all the BCaa mutants were cultured overnight in 1 X AAM and 2 X AAM liquid medium to log phase. Total glutathione (GSX), and oxidized glutathione (GSSG) levels were measured using a DTNB recycling assay. The whole-cell concentrations of the total and the oxidized glutathione were calculated using the regression curve generated from the known GSH and GSSG standards. The amounts of GSH were further calculated by subtracting double GSSG values from GSX values.

The next question I wanted to investigate was: what happens to redox phenotype when the BCaa pathway is non-activated on 2 X AAM? Because it was previously observed that with *GCN4* deletion (which is needed for BCaa pathway activation on 2 X AAM growth condition), the observed growth phenotype was rescued (fig: 29). Surprisingly, the non-activation of BCaa with *GCN4* deletion also rescued the cell from the observed redox phenotype on 2 X AAM growth condition (fig: 43). These findings indicated that either the activation of the BCaa pathway or the unknown upstream component leads to both the redox phenotype and the observed growth phenotype. In summary, both growth and redox phenotype are not caused by each other but rather by a third component, which is probably causing both (either directly or indirectly) in response to the increased amino acid content in the growth medium.

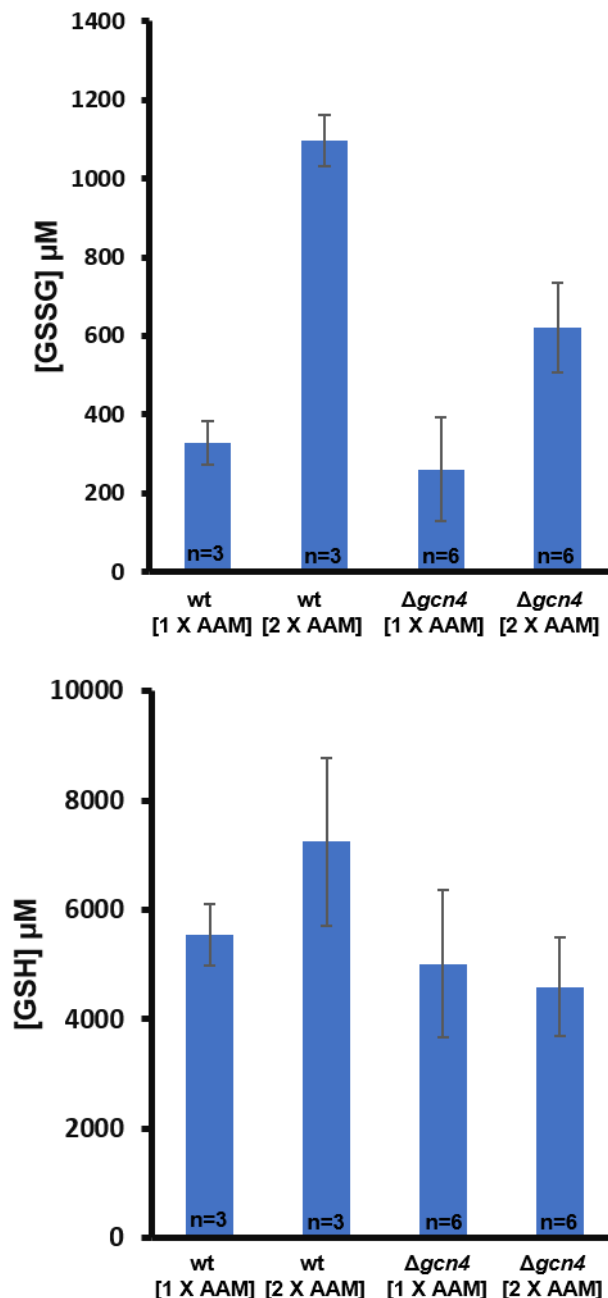


Figure 43: Deleting GCN4 rescues the redox phenotype. BY4742 and $\Delta Gcn4$ were cultured overnight in 1 X AAM and 2 X AAM liquid medium to log phase. Total glutathione (GSX) and oxidized glutathione (GSSG) levels were measured using a DTNB recycling assay. The whole-cell concentrations of the total and the oxidized glutathione were calculated using the regression curve generated from the known GSH and GSSG standards. The amounts of GSH were further calculated by subtracting double GSSG values from GSX values.

We also observed that overexpression of Bat1p was able to rescue the growth phenotype on 2 X AAM, but surprisingly, it could not rescue the cell from the redox phenotype (fig: 44). This result proved that redox and growth phenotype are not linked to each other directly. There is a third unknown factor leading to both growth and redox phenotypes independently of each other. Nevertheless, we could still conclude that the

activation of BCaa pathway synthesis leads to the onset of the redox phenotype in response to the increased amino acid content in the growth medium.

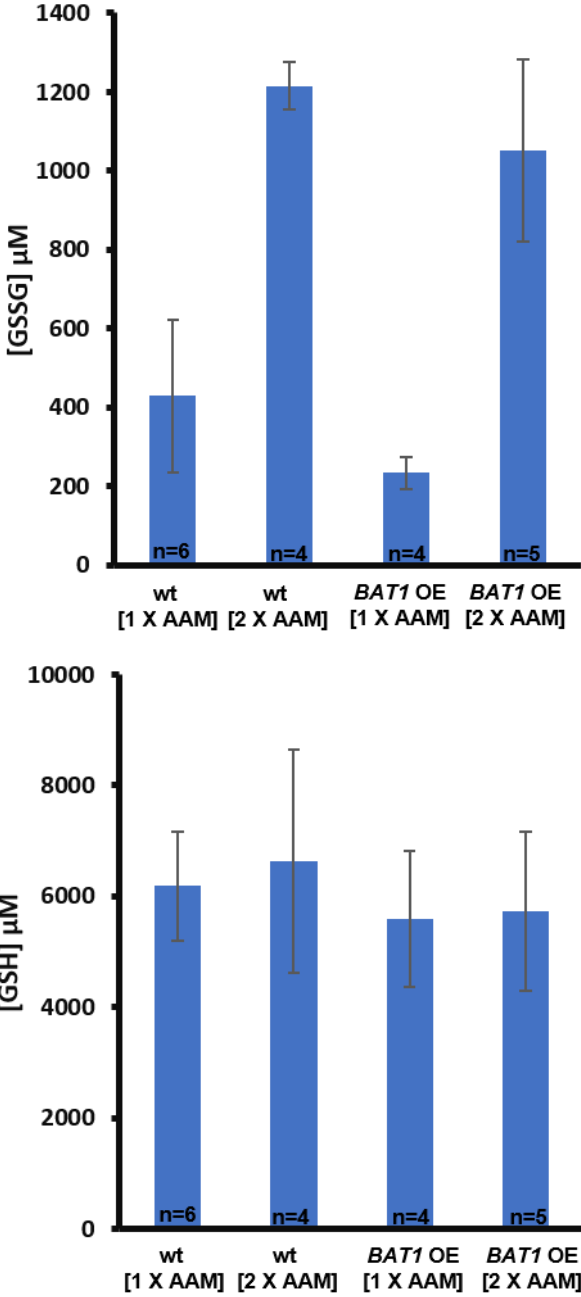


Figure 44: Overexpressing *BAT1* does not rescue the redox phenotype. BY4742 and *BAT1* OE strains were cultured in 1 X AAM and 2 X AAM liquid medium to log phase. Total glutathione (GSX) and oxidized glutathione (GSSG) levels were measured using a DTNB recycling assay. The whole-cell concentrations of total and oxidized glutathione were calculated using the regression curve generated from the known GSH and GSSG standards. The amounts of GSH were further calculated by subtracting double GSSG values from GSX values.

3.5 The potential intermediate behind the growth phenotype

3.5.1 *ILV3* is potentially the switching point for observed growth phenotype

The previous observations suggest that *Ilv3* seems to be the pivot for both growth and redox phenotype. Thus, I asked whether the intermediate keto-isovalerate (KIV) formed during the *ILV3* catalyzed step is causing the observed growth and redox phenotype? There was an equal possibility that instead of KIV or in combination with it, keto-methyl valerate (KMV) could also be contributing to the amino acid dependent growth and redox phenotypes. The latter's contribution was already ruled out since the deletion of *ILV1* (where KMV could not be synthesised; and formation of KIV was the only possibility) did not rescue the growth of BY4742 in the presence of increased amino acid content in the medium.

Looking from the broader view, KIV or 2-oxo-butyrate or deaminated valine are involved in several cellular pathways (fig: 45). In order to investigate the potential pseudo-toxic role (for emphasizing its effect on the growth of cells) of KIV, I either deleted or overexpressed the genes, whose products could be metabolizing KIV (*ECM31*, *BAT1*, and *BAT2*) in the first place or are speculated to play a substantial role (*CIR2* and *AIM45*) during downstream signalling in the cell.

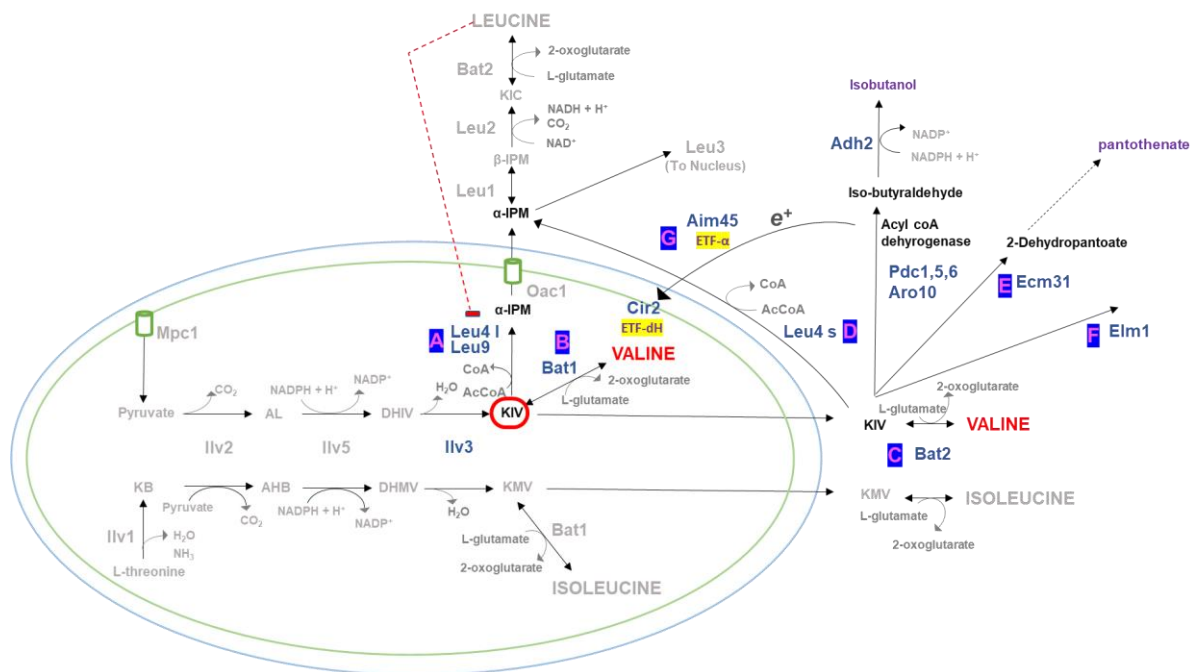


Figure 45: Schematic diagram showing the possible routes and proteins involved where keto-isovalerate (KIV) can be metabolized downstream. KIV can either form valine with Bat1p catalyzed step inside mitochondria or converted to α -IPM leading to leucine synthesis in the cytoplasm. KIV can be exported out of mitochondria via Leu5 transporter where it can again be aminated to valine by Bat2p, or it can be catalyzed by Ecm31 to 2-dehydropantoate, ultimately leading to pantothenate formation via series of reactions. Also, it can be catabolized via the Ehrlich pathway to Isobutanol.

KIV has several possibilities to function downstream inside the cell depending upon its localization and probably also depending upon the local concentration, which no one has reported so far. As a first step, I deleted and overexpressed the genes *ILV3*, *LEU4*, and *LEU9*, whose encoded proteins metabolise KIV inside the mitochondria. As observed from the figure: 46, knockout and overexpression of Leu4 and Leu9 proteins had no additional striking effect on the observed growth phenotype in response to the increased amino acid content in the growth medium. Since the conversion of KIV to IPM is mediated by isopropyl malate synthase, encoded by genes *LEU4* and *LEU9*^{140,206}. Thus, overexpressing both *LEU4* and *LEU9* together could also be a good idea to study its resulting combined effect on the observed growth phenotype. It was also not surprising to observe the variability in the growth phenotype of strains such as BY4742, *ILV3* OE strain, etc., in the current experimental conditions during this study, which might arise due to several technical reasons. Nonetheless, the respective strains exhibited a similar growth pattern as observed from different repeats performed during this study.

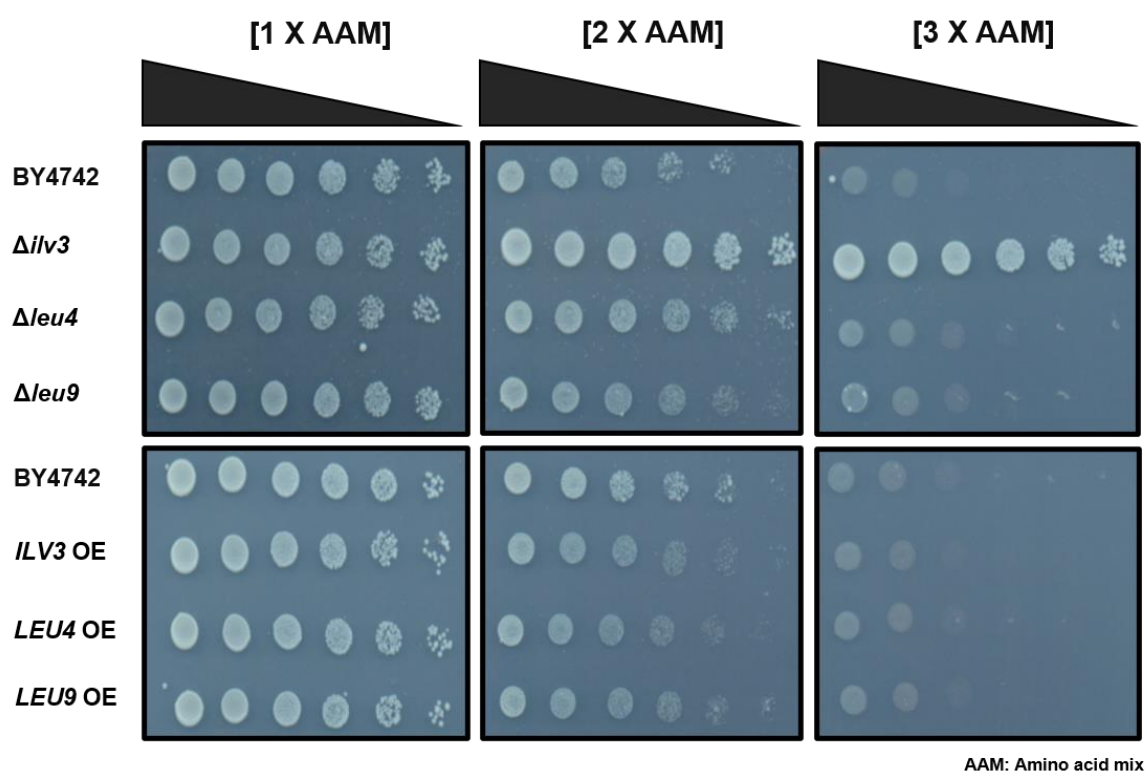


Figure 46: Deleting or overexpressing *LEU4* and *LEU9* has no rescue effect on the growth of cells in conditions with increased amino acid content in the medium. All strains were cultured overnight in HC medium, diluted the next day, and grown to log phase. Cells were harvested, washed, fivefold serially diluted, and spotted on plates containing normal [1 X AAM], double [2 X AAM] or triple [3 X AAM] amount of amino acid dropout mix, containing 2% glucose as carbon substrate. The plates were incubated at 30°C for 42 hours. The top black bar corresponds to the decreasing cell density from left to right. This figure is one of the representative examples from at least three independent experiments performed on different days.

Since knocking out and overexpressing *LEU4* and *LEU9* did not affect the observed growth phenotype. I further decided to look at the growth phenotype of BY4742 with deletion and overexpression of branched-chain aminotransferases, *BAT1* and *BAT2*, which catalyses the conversion of KIV to valine in mitochondria and cytoplasm, respectively¹⁴³. I also chose another potential candidate, *Ecm31*, which metabolises cytoplasmic KIV to 2-dehydropantoate, ultimately leading to pantothenate formation via series of downstream reactions²²¹.

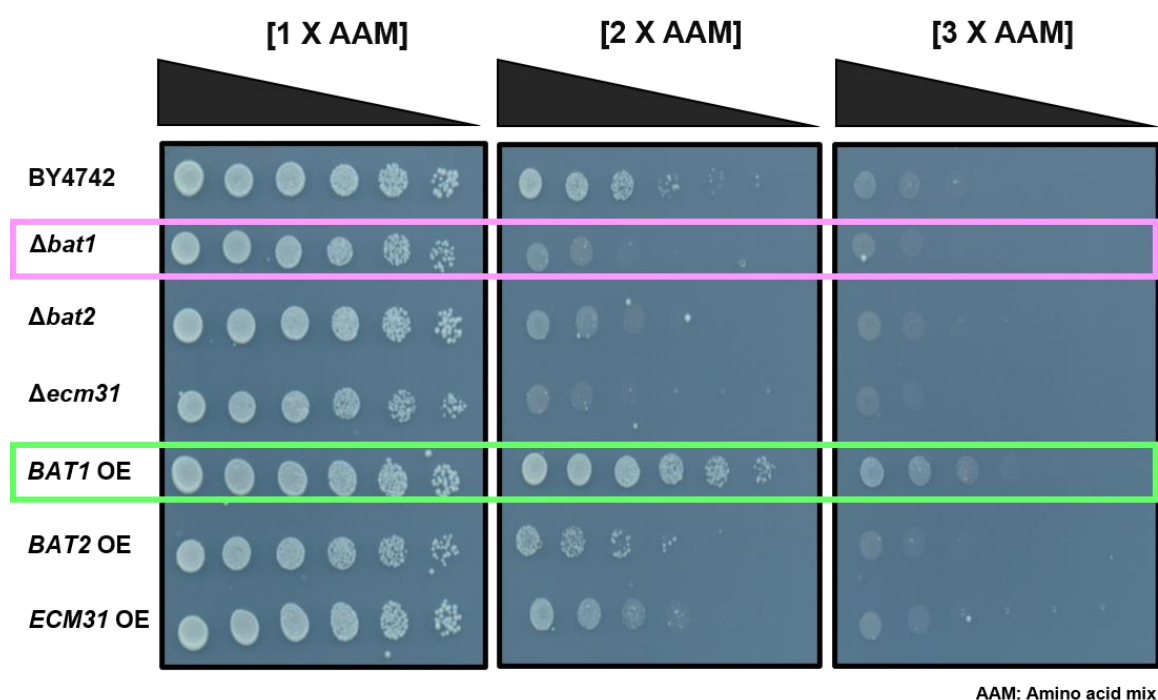


Figure 47: Overexpressing *BAT1* rescues the growth of cells in conditions with increased amino acid content in the medium. All strains were cultured overnight in HC medium, diluted the next day, and grown to log phase. Cells were harvested, washed, fivefold serially diluted, and spotted on plates containing normal [1 X AAM], double [2 X AAM] or triple [3 X AAM] amount of amino acid dropout mix, containing 2% glucose as carbon substrate. The plates were incubated at 30°C for 42 hours. The top black bar corresponds to the decreasing cell density from left to right. This figure is one of the representative examples from at least three independent experiments performed on different days.

The drop dilution assay (fig: 47) showed that deleting the genes *ECM31*, *BAT1*, and *BAT2* further negatively impacted the growth of cells in response to the increased amino acid content in the growth medium. Interestingly, an increased rate of consumption of KIV in the mitochondria mediated by the action of over-expressed Bat1p rescues the growth phenotype. These results strongly indicate that at the first instance, KIV formation (in mitochondria) is creating the problem for the cell (though not quantified yet), which is probably directly leading to the growth phenotype, in an unknown manner so far, on 2 X AAM and 3 X AAM. There is also another possibility,

which cannot be ruled out at this stage, i.e., it could be the downstream product of KIV instead of KIV itself, the actual causative agent, mediating these phenotypes in an undisclosed manner so far.

So far, our results suggested that KIV formation in mitochondria leads to the slow growth phenotype since the overexpression of *BAT1* rescued the observed growth phenotype. As the next step, I also looked at the cytosolic pathway for metabolising KIV that might affect the observed growth phenotype. I deleted or overexpressed *CIR2*, *AIM45* and *ELM1* and studied its impact on the observed growth phenotype.

In mammalian cells, the electron transfer flavoprotein (ETF) transfers electrons from the primary acyl-CoA dehydrogenases to the mitochondrial inner membrane located-ETF dehydrogenases (ETF-DH), which ultimately passes electrons to Ubiquinone in mitochondrial electron transport chain²²². The acyl Co-A dehydrogenases participate in several pathways such as β -oxidation²²³, amino acid catabolism²²⁴, choline catabolism²²⁵. In yeast, the cytoplasmic KIV is converted to Isobutanol via isobutyraldehyde, which is catalyzed by acyl-CoA dehydrogenase. According to the literature, Cir2 is proposed to be the putative ortholog of human ETF-DH. Similarly, Aim45 is proposed to be the putative ortholog of human ETF- α , the subunit of ETF. Both Cir2 and Aim45 are also known to play a role in oxidative stress response²²². If this pathway in a yeast cell has some substantial contribution towards the observed growth phenotype, one must see its contribution (if any) with deletion or overexpression of the ETF or ETF-DH (Aim45 or Cir2, respectively).

Further, Elm1 is a serine-threonine kinase known to phosphorylate and inactivate the α subunit of G-protein, Gpa1, in response to branched-chain α -keto acids or their hydroxy derivatives. Thus, dampening the Gpa1 mediated downstream osmotic stress or pheromone signalling²²⁶. One could also observe whether cytoplasmic KIV (or its hydroxy derivatives) act as a second messenger and recapitulate the osmotic stress response (in Elm1 dependent manner), thus contributing towards the amino acid dependent observed growth phenotype.

As observed from figure: 48, surprisingly, both deletion and overexpression of *CIR2*, *AIM45*, and *ELM1* further worsen the growth phenotype. Since both deletion and overexpression of these genes resulted in a further similar slow growth phenotype compared to BY4742 on 2 X AAM and 3 X AAM. These results indicate that Cir2, Aim45, and Elm1 have no possible contribution mediated by either KIV or its hydroxy derivatives towards the observed growth phenotype upon increased amino acid content in the growth medium.

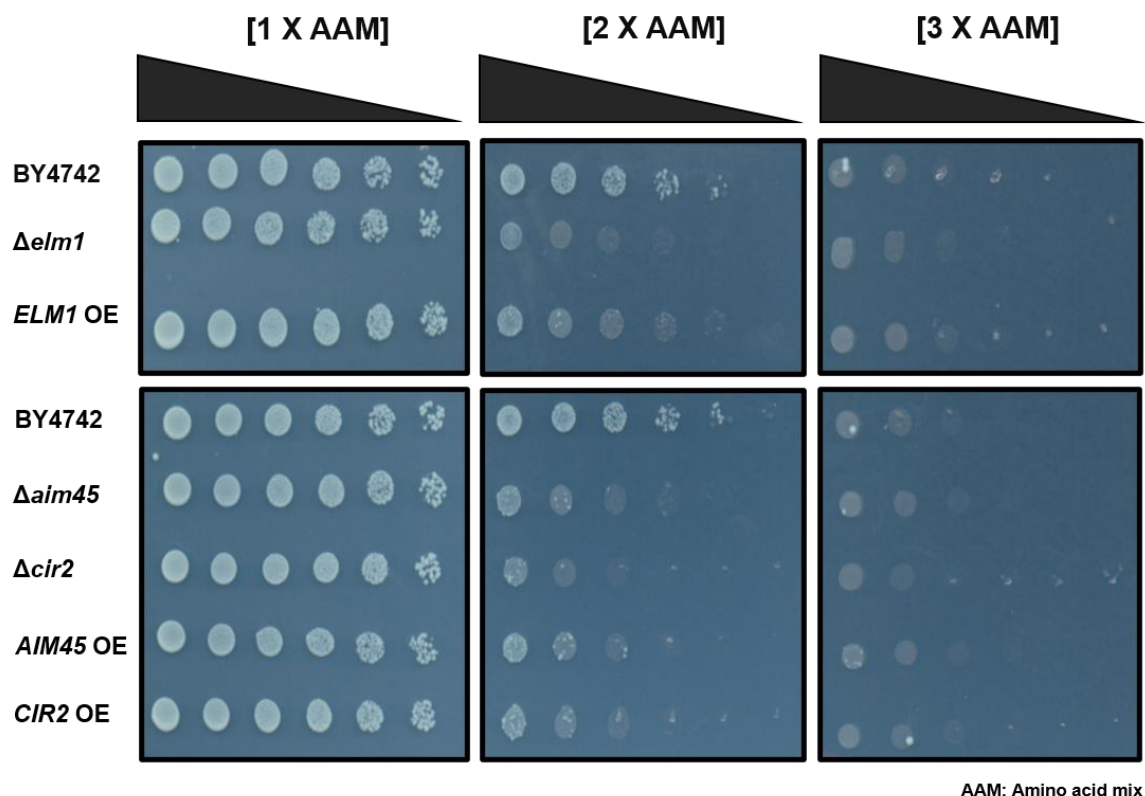


Figure 48: Elm1, Aim45, and Cir2 have no role in plausible signalling mediated via KIV or its downstream intermediates to the growth of the cell in conditions with increased amino acid content. All strains were cultured overnight in HC medium, diluted the next day, and grown to log phase. Cells were harvested, washed, fivefold serially diluted, and spotted on plates containing normal [1 X AAM], double [2 X AAM] or triple [3 X AAM] amount of amino acid dropout mix, containing 2% glucose as carbon substrate. The plates were incubated at 30°C for 42 hours. The top black bar corresponds to the decreasing cell density from left to right. This figure is one of the representative examples from at least three independent experiments performed on different days.

3.5.2 Quantification of intracellular KIV/ α -IPM levels

So far, we observed that *Ilv3* catalyzed step seems to be the pivot point for growth phenotype and redox phenotype in response to the increased amino acid content in the growth medium. Also, overexpression of *Bat1p* could rescue the observed growth phenotype but not the redox phenotype. Thus, at this step, it was quite interesting to investigate which is the key intermediate(s), possibly from the BCAA biosynthetic pathway, leading to the onset of these phenotypes in response to the increased amino acid content in the growth medium.

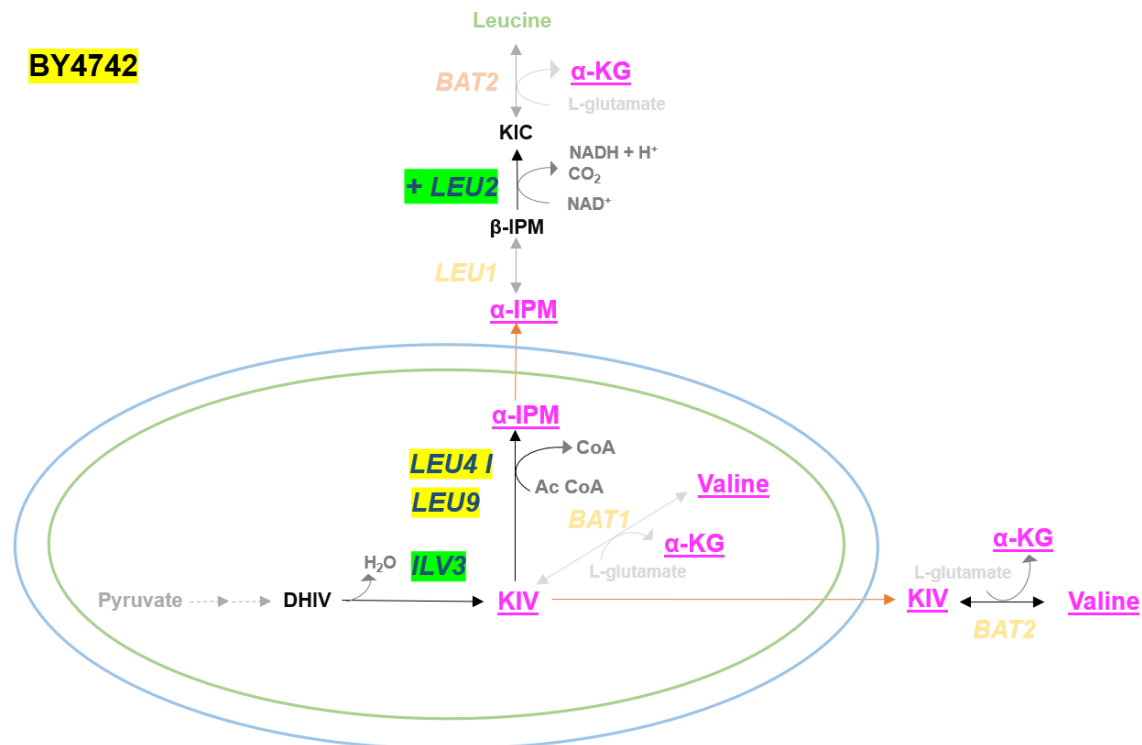


Figure 49: Schematic diagram highlighting the biochemical reactions around the *Ilv3* catalyzed step. The by-product of *Ilv3* catalyzed KIV can either form valine by *Bat1p* catalyzed action inside mitochondria or converted to α -IPM via *LEU4* and can lead to leucine synthesis in the cytoplasm. Since BY4742 is missing the *LEU2*, it cannot synthesise its leucine. KIV can also be further exported out of mitochondria where it can again aminated to valine by *Bat2p*. The potential metabolites that might be involved in inducing the observed phenotypes are represented by pink colour. The red arrows represent the export of the intermediate outside the mitochondria. The dotted grey colour arrow represents the subsequent reaction steps. The yellow (BY4742 or deleting *LEU4* *LEU9*) or green coloured (deleting *ILV3* or transforming the BY4742 cells with missing *LEU2*) represents the conditions, which exhibits or rescues the observed growth phenotype of BY4742 in response to 2 X AAM growth condition, respectively.

After studying the reaction step (fig: 49) around the potential pivot point (*Ilv3* catalyzed step) for the observed growth and redox phenotypes, I shortlisted four downstream metabolites of the *Ilv3* catalyzed step, including KIV. Since these metabolites might be involved in playing a direct or indirect role in inducing the above phenotypes. As the

next step, I investigated the cellular metabolite levels of KIV, valine, α -KG and IPM, in the different yeast strains which either exhibited (BY4742 and $\Delta leu4\Delta leu9$) or rescued ($\Delta ilv3$ and BY4742 transformed with missing *LEU2*) the observed growth phenotype on 2 X AAM and 3 X AAM growth conditions.

The different yeast strains were grown overnight in 1 X AAM and 2 X AAM liquid medium. The following day appropriate volumes of cell broths were processed using the cold extraction protocol (as described in detail under methods section 2.2.5) and were analysed using GC-MS. Thus, the metabolites' levels analysed in different yeast strains represented the combined intracellular plus supernatant concentration (if excreted out by the cell) of the metabolites since there was no separation of biomass and the supernatant during the extraction procedure. Therefore, we observed different valine levels than the previously determined total intracellular valine levels in the BY4742 when grown on 1 X AAM versus 2 X AAM growth conditions.

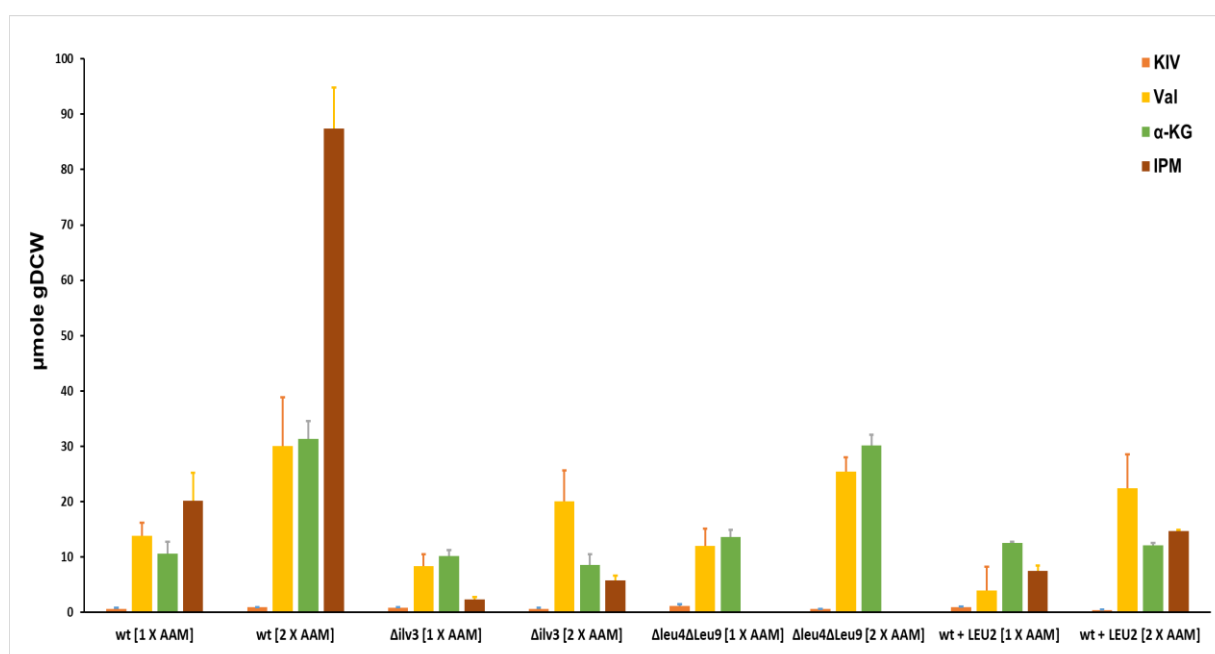


Figure 50: The total cellular metabolites levels. BY4742, $\Delta ilv3$, $\Delta leu4\Delta leu9$, and wt transformed with p415 empty vector (containing *LEU2*) were cultured overnight in HC medium, inoculated in fresh 1 X AAM and 2 X AAM liquid medium the next day and were grown till late exponential phase. The following day, using a cold quenching extraction procedure, an appropriate volume of cell broth (O.D.₆₀₀ of at the time of harvest was around ~ 3) was harvested in a pre-cooled falcon tube. Immediately 35 mL of quenching buffer (95% Acetonitrile, 25 mM formic acid, pre-cooled at -20 °C) was added to the above cell suspension (with the appropriate amount of keto caproic acid, as internal standard, in 2 mL of dH₂O) and was further subjected to incubation on ice for 15 min, vortexed thoroughly in between, and was clarified of cell debris. The supernatant was harvested. The pellet fraction was further washed with supercooled deionized water. The supernatant was harvested again, combined with the first collected fraction, and subsequently frozen at -80 °C. The frozen lysates were lyophilized, re-dissolved in 200 μ L volume of resuspension buffer (100 μ L MeOX + 100 μ L MSTFA, 4 °C), and filtered before injecting to GC-MS. The graphs represent individual metabolite levels (μ mol per cell density weight) from an average of three independent biological replicates. Orange,

and yellow, green, and maroon-coloured bars represent cellular levels (intracellular plus possibly excreted supernatant fraction) of KIV, Valine, α -KG, and IPM, respectively, in different yeast strains grown on 1 X AAM and 2 X AAM growth condition. In this experiment, I prepared the various cell lysates, which were further processed, analysed by Dr Michael Kohlstedt (Wittman's group, at the Saarland University) as a part of the collaboration work.

Surprisingly, nearly no KIV levels were detected in the yeast strains (fig: 50). It could probably mean that KIV is either readily converted to either IPM, valine or any other unknown downstream product in the mitochondria or transported out to the cytoplasm and converted to valine by Bat2. Interestingly, there was approximately 2, 3 and a 4-fold increase in valine, α -KG, and IPM levels, respectively, in BY4742 on 2 X AAM compared to 1 X AAM growth condition (fig: 50). With the previous observation of increased valine synthesis and activation of BCaa pathway genes in BY4742 under 2 X AAM growth conditions, the observation of 4-fold accumulation of IPM levels also is quite convincing. IPM is known to bind to the Leu3 transcription factor in the nucleus, where the Leu3-IPM complex binds to the BCaa pathway genes, *ILV2*, *ILV5*, *LEU4*, *LEU1*, *LEU2* and enhance their expression by many folds¹⁴⁰. It is very likely that massive levels of IPM formed in BY4742 on 2 X AAM growth condition could be activating the BCaa bio-synthesis pathway resulting in a never-ending loop, which could result in a severe problem for the yeast cell which could be leading to the onset of the growth phenotype.

It was also good to observe that since the double mutant *LEU4 LEU9* lacks the α -isopropyl synthase activity, we could not detect any IPM levels in this yeast mutant strain. However, it was observed to still exhibit the growth phenotype on 2 X AAM growth condition. This result implied that IPM might not be the primary causative agent *per se* leading to the observed growth phenotype of BY4742 on 2 X AAM.

I also observed that on 2 X AAM growth condition, levels of α -KG looked similar in amounts for BY4742 and the double mutant *LEU4 LEU9*, which were nearly half in $\Delta ilv3$ and BY4742 + *LEU2* strains (fig: 51), which did not exhibit the observed growth phenotype. This observation indicated that α -KG might have some underlying role in the observed growth phenotype. It was challenging to explain the significance of this α -KG accumulation and its plausible contribution towards the growth phenotype at this point. However, this observation contradicted the previous rescuing growth phenotype of Bat1 overexpression in the mitochondria. Where theoretically, one expects that the Bat1p overexpression diverts the flux from KIV, via *Ilv3* catalyzed step, to valine synthesis (thus favouring the forward reaction) and concomitant α -KG formation, rather than diverting the flux to the *Leu4 Leu9* catalyzed step with IPM formation and subsequent BCaa pathway activation (in a continuous loop).

Nevertheless, the quantification of the potential metabolites: KIV, valine, α -KG, and IPM, strengthen our previous idea that KIV formation via the *Ilv3* catalyzed step is a very crucial step and is a potential switching point for the observed growth and redox phenotypes. Even though we could not detect KIV in the present experimental conditions, KIV might be readily converted to IPM or valine within the mitochondria or an unknown downstream product, ultimately leading to the onset of these phenotypes. Thus, all the results taken together proposed that KIV (or its downstream product)

could still be responsible for triggering the onset of the observed phenotypes (growth and redox both) in response to the increased concentration of Ehrlich amino acids in the growth medium.

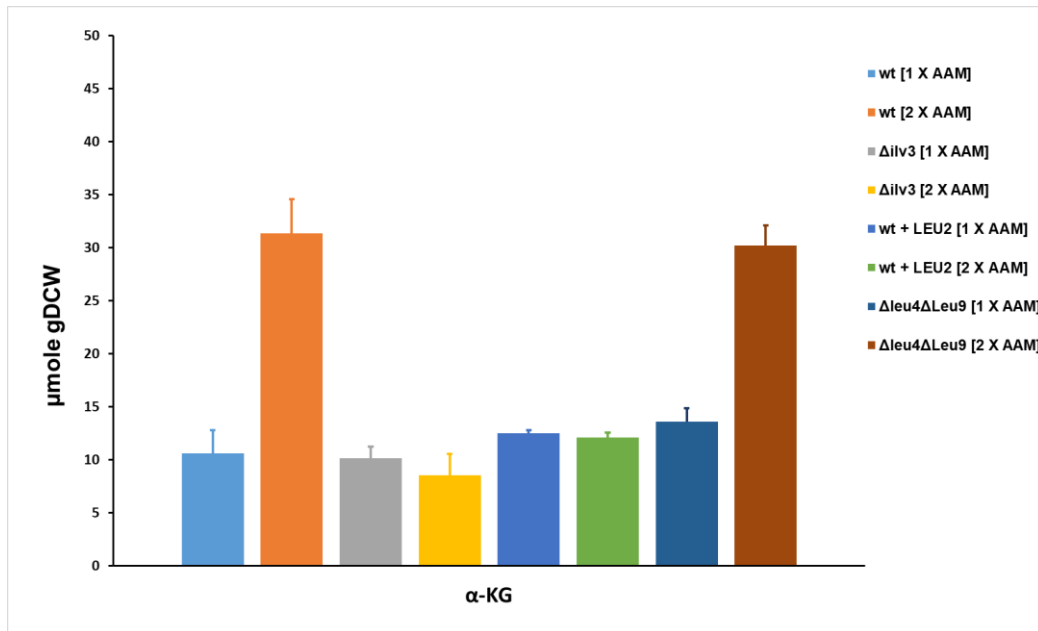


Figure 51: The total cellular alpha-ketoglutarate levels. BY4742, $\Delta ilv3$, $\Delta leu4\Delta leu9$, and wt transformed with p415 empty vector (containing *LEU2*) were cultured overnight in HC medium and the next day were inoculated in fresh HC medium (with either normal [1 X AAM] or double amount [2 X AAM] of amino acid dropout mix) and were grown till late exponential phase. The following day, using a cold quenching extraction procedure, an appropriate volume of cell broth (O.D.₆₀₀ of at the time of harvest was around ~ 3) was harvested in a pre-cooled falcon tube. Immediately 35 mL of quenching buffer (95% Acetonitrile, 25 mM formic acid, pre-cooled at -20 °C) was added to the above cell suspension (with the appropriate amount of keto caproic acid, as internal standard, in 2 mL of dH₂O) and was further subjected to incubation on ice for 15 min, vortexed thoroughly in between, and was clarified of cell debris. The supernatant was harvested. The pellet fraction was further washed with supercooled deionized water. The supernatant was harvested again, combined with the first collected fraction, and subsequently frozen at -80 °C. The frozen lysates were lyophilized, re-dissolved in 200 μL volume of resuspension buffer (100 μL MeOX + 100 μL MSTFA, 4 °C), and filtered before injecting to GC-MS. The graphs represent α-KG levels (μmol per cell density weight) from an average of three independent biological replicates.

4 DISCUSSION

Cells are remarkably tuned to sense extracellular nutrients and adapt to changing nutrient availability by modulating several downstream molecular processes. The rewiring of metabolic processes in non-physiological conditions can be short or long-term, depending upon the exposure time. We know so much about yeast cell growth in various kinds of carbon and nitrogen sources, amino acid-rich or poor conditions and stress factors like high salt, etc. However, there are still many unanswered questions whose insights would positively impact our understanding of various human pathologies (metabolic disorders or aminoacidopathies) and their remedies. The findings of the current study tried to address the impact of the presence of increased amino acids on the growth of a leucine auxotrophic yeast strain.

4.1 The case of leucine limitation

In a recent study, it was shown in mice that the animal's lifespan highly depends on the quality of the amino acid content present in the diet. If the diet is based 100% on essential amino acids, it positively affects the lifespan. The mice lived longer but with the lowest body weight compared to the mice fed with the control diet. Any disturbance to the ratio of essential/non-essential amino acids in the diet resulted in a severe catabolite imbalance response, further resulting in the premature death of the mice²²⁷. When mice were fed with a leucine deprived diet, it activates several physiological responses in the body. It down-regulates the adipose tissue's and liver's lipogenic genes, increases the energy expenditure, and up-regulates oxidative genes in the white adipose tissues and the thermogenic genes. It also decreases the food intake of the animal by 20-30%. Further, 85% leucine restricted diet exhibits a few similar responses like that of methionine restricted diet. It is fascinating to note that the body can sense the minute changes in the concentration of the various essential amino acids in the diet in either restriction or deprivation and arouses both common and unique types of physiological responses in the body²²⁸⁻²³⁰.

Interestingly, I also observed a similar observation where leucine auxotrophs experienced a slow growth phenotype and possibly be starved of leucine (and not due to other essential amino acids) in the presence of increased Ehrlich amino acid content in the growth medium, in comparison to the growth of leucine prototrophs. Further, when leucine was increased in proportion to the increase in the Ehrlich amino acids, this rescued the cell from all of the observed phenotypes. Thus, considering all the above findings from the literature and our current observations, it suggests that the limitation of leucine (which is an essential amino acid for the auxotrophs employed during the study) could be the underlying governing factor for the observed phenotypes.

There was a plausible case of leucine starvation since the concentration of leucine in the HC medium (80 mg/mL) was just one-fourth of the previously reported minimum concentration of leucine to support the maximal cell growth of leucine auxotrophs¹⁷⁶.

However, I found out that this slow growth phenotype did not result particularly due to the leucine limitation *per se* since $\Delta ilv3$, a mutant from the leucine biosynthetic pathway didn't exhibit the observed growth phenotype, and there was no change in the leucine's total intracellular levels on 1 X AAM versus 2 X AAM growth conditions. Instead, when the leucine auxotroph BY4742 tried to upregulate its leucine biosynthetic pathway in the first place, it resulted in the slow growth phenotypes.

4.2 The potential role of leucine underlying the observed phenotype

We observed that excess of Ehrlich amino acids in the growth medium results in the slow growth phenotype of leucine auxotroph BY4742. Either re-establishing functional leucine biosynthetic pathway or increasing leucine in proportion to increasing AAM in the medium (X [AAM + Leu]) could also rescue the cells from the slow-growth phenotype. Interestingly, we also observed that Sit4 activation and resultant enhanced Gcn4 transcription underlies upstream to the observed phenotype. The following intriguing question we came across during the study was what underlies upstream of Sit4 and Gcn4 activation? According to the literature, Sit4 phosphatase is activated upon TOR inhibition. Although, we already addressed and ruled out the possibility of leucine limitation as to the underlying cause for the observed growth phenotype. It was still interesting to figure out how Sit4 is activated in the current growing conditions. Secondly, how increasing leucine content in proportion to increasing AAM in the medium rescues the cells from the slow-growth phenotype? Is there any possible link between leucine availability and TOR-mediated signalling in response to the increase in the amino acid content in the growth medium?

Various studies have underlined the role of amino acids, especially leucine, in mediating and activating the TOR signalling. Conversely, upon amino acids or leucine starvation TORC1 mediated signalling is inhibited. The leucine availability is known to affect the binding of Vam6, which is one of the GEFs for Gtr1, and thus positively modulate the TORC1 signalling in a Gtr1-dependent manner¹⁰⁰. Similarly, Cdc60, the leucine binding LRS is also known to positively regulate TORC1 signalling in leucine's dependent manner. In the abundance of leucine, the CP1 domain of Cdc60 interacts with Gtr1 bound to GTP. However, when cells are starved of leucine, Cdc60, instead of interacting with Gtr1, turns to proof read the mischarged tRNA^{Leu}. Thus, GTP bound to Gtr1 is easily susceptible to GAP activity resulting in inhibition of TOR signalling¹⁰⁶. In another study, Sabatini et al. showed that Iml1 could interact transiently with GTP loaded Gtr1, which is also supported by other SEACIT complex components during the leucine deprivation conditions. These transient interactions activate the GAP activity of SEACIT complex towards the Gtr1^{GTP}, converting it to Gtr1^{GDP} and thus inhibiting the TOR signalling¹⁰⁹.

With these deep insights from the literature about the role of leucine in activating TOR signalling, it was quite intriguing to explore the contribution of leucine underlying the observed growth phenotype. As the next step, I looked at the phenotype of the BY4742 deleted for or overexpressing the *IML1* gene under the control of the TEF promoter. As expected, overexpressing Iml1 enhanced the GAP activity of SEACIT complex, subsequently leading to diminished TOR signalling and retarding the growth of cells.

However, unexpectedly deleting *IML1* contributed to the even slower growth of cells rather than rescuing it in response to an increase in amino acid content in the growth medium. These results again strongly proved that leucine deprivation had no possible contribution towards the observed growth phenotype.

We also observed the activation of the BCaa biosynthetic pathway using ^{13}C glucose labelling and RNA seq studies on 2 X AAM growth conditions. Interestingly, leucine is also reported to inhibit the α -isopropyl malate synthase (Leu4) activity via the negative feedback mechanism, leading to reduced IPM levels and thus ultimately downregulating the BCaa biosynthesis pathway^{134,140}. Thus, implying that supplementation of leucine in the growth medium, in proportion to an increase in the AAM content, should also inhibit the BCaa biosynthetic pathway. Thus one could conclude that rescue of the observed growth phenotype by supplementation of leucine in proportion to the increase in the AAM content in the medium was probably due to inhibition of the potential activation of the BCaa biosynthetic pathway, which is triggering the onset of this phenotype.

4.3 The plausible contribution of the Gap1 permease towards the observed growth phenotype

Interestingly, the increase in amino acids due to mutations leading to increased glutamate/glutamine synthesis de-novo or the abundance of extracellular amino acids in the growth medium induces sorting of the Gap1 permease to the vacuole²³¹. Conversely, the gene mutations affecting this intracellular trafficking of Gap1 permease to the vacuole should be able to sort the Gap1 to the plasma membrane instead. Additionally, it is also studied that the arrestin like adaptor proteins: Bul1 and Bul2, which assist the vacuolar degradation of Gap1 permease, are phosphorylated and inactivated by Npr1 kinase in the presence of poor nitrogen sources in the growth medium. Upon replete nitrogen conditions, further Sit4 phosphatase de-phosphorylate and activates Bul1 and Bul2 proteins, mediating the Gap1 endocytosis and degradation⁸³.

This idea was quite interesting since yeast cells are also exposed to increased extracellular amino acids in the growth medium in the current experimental conditions. This raised several questions like, whether Gap1 also downregulated or not expressed on PM in our current growth conditions and thus leads to the observed growth phenotype. If this holds true, does having the stable expression of broad-spectrum Gap1 amino acid transporter on the plasma membrane could rescue the cells from the observed growth phenotype? To address this possibility, I initially tried to express the Gap1 AAT under the strong TEF promoter's control (fig: 15), which did not exhibit any striking rescuing phenotype.

Since it is well understood that the expression and localization of these AATs are tightly controlled at transcriptional and post-transcriptional level⁴³⁻⁴⁵, over-expressing the AAT itself does not ensure stable expression of these transporters at PM ultimately. Further, in the presence of the preferred nitrogen sources, PM sorted Gap1 is rapidly polyubiquitinated by Rsp5p ubiquitin ligase and is targeted for vacuolar degradation by

Bul1 and Bul2 adaptor proteins^{81,92,232}. Further, Bul1 and Bul2 deleted strains were also observed as the top hits (were resistant to increased amino acid concentration in the growth medium) from the preliminary results from the yeast genetic screen, where the entire yeast deletion library was plated on 1, 2, 3 X AAM containing HC medium plates using the robotic arm (done in collaboration with Blanch Schwappach group, University of Göttingen, Germany). As the next step, a former bachelor student Basile Christou established *BUL1* and *BUL2* deleted BY4742 strains (obtained from the yeast deletion library) and studied their effect on the observed growth phenotype. Deleting Bul1 and Bul2 could not rescue the growth of the BY4742 in response to the increase in amino acid content in the growth medium (2 and 3 X AAM: data not shown).

Secondly, if we also have a look at the total intracellular amino acid levels in a yeast cell grown in 1 X AAM vs 2 X AAM growth conditions, there was no striking decrease in the total amino acid levels of amino acids apart from arginine (imported more on 2 X AAM). By combining all these above observations, one could conclude that Gap1 downregulation has no possible contribution underlying the observed growth phenotype in response to the increase in amino acid content in the growth medium.

4.4 pH-dependent activation of PKA pathway and TORC1 mediated signalling

The activation of the PKA and TORC1 pathway in response to Glucose promotes yeast cell growth and viability¹⁰³. Inactivation of either of these essential pathways severely impacts the growth of the cells leading to cell-cycle arrest at the G1 phase²³³. It is also reported that cytosolic pH changes, indirectly induced in response to quality and quantity of the carbon source, such as Glucose, leads to activation of V-ATPase by protonated of its 'a' subunit, which acts as the cytosolic pH sensor^{234,235}. The activated V-ATPase further interacts with two different GTPases Arf1 and Gtr1, thus regulating the Ras/PKA pathway and TORC1 signalling²³⁵. This idea was quite intriguing since the presence of increased amino acid content in the growth medium could argue that possibly the downregulation of TORC1 mediated signalling, which we speculate to be the upstream factor for the observed phenotype, could potentially stem from the drop in the cytosolic pH. To investigate this idea, I also looked at the changes in the cytosolic pH in the cell in response to increased amino acid content in the growth medium. Surprisingly, there was no considerable change in the cytosolic pH levels in BY4742 and *ILV3* mutant studied using the pHluorin probe when growth in 1 X AAM versus 2 X AAM growth conditions.

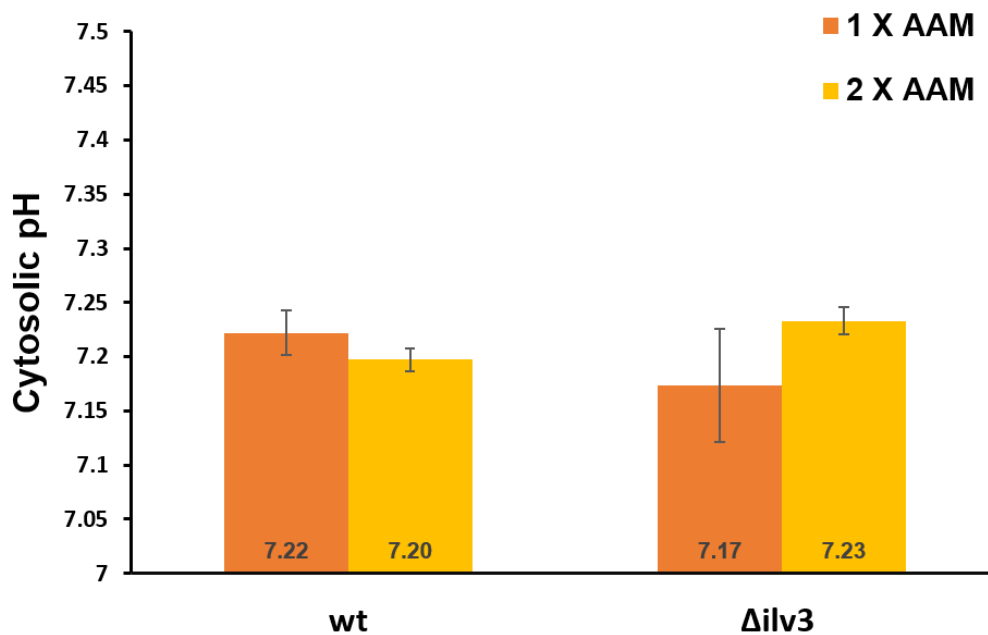


Figure 52: No significant change in the cytosolic pH in BY4742 (wt) and $\Delta ilv3$ due to increased amino acid content in the growth medium. All strains (transformed with empty vector and the cytosolic pHluorin probe^{183,184}) were cultured overnight in HC medium (-histidine) and inoculated to fresh medium (1 X AAM and 2 X AAM) the next day. Cells were harvested (in the O.D. range ~3), resuspended and incubated in the different pH buffers (pH 6 to 7.5) with 0.1% digitonin (for generating the calibration plot) and in the medium (for steady-state value) in a 96 well plate. The cells were settled at the bottom of the plate using the plate centrifuge (15xg; 5 min). Further, the fluorescent response of the pHluorin probe was measured using CLARIOstar plate reader (BMG Labtech) in a time-dependent manner. The histogram represents the average of three independent repeats performed on different days, where error bars represent standard deviation.

In another set of experiments, I also investigated the growth phenotype of mutants (*PDE1*, *PDE2*, *MSN2*, and *MSN4* mutant strains) for the PKA signalling pathway in the presence of increased amino content in the growth medium. Cells deleted for phosphodiesterase Pde1, or Pde2 maintains high cAMP levels and hence have hyperactive PKA signalling²³⁶. Msn2 and Msn4 transcription factors, regulating the general stress responses in a yeast cell, are known to be the downstream effectors of PKA-mediated signalling^{237,238}. As observed from figure 53, *PDE1*, *PDE2*, *MSN2*, and *MSN4* mutant strains didn't alter the observed growth phenotype upon increasing amino acid content in the growth medium. These results gave us a hint that PKA signalling has no substantial role underlying the observed growth phenotype.

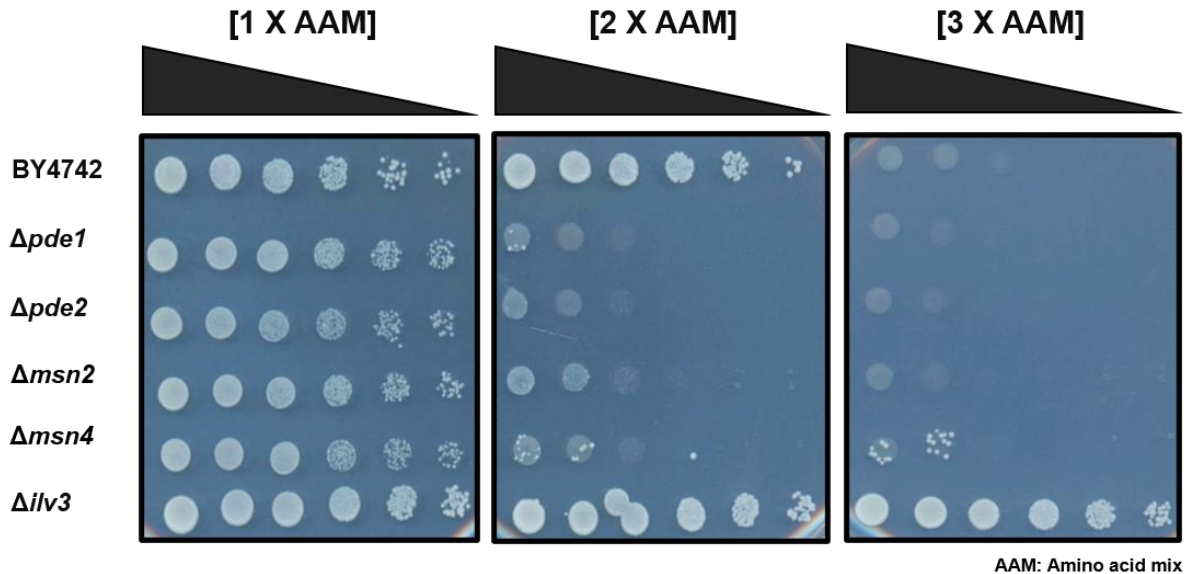


Figure 53: PKA signalling components have no plausible contribution towards the impaired growth phenotype of BY4742 in growth conditions with increased amino acid content. All strains were cultured overnight in HC medium, diluted the next day, and grown to log phase. Cells were harvested, washed, fivefold serially diluted, and spotted on plates containing normal [1 X AAM], double [2 X AAM] or triple [3 X AAM] amount of amino acid dropout mix, containing 2% glucose as carbon substrate. The plates were incubated at 30°C for 42 hours. The top black bar corresponds to the decreasing cell density from left to right. This figure is one of the representative examples from two independent experiments performed on different days.

4.5 The role of branched-chain aminotransferases

We observed that *Ilv3* catalyzed step in the BCaa biosynthetic pathway acts as a potential switch point for the observed growth phenotype. Further, *Bat1* overexpression was also able to rescue the slow growth phenotype in response to the increase in the amino acid content in the growth medium. The role of branched-chain amino transaminases, affecting (either directly or indirectly) various cellular processes, is nicely elucidated in the literature and is described below.

Bat1 was initially identified in a genetic screen as a high-copy suppressor for the mitochondrial ABC transporter- *Atm1*¹⁴³. It was also shown that the yeast *Bat1*, but not *Bat2*, physically interacts with certain BCaa biosynthetic (*Ilv5*, *Ilv3*, *leu4*) and TCA pathway (*Aco1*, *Pdh*) enzymes and might exist in a multi-protein metabolon complex like the mammalian BCAT, Pyruvate carboxylase and BCKDC supercomplex. These experimental pieces of evidence further propose that branched-chain aminotransaminase might couple BCaa pathway (leucine and KIC availability), TCA-pathway flux to activating TOR signalling⁹⁷.

The yeast *Taz1* is the human orthologue of the *TAZ* (taffazin) gene encoding the monolysocardiolipin (MLCL) transacylase enzyme, which is involved in the metabolism of mitochondrial-specific phospholipid cardiolipin (CL)²³⁹. Mutations in the human *TAZ* gene, conserved from yeasts to humans, leads to the onset of Barth syndrome (BTHS).

The BTHS patients suffer from skeletal, cardio-myopathy and neutropenia and have a characteristic accumulation of MLCL, aberrant CL species and overall reduced CL levels in their fibroblasts and platelets²⁴⁰. Rapaport et al. showed that overexpression of the mitochondrial aminotransaminase Bat1 could rescue the severe growth phenotype of $\Delta taz1$ when grown on the synthetic medium using ethanol as a sole carbon source²⁴¹. The findings of this study clearly indicated that Bat1 overexpression did not restore the reported defects of $\Delta taz1$ cells, such as reduced mitochondrial membrane potential or increased MLCL to CL ratio. Instead, it increased the levels of specific Krebs cycle's metabolites (fig: 54).

Interestingly, valine supplementation in the medium also recapitulated the same growth rescue effect for $\Delta taz1$ yeast cells and TAZ-knockdown mouse embryonic fibroblasts cells. In a nutshell, these results strengthen the idea that amino acid metabolism plays an essential role in such disease-relevant mutated cells. Also, supplementation of amino acids such as valine, histidine could help reduce the symptoms of BTHS patients²⁴¹. All these findings from different studies exemplify the role of the BCaa pathway associated with Bat1p in other cellular processes.

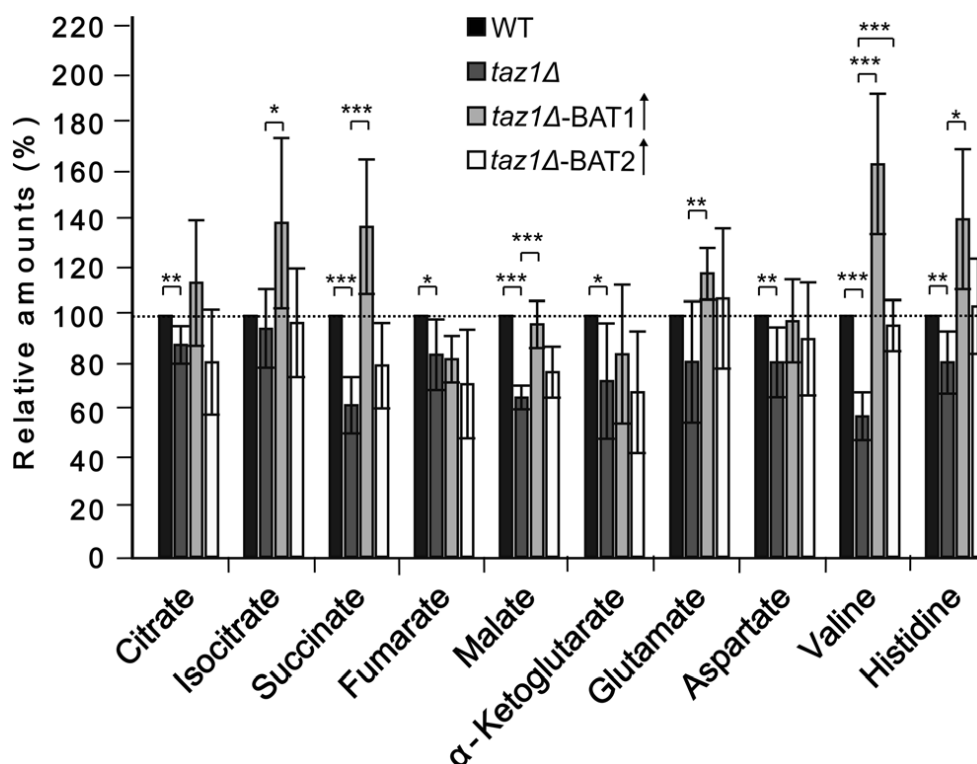


Figure 54: The levels of some metabolites are altered in *taz1Δ* cells and restored upon overexpression of *BAT1*. The indicated metabolites were extracted from the specified cells grown in ethanol-containing medium and were analyzed by LC-MS. The relative peak area of each metabolite was determined, and the levels in control WT cells were taken as 100%. Mean values \pm S.D. of six independent experiments is shown. *, $p < 0.05$; **, $p < 0.01$; ***, $p < 0.001$. This figure and legends are directly adapted from its source: Rapaport et al. ²⁴¹.

It was quite fascinating to observe that the overexpression of Bat1 in $\Delta taz1$ cells probably catalyzing the reversible enzymatic reaction of KIV and glutamate towards the α -KG and valine formation (as interpreted from massive valine levels; fig: 50). Additionally, levels of specific TCA-cycle metabolites are also increased (fig: 54), which subsequently aids in rescuing the observed severe growth phenotype of $\Delta taz1$ cells²⁴¹. Does this mean that favouring the Bat1 catalyzed reaction towards valine synthesis and fueling metabolites and driving the TCA cycle could enhance the overall mitochondrial functional state, ultimately preparing the cell to adapt better and overcome the growth defects observed for $\Delta taz1$ cells?

Interestingly findings from the current study also reported a similar observation. We also observed the slow growth phenotype of BY4742 and increased valine synthesis on 2 X AAM growth conditions. Further, this growth phenotype was rescued by knockdown of *Ilv3* or with overexpression of Bat1. Does this imply that the α -keto acid: KIV (or its downstream product) could be the actual causative agent?

4.6 The role of α -keto acids

The α -keto acids or 2-oxo acids have a ketone group next to the carboxylic acid group. These organic compounds are generally the intermediates in the glycolysis or TCA cycle. The deaminated leucine, valine and isoleucine products, i.e., KIC, KIV, and KMV, respectively, as per the structure, are also known as branched-chain α -keto acids (BCKA). Lill et al. also proposed that mitochondrial branched-chain α -keto acids could play the role of the iron chelator, enabling iron transport through Atm1 transporter in the soluble state from the mitochondrial matrix to cytosol, where it can be incorporated into Fe-S clusters or used for other cellular processes¹⁴³.

As described before, MSUD is a rare metabolic disorder with either zero or reduced BCKDH activity leading to accumulation of the BCaa's and their BCKAs in plasma of the affected individuals. Many clinical studies showed that accumulation of BCaa and their BCKA in mice models of MSUD impacted their brain function and observed lipid-peroxidation in their brain homogenates. So, far we don't understand the pathomechanism behind how BCaa's and their respective BCKA's contributes to neurological damage. Further, in-vitro studies with these mouse brain homogenates indicated that cells experienced high oxidative stress levels and had a less anti-oxidative defence mechanism.

Interestingly, we also observed during this study that the leucine auxotrophic BY4742 exhibited an unusual redox phenotype (high GSSG levels) along with the severe growth phenotype when grown in the presence of increased amino acid content in the growth medium consuming glucose as a sole carbon source. We also observed that both growth and redox phenotypes arose due to the activation of the BCaa biosynthetic pathway on 2 X AAM growth conditions. If the formation of KIV (the potential causative agent) was somehow inhibited ($\Delta ilv3$ or $\Delta sit4$), it rescued both growth and redox phenotype. However, we could not detect the accumulation of KIV levels in our study. Our findings indicate that yeast could be used as a simple eukaryotic model organism to study the mechanisms of how α -keto acids accumulation leads to oxidative stress

and damage to the cell. Such insights would increase our knowledge of the pathomechanism of MSUD.

4.7 The interplay between amino acid homeostasis, mitochondrial function and the cell growth

The mitochondrial TCA cycle not only provides electron donors for ATP production but also fulfils an additional function by synthesizing certain amino acids and other biomolecules such as glutamic acid, aspartate, arginine, and α -ketoglutarate derived amino acids^{242–244}. Further, the blocked respiration activity can be rescued by pyruvate supplementation, which restores the respiration mediated aspartate bio-synthesis in the proliferating mammalian cells^{242,245}. Therefore, the TCA cycle derived products could act as a growth-limiting factor for proliferating mammalian cells. However, some single-celled organisms, such as *S. cerevisiae*, are known to grow with the absence of respiration activity (and even without the mitochondrial genome) under the anaerobic growth conditions²⁴⁶. Under fermentative growth conditions, *S. cerevisiae* utilises the glyoxylate cycle to replenish the TCA cycle intermediates^{247,248}. This in turn, eliminates the need of succinate dehydrogenase activity and further maintains the redox homeostasis under non-respiratory conditions²⁴⁹. These molecular adaptations help budding yeast to cope with non-functional oxidative phosphorylation. On the other hand, *Schizosaccharomyces pombe* has still higher respiration activity under fermentative growth conditions²⁵⁰. Blocking the respiratory activity leads to TOR activity inhibition, amino acids auxotrophy, indicating that respiration activity is essential to support the amino acid metabolism in *S. pombe*²⁵¹. Budding yeast also exhibits a similar phenotypic response for blockage of the TCA cycle but not towards the respiration activity block⁹⁷. It is also known that the cellular mitochondrial function is required for cell survival during the laboratory-induced leucine starvation in *S. cerevisiae*²⁵². These findings suggest that the mitochondrial function, but probably not its respiration activity, is essential for sustaining the amino acid metabolism in *S. cerevisiae*.

Interestingly, it is also shown that overexpression of Bat1-the mitochondrial BCAT or excess supplementation of valine was able to enhance the TCA flux. Thus, increased TCA metabolites levels could rescue the ethanol sensitivity and the growth phenotype of the *TAZ1* deletion strains, where it encodes for the highly conserved phospholipid transacylase enzyme involved in cardiolipin remodelling²⁴¹. Further, both BCATs are also known to activate the TORC1 mediated signalling. Mutations in BCAT lead to a decrease in the TCA metabolites, ATP production and hampered the TOR signalling⁹⁷. Collectively these findings implied that enhanced amino acid metabolism could rescue some of the cellular and mitochondrial dysfunctions by increasing the TCA flux and indirectly by affecting the TORC1 mediated signalling. Furthermore, amino acid metabolism and homeostasis play an essential disease-relevant role in mitochondrial related pathologies^{119,123,253}.

Results from the current study also exhibited similar observations. It was observed that the presence of increased amino acid content, namely Ehrlich amino acids, in the fermentative growth medium induced a slow growth phenotype for leucine auxotrophs,

which was absent in the non-fermentative growth conditions. Further, it was observed that the BCaa biosynthetic pathway was upregulated under these growth conditions, which was plausibly leading to the observed growth phenotypes. There was also a concomitant increase in the α -ketoglutarate levels on 2 X AAM, which is also a by-product of the BCaa pathway along with the TCA cycle. Since, deletion of *ILV3*, encoding for a BCaa pathway enzyme-dihydroxyacid dehydratase, rescued the growth of leucine auxotroph BY4742 on 2 X AAM and 3 X AAM growth conditions. Surprisingly either removing isoleucine and valine from the growth medium or overexpression of mitochondrial BCAT- Bat1 only could also rescue the observed growth phenotype. Our findings suggest that the KIV, α -ketoacid formed during the *Ilv3* catalysed step in the mitochondria, or its unknown downstream product is probably the actual causative agent leading to the onset of the observed phenotypes. However, we could not detect the accumulation of KIV in the current experimental conditions and technical setup. Clearly, with observations from the present study, it seems that the mitochondrial BCaa homeostasis is tightly linked and affecting the other cellular functions in an unknown manner due to the increased presence of Ehrlich amino acids in the growth medium. Hence, all these observations mentioned above and the findings of the current study establish a link between cellular amino acid homeostasis, mitochondrial function and cell growth.

WORKING MODEL

BY4742

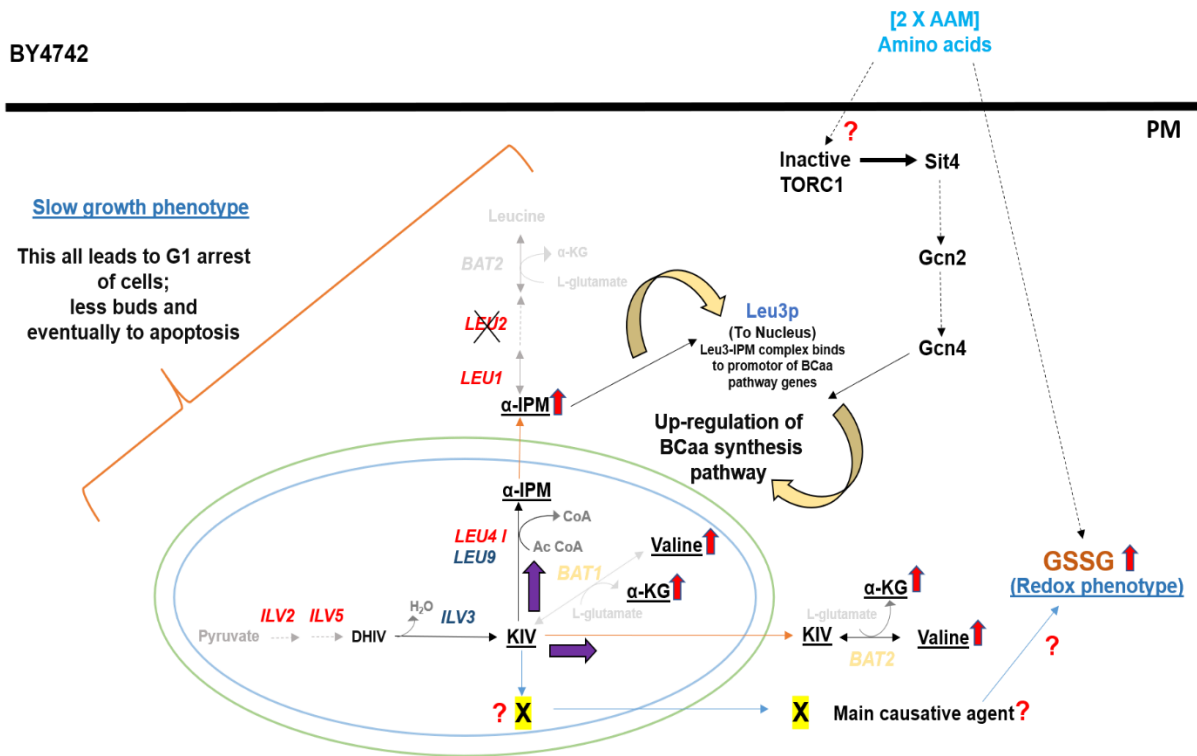


Figure 55: Schematic representation summarising the plausible mechanism contributing to the slow growth phenotype of leucine auxotroph BY4742 on 2 X AAM growth condition. The leucine auxotrophic strain's growth is severely impacted in response to the increased amino acids in the growth medium, especially Ehrlich amino acids. ¹³C glucose labelling RNA sequencing studies indicated the activation of the BCaa pathway on 2 X AAM growth conditions, probably because of Gcn4 mediated signalling. Deleting either *ILV2* or *ILV3* or overexpressing the *Bat1* makes the cell resistant to the observed growth phenotype. These results indicated that *Ilv3* catalysed step acted as the potential switch point. There is a massive accumulation of IPM, valine and α-KG in BY4742 when grown on 2 X AAM. IPM is known to bind to Leu3p in the nucleus and further enhances the transcription of its downstream BCaa gene targets, shown in red colour. Though we could not detect the accumulation of KIV in the current setup, we could not also overlook the possibility that there could be a downstream product X, which could lead to this phenotype. The dotted black arrows indicate the plausible links which are not proven experimentally.

CONCLUSION

We observed that the leucine auxotrophic BY4742 strain exhibited slow growth and redox phenotypes compared to leucine prototrophic yeast strains in response to an increase in Ehrlich amino acids in the growth medium. However, establishing a functional leucine biosynthetic pathway or increasing the concentration of leucine in proportion to the increase in the concentration of amino acid dropout mix in the medium helped rescue the observed slow growth phenotype. Interestingly, from the ^{13}C glucose labelling studies, we also observed that in BY4742, valine synthesis is triggered on 2 X AAM. Total intracellular levels of arginine are also increased tremendously in BY4742 in response to 2 X AAM growth conditions. The idea of upregulation of the BCaa bio-synthesis pathway was also further strengthened by RNA sequencing analysis. It was observed that deleting any gene upstream or *ILV3* could rescue the cell from the observed phenotypes.

Conversely, overexpressing *ILV3* leads to slower growth, probably leading to enhanced IPM production and upregulation of the BCaa bio-synthesis pathway. The activation of the Gcn4 transcription factor upon Sit4 phosphatase activation (possibly due to TORC1 inactivation via an unknown mechanism) resulted in the upregulation of the BCaa bio-synthesis pathway. The presence of increased amino acid content in the growth medium also resulted in apoptosis of BY4742 with a concomitant decrease in global protein synthesis and G1 cell cycle arrest for the remaining live cells. Since IPM, intermediate from the leucine bio-synthesis pathway, binds to Leu3 TF in the nucleus. This Leu3-IPM complex acts as an activator for transcription of BCaa pathway genes¹⁴⁹ (shown in red; figure: 56). Thus, the accumulation of IPM possibly results in continuous hyper-activation of the BCaa pathway, which seems detrimental for the cell.

Interestingly, we also saw the simultaneous accumulation of α -KG in the yeast strains (BY4742 and $\Delta leu4 \Delta leu9$), which exhibited slow growth phenotype on 2 X AAM growth conditions. This observation is quite challenging to interpret and correlate with the observed growth phenotype. Even though we could not detect KIV in the current conditions, it was difficult to rule out the possibility that an unknown downstream product of KIV could be the actual causative agent inducing the observed phenotypes. In conclusion, the *Ilv3* catalyzed step seems to be the switching point for the growth and redox phenotypes in response to the increased Ehrlich amino acid content in the growth medium.

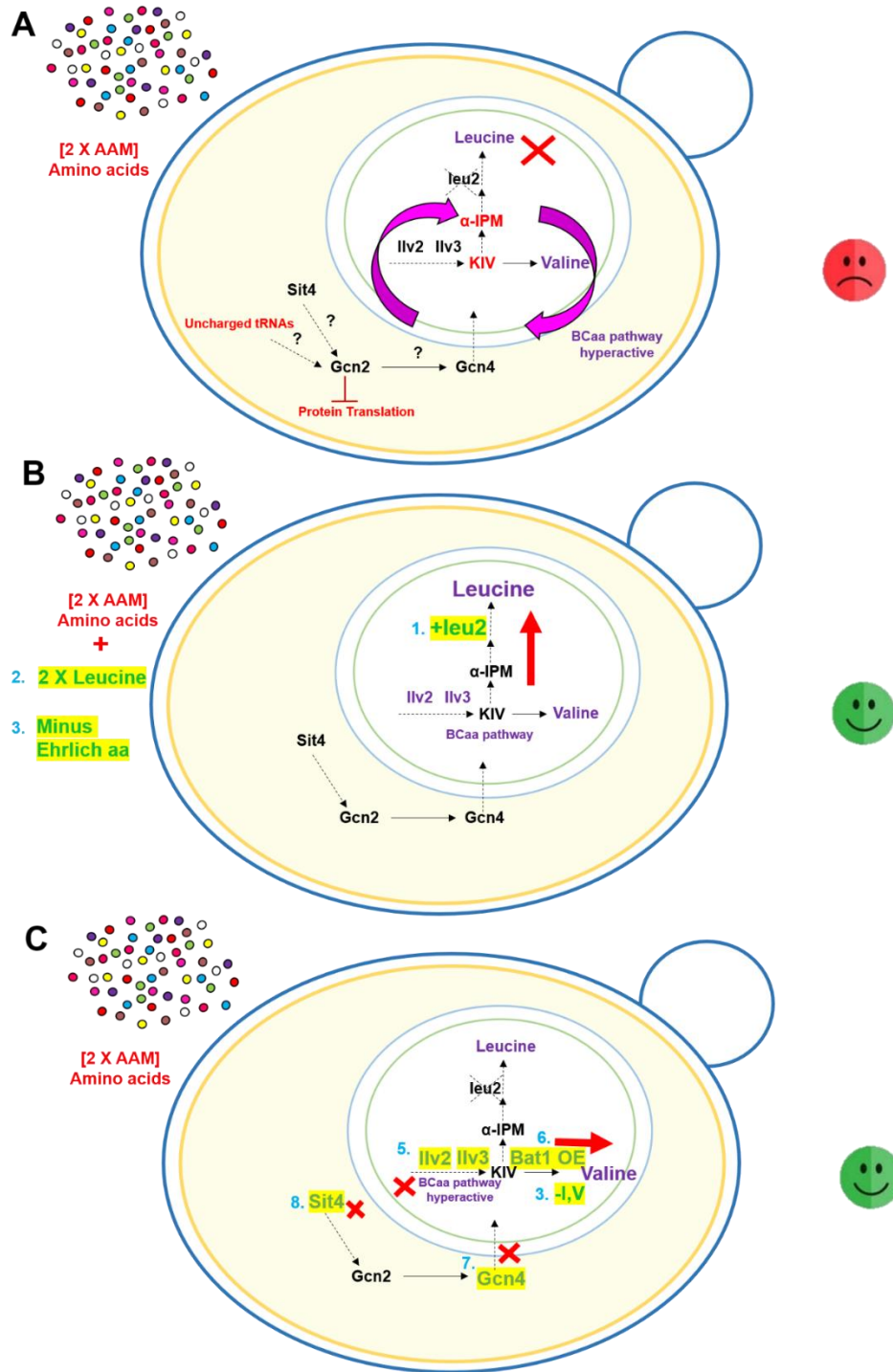
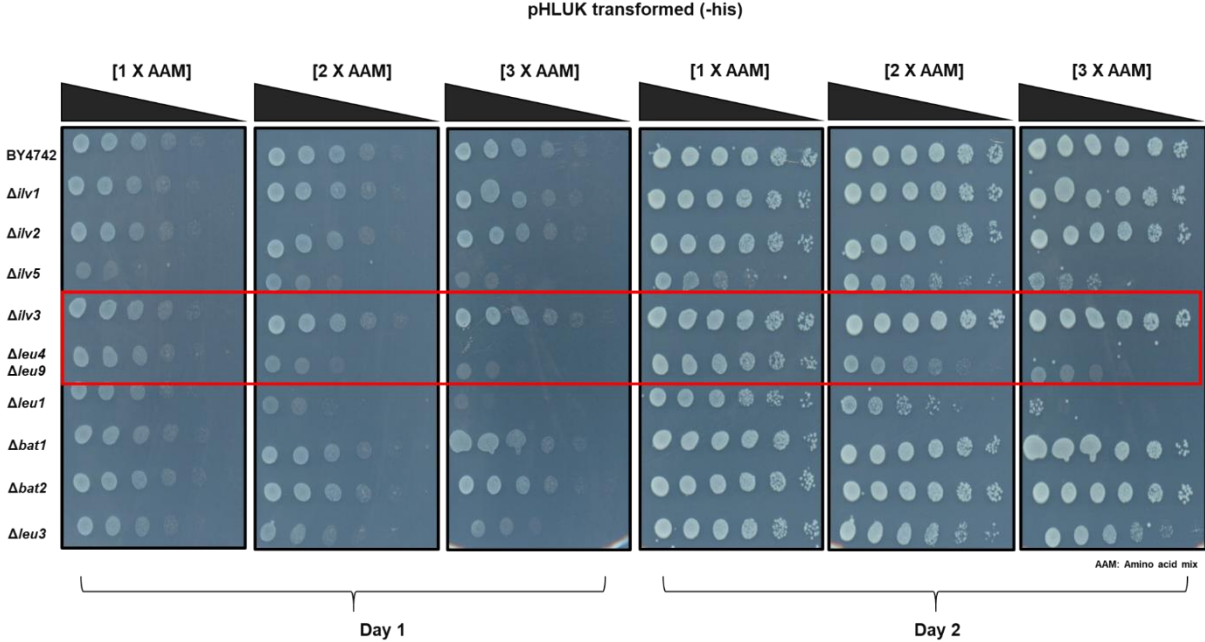


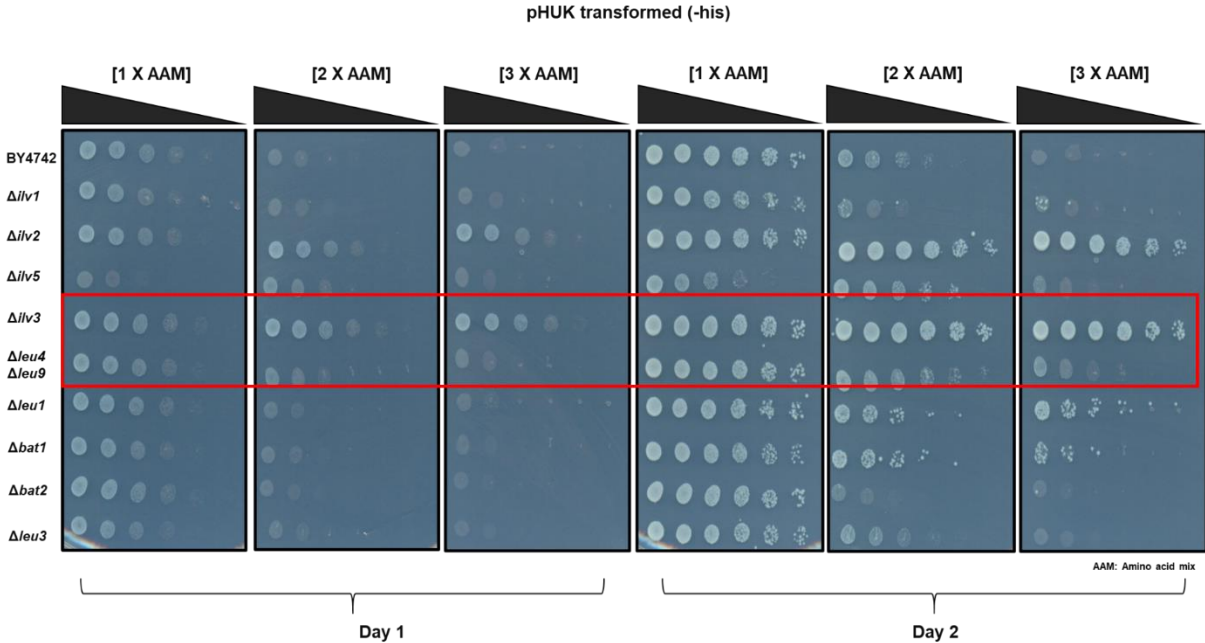
Figure 56: Schematic representation summarizing the observations of the current study. **A:** The aberrant activation of the BCAA pathway possibly contributing to the slow growth phenotype in response to the increased amino acid, especially Ehrlich amino acids, content in the growth medium. **B:** Extra supplementation of leucine in proportion to increase in the amino acid content (AAM) or re-establishment of functional leucine biosynthetic pathway rescues the cell from this phenotype. **C:** Deleting the genes (*SIT4*, *GCN4*, *ILV2*, or *ILV3*), which is observed to lie upstream of the potential switch point, contributed towards the observed growth phenotype of BY4742 on 2 X AAM. Further, overexpression of Bat1 or removing isoleucine and valine from the growth medium also made BY4742 resistant to the observed growth phenotype.

SUPPLEMENTARY FIGURES

A



B



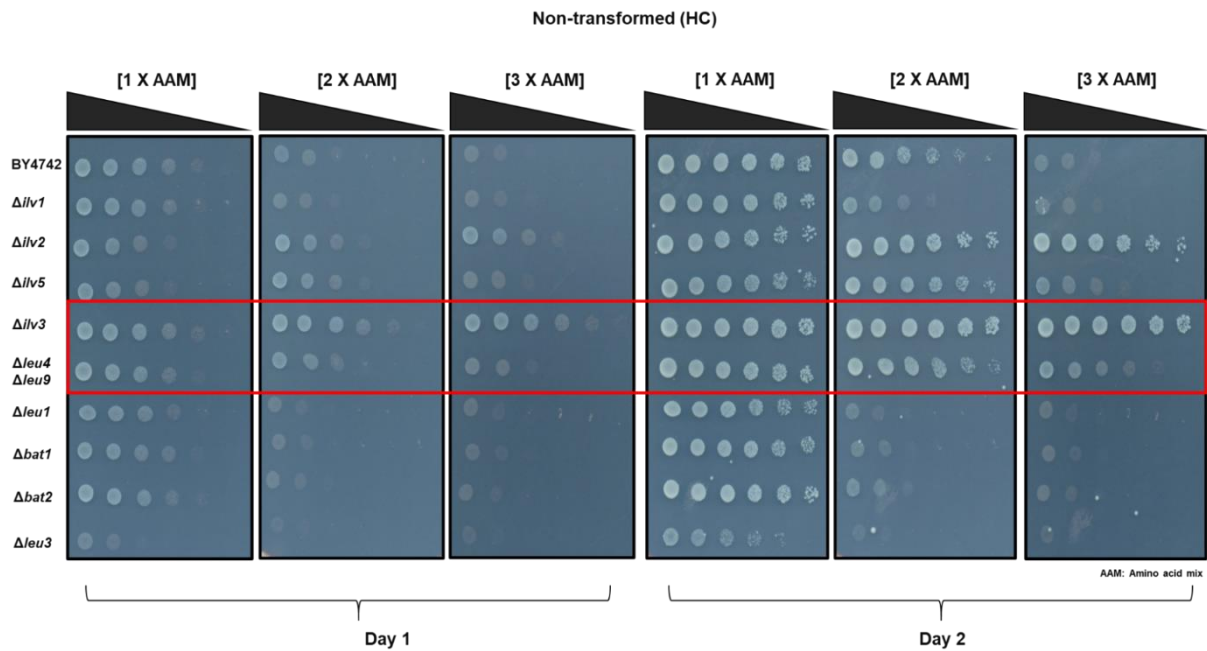
C

Figure 57: Deleting *ILV2* or *ILV3*, and not *LEU4* *LEU9*, rescues the growth of cells in conditions with increased amino acid content. Several mutants of the BCaa pathway were made during this study via homologous recombination. To restore the missing *LEU2*, which also belongs to this BCaa pathway, the BY4742 and all mutants were transformed with either pHUK or pHLUK plasmids. All the transformed (pHLUK-A and pHUK-B) and non-transformed (C) strains were cultured overnight in HC (minus histidine, to maintain the plasmid selection), diluted the next day, and grown to log phase. Cells were harvested, washed, fivefold serially diluted, and spotted on plates containing normal [1 X AAM], double [2 X AAM] or triple [3 X AAM] amount of amino acid dropout mix (without histidine to maintain the selection for cells transformed with plasmids), containing 2% glucose as carbon substrate. The plates were scanned following incubation at 30°C after 24 and 48 hours of the incubation time. The top black bar corresponds to the decreasing cell density from left to right. This figure is one of the representative examples from at least three independent experiments performed on different days.

REFERENCES

1. Berg Jeremy M, Tymoczko John L & Stryer Lubert. *Biochemistry* . (W H Freeman and company, 2002).
2. Wu, G. Amino acids: Metabolism, functions, and nutrition. *Amino Acids* vol. 37 1–17 (2009).
3. Rosenberg, L. E. *Diagnosis and Management of Inherited Aminoacidopathies in the Newborn and the Unborn**. *Clinics in Endocrinology and Metabolism* vol. 3, no 1 145–152 (Baillière Tindall, 1974).
4. Chen, X. & Yang, W. *Branched-chain amino acids and the association with type 2 diabetes*. *Journal of Diabetes Investigation* vol. 6 369–370 (Blackwell Publishing, 2015).
5. Bloomgarden, Z. *Diabetes and branched-chain amino acids: What is the link?* *Journal of Diabetes* vol. 10 350–352 (John Wiley and Sons Inc., 2018).
6. Bridi, R. *et al.* α -keto acids accumulating in maple syrup urine disease stimulate lipid peroxidation and reduce antioxidant defences in cerebral cortex from young rats. *Metab. Brain Dis.* **20**, 155–167 (2005).
7. Bridi, R. *et al.* Induction of oxidative stress in rat brain by the metabolites accumulating in maple syrup urine disease. *Int. J. Dev. Neurosci.* **21**, 327–332 (2003).
8. Funchal, C. *et al.* Morphological alterations and induction of oxidative stress in glial cells caused by the branched-chain α -keto acids accumulating in maple syrup urine disease. *Neurochem. Int.* **49**, 640–650 (2006).
9. Lima Pelaez, P. *et al.* Branched-chain amino acids accumulating in maple syrup urine disease induce morphological alterations in C6 glioma cells probably through reactive species. *Int. J. Dev. Neurosci.* **25**, 181–189 (2007).
10. What are yeasts?
https://web.archive.org/web/20090226151906/http://www.yeastgenome.org/VL-what_are_yeast.html.
11. Legras, J. L., Merdinoglu, D., Cornuet, J. M. & Karst, F. Bread, beer and wine: *Saccharomyces cerevisiae* diversity reflects human history. *Mol. Ecol.* **16**, 2091–2102 (2007).
12. Michel, R. H., McGovern, P. E. & Badler, V. R. Chemical evidence for ancient beer [12]. *Nature* vol. 360 24 (1992).
13. Kurtzman, C. P. Molecular taxonomy of the yeasts. *Yeast* **10**, 1727–1740 (1994).
14. Herskowitz, I. Life cycle of the budding yeast *Saccharomyces cerevisiae*. *Microbiological Reviews* vol. 52 536–553 (1988).
15. Gow, N. A. R. & Yadav, B. Microbe profile: *Candida albicans*: A shape-changing, opportunistic pathogenic fungus of humans. *Microbiol. (United Kingdom)* **163**, 1145–1147 (2017).

16. Liti, G. *The fascinating and secret wild life of the budding yeast S. cerevisiae*. *eLife* vol. 4 (eLife Sciences Publications Ltd, 2015).
17. Eduard Buchner - Biographical. <https://www.nobelprize.org/prizes/chemistry/1907/buchner/biographical/>.
18. Szybalski, W. My road to Øjvind Winge, the father of yeast genetics. *Genetics* vol. 158 1–6 (2001).
19. Leland H. Hartwell - Facts - NobelPrize.org. <https://www.nobelprize.org/prizes/medicine/2001/hartwell/facts/>.
20. Sir Paul Nurse - Facts. <https://www.nobelprize.org/prizes/medicine/2001/nurse/facts/>.
21. Randy W. Schekman - Facts - NobelPrize.org. <https://www.nobelprize.org/prizes/medicine/2013/schekman/facts/>.
22. Yoshinori Ohsumi - Facts. <https://www.nobelprize.org/prizes/medicine/2016/ohsumi/facts/>.
23. H Nakatogawa, K. S. Y. K. Y. O. Dynamics and diversity in autophagy mechanisms: lessons from yeast. *Nat. Rev. Mol. Cell Biol.* **10**, 458–467 (2009).
24. Hohmann, S. Nobel Yeast Research. *FEMS Yeast Res.* **16**, fow094 (2016).
25. Aitman, T. J. *et al.* *The future of model organisms in human disease research*. *Nature Reviews Genetics* vol. 12 575–582 (Nature Publishing Group, 2011).
26. Hao, H. X. *et al.* SDH5, a gene required for flavination of succinate dehydrogenase, is mutated in paraganglioma. *Science* (80-.). **325**, 1139–1142 (2009).
27. Khurana, V. & Lindquist, S. Modelling neurodegeneration in *Saccharomyces cerevisiae*: Why cook with baker's yeast? *Nature Reviews Neuroscience* vol. 11 436–449 (2010).
28. Botstein, D. & Fink, G. R. Yeast: An experimental organism for 21st century biology. *Genetics* **189**, 695–704 (2011).
29. D Botstein, G. F. Yeast: an experimental organism for modern biology. *Science* (80-.). **240**, 1439–1443 (1988).
30. D Botstein, S. C. J. C. Yeast as a model organism. *Science* (80-.). **277**, 1259–1260 (1997).
31. Goffeau, A. *et al.* Life with 6000 genes. *Science* (80-.). **274**, 546–567 (1996).
32. Giaever, G. *et al.* Functional profiling of the *Saccharomyces cerevisiae* genome. *Nature* **418**, 387–391 (2002).
33. Sopko, R. *et al.* Mapping pathways and phenotypes by systematic gene overexpression. *Mol. Cell* **21**, 319–330 (2006).
34. Huh, W. K. *et al.* Global analysis of protein localization in budding yeast. *Nature* **425**, 686–691 (2003).
35. Ertugay, N. & Hamamci, H. Continuous Cultivation of Bakers' Yeast: Change in Cell Composition at Different Dilution Rates and Effect of Heat Stress on

- Trehalose Level. *Folia Microbiol. (Praha)*. **42**, 463–467 (1997).
36. Stadtman, T. C. Selenocysteine. *Annual Review of Biochemistry* vol. 65 83–100 (1996).
 37. Krzycki, J. A. The direct genetic encoding of pyrrolysine. *Current Opinion in Microbiology* vol. 8 706–712 (2005).
 38. Hou, Y. & Wu, G. Nutritionally essential amino acids. *Adv. Nutr.* **9**, 849–851 (2018).
 39. Hou, Y., Yin, Y. & Wu, G. Dietary essentiality of “nutritionally non-essential amino acids” for animals and humans. *Exp. Biol. Med.* **240**, 997–1007 (2015).
 40. Reeds, P. J. Dispensable and indispensable amino acids for humans. in *Journal of Nutrition* vol. 130 1835S-1840S (American Institute of Nutrition, 2000).
 41. Millward, D. J. Human amino acid requirements. *Journal of Nutrition* vol. 127 1842–1846 (1997).
 42. Berg, J. M., Tymoczko, J. L. & Stryer, L. Carbon Atoms of Degraded Amino Acids Emerge as Major Metabolic Intermediates. (2002).
 43. Hazelwood, L. A., Daran, J. M., Van Maris, A. J. A., Pronk, J. T. & Dickinson, J. R. The Ehrlich pathway for fusel alcohol production: A century of research on *Saccharomyces cerevisiae* metabolism. *Applied and Environmental Microbiology* vol. 74 2259–2266 (2008).
 44. Klasson, H., Fink, G. R. & Ljungdahl, P. O. Ssy1p and Ptr3p Are Plasma Membrane Components of a Yeast System That Senses Extracellular Amino Acids. *Mol. Cell. Biol.* **19**, 5405–5416 (1999).
 45. Forsberg, H., Gilstring, C. F., Zargari, A., Martínez, P. & Ljungdahl, P. O. *The role of the yeast plasma membrane SPS nutrient sensor in the metabolic response to extracellular amino acids. Molecular Microbiology* vol. 42 215–228 (John Wiley & Sons, Ltd, 2008).
 46. Didion, T., Regenber, B., Jørgensen, M. U., Kielland-Brandt, M. C. & Andersen, H. A. The permease homologue Ssy1p controls the expression of amino acid and peptide transporter genes in *Saccharomyces cerevisiae*. *Mol. Microbiol.* **27**, 643–650 (1998).
 47. Ljungdahl, P. O. Amino-acid-induced signalling via the SPS-sensing pathway in yeast. *Biochem. Soc. Trans.* **37**, 242–247 (2009).
 48. Conrad, M. *et al.* *Nutrient sensing and signaling in the yeast Saccharomyces cerevisiae. FEMS Microbiology Reviews* vol. 38 254–299 (2014).
 49. Abdel-Sater, F., El Bakkoury, M., Urrestarazu, A., Vissers, S. & André, B. Amino Acid Signaling in Yeast: Casein Kinase I and the Ssy5 Endoprotease Are Key Determinants of Endoproteolytic Activation of the Membrane-Bound Stp1 Transcription Factor. *Mol. Cell. Biol.* **24**, 9771–9785 (2004).
 50. Abdel-Sater, F., Jean, C., Merhi, A., Vissers, S. & André, B. Amino acid signaling in yeast: Activation of Ssy5 protease is associated with its phosphorylation-induced ubiquitylation. *J. Biol. Chem.* **286**, 12006–12015

- (2011).
51. Omnus, D. J., Pfirrmann, T., Andréasson, C. & Ljungdahl, P. O. A phosphodegron controls nutrient-induced proteasomal activation of the signaling protease Ssy5. *Mol. Biol. Cell* **22**, 2754–2765 (2011).
 52. De Boer, M. *et al.* Stp1p, Stp2p and Abf1p are involved in regulation of expression of the amino acid transporter gene BAP3 of *Saccharomyces cerevisiae*. *Nucleic Acids Res.* **28**, 974–981 (2000).
 53. Andréasson, C. & Ljungdahl, P. O. Receptor-mediated endoproteolytic activation of two transcription factors in yeast. *Genes Dev.* **16**, 3158–3172 (2002).
 54. Boban, M. *et al.* Asi1 is an inner nuclear membrane protein that restricts promoter access of two latent transcription factors. *J. Cell Biol.* **173**, 695–707 (2006).
 55. Zargari, A. *et al.* Inner nuclear membrane proteins Asi1, Asi2, and Asi3 function in concert to maintain the latent properties of transcription factors Stp1 and Stp2. *Journal of Biological Chemistry* vol. 282 594–605 (J Biol Chem, 2007).
 56. Shin, C. S., Kim, S. Y. & Huh, W. K. TORC1 controls degradation of the transcription factor Stp1, a key effector of the SPS amino-acidsensing pathway in *Saccharomyces cerevisiae*. *J. Cell Sci.* **122**, 2089–2099 (2009).
 57. Hinnebusch, A. G. & Fink, G. R. The general control of amino acid biosynthetic genes in the yeast *saccharomyces cerevisia*. *Crit. Rev. Biochem. Mol. Biol.* **21**, 277–317 (1986).
 58. Rolfes, R. J. & Hinnebusch, A. G. Translation of the yeast transcriptional activator GCN4 is stimulated by purine limitation: implications for activation of the protein kinase GCN2. *Mol. Cell. Biol.* **13**, 5099–5111 (1993).
 59. Yang, R., Wek, S. A. & Wek, R. C. Glucose Limitation Induces GCN4 Translation by Activation of Gcn2 Protein Kinase. *Mol. Cell. Biol.* **20**, 2706–2717 (2000).
 60. Hinnebusch, A. G. *Translational regulation of GCN4 and the general amino acid control of yeast.* *Annual Review of Microbiology* vol. 59 407–450 (Annu Rev Microbiol, 2005).
 61. Wek, R. C., Staschke, K. A. & Narasimhan, J. 7 Regulation of the yeast general amino acid control pathway in response to nutrient stress. in 171–199 (Springer, Berlin, Heidelberg, 2004). doi:10.1007/978-3-540-39898-1_8.
 62. Simpson, C. E. & Ashe, M. P. Adaptation to stress in yeast: To translate or not? in *Biochemical Society Transactions* vol. 40 794–799 (Biochem Soc Trans, 2012).
 63. Vattem, K. M. & Wek, R. C. Reinitiation involving upstream ORFs regulates ATF4 mRNA translation in mammalian cells. *Proc. Natl. Acad. Sci. U. S. A.* **101**, 11269–11274 (2004).
 64. Wek, R. C., Jiang, H. Y. & Anthony, T. G. Coping with stress: EIF2 kinases and translational control. in *Biochemical Society Transactions* vol. 34 7–11 (Portland Press Ltd, 2006).

65. Mittal, N. *et al.* The Gcn4 transcription factor reduces protein synthesis capacity and extends yeast lifespan. *Nat. Commun.* **8**, 1–12 (2017).
66. Steffen, K. K. *et al.* Yeast Life Span Extension by Depletion of 60S Ribosomal Subunits Is Mediated by Gcn4. *Cell* **133**, 292–302 (2008).
67. Pavitt, G. D., Yang, W. & Hinnebusch, A. G. Homologous segments in three subunits of the guanine nucleotide exchange factor eIF2B mediate translational regulation by phosphorylation of eIF2. *Mol. Cell. Biol.* **17**, 1298–1313 (1997).
68. Kimball, S. R. *Eukaryotic initiation factor eIF2*. *International Journal of Biochemistry and Cell Biology* vol. 31 25–29 (Int J Biochem Cell Biol, 1999).
69. Jackson, R. J., Hellen, C. U. T. & Pestova, T. V. The mechanism of eukaryotic translation initiation and principles of its regulation. *Nature Reviews Molecular Cell Biology* vol. 11 113–127 (2010).
70. Wek, R. C., Jackson, B. M. & Hinnebusch, A. G. Juxtaposition of domains homologous to protein kinase and histidyl-tRNA synthetases in GCN2 protein suggests a mechanism for coupling GCN4 expression to amino acid availability. *Proc. Natl. Acad. Sci. U. S. A.* **86**, 4579–4583 (1989).
71. Dong, J., Qiu, H., Garcia-Barrio, M., Anderson, J. & Hinnebusch, A. G. *Uncharged tRNA activates GCN2 by displacing the protein kinase moiety from a bipartite tRNA-binding domain*. *Molecular Cell* vol. 6 269–279 (Cell Press, 2000).
72. Cherkasova, V. A. & Hinnebusch, A. G. Translational control by TOR and TAP42 through dephosphorylation of eIF2 α kinase GCN2. *Genes Dev.* **17**, 859–872 (2003).
73. Rawal, Y., Qiu, H. & Hinnebusch, A. G. *Accumulation of a Threonine Biosynthetic Intermediate Attenuates General Amino Acid Control by Accelerating Degradation of Gcn4 via Pho85 and Cdk8*. *PLoS Genetics* vol. 10 e1004534 (Public Library of Science, 2014).
74. Natarajan, K. *et al.* *Transcriptional Profiling Shows that Gcn4p Is a Master Regulator of Gene Expression during Amino Acid Starvation in Yeast*. *Molecular and Cellular Biology* vol. 21 4347–4368 (American Society for Microbiology, 2001).
75. Jia, M. H. *et al.* Global expression profiling of yeast treated with an inhibitor of amino acid biosynthesis, sulfometuron methyl. *Physiol. Genomics* **2000**, 83–92 (2000).
76. Zhang, W., Du, G., Zhou, J. & Chen, J. Regulation of Sensing, Transportation, and Catabolism of Nitrogen Sources in *Saccharomyces cerevisiae*. *Microbiol. Mol. Biol. Rev.* **82**, (2018).
77. André, B. An overview of membrane transport proteins in *Saccharomyces cerevisiae*. *Yeast* **11**, 1575–1611 (1995).
78. Regenberg, B., Düring-Olsen, L., Kielland-Brandt, M. C. & Holmberg, S. Substrate specificity and gene expression of the amino acid permeases in *Saccharomyces cerevisiae*. *Curr. Genet.* **36**, 317–328 (1999).
79. Sophianopoulou, V. & Diallinas, G. Amino acid transporters of lower

- eukaryotes: regulation, structure and topogenesis. *FEMS Microbiol. Rev.* **16**, 53–75 (1995).
80. Magasanik, B. & Kaiser, C. A. Nitrogen regulation in *Saccharomyces cerevisiae*. *Gene* vol. 290 1–18 (2002).
 81. Rubio-Texeira, M. & Kaiser, C. A. Amino Acids Regulate Retrieval of the Yeast General Amino Acid Permease from the Vacuolar Targeting Pathway. *Mol. Biol. Cell* **17**, 3031–3050 (2006).
 82. Ruiz, S. J., van 't Klooster, J. S., Bianchi, F. & Poolman, B. Growth inhibition by amino acids in *Saccharomyces cerevisiae*. *Microorganisms* **9**, 1–17 (2021).
 83. Merhi, A. & Andre, B. Internal Amino Acids Promote Gap1 Permease Ubiquitylation via TORC1/Npr1/14-3-3-Dependent Control of the Bul Arrestin-Like Adaptors. *Mol. Cell. Biol.* **32**, 4510–4522 (2012).
 84. Bernard, F. & André, B. Ubiquitin and the SCFGrr1 ubiquitin ligase complex are involved in the signalling pathway activated by external amino acids in *Saccharomyces cerevisiae*. *FEBS Lett.* **496**, 81–85 (2001).
 85. Huibregtse, J. M., Scheffner, M., Beaudenon, S. & Howley, P. M. A family of proteins structurally and functionally related to the E6-AP ubiquitin-protein ligase. *Proc. Natl. Acad. Sci. U. S. A.* **92**, 2563–2567 (1995).
 86. Hein, C., Springael, J. -Y, Volland, C., Haguenaer-Tsapis, R. & André, B. NPI1, an essential yeast gene involved in induced degradation of Gap1 and Fur4 permeases, encodes the Rsp5 ubiquitin—protein ligase. *Mol. Microbiol.* **18**, 77–87 (1995).
 87. Lauwers, E., Erpapazoglou, Z., Haguenaer-Tsapis, R. & André, B. The ubiquitin code of yeast permease trafficking. *Trends in Cell Biology* vol. 20 196–204 (2010).
 88. Grenson, M., Hou, C. & Crabeel, M. Multiplicity of the amino acid permeases in *Saccharomyces cerevisiae*. IV. Evidence for a general amino acid permease. *J. Bacteriol.* **103**, 770–777 (1970).
 89. Kriel, J., Haesendonckx, S., Rubio-Texeira, M., Van Zeebroeck, G. & Thevelein, J. M. From transporter to transceptor: Signaling from transporters provokes re-evaluation of complex trafficking and regulatory controls: Endocytic internalization and intracellular trafficking of nutrient transceptors may, at least in part, be governed by their signaling function. *BioEssays* **33**, 870–879 (2011).
 90. Holsbeeks, I., Lagatie, O., Van Nuland, A., Van De Velde, S. & Thevelein, J. M. The eukaryotic plasma membrane as a nutrient-sensing device. *Trends in Biochemical Sciences* vol. 29 556–564 (2004).
 91. Donaton, M. C. V. *et al.* The Gap1 general amino acid permease acts as an amino acid sensor for activation of protein kinase A targets in the yeast *Saccharomyces cerevisiae*. *Mol. Microbiol.* **50**, 911–929 (2003).
 92. Springael, J. Y. & André, B. Nitrogen-regulated ubiquitination of the Gap1 permease of *Saccharomyces cerevisiae*. *Mol. Biol. Cell* **9**, 1253–1263 (1998).
 93. Schmidt, A., Beck, T., Koller, A., Kunz, J. & Hall, M. N. The TOR nutrient

- signalling pathway phosphorylates NPR1 and inhibits turnover of the tryptophan permease. *EMBO J.* **17**, 6924–6931 (1998).
94. Crapeau, M., Merhi, A. & André, B. Stress conditions promote yeast Gap1 permease ubiquitylation and down-regulation via the arrestin-like bul and aly proteins. *J. Biol. Chem.* **289**, 22103–22116 (2014).
 95. O'Donnell, A. F., Apffel, A., Gardner, R. G. & Cyert, M. S. α -arrestins Aly1 and Aly2 regulate intracellular trafficking in response to nutrient signaling. *Mol. Biol. Cell* **21**, 3552–3566 (2010).
 96. Loewith, R. & Hall, M. N. Target of rapamycin (TOR) in nutrient signaling and growth control. *Genetics* vol. 189 1177–1201 (2011).
 97. Kingsbury, J. M., Sen, N. D. & Cardenas, M. E. Branched-Chain Aminotransferases Control TORC1 Signaling in *Saccharomyces cerevisiae*. **11**, (2015).
 98. Helliwell, S. B. *et al.* TOR1 and TOR2 are structurally and functionally similar but not identical phosphatidylinositol kinase homologues in yeast. *Mol. Biol. Cell* **5**, 105–118 (1994).
 99. Kim, J. & Guan, K. L. Amino acid signaling in TOR Activation. *Annu. Rev. Biochem.* **80**, 1001–1032 (2011).
 100. Binda, M. *et al.* The Vam6 GEF Controls TORC1 by Activating the EGO Complex. *Mol. Cell* **35**, 563–573 (2009).
 101. Sancak, Y. *et al.* The rag GTPases bind raptor and mediate amino acid signaling to mTORC1. *Science (80-.)*. **320**, 1496–1501 (2008).
 102. Kim, E., Goraksha-Hicks, P., Li, L., Neufeld, T. P. & Guan, K. L. Regulation of TORC1 by Rag GTPases in nutrient response. *Nat. Cell Biol.* **10**, 935–945 (2008).
 103. Broach, J. R. Nutritional control of growth and development in yeast. *Genetics* vol. 192 73–105 (2012).
 104. Georis, I., Feller, A., Vierendeels, F. & Dubois, E. The Yeast GATA Factor Gat1 Occupies a Central Position in Nitrogen Catabolite Repression-Sensitive Gene Activation. *Mol. Cell. Biol.* **29**, 3803–3815 (2009).
 105. Stracka, D., Jozefczuk, S., Rudroff, F., Sauer, U. & Hall, M. N. Nitrogen source activates TOR (Target of Rapamycin) complex 1 via glutamine and independently of Gtr/Rag proteins. *J. Biol. Chem.* **289**, 25010–25020 (2014).
 106. Bonfils, G. *et al.* Leucyl-tRNA Synthetase Controls TORC1 via the EGO Complex. *Mol. Cell* **46**, 105–110 (2012).
 107. Panchaud, N., Péli-Gulli, M. P. & De Virgilio, C. SEACing the GAP that nEGOCiates TORC1 activation: Evolutionary conservation of Rag GTPase regulation. *Cell Cycle* **12**, 2948–2952 (2013).
 108. Panchaud, N., Péli-Gulli, M. P. & De Virgilio, C. Amino acid deprivation inhibits TORC1 through a GTPase-activating protein complex for the Rag family GTPase Gtr1. *Sci. Signal.* **6**, (2013).
 109. Bar-Peled, L. *et al.* A tumor suppressor complex with GAP activity for the Rag

- GTPases that signal amino acid sufficiency to mTORC1. *Science* (80-). **340**, 1100–1106 (2013).
110. González, A. & Hall, M. N. Nutrient sensing and TOR signaling in yeast and mammals . *EMBO J.* **36**, 397–408 (2017).
 111. Chen, X. *et al.* Whi2 is a conserved negative regulator of TORC1 in response to low amino acids. (2018) doi:10.1371/journal.pgen.1007592.
 112. Wang, S. *et al.* Lysosomal amino acid transporter SLC38A9 signals arginine sufficiency to mTORC1. *Science* (80-). **347**, 188–194 (2015).
 113. Jung, J., Genau, H. M. & Behrends, C. Amino Acid-Dependent mTORC1 Regulation by the Lysosomal Membrane Protein SLC38A9. *Mol. Cell. Biol.* **35**, 2479–2494 (2015).
 114. Russnak, R., Konczal, D. & McIntire, S. L. A Family of Yeast Proteins Mediating Bidirectional Vacuolar Amino Acid Transport. *J. Biol. Chem.* **276**, 23849–23857 (2001).
 115. Sutter, B. M., Wu, X., Laxman, S. & Tu, B. P. XMethionine inhibits autophagy and promotes growth by inducing the SAM-responsive methylation of PP2A. *Cell* **154**, 403 (2013).
 116. Van Vliet, D. *et al.* Single amino acid supplementation in aminoacidopathies: A systematic review. *Orphanet Journal of Rare Diseases* vol. 9 7 (2014).
 117. Camp, K. M., Lloyd-Puryear, M. A. & Huntington, K. L. Nutritional treatment for inborn errors of metabolism: Indications, regulations, and availability of medical foods and dietary supplements using phenylketonuria as an example. *Molecular Genetics and Metabolism* vol. 107 3–9 (2012).
 118. Walter, J. H. & MacDonald, A. The use of amino acid supplements in inherited metabolic disease. *J. Inherit. Metab. Dis.* **29**, 279–280 (2006).
 119. Manoli, I. & Venditti, C. P. Disorders of branched chain amino acid metabolism. *Transl. Sci. Rare Dis.* **1**, 91–110 (2016).
 120. Tuncel, A. T. *et al.* *Organic acidurias in adults: late complications and management.* *Journal of Inherited Metabolic Disease* vol. 41 765–776 (Springer Netherlands, 2018).
 121. Ah Mew, N. *et al.* *Urea Cycle Disorders Overview.* *GeneReviews®* (University of Washington, Seattle, 1993).
 122. Knerr, I., Weinhold, N., Vockley, J. & Gibson, K. M. Advances and challenges in the treatment of branched-chain amino/keto acid metabolic defects. *J. Inherit. Metab. Dis.* **35**, 29–40 (2012).
 123. Stauss, K., Puffenberger, E. & Morton, D. Maple Syrup Urine Disease. 2006 Jan 20 [Updated 2013 May 9]. in *Gene Reviews* (eds. Pagon, R., Adam, M. & Ardinger, H.) (University of Washington, Seattle, 2020).
 124. Quental, S. *et al.* Molecular and structural analyses of maple syrup urine disease and identification of a founder mutation in a Portuguese Gypsy community. *Mol. Genet. Metab.* **94**, 148–156 (2008).
 125. Edelmann, L. *et al.* *Maple syrup urine disease: Identification and carrier-*

- frequency determination of a novel founder mutation in the Ashkenazi Jewish population. American Journal of Human Genetics* vol. 69 863–868 (Elsevier, 2001).
126. Chapman, K. A., Gramer, G., Viall, S. & Summar, M. L. *Incidence of maple syrup urine disease, propionic acidemia, and methylmalonic aciduria from newborn screening data. Molecular Genetics and Metabolism Reports* vol. 15 106–109 (Elsevier Inc., 2018).
 127. Chuang, D. T., Chuang, J. L. & Wynn, R. M. Lessons from genetic disorders of branched-chain amino acid metabolism. in *Journal of Nutrition* vol. 136 (American Institute of Nutrition, 2006).
 128. Blackburn, P. R. *et al.* Maple syrup urine disease: Mechanisms and management. *Application of Clinical Genetics* vol. 10 57–66 (2017).
 129. Richard, E. *et al.* *Altered redox homeostasis in branched-chain amino acid disorders, organic acidurias, and homocystinuria. Oxidative Medicine and Cellular Longevity* vol. 2018 (Hindawi Limited, 2018).
 130. Friedrich, T., Lambert, A. M., Masino, M. A. & Downes, G. B. Mutation of zebrafish dihydrolipoamide branched-chain transacylase E2 results in motor dysfunction and models maple syrup urine disease. *DMM Dis. Model. Mech.* **5**, 248–258 (2012).
 131. Zinnanti, W. J. *et al.* Dual mechanism of brain injury and novel treatment strategy in maple syrup urine disease. *Brain* **132**, 903–918.
 132. Barschak, A. G. *et al.* Oxidative stress in plasma from maple syrup urine disease patients during treatment. *Metab. Brain Dis.* **23**, 71–80 (2008).
 133. Mescka, C. P. *et al.* Protein and lipid damage in maple syrup urine disease patients: L-carnitine effect. *Int. J. Dev. Neurosci.* **31**, 21–24 (2013).
 134. Bussey' And, H. & Umbarger, H. E. *Biosynthesis of the Branched-Chain Amino Acids in Yeast: a Leucine-Binding Component and Regulation of Leucine Uptake. JOURNAL OF BACTERIOLOGY* vol. 103 <http://jb.asm.org/> (1970).
 135. Xing, R. & Whitman, W. B. Characterization of enzymes of the branched-chain amino acid biosynthetic pathway in *Methanococcus* spp. *J. Bacteriol.* **173**, 2086–2092 (1991).
 136. Gross, S. R. Genetic Regulatory Mechanisms in the Fungi. *Annu. Rev. Genet.* **3**, 395–424 (1969).
 137. Hagelstein, P. & Schultz, G. Leucine Synthesis in Spinach Chloroplasts: Partial Characterization of 2-Isopropylmalate Synthase. *Biol. Chem. Hoppe. Seyler.* **374**, 1105–1108 (1993).
 138. Lee, Y. T. & Duggleby, R. G. Identification of the regulatory subunit of *Arabidopsis thaliana* acetohydroxyacid synthase and reconstitution with its catalytic subunit. *Biochemistry* **40**, 6836–6844 (2001).
 139. Amorim Franco, T. M. & Blanchard, J. S. Bacterial Branched-Chain Amino Acid Biosynthesis: Structures, Mechanisms, and Drugability. *Biochemistry* vol. 56 5849–5865 (2017).

140. Kohlhaw, G. B. Leucine Biosynthesis in Fungi: Entering Metabolism through the Back Door. *Microbiol. Mol. Biol. Rev.* **67**, 1–15 (2003).
141. Satyanarayana, T., Umbarger, H. E. & Lindegren, G. Biosynthesis of branched-chain amino acids in yeast: regulation of leucine biosynthesis in prototrophic and leucine auxotrophic strains. *J. Bacteriol.* **96**, 2018–2024 (1968).
142. Ryan, E. D. & Kohlhaw, G. B. Subcellular localization of isoleucine-valine biosynthetic enzymes in yeast. *J. Bacteriol.* **120**, 631–637 (1974).
143. Kispal, G., Steiner, H., Court, D. A., Rolinski, B. & Lill, R. Mitochondrial and cytosolic branched-chain amino acid transaminases from yeast, homologs of the myc oncogene-regulated Eca39 protein. *J. Biol. Chem.* **271**, 24458–24464 (1996).
144. Ryan, E. D., Tracy, J. W. & Kohlhaw, G. B. Subcellular localization of the leucine biosynthetic enzymes in yeast. *J. Bacteriol.* **116**, 222–225 (1973).
145. Baichwal, V. R., Cunningham, T. S., Gatzek, P. R. & Kohlhaw, G. B. Leucine biosynthesis in yeast - Identification of two genes (LEU4, LEU5) that affect α -Isopropylmalate synthase activity and evidence that LEU1 and LEU2 gene expression is controlled by α -Isopropylmalate and the product of a regulatory gene. *Curr. Genet.* **7**, 369–377 (1983).
146. Kirkpatrick, C. R. & Schimmel, P. Detection of leucine-independent DNA site occupancy of the yeast Leu3p transcriptional activator in vivo. *Mol. Cell. Biol.* **15**, 4021–4030 (1995).
147. Wang, D., Zheng, F., Holmberg, S. & Kohlhaw, G. B. Yeast transcriptional regulator Leu3p. Self-masking, specificity of masking, and evidence for regulation by the intracellular level of Leu3p. *J. Biol. Chem.* **274**, 19017–19024 (1999).
148. Zhou, K., Bai, Y. & Kohlhaw, G. B. Yeast regulatory protein LEU3: A structure-function analysis. *Nucleic Acids Res.* **18**, 291–298 (1990).
149. Friden, P. & Schimmel, P. LEU3 of *Saccharomyces cerevisiae* activates multiple genes for branched-chain amino acid biosynthesis by binding to a common decanucleotide core sequence. *Mol. Cell. Biol.* **8**, 2690–2697 (1988).
150. Chang, L. L., Cunningham, T. S. & Gatzek, P. R. Cloning and characterization of yeast LEU4, one of two genes responsible for α -isopropylmalate synthesis. *Genetics* **108**, 91–106 (1984).
151. Hsu, Y. P., Kohlhaw, G. B. & Niederberger, P. Evidence that α -isopropylmalate synthase of *Saccharomyces cerevisiae* is under the 'general' control of amino acid biosynthesis. *J. Bacteriol.* **150**, 969–972 (1982).
152. Peters, M. H., Beltzer, J. P. & Kohlhaw, G. B. Expression of the yeast LEU4 gene is subject to four different modes of control. *Arch. Biochem. Biophys.* **276**, 294–298 (1990).
153. Linnane, A. W. & Haslam, J. M. The Biogenesis of Yeast Mitochondria. in *Current Topics in Cellular Regulation* vol. 2 101–172 (Academic Press, 1970).
154. Wurtz, P. *et al.* Branched-chain and aromatic amino acids are predictors of insulin resistance in young adults. *Diabetes Care* **36**, 648–655 (2013).

155. Connelly, M. A., Wolak-Dinsmore, J. & Dullaart, R. P. F. Branched Chain Amino Acids Are Associated with Insulin Resistance Independent of Leptin and Adiponectin in Subjects with Varying Degrees of Glucose Tolerance. *Metab. Syndr. Relat. Disord.* **15**, 183–186 (2017).
156. Felig, P., Marliss, E. & Cahill, G. F. Plasma Amino Acid Levels and Insulin Secretion in Obesity. *N. Engl. J. Med.* **281**, 811–816 (1969).
157. Newgard, C. B. *et al.* A Branched-Chain Amino Acid-Related Metabolic Signature that Differentiates Obese and Lean Humans and Contributes to Insulin Resistance. *Cell Metab.* **9**, 311–326 (2009).
158. Boye, J., Wijesinha-Bettoni, R. & Burlingame, B. Protein quality evaluation twenty years after the introduction of the protein digestibility corrected amino acid score method. *Br. J. Nutr.* **108**, (2012).
159. Elshorbagy, A. *et al.* Amino acid changes during transition to a vegan diet supplemented with fish in healthy humans. *Eur. J. Nutr.* **56**, 1953–1962 (2017).
160. Schmidt, J. A. *et al.* Plasma concentrations and intakes of amino acids in male meat-eaters, fish-eaters, vegetarians and vegans: A cross-sectional analysis in the EPIC-Oxford cohort. *Eur. J. Clin. Nutr.* **70**, 306–312 (2016).
161. Fontana, L. *et al.* Decreased Consumption of Branched-Chain Amino Acids Improves Metabolic Health. *Cell Rep.* **16**, 520–530 (2016).
162. Solon-Biet, S. M. *et al.* The ratio of macronutrients, not caloric intake, dictates cardiometabolic health, aging, and longevity in ad libitum-fed mice. *Cell Metab.* **19**, 418–430 (2014).
163. Richardson, N. E. *et al.* Lifelong restriction of dietary branched-chain amino acids has sex-specific benefits for frailty and life span in mice. *Nat. Aging* **1**, 73–86 (2021).
164. Cummings, N. E. *et al.* *Restoration of metabolic health by decreased consumption of branched-chain amino acids.* *Journal of Physiology* vol. 596 623–645 (Blackwell Publishing Ltd, 2018).
165. Yu, D. *et al.* The adverse metabolic effects of branched-chain amino acids are mediated by isoleucine and valine. *Cell Metab.* **33**, 905-922.e6 (2021).
166. Mülleder, M. *et al.* *Functional Metabolomics Describes the Yeast Biosynthetic Regulome.* *Cell* vol. 167 553-565.e12 (Cell Press, 2016).
167. Chopra, R., Sharma, V. M. & Ganesan, K. Elevated growth of *Saccharomyces cerevisiae* ATH1 null mutants on glucose is an artifact of nonmatching auxotrophies of mutant and reference strains. *Appl. Environ. Microbiol.* **65**, 2267–2268 (1999).
168. WENZEL, T. J., VAN DEN BERG, M. A., VISSER, W., VAN DEN BERG, J. A. & STEENSMA, H. Y. *Characterization of Saccharomyces cerevisiae mutants lacking the E1 α subunit of the pyruvate dehydrogenase complex.* *European Journal of Biochemistry* vol. 209 697–705 (1992).
169. Petek Çakar, Z. *et al.* Vacuolar morphology and cell cycle distribution are modified by leucine limitation in auxotrophic *Saccharomyces cerevisiae*. *Biol. Cell* **92**, 629–637 (2000).

170. Alper, H., Moxley, J., Nevoigt, E., Fink, G. R. & Stephanopoulos, G. Engineering yeast transcription machinery for improved ethanol tolerance and production. *Science (80-.)*. **314**, 1565–1568 (2006).
171. Baerends, R. J. S., Qiu, J.-L., Rasmussen, S., Nielsen, H. B. & Brandt, A. Impaired Uptake and/or Utilization of Leucine by *Saccharomyces cerevisiae* Is Suppressed by the SPT15-300 Allele of the TATA-Binding Protein Gene. *Appl. Environ. Microbiol.* **75**, 6055–6061 (2009).
172. Reynaldo, H., Lo´lo´pez-Mirabal, L., Winther, J. R. & Kielland-Brandt, M. C. Genetic Interaction between the *ero1-1* and *leu2* Mutations in *Saccharomyces cerevisiae*. doi:10.1271/bbb.70323.
173. Mülleder, M. *et al.* A prototrophic deletion mutant collection for yeast metabolomics and systems biology. *Nature Biotechnology* vol. 30 1176–1178 (2012).
174. Alam, M. T. *et al.* The metabolic background is a global player in *Saccharomyces* gene expression epistasis. *Nat. Microbiol.* **1**, 15030 (2016).
175. Pronk, J. T. Auxotrophic yeast strains in fundamental and applied research. *Applied and Environmental Microbiology* vol. 68 2095–2100 (2002).
176. Çakar, Z. P., Sauer, U. & Bailey, J. E. Metabolic engineering of yeast: The perils of auxotrophic hosts. *Biotechnol. Lett.* **21**, 611–616 (1999).
177. Van Dijken, J. P. *et al.* An interlaboratory comparison of physiological and genetic properties of four *Saccharomyces cerevisiae* strains. in *Enzyme and Microbial Technology* vol. 26 706–714 (Elsevier Science Inc, 2000).
178. Cohen, R. & Engelberg, D. Commonly used *Saccharomyces cerevisiae* strains (e.g. BY4741, W303) are growth sensitive on synthetic complete medium due to poor leucine uptake. *FEMS Microbiol. Lett.* **273**, 239–243 (2007).
179. Gomes, P., Sampaio-Marques, B., Ludovico, P., Rodrigues, F. & Leão, C. Low auxotrophy-complementing amino acid concentrations reduce yeast chronological life span. *Mech. Ageing Dev.* **128**, 383–391 (2007).
180. Gietz, R. D. & Woods, R. A. Yeast transformation by the LiAc/SS Carrier DNA/PEG method. *Methods Mol. Biol.* **313**, 107–120 (2006).
181. Mumberg, D., Müller, R. & Funk, M. Yeast vectors for the controlled expression of heterologous proteins in different genetic backgrounds. *Gene* **156**, 119–122 (1995).
182. Ralser, M., Mülleder, M., Campbell, K., Matsarskaia, O. & Eckerstorfer, F. *Saccharomyces cerevisiae* single-copy plasmids for auxotrophy compensation, multiple marker selection, and for designing metabolically cooperating communities. *F1000Research* **5**, (2016).
183. Miesenböck, G., De Angelis, D. A. & Rothman, J. E. Visualizing secretion and synaptic transmission with pH-sensitive green fluorescent proteins. *Nature* **394**, 192–195 (1998).
184. Marešová, L., Hošková, B., Urbánková, E., Chaloupka, R. & Sychrová, H. New applications of pHluorin - Measuring intracellular pH of prototrophic yeasts and determining changes in the buffering capacity of strains with affected

- potassium homeostasis. *Yeast* **27**, 317–325 (2010).
185. Janke, C. *et al.* A versatile toolbox for PCR-based tagging of yeast genes: new fluorescent proteins, more markers and promoter substitution cassettes. *Yeast* **21**, 947–962 (2004).
 186. Rahman, I., Kode, A. & Biswas, S. K. Assay for quantitative determination of glutathione and glutathione disulfide levels using enzymatic recycling method. *Nat. Protoc.* **1**, 3159–3165 (2007).
 187. Morgan, B. *et al.* Real-time monitoring of basal H₂O₂ levels with peroxiredoxin-based probes. *Nat. Chem. Biol.* **12**, 437–443 (2016).
 188. Bolten, C. J., Kiefer, P., Letisse, F., Portais, J. C. & Wittmann, C. Sampling for metabolome analysis of microorganisms. *Anal. Chem.* **79**, 3843–3849 (2007).
 189. Wittmann, C., Krömer, J. O., Kiefer, P., Binz, T. & Heinzle, E. Impact of the cold shock phenomenon on quantification of intracellular metabolites in bacteria. *Anal. Biochem.* **327**, 135–139 (2004).
 190. Bolten, C. J. & Wittmann, C. Appropriate sampling for intracellular amino acid analysis in five phylogenetically different yeasts. *Biotechnol. Lett.* **30**, 1993–2000 (2008).
 191. Picelli, S. *et al.* Smart-seq2 for sensitive full-length transcriptome profiling in single cells. *Nat. Methods* **10**, 1096–1100 (2013).
 192. Dobin, A. *et al.* STAR: Ultrafast universal RNA-seq aligner. *Bioinformatics* **29**, 15–21 (2013).
 193. Li, B. & Dewey, C. N. RSEM: Accurate transcript quantification from RNA-Seq data with or without a reference genome. *BMC Bioinformatics* **12**, 1–16 (2011).
 194. Robinson, M. D., McCarthy, D. J. & Smyth, G. K. edgeR: A Bioconductor package for differential expression analysis of digital gene expression data. *Bioinformatics* **26**, 139–140 (2009).
 195. Jiao, X. *et al.* DAVID-WS: A stateful web service to facilitate gene/protein list analysis. *Bioinformatics* **28**, 1805–1806 (2012).
 196. Wittmann, Christoph Heinzle, E. *Methods in Biotechnology, Vol. 18: Microbial Processes and Products*. (Humana Press Inc., Totowa, NJ, 2020).
 197. Grauslund, M., Didion, T., Kielland-Brandt, M. C. & Andersen, H. A. *BAP2, a gene encoding a permease for branched-chain amino acids in Saccharomyces cerevisiae*. *BBA - Molecular Cell Research* vol. 1269 275–280 (Elsevier, 1995).
 198. Sáenz, D. A., Chianelli, M. S. & Stella, C. A. L-Phenylalanine Transport in *Saccharomyces cerevisiae*: Participation of GAP1, BAP2, and AGP1. *J. Amino Acids* **2014**, 1–9 (2014).
 199. Iraqui, I. *et al.* Amino Acid Signaling in *Saccharomyces cerevisiae*: a Permease-Like Sensor of External Amino Acids and F-Box Protein Grr1p Are Required for Transcriptional Induction of the AGP1 Gene, Which Encodes a Broad-Specificity Amino Acid Permease. *Mol. Cell. Biol.* **19**, 989–1001 (1999).
 200. Schreve, J. L., Sin, J. K. & Garrett, J. M. The *Saccharomyces cerevisiae* YCC5 (YCL025c) gene encodes an amino acid permease, Agp1, which transports

- asparagine and glutamine. *J. Bacteriol.* **180**, 2556–2559 (1998).
201. Ehrlich, F. Über die Bedingungen der Fuselölbildung und über ihren Zusammenhang mit dem Eiweißaufbau der Hefe. *Berichte der Dtsch. Chem. Gesellschaft* **40**, 1027–1047 (1907).
 202. Chen, E. C.-H. The Relative Contribution of Ehrlich and Biosynthetic Pathways to the Formation of Fusel Alcohols. *J. Am. Soc. Brew. Chem.* **36**, 39–43 (1978).
 203. SMITH, Q. R. & TAKASATO, Y. Kinetics of Amino Acid Transport at the Blood-Brain Barrier Studied Using an in Situ Brain Perfusion Technique. *Ann. N. Y. Acad. Sci.* **481**, 186–201 (1986).
 204. Thevelein, J. M. Signal transduction in yeast. *Yeast* **10**, 1753–1790 (1994).
 205. Thevelein, J. M. & De Winde, J. H. Novel sensing mechanisms and targets for the cAMP-protein kinase A pathway in the yeast *Saccharomyces cerevisiae*. *Molecular Microbiology* vol. 33 904–918 (1999).
 206. Marobbio, C. M. T., Giannuzzi, G., Paradies, E., Pierri, C. L. & Palmieri, F. α -Isopropylmalate, a leucine biosynthesis intermediate in yeast, is transported by the mitochondrial oxalacetate carrier. *J. Biol. Chem.* **283**, 28445–28453 (2008).
 207. Zelenaya-Troitskaya, O., Perlman, P. S. & Butow, R. A. *An enzyme in yeast mitochondria that catalyzes a step in branched-chain amino acid biosynthesis also functions in mitochondrial DNA stability.* *EMBO Journal* vol. 14 3268–3276 (Wiley-VCH Verlag, 1995).
 208. Santhanam, A., Hartley, A., Düvel, K., Broach, J. R. & Garrett, S. PP2A phosphatase activity is required for stress and Tor kinase regulation of yeast stress response factor Msn2p. *Eukaryot. Cell* **3**, 1261–1271 (2004).
 209. Jacinto, E., Guo, B., Arndt, K. T., Schmelzle, T. & Hall, M. N. TIP41 interacts with TAP42 and negatively regulates the TOR signaling pathway. *Mol. Cell* **8**, 1017–1026 (2001).
 210. Van Engeland, M., Nieland, L. J. W., Ramaekers, F. C. S., Schutte, B. & Reutelingsperger, C. P. M. Annexin V-affinity assay: A review on an apoptosis detection system based on phosphatidylserine exposure. *Cytometry* vol. 31 1–9 (1998).
 211. Vermes, I., Haanen, C., Steffens-Nakken, H. & Reutelingsperger, C. A novel assay for apoptosis Flow cytometric detection of phosphatidylserine expression on early apoptotic cells using fluorescein labelled Annexin V. *J. Immunol. Methods* **184**, 39–51 (1995).
 212. Koopman, G. *et al.* Annexin V for flow cytometric detection of phosphatidylserine expression on B cells undergoing apoptosis. *Blood* vol. 84 1415–1420 (American Society of Hematology, 1994).
 213. Martin, S. J. *et al.* Early redistribution of plasma membrane phosphatidylserine is a general feature of apoptosis regardless of the initiating stimulus: Inhibition by overexpression of BCL-2 and Abl. *J. Exp. Med.* **182**, 1545–1556 (1995).
 214. Fadok, V. A., Bratton, D. L., Frasch, S. C., Warner, M. L. & Henson, P. M. The role of phosphatidylserine in recognition of apoptotic cells by phagocytes. *Cell Death and Differentiation* vol. 5 551–562 (1998).

215. Brumatti, G., Sheridan, C. & Martin, S. J. Expression and purification of recombinant annexin V for the detection of membrane alterations on apoptotic cells. *Methods* **44**, 235–240 (2008).
216. NATHANS, D. PUROMYCIN INHIBITION OF PROTEIN SYNTHESIS: INCORPORATION OF PUROMYCIN. *Proc. Natl. Acad. Sci. United States* **51**, 585–592 (1964).
217. Yarmolinsky, M. B. & Haba, G. L. D. L. INHIBITION BY PUROMYCIN OF AMINO ACID INCORPORATION INTO PROTEIN. *Proc. Natl. Acad. Sci.* **45**, 1721–1729 (1959).
218. Aviner, R. The science of puromycin: From studies of ribosome function to applications in biotechnology. *Computational and Structural Biotechnology Journal* vol. 18 1074–1083 (2020).
219. Morgan, B., Sobotta, M. C. & Dick, T. P. Measuring EGSH and H₂O₂ with roGFP2-based redox probes. *Free Radical Biology and Medicine* vol. 51 1943–1951 (2011).
220. Oestreicher, J. & Morgan, B. *Glutathione: Subcellular distribution and membrane transport. Biochemistry and Cell Biology* vol. 97 270–289 (Canadian Science Publishing, 2019).
221. White, W. H., Gunyuzlu, P. L. & Toyn, J. H. *Saccharomyces cerevisiae* Is Capable of de Novo Pantothenic Acid Biosynthesis Involving a Novel Pathway of β -Alanine Production from Spermine. *J. Biol. Chem.* **276**, 10794–10800 (2001).
222. Lopes, J. J., Pinto, M. J., Rodrigues, A., Vasconcelos, F. & Oliveira, R. The *Saccharomyces cerevisiae* Genes, AIM45, YGR207c/CIR1 and YOR356w/CIR2, Are Involved in Cellular Redox State Under Stress Conditions. **4**, 75–82 (2010).
223. Thorpe, C. & Kim, J. P. Structure and mechanism of action of the Acyl-CoA dehydrogenases 1. *FASEB J.* **9**, 718–725 (1995).
224. H-atroon And, J. R. & Haight, R. D. *Glutaric Acid Accumulation by a Lysine-requiring Yeast Mutant**. *THEJOURNAL o.B-o~oorcn~ CHEMISTRY* vol. 237 (1962).
225. Spaan, A. N. *et al.* Identification of the human mitochondrial FAD transporter and its potential role in multiple acyl-CoA dehydrogenase deficiency. *Mol. Genet. Metab.* **86**, 441–447 (2005).
226. Shellhammer, J. P. *et al.* Amino acid metabolites that regulate G protein signaling during osmotic stress. *PLOS Genet.* **13**, e1006829 (2017).
227. Romano, C. *et al.* Influence of Diets with Varying Essential/Nonessential Amino Acid Ratios on Mouse Lifespan. *Nutrients* **11**, (2019).
228. Wanders, D. *et al.* Metabolic responses to dietary leucine restriction involve remodeling of adipose tissue and enhanced hepatic insulin signaling. *BioFactors* **41**, 391–402 (2015).
229. Wanders, D. *et al.* *UCP1 is an essential mediator of the effects of methionine restriction on energy balance but not insulin sensitivity.* *FASEB Journal* vol. 29

- 2603–2615 (FASEB, 2015).
230. Cheng, Y. *et al.* Leucine deprivation decreases fat mass by stimulation of lipolysis in white adipose tissue and upregulation of uncoupling protein 1 (UCP1) in brown adipose tissue. *Diabetes* **59**, 17–25 (2010).
 231. Chen, E. J. & Kaiser, C. A. Amino acids regulate the intracellular trafficking of the general amino acid permease of *Saccharomyces cerevisiae*. *Proc. Natl. Acad. Sci. U. S. A.* **99**, 14837–14842 (2002).
 232. Helliwell, S. B., Losko, S. & Kaiser, C. A. Components of a ubiquitin ligase complex specify polyubiquitination and intracellular trafficking of the general amino acid permease. *J. Cell Biol.* **153**, 649–662 (2001).
 233. Dechant, R. & Peter, M. Nutrient signals driving cell growth. *Curr. Opin. Cell Biol.* **20**, 678–687 (2008).
 234. Dechant, R. *et al.* Cytosolic pH is a second messenger for glucose and regulates the PKA pathway through V-ATPase. *EMBO Journal* vol. 29 2515–2526 (European Molecular Biology Organization, 2010).
 235. Dechant, R., Saad, S., Ibá, A. J. & Peter, M. Cytosolic pH Regulates Cell Growth through Distinct GTPases, Arf1 and Gtr1, to Promote Ras/PKA and TORC1 Activity. *Mol. Cell* (2014) doi:10.1016/j.molcel.2014.06.002.
 236. Wilson, R. B., Renault, G., Jacquet, M. & Tatchell, K. The *pde2* gene of *Saccharomyces cerevisiae* is allelic to *rcal* and encodes a phosphodiesterase which protects the cell from extracellular cAMP. *FEBS Lett.* **325**, 191–195 (1993).
 237. Schmitt, A. P. & Mcentee, K. Msn2p, a zinc finger DNA-binding protein, is the transcriptional activator of the multistress response in *Saccharomyces cerevisiae*. *Proc. Natl. Acad. Sci. U. S. A.* **93**, 5777–5782 (1996).
 238. Martínez-Pastor, M. T. *et al.* The *Saccharomyces cerevisiae* zinc finger proteins *Msn2p* and *Msn4p* are required for transcriptional induction through the stress-response element (STRE). *EMBO Journal* vol. 15 2227–2235 (Wiley-VCH Verlag, 1996).
 239. Xu, Y., Malhotra, A., Ren, M. & Schlame, M. The enzymatic function of tafazzin. *J. Biol. Chem.* **281**, 39217–39224 (2006).
 240. Claypool, S. M., Whited, K., Srijumng, S., Han, X. & Koehler, C. M. Barth syndrome mutations that cause tafazzin complex lability. *J. Cell Biol.* **192**, 447–462 (2011).
 241. Antunes, D. *et al.* Overexpression of branched-chain amino acid aminotransferases rescues the growth defects of cells lacking the Barth syndrome-related gene TAZ1. *J. Mol. Med.* **97**, 269–279 (2019).
 242. Sullivan, L. B. *et al.* Supporting Aspartate Biosynthesis Is an Essential Function of Respiration in Proliferating Cells. *Cell* **162**, 552–563 (2015).
 243. Gombert, A. K., Dos Santos, M. M., Christensen, B. & Nielsen, J. Network identification and flux quantification in the central metabolism of *Saccharomyces cerevisiae* under different conditions of glucose repression. *J. Bacteriol.* **183**, 1441–1451 (2001).

244. Camarasa, C., Grivet, J. P. & Dequin, S. Investigation by ¹³C-NMR and tricarboxylic acid (TCA) deletion mutant analysis of pathways of succinate formation in *Saccharomyces cerevisiae* during anaerobic fermentation. *Microbiology* **149**, 2669–2678 (2003).
245. Birsoy, K. *et al.* An Essential Role of the Mitochondrial Electron Transport Chain in Cell Proliferation Is to Enable Aspartate Synthesis. *Cell* **162**, 540–551 (2015).
246. Chen, X. J. & Clark-Walker, G. D. The petite mutation in yeasts: 50 years on. *International Review of Cytology* vol. 194 197–238 (1999).
247. Liao, X. & Butow, R. A. RTG1 and RTG2: Two yeast genes required for a novel path of communication from mitochondria to the nucleus. *Cell* **72**, 61–71 (1993).
248. Liu, Z. & Butow, R. A. A Transcriptional Switch in the Expression of Yeast Tricarboxylic Acid Cycle Genes in Response to a Reduction or Loss of Respiratory Function. *Mol. Cell. Biol.* **19**, 6720–6728 (1999).
249. Rodrigues, F., Ludovico, P. & Leão, C. Sugar Metabolism in Yeasts: an Overview of Aerobic and Anaerobic Glucose Catabolism. in *Biodiversity and Ecophysiology of Yeasts* 101–121 (Springer-Verlag, 2006). doi:10.1007/3-540-30985-3_6.
250. Malecki, M. *et al.* Functional and regulatory profiling of energy metabolism in fission yeast. *Genome Biol.* **17**, (2016).
251. Malecki, M., Kamrad, S., Ralser, M. & Bähler, J. Mitochondrial respiration is required to provide amino acids during fermentative proliferation of fission yeast. *EMBO Rep.* **21**, e50845 (2020).
252. Gresham, D. *et al.* System-level analysis of genes and functions affecting survival during nutrient starvation in *Saccharomyces cerevisiae*. *Genetics* **187**, 299–317 (2011).
253. Streck, E. L. *et al.* Administration of branched-chain amino acids alters epigenetic regulatory enzymes in an animal model of Maple Syrup Urine Disease. *Metab. Brain Dis.* **36**, 247–254 (2021).

LIST OF ABBREVIATIONS

aa	Amino acid
AAM	Amino acid mix
AAP	Amino acid permease
AAT	Amino acid transporter
AHB	α -aceto α -hydroxybutyrate
AL	Acetolactate
BCaa	Branched chain amino acid
BCAT	Branched chain aminotransferases
DAPI	4,6-diamidino-2-phenylindole
ddH ₂ O	Double distilled water
DHIV	α , β -dihydroxyisobutyrate
DHMV	α , β -dihydroxy β -methylvalerate
DNA	Deoxyribonucleic acid
dNTP	Deoxyribonucleotide triphosphate
DTT	Dithiothreitol
<i>E. coli</i>	<i>Escherichia coli</i>
EDTA	Ethylene diamine tetraacetate
g	Gravity of earth
GSH	Reduced glutathione
GSSG	Oxidized glutathione
GSX	Total glutathione
H ₂ O ₂	Hydrogen peroxide
HC	Hartwell's Complete
HEPES	4-(2-hydroxyethyl)-1-piperazine-ethane sulfonic acid
kb	Kilobase
KB	α -ketobutyrate
KIC	α -keto-isocaproate
KIV	α -keto-isovalerate
KMV	α -keto β -methylvalerate
L	litre
mL	Milli litre
LB	Lysogeny broth media
M	Molarity
mg	Milligram
milliQ-H ₂ O	Double distilled water
min	Minute
ml	Millilitre
mM	Millimolar
MSUD	Maple syrup urine disease
NADH	Nicotinamide adenine dinucleotide
NADPH	Nicotinamide adenine dinucleotide phosphate
NEM	N-Ethylmaleimide
Oac1	Oxaloacetate carrier 1
O.D. ₆₀₀	Optical density at 600 nm
PCR	Polymerase chain reaction

PI	Propidium iodide
PKA	Protein kinase A
PM	Plasma membrane
PS	Phosphatidylserine
RNA	Ribonucleic acid
roGFP2	Redox sensitive green fluorescent protein 2
ROS	Reactive oxygen species
rpm	Revolutions per minute
RT	Room temperature
<i>S. cerevisiae</i>	<i>Saccharomyces cerevisiae</i>
<i>S. pombe</i>	<i>Saccharomyces pombe</i>
T2D	Type-2 diabetes
TOR	Target of rapamycin
TORC1	Target of rapamycin complex1
Tris	Tris-(hydroxymethyl)-aminomethane
U	Units
UV	Ultraviolet
v/v	Volume per volume
w/v	Weight per volume
α -IPM	α -isopropylmalate
β -IPM	β -isopropylmalate
°C	Grade Celsius
μ g	Microgram
μ l	Microlitre
μ M	Micromolar

CURRICULUM VITAE

Gurleen Kaur Khandpur

Master of Science

Education

- 2016-2021 **Ph.D.**, Technische Universität Kaiserslautern.
Thesis lab: Prof. Dr. Bruce Morgan's group, Department of Biochemistry, Universität des Saarlandes.
Thesis title: *Investigating the mechanism of cellular toxicity during aberrant branched-chain amino acid metabolism.*
- 2012-2015 **Master of Science, Molecular Biology and Biotechnology**
Universität Bonn, Germany (Grade-1.6).
Thesis lab: Dr. Carsten Schultz group, Cell Biology and Biophysics Unit, EMBL, Heidelberg, Germany.
Thesis title: *Application of chemical dimerizers for studying of G-proteins signaling involved in the regulation of insulin secretion in beta cells.*
- 2007-2011 **Bachelor of Engineering in Biotechnology**
Ambala College of Engineering and Applied Research (ACE), Kurukshetra University (84 %).
Thesis lab: Prof. Dr. G. Lakshmi, Applied Biotechnology Engineering Centre, Biotechnology Department, ACE, Ambala.
Project title: *Preparation of Subunits of Human Chorionic Gonadotropin (hCG) and their Characterization.*
- 2006-2007 **Senior Secondary Education**
S. S. Mota Singh Model School, New Delhi (86 %).
- 2004-2005 **Higher Secondary Education**
S. S. Mota Singh Model School, New Delhi (88 %).

Research Experience and Internship

- **Research Stay, IRTG graduate school (April-July 2018)**
Dr. Nicolas Touret, Department of Biochemistry, University of Alberta, Edmonton.
- **Visiting Scientist (November 2015-February 2016)**
Dr. Dmytro Yushchenko, Institute of Organic Chemistry and Biochemistry (IOCB), Prague.
- **Research training (July-August 2013)**
Dr. Sven Perner, Department of Prostate Cancer Research, Institute of Pathology, University Hospital Bonn, Germany.

Project title: *Characterization of FOXF1 gene, a potent tumour suppressor gene in prostate cancer (PCa) cell lines.*
- **Three weeks training experience (September 2010)**
Intensive course on Human Centered Approaches in Biomedical Engineering, at University of Applied Sciences, Wilhelmshaven, Germany.
- **Summer Internship (July-August 2010)**
Stem Cells department at INMAS, DRDO), New Delhi

Project title: *Sub cloning of c-kit cDNA V560G into pTre2 Vector, Transfection into U-937 cell lines and Its Protein Detection.*

Other Achievements

- Member of **German & Canadian Research Training Group (IRTG) 1830**, collaboration between German and Canadian Universities (Technische Universität Kaiserslautern, Universität des Saarlandes and University of Alberta, Edmonton).
- 2012-2014 “Scholarship plus” holder and students’ representative (CEMBIO) at University of Bonn.
- 2007-2011 Gold Medalist for 1st Rank in Kurukshetra University.
- 06/2011 Qualified National Eligibility Test for CSIR Lectureship.
- 03/2011 Qualified Graduate Aptitude Test (GATE) with 86 % percentile.

Publications

- Duarte, M., Ferreira, C., **Khandpur, G. K.**, Zimmermann, Flohr, T., Herrmann, J., Castro, H., Morgan, B., Tomás, A. M., Duarte, M. *Leishmania* type II dehydrogenase is essential for parasite viability and renders complex I activity dispensable. Under revision at PNAS (2021).

ACKNOWLEDGEMENTS

“The woods are lovely, dark and deep, But I have promises to keep, And miles to go before I sleep, And miles to go before I sleep”. This famous quote from Robert Frost always inspired me since I recited this poem in the school assembly in the seventh standard. I was always fascinated to learn something new and interact with new people. Visiting a summer school in Germany during my bachelor ignited my love for studying further in Germany. That’s how this beautiful journey in Germany started 11 years ago. Wherein my lovely family always supported me and my plans and decisions. Especially my mother who gave me the heart to believe in me, my father, who gave me courage and wings to fly and my grandfather, who always prayed for me. No words are enough to express my thankfulness and gratitude towards the support my parents and my family gave me all these years. Without their belief, encouragement and prayers, it would have been impossible for me to pursue the PhD study and to be able to write all this.

The next person I owe a big thank you is my professor and mentor Dr. Bruce Morgan. Dear **Bruce**, I really feel so lucky to have you as my supervisor. Your guidance at work not only motivated and encouraged me in several instances during these years. But also, your words taught me many great lessons for my life. Thank you, Bruce, for believing in me and helping me to overcome my talk fears. Many times in the lab, I felt hopeless and depressed, which I think is a must phase of being a PhD student. Your kind words and inspiration always made me bounce back stronger. Your approach provided me with the flexibility to think in different directions, which in turn helped me to build my knowledge. I also genuinely appreciate your quality of being an easily approachable mentor cum person. Thank you, Bruce, for giving me an opportunity to be a part of Morgan lab.

Dear **Zuzanna**, first of all, thank you for letting me work in your lab with Dr. Galal. It was very comfortable working with you and Galal. My PhD project gained good insights during this collaboration. I am also grateful to you for accepting to become the second examiner for my thesis examination.

Dear **Hannes**, I am delighted that I also got to work in the cell biology department during the initial years of my PhD. I appreciate your quality for passionately teaching the students. I want to thank you for accepting to be the ‘Vorsitz’ for my thesis examination. I want to thank Sabine Knaus, Vera Nehr, Cornelia Parent and Andrea Trinkaus from the cell biology department for their technical support and wonderful conversations. You guys helped me settle quickly in Kaiserslautern. I would also like to thank Simone Adkins for all the administrative help and for arranging my initial stay in Germany. Thanks for being very friendly and cheerful always. You always reminded me of my grandmother :D

I would like to thank Prof. Wittman and Prof. Walter for agreeing to collaborate on my project. It was a good learning experience to work with you, Michael, and Kathrin. You both made these collaborations really worth it. Thank you for all your assistance and for helping me to achieve more results in this project.

I would also like to convey my thanks to Prof. Ekkehard Neuhaus and Dr. Gabriele Amoroso for letting me be a part of the IRTG 1830 graduate school. Thank you, Gabi, Malika, and students' representatives, for organizing different meetings, workshops, and seminars beneficial for academic and personal growth. I sincerely thank Dr. Nicolas Touret and Swai for hosting my stay at the University of Alberta in Canada for three months and allowing me to research his lab. I would like to also thank Swai, Nada, Luana, Rawad, Shahid, Annissa and Claude for making my stay in Edmonton a pleasant time.

To my dearest Morganities, thank you all for providing a healthy lab environment to work in and being the best colleagues so far. Dear **Prince Amponsah, Julian Östreicher, Marie Mai** and **Jannik Zimmermann** thank you for being there for me always! I have shared many beautiful memories with you all that I am always going to relish. Julian and Jannik, I wish we guys could have actually worked upon tiger GRXs :P :P. Thank you both also for being wonderful travelling partners. Dear Antje, Birgit, Frank, and Gabi, thank you all for welcoming and make working in the lab in Saarbrücken so smooth. I would like to specially mention **Vera Nehr** here. She was the one who taught me how to pour plates and perform tüfel tests in my first two weeks of PhD, which became my staple experiments in the lab.

I would also like to quote a few of my students which I got to work along during these PhD years. Dear Neus, Basile, Gemer, Zahra and Lorraine, it was a pleasant meeting and working with you. I believe, more than me, you guys have taught me things. I am really happy that I met you and supervised your lab projects.

Usually, one's family is the only family they refer to. I believe I am lucky to have my friends as a part of my family, which is equally dear and special for me. I am blessed to have friends: Deepika, Jaspreet, Gaurav, Sarita, Rohit and Karan back in Delhi. These people never made me feel that I was thousands of miles apart from them. They were and always are just a message/call away from me! Dear **Shibu, Himanshu, Akash, Neha** and **Sushmitha**, the end of this academic journey would not have complete without you. Your presence in my life made me all a better person. It's like I have found my cousins next to me in Germany in you all. Not to forget my lovelies: **Preet, Neha, Anmol, Teddy**, and **Copper**. I love you guys 😊

I would also like to mention my Kaiserslautern friends and curry house family, which means more than home away from home to me. You guys stood by me constantly and made a living in Kaiserslautern for me, like back with my family in Delhi. Thank you, Sreedivya, Rumpa, Subrata bhaiya, Deeba, Eman, Akash, Manikantan, Dalbir, Sushmitha and Lily2.0, for the beautiful times we spent together!

A dream that I saw many years ago will be fulfilled, and I feel very much delighted and blessed to have lived and achieved it (soon 😊). I am deeply grateful to my **Babajee** for everything he has bestowed on me. Thank you, Babajee, for making me also meet **Vikrant** in KL. He came as a good friend in my life and became my lovely husband. Literally without him, his support, and his tasty culinary delights, these years (and coming ones) would not have been like "Zindagi Gulzar hai": Like the way of life I have always envisioned. Finally, and most importantly, I would like to express my thanks, and love for my dear **Peanut**-who made me endure all my PhD fears and mood swings finally. She made me realize that I am living my dream. She is truly a blessing for Vikrant and me!

DECLARATION

I hereby declare that this thesis is a record of bonafide work carried out by me, under the supervision of Prof. Dr. Bruce Morgan, for the award of a Doctorate degree at the Technische Universität, Kaiserslautern. No other sources or aids for assistance, other than those specified, were used in the writing of this thesis.

I further declare that the work reported in this thesis has not been submitted and will not be submitted, either in part or full, for the award of any other degree or diploma in this institute or any other institute or University.

Gurleen kaur Khandpur
Kaiserslautern, 07.07.2021

ਜਪੁ ॥
ਆਦਿ ਸਚੁ ਜੁਗਾਦਿ ਸਚੁ ॥
ਹੈ ਭਿ ਸਚੁ ਨਾਨਕ ਹੋਸੀ ਭਿ ਸਚੁ ॥੧॥

Source: Sri Guru Nanak Dev ji, Raag Gauri, page 1,
Sri Guru Granth Sahib Ji

Translation:

You should meditate on Truth,

“Truth is, Truth was before time, Truth is now, and Nanak, Truth shall ever be.”